Targeting cholesterol crystals in atherosclerosis with cholesterol solubilizing 2-hydroxypropyl-β-cyclodextrin

Dissertation

zur
Erlangung des Doktorgrades (Dr. rer. nat.)
der
Mathematisch-Naturwissenschaftlichen Fakultät
der
Rheinischen Friedrich-Wilhelms-Universität Bonn

vorgelegt von
Alena Grebe
aus
Siegen

Bonn, März 2016

Angefertigt mit Genehmigung der Mathematisch-Naturwissenschaftlichen Fakultät
der Rheinischen Friedrich-Wilhelms-Universität Bonn.

1. Gutachter: Prof. Dr. med. Eicke Latz
2. Gutachter: Prof. Dr. rer. nat. Waldemar Kolanus

Tag der Promotion: 17.10.2016

Erscheinungsjahr: 2016

Ein Teil der vorgelegten Arbeit wurde in folgenden Originalpublikationen veröffentlicht:

Sheedy FJ, **Grebe A**, Rayner KJ, Kalantari P, Ramkhelawon B, Carpenter SB, Becker CE, Ediriweera HN, Mullick AE, Golenbock DT, Stuart LM, Latz E, Fitzgerald KA, Moore KJ. **CD36 coordinates NLRP3 inflammasome activation by facilitating intracellular nucleation of soluble ligands into particulate ligands in sterile inflammation.** *Nat Immunol. 2013 Aug;14(8):812-20.*

Zimmer S*****, **Grebe A***, Bakke SS, Bode N, Halvorsen B, Ulas T, Skjelland M, De Nardo D, Labzin LI, Kerksiek A, Hempel C, Heneka MT, Hawxhurst V, Fitzgerald ML, Trebicka J, Björkhem I, Gustafsson JA, Westerterp M, Tall AR, Wright SD, Espevik T, Schultze JL, Nickenig G, Lütjohann D, Latz E. **Cyclodextrin promotes atherosclerosis regression via macrophage reprogramming.** *Sci Transl Med. 2016 Apr 6;8(333):333ra50.*

***** These authors contributed equally.

Table of Contents

1 Zusammenfassung

Kardiovaskuläre Erkrankungen sind die häufigste Todesursache weltweit. In den meisten Fällen ist die Atherosklerose, eine progressive, chronische Entzündungskrankheit der Blutgefäße, die pathologische Ursache dieser kardiovaskulären Erkrankungen. Ein erhöhter Cholesterinspiegel im Blut gilt als wichtiger Risikofaktor für die Entstehung der Atherosklerose, und die medikamentöse Senkung von zirkulierendem LDL-Cholesterin ist derzeit eine der erfolgreichsten Behandlungsmethoden. Ablagerungen von kristallinem Cholesterin in den Gefäßwänden gelten als Merkmal fortgeschrittener atherosklerotischer Plaques. Darüberhinaus sind Cholesterinkristalle aber bereits in den frühen Entwicklungsstadien der Atherosklerose vorhanden. Makrophagen, die häufigsten und bedeutendsten Zellen in atherosklerotischen Plaques, erkennen Cholesterinkristalle mithilfe des NLRP3 Inflammasoms. Dieser Multiproteinkomplex des angeborenen Immunsystems verursacht die Ausschüttung der pro-inflammatorischen Zytokine Interleukin (IL)-1β und IL-18, die entscheidend zur vaskulären Inflammation beitragen und damit für das Voranschreiten der Atherosklerose verantwortlich sind. Eine Reduktion der Cholesterinkristallmenge in atherosklerotischen Plaques könnte voraussichtlich die vaskuläre Inflammation und folglich das Voranschreiten der Atherosklerose verringern.

In dieser Studie wurde im Mausmodell untersucht, ob 2-Hydroxypropyl-β-cyclodextrin (CD), welches Cholesterin in Lösung bringt und aus Zellen entfernen kann, auch die vaskuläre Ablagerung von Cholesterinkristallen reduziert oder diese aus den atherosklerotischen Plaques entfernen kann, und ob dadurch die Entwicklung und das Voranschreiten der murinen Atherosklerose verhindert wird. Tatsächlich beeinträchtigte die Behandlung mit CD die Entwicklung der Atherosklerose in Mäusen, was an einer Reduktion der Plaquegröße und der Cholesterinkristallmenge im Plaque erkennbar war. Zudem bewirkte die Behandlung mit CD sogar die Regression von bereits etablierten atherosklerotischen Plaques. Daraufhin wurden die molekularen Mechanismen des atheroprotektiven Effekts von CD *in vitro* in Makrophagen untersucht. Die Behandlung von Cholesterinkristall-beladenen Makrophagen mit CD führte zur Auflösung der intrazellulären Cholesterinkristalle und förderte die Esterifizierung und den Efflux des aus den Kristallen herausgelösten Cholesterins. Zudem wurde dieses Cholesterin vermehrt zu Oxysterinen, wie zum Beispiel 27-Hydroxycholesterin, metabolisiert. Einige Oxysterine fungieren als endogene Agonisten für LXR (*liver X receptor*) Transkriptionsfaktoren, die wiederum Gene aktivieren, welche den Cholesterinefflux und anti-inflammatorische Prozesse regulieren. Tatsächlich induzierte die Behandlung mit CD eine LXR-basierte transkriptionelle Umprogrammierung der Makrophagen auf erhöhten Cholesterinefflux. Damit einhergehend förderte CD in Abhängigkeit von LXR den reversen Cholesterintransport und die Ausscheidung von ursprünglich kristallinem Cholesterin aus Cholesterinkristall-beladenen Makrophagen. Darüber hinaus war die Aktivierung von LXR

Transkriptionsfaktoren auch für die atheroprotektiven und anti-inflammatorischen Effekte von CD *in vivo* in muriner Atherosklerose erforderlich.

Die vorliegende Studie zeigt eine atheroprotektive Wirkung von CD im Mausmodell, die mit der Auflösung und Beseitigung von Cholesterinkristallen aus atherosklerotischen Plaques einhergeht. Dabei spielt die erhöhte Produktion von Cholesterin-basierten endogenen LXR Agonisten, welche zur Aktivierung anti-atherogener Transkriptionsprozesse führen, eine entscheidende Rolle. Da eine Behandlung mit CD bereits von der FDA (*U.S. food and drug administration*) für die klinische Nutzung zugelassen ist, könnte CD unmittelbar in klinischen Studien zur Prävention und Behandlung von humaner Atherosklerose getestet werden.

1 Summary

Atherosclerosis is the underlying pathology of cardiovascular diseases (CVDs), the leading cause of deaths worldwide. Elevated blood cholesterol levels have been linked to this slowly progressing inflammatory disease and lowering the amount of circulating low-density lipoprotein (LDL) cholesterol is one of the most successful treatment approaches. Crystalline cholesterol deposits in the vessel wall are a hallmark of advanced atherosclerotic plaques, but they actually already occur in early stages of atherosclerosis development. Cholesterol crystals (CCs) can activate the NLRP3 inflammasome, a cytosolic multimolecular signaling complex present in innate immune cells, such as macrophages, which are the most prominent cell type in the developing atherosclerotic plaque. NLRP3 inflammasome activation results in the release of the pro-inflammatory cytokines IL-1β and IL-18, which are key contributors to the vascular inflammation driving atherosclerosis progression. Therefore, presumably a reduction in the amount of CCs in atherosclerotic plaques could also decrease vascular inflammation and consequently atherosclerosis progression.

In this study, whether 2-hydroxypropyl-β-cyclodextrin (CD), a compound that solubilizes cholesterol and removes cholesterol from cells, is effective in reducing vascular CC deposition or removing CCs from atherosclerotic plaques and thereby preventing atherosclerosis development was investigated in mice. CD treatment indeed impaired murine atherosclerosis development, which was indicated by a reduction of atherosclerotic plaque size and CC load. Moreover, CD treatment even mediated the regression of already established atherosclerotic plaques. The molecular mechanisms of CD-mediated atheroprotection were further examined *in vitro* in macrophages. CD treatment of CC-loaded macrophages mediated the dissolution of intracellular CCs and subsequently promoted crystal-derived cholesterol esterification, efflux and metabolism to oxysterols such as 27-hydroxycholesterol. Some oxysterols function as endogenous agonists for liver X receptor (LXR) transcription factors, which in turn activate genes regulating cholesterol efflux and anti-inflammatory processes. Indeed, CD treatment induced LXR-mediated transcriptional reprogramming of macrophages towards increased cholesterol efflux. Thereby, CD promoted the reverse cholesterol transport and excretion of crystal-derived cholesterol from CC-loaded macrophages in an LXR-dependent manner. Moreover, LXR transcription factor activation was required for the atheroprotective and anti-inflammatory effects of CD *in vivo* in murine atherosclerosis.

This study shows that CD is atheroprotective in mice by dissolving and removing CCs from atherosclerotic plaques and by promoting the production of cholesterol-derived endogenous LXR agonists that activate anti-atherogenic transcriptional processes. Since CD treatment is already approved for clinical use by the U.S. food and drug administration (FDA), it could be directly tested in clinical trials for the prevention or treatment of human atherosclerosis.

2 Introduction

2.1 The immune system

The mammalian body is constantly exposed to potentially harmful microorganisms. Consequently, the body has developed several mechanisms to circumvent microbial invasion. Physical, chemical, and microbiological surface barriers, such as skin, epithelial surfaces, mucus, gastric acid, and commensal gut microbiota, provide a first line of host defense against invading microorganisms. When microbes overcome these protective barriers, they encounter the cellular and humoral defense mechanisms of the host immune system.

The immune system is a highly complex system, which has evolved to efficiently protect the body against infection by pathogens. It can basically be subdivided into innate and adaptive immunity. Innate immunity is the evolutionarily ancient arm of the mammalian immune system. The innate immune response is generally non-specific and its purpose is to physically eliminate pathogens before an infection is established. The innate immune system is also required for activating adaptive immunity. The adaptive immune system, in turn, eliminates pathogens in the later phase of an infection and mediates immunological memory, allowing for quicker, more effective immune responses upon re-infection. Adaptive immune responses are mediated by lymphocytes, which express receptors that are somatically recombined and clonally selected for a specific antigen, and cause a long-lasting, pathogen-specific immune response. Efficient elimination of infectious pathogens usually requires both innate and adaptive immune responses.

2.1.1 Innate immunity

The innate immune system is composed of phagocytes (macrophages, dendritic cells (DCs), natural killer (NK) cells), granulocytes (neutrophils, eosinophils, basophils, mast cells), and humoral factors such as the complement system. It provides the initial host response to any pathogens that have breached surface barriers and invaded the host tissue. Tissue-resident innate immune cells, such as macrophages, DCs and mast cells, detect the presence of either pathogens themselves or tissue damage that indicates infection. These cells then secrete inflammatory mediators such as cytokines and chemokines, which recruit further innate immune cells such as monocytes and neutrophils from the circulation. Together, activated tissue-resident and recruited innate immune cells combat the pathogens by phagocytic destruction or secretion of toxic granules and antimicrobial peptides. In addition, the secreted pro-inflammatory cytokines interleukin (IL) 6, IL-1β and tumor necrosis factor (TNF) mediate a systemic acute-phase response by inducing the production of acute phase proteins in the liver. These humoral factors contribute to pathogen clearance by

opsonization-promoted phagocytosis and complement activation. Activation of innate immunity can therefore already result in pathogen clearance before adaptive immunity is even established. However, the initiation of pathogen-specific adaptive immune responses requires phagocytic innate immune cells such as DCs to process phagocytozed microbial antigens for surface presentation to lymphocytes[1]. After the infection has been cleared, the innate immune system, in particular tissue-resident macrophages, are also important in resolving the inflammation as well as mediating tissue repair and restoring tissue homeostasis[2].

2.1.2 Recognition principles of the innate immune system

Innate immune cells express germ line-encoded pattern recognition receptors (PRRs), which allow for the detection of a wide variety of infectious microbes. They recognize pathogens by conserved microbial structures, termed pathogen-associated molecular patterns (PAMPs). PAMPs are often molecules, which are essential for microbial survival and are therefore highly conserved across microbial species and unlikely to mutate during evolution. As most of these microbial patterns are not present on host molecules, the concept that PRRs allow innate immune cells react to infection by discriminating between self and non-self structures was proposed[3]. However, this theory was altered when it became evident that PRRs also recognize endogenous molecules that indicate tissue injury or infection, such as molecules released from damaged or dying cells[4]. Analogously to PAMPs these endogenous PRR ligands were therefore termed damage-associated molecular patterns (DAMPs) (also known as danger-associated molecular patterns).

PRRs are expressed in different cellular compartments of innate immune cells, for example on the cell surface, in the cytoplasm or in endosomes. PRRs are grouped into five different classes according to their molecular structure: the membrane-bound C-type lectin receptors (CLRs) and Toll-like receptors (TLRs), and the cytosolic absent in melanoma (AIM)-like receptors (ALRs), Retinoic acid-inducible gene (RIG)-I-like receptors (RLRs) and nucleotide-binding and oligomerization domain (NOD)-like receptors (NLRs)[5]. These receptors are all composed of a ligand binding domain and a signaling domain, and their activation is often regulated by dimerization, oligomerization or conformational changes induced upon ligand binding. Adaptor molecules are subsequently recruited to the receptor signaling domain, which activates intracellular signaling cascades culminating in inflammatory gene expression and the release of inflammatory mediators. PRRs of different classes can have synergistic or complementary effects, for example, when the same inflammatory pathways are induced upon recognition of different PAMPS derived from the same infectious organism. Similarly, sufficient activation of certain PRRs often requires the engagement of other PRR classes or

signaling pathways[6]. This cooperative signaling of different PRRs facilitates controlled but effective pathogen detection and elimination.

2.1.2.1 TLRs

The first PRRs identified were TLRs, which are as such the best-characterized class of PRRs. So far, 10 human (TLR 1-10) and 12 functional murine (TLR 1-9 and 11-13) TLRs have been described[7]. Most TLRs are expressed on the cell surface (TLR 1, 2, 4, 5, 6, and 10), where they mainly detect microbial membrane components. However, the TLRs that are responsible for nucleic acid sensing (TLR 3, 7, 8, 9) are localized in intracellular endosomal compartments. Together, these TLRs can sense a wide variety of PAMPs from bacteria, viruses, fungi and protozoa as well as several endogenous DAMPs. To achieve recognition of such a broad spectrum of different ligands, TLRs cooperate with each other, such as TLR2, which forms heterodimers with TLR1 or TLR6 to sense triacylated lipopeptides from Gram-negative bacteria and diacylated lipopeptides from Gram-positive bacteria, respectively. Moreover, TLR4 is known to form a complex with myeloid differentiation factor 2 (MD2) and cluster of differentiation 14 (CD14) to recognize lipopolysaccharide (LPS), a cell wall component of Gram-negative bacteria[7], but it can also cooperate with TLR6 and the scavenger receptor cluster of differentiation 36 (CD36) to recognize DAMPs, such as endogenous oxidized low density lipoprotein (oxLDL)[8]. Therefore, cooperative interactions between TLRs and other signaling molecules and cell surface receptors can expand TLR ligand diversity.

TLRs are type I integral membrane glycoproteins consisting of an extracellular ligand-binding domain containing leucine-rich repeat (LRR) motifs, a transmembrane domain and a cytoplasmic Toll/IL-1 receptor (TIR) domain. Upon ligand binding, TLRs form homo- or heterodimers, which initiates the recruitment of TIR domain-containing adaptor proteins, including myeloid differentiation factor 88 (MyD88), TIR domain-containing adaptor protein-inducing IFN-β (TRIF), TRIF-related adaptor molecule (TRAM), TIR-associated protein (TIRAP, also known as MyD88 adaptor-like (MAL)) and sterile-α and HEAT-Armadillo motifs (SARM)[9]. MyD88 is utilized by all TLRs with the exception of TLR3 and mediates the activation of mitogen-activated protein (MAP) kinases and nuclear factor kappa B (NF-κB). In turn, the activated transcription factors regulate the expression of pro-inflammatory cytokines, such as IL-6, IL-12 and TNF, as well as other inflammatory genes. MyD88 recruitment to TLR7 and TLR9 additionally results in the production of type I interferons (IFNs) via activation of IFN regulatory factor (IRF) 7 in plasmacytoid DCs, which represent a subset of immune cells that is specialized on the detection of viruses[10]. TRIF is used by TLR3 and TLR4 and, besides pro-inflammatory cytokine induction via NF-κB and MAP kinases, also initiates an alternative pathway leading to activation of IRF3, which subsequently induces the production of type I IFN. TLR4 is unusual as it can recruit both

TIRAP and TRAM as linking adaptors for MyD88 and TRIF, respectively. The TIRAP-MyD88 adaptor complex drives an early induction of pro-inflammatory cytokines via MAP kinases and NF-κB, whereas the TRAM-TRIF adaptor complex induces type I IFN via IRF3 as well as late induction of pro-inflammatory cytokines via MAP kinases and NF-κB[11]. The fifth TIR domain-containing adaptor molecule SARM was described to act as an inhibitor of TRIF-dependent signaling in humans[12].

2.1.2.2 NLRs

NLRs represent a large family of cytoplasmic PRRs, which are composed of three functional domains: C-terminal LRRs that might contribute to ligand recognition, a central NOD domain that possesses ATPase activity and is responsible for receptor oligomerization, and an N-terminal protein-protein interaction domain that is required for downstream signal transduction. In the absence of a ligand the C-terminal LRRs conceal the N-terminal domain thereby preventing uncontrolled downstream NLR signaling[13,14].

Several NLR orthologues are found among the plant resistance (R) proteins, which are the PRRs of the plant immune system[15]. This evolutionary conservation across species and kingdoms (from plants to humans) indicates a vital role for these receptors in host defense. Interestingly, plant pathogen recognition by R proteins mainly relies on an indirect detection mechanism through interaction with host proteins that have been altered (e.g. by proteolytic cleavage or phosphorylation) in response to infection (described as the “guard hypothesis”)[16]. Indirect recognition of PAMPs or DAMPs might also play a role in sensing of infection or tissue damage by mammalian NLRs.

In humans, 22 NLRs have been identified so far[14], which are subdivided into several subfamilies according to their N-terminal domain NLRA (NOD, LRR and acidic transactivation domain containing), NLRB (NOD, LRR and baculovirus inhibitor of apoptosis protein repeat (BIR) domain containing), NLRC (NOD, LRR and caspase activation and recruitment domain (CARD) containing), NLRP (NOD, LRR and pyrin domain (PYD) containing) and NLRX (NOD, LRR and CARD-related X effector domain containing)[17].

The NLRC family members NOD1 and NOD2 recognize similar ligands as TLRs, such as bacterial peptidoglycan or viral ribonucleic acids (RNAs), thereby activating downstream signaling via NF-κB or IRFs, which results in similar pro-inflammatory responses. Therefore, it has been suggested that TLRs and NLRs might cooperate in synergistically activating pro-inflammatory cytokine production[10].

Other members of the NLR family, mainly members of the NLRP subfamily, are the sensor proteins in cytosolic multimolecular signaling platforms termed inflammasomes. The heart of these multimeric protein complexes is the inflammasome adaptor molecule apoptosis associated speck-like protein containing a CARD (ASC), which links the inflammasome sensor to the inflammatory protease caspase-1. Upon activation of the inflammasome

sensor, the C-terminal LRRs undergo a conformational change, uncovering the N-terminal protein-protein interaction domain, which is typically the PYD domain[14]. This allows recruitment of ASC, which promotes the multimerization of the adaptor molecule causing the formation of a so-called ASC speck[13]. ASC recruits pro-caspase-1 via homotypic CARD interactions, which enables the self-cleavage of pro-caspase-1 molecules. Activated caspase-1 in turn proteolytically cleaves the pro-forms of the pro-inflammatory cytokines IL-1β and IL-18 into their active forms. Furthermore, upon inflammasome activation, cells undergo a rapid, inflammatory form of cell death, called pyroptosis[13].

The inflammasome sensors described so far include NLRs, such as NLRP1, NLRP3, NLRP6, NLRP12 and NLRC4 (also known as IL-1β-converting enzyme protease-activating factor (IPAF)). Furthermore, the ALR members AIM2 and IFNγ-inducible protein 16 (IFI16) as well as the RLR family member RIG-I can function as inflammasome sensors in response to microbial nucleic acids[13]. In contrast, most NLR-containing inflammasomes have mainly been implicated in the recognition of bacterial components, such as bacterial peptidoglycan, toxins, flagellin and components of type III and type IV secretion systems[18]. The NLRP3 inflammasome is unique in terms of its activating ligands, as it is activated by a large number of structurally diverse endogenous, exogenous and pathogenic activators, and has been implicated in the pathogenesis of many diseases.

2.1.3 NLRP3 inflammasome in infection and inflammatory diseases

Immune responses are required for efficient elimination of potentially harmful microorganisms, but excessive activation of inflammatory responses and dysregulated inflammation can harm the host and result in detrimental chronic inflammatory diseases. Therefore, inflammatory responses are typically tightly regulated. NLRP3 inflammasome activation is a pertinent example of how the innate immune response can be both protective or pathogenic depending on context. While NLRP3 importantly contributes to the elimination of bacterial, viral, fungal and parasitic infections, it has also been implicated in the pathology of a large number of chronic inflammatory diseases[14,18].

2.1.3.1 NLRP3 inflammasome in chronic inflammatory diseases

NLRP3 was originally discovered when mutations in this gene were identified in patients suffering from cryopyrin-associated periodic syndromes (CAPS) such as familial cold autoinflammatory syndrome and Muckle-Wells syndrome[19]. Due to its structural homology to NLRP1, the role of NLRP3 as an inflammasome-forming innate immune receptor was established, and the CAPS-related mutations were found to be gain-of-function mutations resulting in hyper-activation of the NLRP3 inflammasome and overproduction of IL-1β[20].

These findings already indicated the detrimental effects of dysregulated NLRP3 inflammasome function.

Table 2-1: NLRP3 inflammasome in chronic inflammatory diseases.

Various crystalline and aggregated endogenous and exogenous molecules, which are characteristic of chronic inflammatory diseases, activate NLRP3 inflammasome-mediated inflammatory responses, therefore linking the NLRP3 inflammasome to disease pathology.

DAMP	Origin of DAMP	Disease	Ref
Monosodium urate (MSU) crystals	Uric acid released during cell death precipitates in extracellular space	Gout	[21]
Calcium pyrophosphate (CPPD) crystals	Spontaneous crystallization of calcium pyrophosphate	Pseudogout	[21]
Fibrillar amyloid β	Spontaneous aggregation of Amyloid β	Alzheimer's disease	[22]
Islet amyloid polypeptide (IAPP)	Increased insulin secretion promotes secretion and subsequent oligomerization and amyloid deposition of IAAP	Type 2 diabetes mellitus (T2DM)	[23]
Cholesterol crystals	Extracellular cholesterol crystal precipitation or intracellular cholesterol crystal formation upon uptake of modified low density lipoprotein (e.g. oxidized LDL)	Atherosclerosis	[24,25]
Silica crystals	Inhalation of exogenous inorganic silica crystals	Silicosis	[26,27]
Asbestos	Inhalation of exogenous inorganic asbestos fibers	Asbestosis	[27]

Since the discovery of NLRP3, plenty of molecules that trigger NLRP3 inflammasome activation have been identified. These NLRP3 inflammasome activators comprise a broad spectrum of endogenous as well as exogenous molecules of environmental or pathogenic origin, such as bacterial toxins and cell wall components or microbial nucleic acids. A well-described DAMP among the NLRP3 activators is extracellular adenosine triphosphate (ATP), which is released by dying cells during tissue damage. Furthermore, many DAMPs sensed by the NLRP3 inflammasome are aggregated or crystalline endogenous or exogenous molecules, which are related to chronic inflammatory diseases (Table 2-1). For example, the NLRP3 inflammasome is activated by environmental stimuli like asbestos and silica crystals, the causative agents of asbestosis and silicosis; but it can also recognize aggregated or crystallized host molecules such as uric acid crystals, cholesterol crystals and amyloid β fibrils and as such the NLRP3 inflammasome is also involved in metabolic disorders like gout, atherosclerosis and Alzheimer's disease.

2.1.3.2 NLRP3 inflammasome activation

Since NLRP3 inflammasome activation has been linked to several chronic inflammatory diseases, the mechanisms of NLRP3 inflammasome activation are the subject of intense

study. Given the multitude of endogenous and exogenous NLRP3 activators of various origin and diverse structures, it is unlikely that one PRR can directly sense all these structurally diverse molecules and indeed no direct interaction between NLRP3 and it's activators has been observed so far. It has therefore been postulated that NLRP3 is activated indirectly, for example by sensing changes in the cellular environment[28]. This is in line with the suggestion that mammalian NLRs might, similar to their plant orthologues, indirectly detect infection or tissue damage[15].

Activation of the NLRP3 inflammasome is a two-step process. Firstly, a priming step induces adequate expression levels of the inflammasome sensor NLRP3 and the caspase-1 substrate pro-IL-1β. Secondly, detection of NLRP3 activators results in conformational changes in NLRP3 that enable assembly and activation of the NLRP3 inflammasome.

The priming signal (signal 1) is provided by the activation of the transcription factor NF-κB during TLR, NLR or cytokine receptor (e.g. IL-1 receptor (IL-1R)) signaling[29]. *In vitro*, the TLR4 ligand LPS is commonly used as a priming stimulus for NLRP3 inflammasome assays in macrophages. However, some NLRP3 inflammasome activators such as oxLDL[24] or amyloid-β[22] were shown to mediate both NLRP3 priming via activation of TLRs and subsequent NLRP3 activation. However, additional priming stimuli can considerably potentiate the response to these crystallizing and aggregating ligands indicating a regulatory role of the priming step in determining the extent of the subsequent NLRP3-mediated inflammatory response[13].

The signal activating the NLRP3 inflammasome (signal 2) is not entirely understood yet[30]. As mentioned above, direct ligand-receptor activations are implausible; instead the current consensus is that NLRP3 activators induce common pathways upstream of NLRP3. Intensive research into the molecular mechanisms of NLRP3 inflammasome activation has generated various hypotheses for potential upstream events that trigger NLRP3 activation. In brief, ion fluxes such as potassium efflux and calcium fluxes, production of mitochondrial reactive oxygen species (ROS), or sensing of mitochondrial dysfunction via cardiolipin or mitochondrial deoxyribonucleic acid (DNA) release and the subsequent cellular re-localization of NLRP3 to mitochondria have all been implicated in mediating NLRP3 inflammasome activation. Furthermore, post-translational modification of NLRP3 might also regulate inflammasome assembly; for instance deubiquitination was reported to be required for NLRP3 activation[30]. Another hypothesis is that phagocytozed protein aggregates or crystalline material induce lysosomal damage, resulting in the release of the lysosomal proteases such as cathepsins into the cytoplasm. NLRP3, similar to plant NLR orthologues, might then indirectly detect this unusual cytosolic protease activity, for example in the proteolytic cleavage of NLRP3 inhibitor proteins or sensing of proteolytically cleaved host molecules[31]. A further hypothesis based on the similarity between plant NLR orthologues and

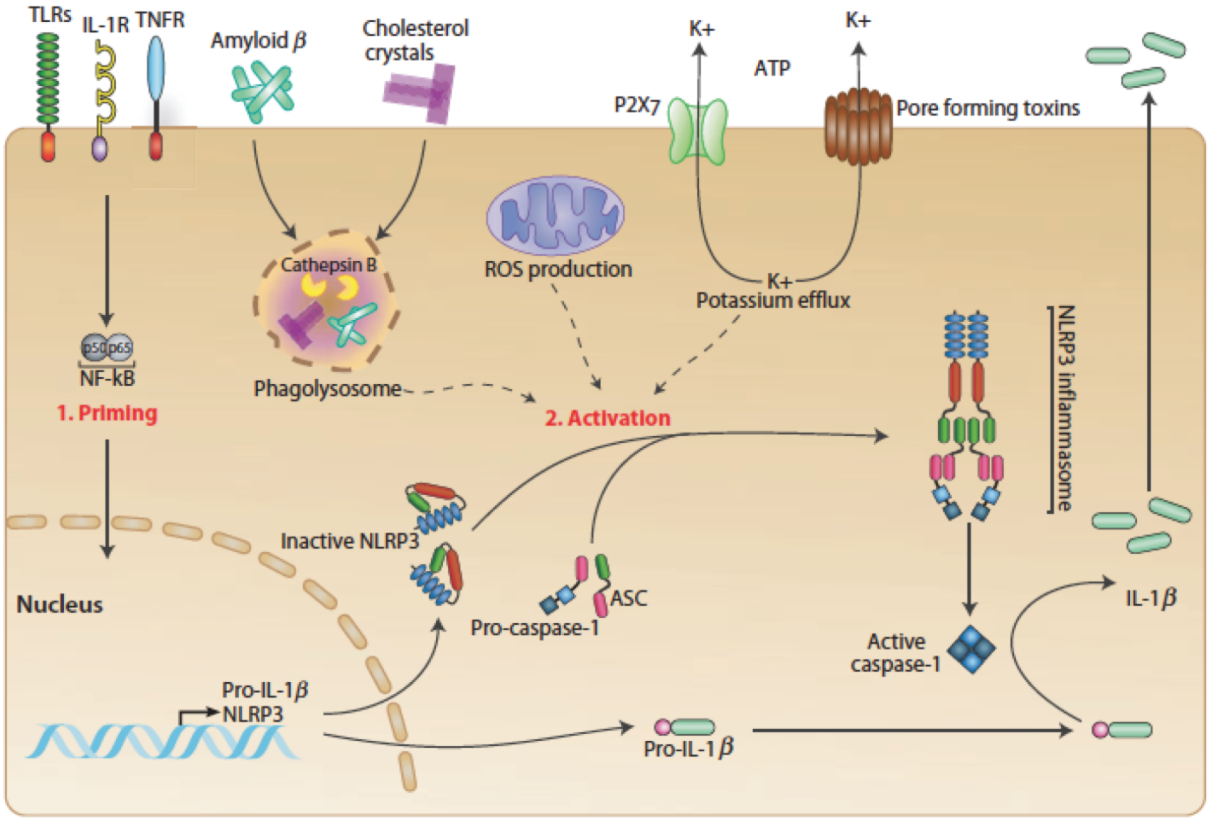

Figure 2-1: NLRP3 inflammasome activation.

NLRP3 inflammasome activation is controlled by a two-checkpoint mechanism. It requires a priming signal activating NF-κB-dependent transcription of NLRP3 and pro-IL-1β, and a subsequent activation signal that induces conformational changes in NLRP3 allowing for recruitment of ASC and caspase-1 to form the mulitmeric inflammasome complex. The activation signal is not entirely understood yet, but mechanisms like release of lysosomal proteins upon lysosome disruption, production of mitochondrial ROS and cellular potassium efflux are proposed to contribute to the activation signal mediating NLRP3 inflammasome assembly and subsequent cleavage and secretion of IL-1β. Figure from Horvath *et al.*[28] with reprint permission (see appendix).

NLRP3 is, that suppressor of G2 allele of S-phase kinase-associated protein 1 (SGT1) and heat shock protein (HSP) 90, which form complexes with R proteins to keep them inactive, also keeps NLRP3 in an inactive conformation. Indeed SGT1 and HSP90 were shown to directly interact with NLRP3[32].

In summary, a variety of potential molecular mechanisms involved in NLRP3 inflammasome activation have been described within the last years (Fig. 2-1), but no distinct mechanism has been elucidated. Therefore, it is likely that NLRP3 inflammasome activation is controlled at several levels and requires more than one particular pathway to be activated. Nevertheless, despite a tightly controlled, two-checkpoint activation mechanism, the NLRP3 inflammasome is efficiently activated by several danger molecules, which are present during metabolic disorders and therefore contributes to the chronic inflammation underlying the pathology of these diseases.

2.2 Atherosclerosis

Cardiovascular diseases (CVDs), which comprise all diseases affecting the cardiovascular system, are the most prevalent cause of mortality worldwide*. The major cause of CVD is atherosclerosis, which is a progressive chronic inflammatory disease characterized by the formation of lipid-rich plaques in the subendothelial space of the large arteries. Atherosclerosis develops as a result of an imbalanced lipid metabolism and the associated excessive cardiovascular inflammation. While atherosclerosis remains asymptomatic for many years, the continuous growth and increasing complexity of the atherosclerotic plaques raise the risk of acute clinical events such as myocardial infarction (heart attack) or cerebral infarction (stroke).

2.2.1 Risk factors and clinical treatment

Epidemiological, clinical and animal studies have revealed important environmental, behavioral and genetic risk factors for atherosclerosis, including hyperlipidemia, consumption of a high-fat diet, lack of exercise, cigarette smoking, hypertension, diabetes, gender (male) and aging. One of the major risk factors of atherosclerosis is an increase in blood cholesterol levels, which has been causally linked to the pathogenesis of atherosclerosis. In turn, lowering blood cholesterol levels, or more precisely low-density lipoprotein (LDL) cholesterol levels, by pharmacological inhibition of cholesterol synthesis with statins, is amongst the most successful therapeutic approaches for delaying atherosclerosis and decreasing the risk of cardiovascular events. Besides drug therapy, current clinical treatment mainly relies on surgical interventions including balloon angioplasty, endarterectomies and bypass grafting[33].

2.2.2 Atherosclerotic plaque formation

The process of atherosclerotic plaque formation (atherogenesis) (Fig. 2-2) is initiated when apolipoprotein (Apo) B-containing lipoproteins such as LDL are retained in the arterial intima (the area between endothelial layer and the smooth muscle cells of the arterial media). This accumulation and oxidative or enzymatic modification of the cholesterol-rich lipoproteins activates endothelial cells to produce pro-inflammatory molecules such as adhesion molecules and chemotactic proteins. This inflammatory response results in the recruitment of monocytes to the intima, where they primarily differentiate into macrophages. These monocyte-derived macrophages then ingest the accumulated lipoproteins, and thereby develop into lipid-laden cells with cytoplasmic lipid droplets that are called foam cells. As a

* World Health Organization (WHO) - Fact sheet N°317 on Cardiovascular diseases CVDs); http://www.who.int/mediacentre/factsheets/fs317/en/ - 14th March, 2016, 10:37 am (see appendix)

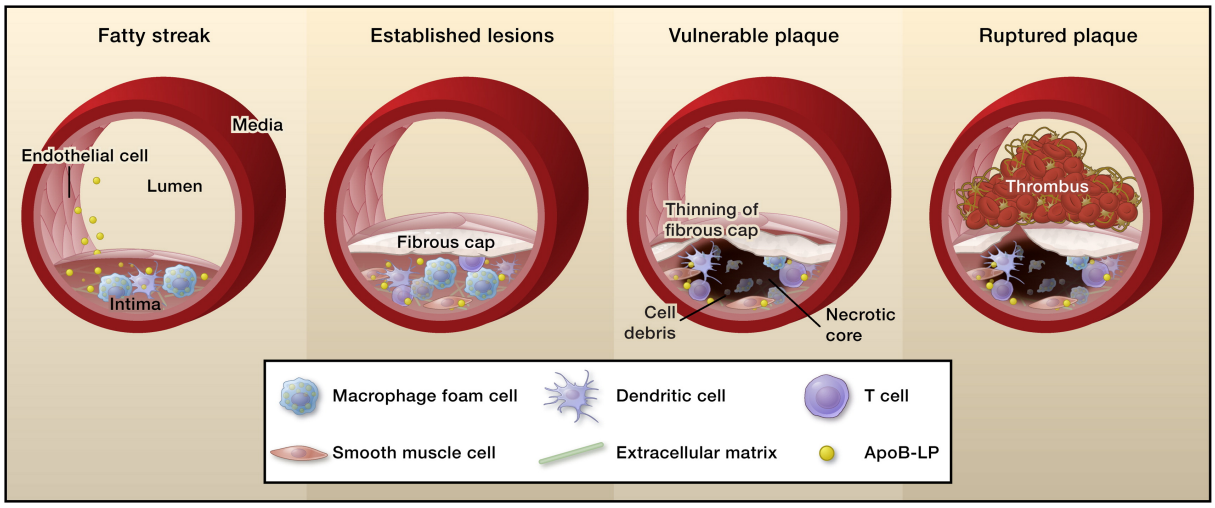

Figure 2-2: Atherosclerosis plaque development and progression.

Atherosclerotic plaque formation starts with the formation of so-called fatty streak lesions in the arterial intima, which are characterized by accumulation of ApoB-containing lipoproteins (ApoB-LP) and resultant recruitment of macrophages and DCs. Due to continuous ApoB-LP retention, infiltration of lymphocytes and smooth muscle cells as well as the deposition of extracellular matrix components fatty streak lesions develop into more complex established atherosclerotic plaques that are covered by a fibrous cap. Accumulation of apoptotic cells as a result of defective efferocytosis causes the formation of a lipid-rich necrotic core, which is characteristic of advanced atherosclerotic plaques. Due to thinning of the fibrous cap advanced atherosclerotic plaques become instable and vulnerable to rupture resulting in subsequent thrombus formation. Figure from Moore and Tabas[34] with reprint permission (see appendix).

result of imbalanced macrophage lipid metabolism, these macrophage foam cells are retained in the subendothelial space where they contribute to atherosclerotic plaque progression by amplifying pro-inflammatory responses in the early fatty streak lesions[35]. The ongoing accumulation of lipids and immune cells, including monocytes and lymphocytes, as well as smooth muscle cell infiltration causes the expansion of the arterial intima towards the vessel lumen. A fibrous cap, consisting of smooth muscle cells and secreted extracellular matrix components, which forms underneath the endothelial cell layer, subsequently covers the accumulated lipoproteins and immune cells. At this stage of atherosclerosis a non-resolving pro-inflammatory immune response causes further atherosclerotic plaque progression. In particular, increased apoptotic cell death within the plaque, combined with defective phagocytic clearance of apoptotic cells (efferocytosis) causes the build-up of extracellular lipids and the formation of a lipid-rich necrotic plaque core, which is a sign of advanced atherosclerotic plaques. Concurrently, the release of matrix degrading proteases results in the thinning of the fibrous cap. These events destabilize the atherosclerotic plaques and make them vulnerable to rupture. Plaque rupture exposes thrombogenic plaque content to the bloodstream resulting in platelet aggregation and the formation of a lumenal thrombus. Thrombotic occlusion of the already narrowed artery finally manifests clinically by myocardial or cerebral infarction due to insufficient oxygen supply to the heart or the brain.

2.2.3 Mouse models of atherosclerosis

Animal models have greatly advanced our understanding of the key steps in the development and progression of atherosclerosis. Common animal models for studying diet-induced atherosclerosis include rabbits, pigs and non-human primates, but the most preferred animal for these studies is the mouse. However, wild type (WT) mice are highly resistant to diet-induced atherosclerosis and only develop small fatty streak-like lesions even when fed a prolonged high-fat, high-cholesterol diet, which is an insufficient model for human atherosclerosis. To overcome this, various genetically modified mouse models have been generated within the last decades. In these models, the mice develop atherosclerotic plaques that more closely mirror human disease, due to dyslipidemia induced upon feeding of an atherogenic diet[36]. ApoE- or LDL receptor (LDLR)-deficient mice fed a high-fat diet are the most frequently used and best-characterized mouse models of atherosclerosis. ApoE is one of the major ligands of the LDLR, the cell surface receptor responsible for clearing ApoB- or ApoE-containing lipoproteins from the plasma. Hence, the absence of either the ligand (ApoE) or the receptor (LDLR) impairs LDL cholesterol clearance and thus causes high serum cholesterol levels in response to a cholesterol-rich diet[37]. While both mouse models develop atherosclerotic plaques that morphologically resemble human atherosclerotic plaques, diet-induced atherosclerosis progression is faster and more severe in ApoE knockout ($ApoE^{-/-}$) mice, which even develop spontaneous atherosclerosis under chow diet[38]. In contrast, LDLR knockout ($LDLR^{-/-}$) mice, which are a model of human familial hypercholesterolemia, require a cholesterol-rich diet for induction of hypercholesterolemia and atherosclerosis[36]. The major limitation of these murine atherosclerosis models is the lack of vulnerable plaque formation, which hampers proper studies on plaque rupture and subsequent thrombosis - the clinically important events in atherosclerosis[37]. Nevertheless, these models are very useful for investigating the mechanisms of atherosclerosis initiation, early atherosclerotic plaque development and atherosclerosis progression up to advanced atherosclerotic plaques.

2.2.4 Chronic cardiovascular inflammation

Inflammatory changes in the atherosclerotic vessel wall were already described in the 19th century. However, for a long time it was unclear whether this inflammation was a coincidental result of atherosclerotic alterations in the vessels, or whether the cellular inflammatory changes were of primary importance and actually the causal effectors of the disease[39,40]. Today it is well established that atherosclerosis is a chronic inflammatory disease and that cardiovascular inflammation plays a key role in atherogenesis.

The overabundance of immune cells in atherosclerotic plaques is the first indication for an important role of inflammation in atherosclerosis development. These cells, in particular

macrophages and DCs, secrete pro-inflammatory cytokines and chemokines, such as IL-1β, IL-6, IL-12, TNF-α and monocyte chemotactic protein (MCP)-1, which have all been shown to promote atherosclerosis progression[41]. Local non-resolving inflammatory responses in the vessel wall result in further immune cell recruitment and lipid deposition in the intimal space. This, in turn, leads to a systemic increase of pro-inflammatory cytokines in the blood and subsequent activation of acute-phase reactants in the liver. Indeed, high serum levels of TNF-α, IL-6 and particularly high sensitivity C-reactive protein (hsCRP) have been associated with increased risk of future cardiovascular events and represent inflammatory biomarkers for prediction of CVD. Amongst those, hsCRP, which is clinically used as inflammatory biomarker, has been shown to be as predictive as total cholesterol or HDL-cholesterol levels for determining CVD risk[42], which supports the importance of systemic inflammation in atherosclerosis. Another link between systemic inflammation and atherosclerosis is derived from the finding that patients with chronic inflammatory diseases, such as rheumatoid arthritis and systemic lupus erythematosus, have an increased risk for cardiovascular events[43,44].

Since the major function of the immune system is to protect the body from invading pathogens, and the vasculature is an important interface for pathogen recognition, a popular hypothesis was that vascular inflammation deriving from microbial infections might contribute to the pathogenesis of atherosclerosis. Indeed, some bacterial and viral pathogens, such as *C. pneumoniae*, *H. pylori*, Influenza and HIV, were associated with human atherosclerosis development[45]. However, while it is likely that the systemic inflammation caused by chronic infection with these pathogens might increase the risk of developing atherosclerosis there is no evidence for a direct causative effect of microbial infection on atherogenesis[45]. Moreover, a study using germ-free mice provided evidence that atherogenesis occurs independently of microbial infections[46], which indicates that endogenous danger signals rather than microbial molecules might elicit the inflammation responsible for atherosclerosis progression. Indeed, several DAMPs are present in atherosclerotic plaques and have been linked to cardiovascular inflammation and atherosclerosis development (Table 2-2).

Therefore, atherosclerosis is no longer considered to develop from passive accumulation of cholesterol and lipoproteins in the vessel wall, but it is rather regarded as complex chronic inflammatory disease, in which sterile cardiovascular inflammation initially caused by imbalances in cholesterol metabolism is the main driver of disease progression.

Consequently, a plethora of anti-inflammatory therapies for atherosclerosis, including generic anti-inflammatory agents such as colchicine and methotrexate, are currently being tested[42]. Currently, the most promising approach is the inhibition of the pro-inflammatory cytokine IL-1β, which is a potent pro-atherogenic cytokine with pleitropic effects, such as promoting

Table 2-2: Triggers of sterile inflammation in atherosclerosis.

Several endogenous danger signals accumulate in atherosclerotic plaques and have been associated with cardiovascular inflammation, the main driver of atherogenesis[45].

Origin of DAMP	DAMP
Extracellular matrix	Fibronectin, Hyaluron, Heparan sulfate
Oxidation epitopes	Oxidized LDL, Oxidized phospholipids, Minimally modified LDL
Cell death	Advanced glycation end-products (AGEs), Heat shock proteins, HMGB1, Fatty acids, Nucleic acids, ATP
Metabolic products	Cholesterol crystals, Uric acid crystals
Microenvironment	Acidosis, Hyperglycemia

the proliferation and differentiation of monocyte-derived cells, augmenting local cytokine and growth factor production and increasing endothelial adhesion molecule and coagulation factor expression, thereby favoring thrombus formation. In human coronary arteries of atherosclerosis patients macrophage and endothelial cell-derived IL-1β levels correlate with atherosclerosis severity[47]. Furthermore, murine atherosclerosis progression is attenuated in mice lacking IL-1β, confirming that IL-1β has atherogenic activity[24,48]. Several animal models have suggested the protective role of IL-1β blockade in atherosclerosis[48-51], and a clinical trial is currently testing the effectiveness and safety of canakinumab, a human monoclonal neutralizing IL-1β antibody, in patients with coronary artery disease (CANTOS trial)[52]. While targeting vascular inflammation appears to be a promising approach for the development of anti-atherogenic therapies, the inhibition or modulation of systemic inflammation always carries the caveat of disturbing immune homeostasis, which might therefore cause detrimental side effects for example during infection and therefore requires careful evaluation of risks and benefits.

2.2.5 Cholesterol uptake, metabolism and elimination

In vertebrates, cholesterol is an essential lipid that is either derived from endogenous *de novo* synthesis or taken up via the diet. Cholesterol is a fundamental component of cell membranes, where it is crucial for maintaining membrane structure, function and permeability and is also importantly involved in cellular signal transduction. Moreover, cholesterol metabolites such as oxysterols, vitamin D, bile acids and steroid hormones are also essential for several physiological processes. Despite these essential functions, excessive amounts of cholesterol in the body can be detrimental. Therefore, cellular cholesterol uptake, biosynthesis, metabolism and elimination need to be tightly regulated.

2.2.5.1 The “good” and the “bad” cholesterol

The hydrophobic nature of cholesterol requires that lipoprotein carriers in the blood transport it through the body. The major cholesterol-carrying lipoprotein in humans is LDL, which delivers cholesterol, including dietary cholesterol from the liver, to the peripheral tissues. In contrast, high-density lipoprotein (HDL) is responsible for removing excess cholesterol from peripheral tissues to the liver for bile acid synthesis and fecal excretion from the body in a process known as reverse cholesterol transport (RCT).

Since high LDL cholesterol levels increase the risk of developing atherosclerosis, it has been commonly referred to as the “bad” cholesterol for a long time. Because LDL accumulates in the subendothelial space where it triggers inflammatory responses and initiates atherosclerosis plaque formation, it is still regarded as the major atherogenic lipoprotein[53]. In contrast, HDL cholesterol levels have been inversely correlated to CVD risk, and since HDL cholesterol levels were observed to be protective in epidemiological studies[54], it was subsequently referred to as the “good” cholesterol. However, more recent studies have elucidated that HDL function, or more specifically, its capacity to efflux cholesterol from macrophages, is a more important predictor atherosclerosis risk than HDL cholesterol levels alone[55]. Besides its important role in RCT, HDL has anti-oxidative, anti-thrombotic, anti-apoptotic and anti-inflammatory effects, and is therefore regarded as anti-atherogenic lipoprotein[53,56].

2.2.5.2 Cellular cholesterol uptake and storage

Cells in peripheral tissues obtain cholesterol from the circulation by receptor-mediated endocytosis of LDL particles by the LDLR. Upon endocytic uptake, the LDLR is recycled back to the plasma membrane, whereas its cholesterol cargo is exported from late endosomal compartments by the proteins Niemann-Pick type C (NPC) 1 and NPC2. This LDL-derived cholesterol is then either directly integrated into cellular membranes or it is enzymatically converted to cholesterol esters by acyl-coenzyme A (CoA):cholesterol acyltransferase (ACAT) in the endoplasmic reticulum (ER). This esterification of cholesterol is of importance as the accumulation of free cholesterol is toxic for the cells[57], while cholesterol esters are a nontoxic storage form of cholesterol, which can be stored in cytoplasmic lipid droplets. Cholesterol ester hydrolase (CEH) hydrolyzes esterified cholesterol from lipid droplets and thus makes the stored cholesterol available for cellular cholesterol metabolism[58].

2.2.5.3 Cellular cholesterol efflux and reverse cholesterol transport

A key mechanism for maintaining cellular cholesterol homeostasis is the efflux of excess cholesterol from peripheral cells, such as cholesterol-rich macrophage foam cells in the

arterial walls. Cholesterol efflux is mainly mediated via the transmembrane ATP-binding cassette transporters A1 (ABCA1) and G1 (ABCG1), which initiate RCT by loading cholesterol into HDL (Fig. 2-3). ABCA1 transfers cholesterol to lipid-poor ApoA1 particles, thereby forming nascent HDL particles. Lecithin-cholesterol acyltransferase (LCAT) generates mature HDL particles esterifying the cholesterol present in these nascent HDL particles. In contrast to ABCA1-mediated cholesterol efflux, ABCG1 transfers cellular cholesterol to lipid-rich mature HDL particles. While some cholesterol can be transferred directly from mature HDL to VLDL and LDL particles by cholesterol ester transfer protein (CETP), HDL mainly delivers its incorporated cholesterol to the liver, where it is removed from the circulation via hepatic scavenger receptor B1 (SR-B1). In the liver, HDL-derived cholesterol esters are converted back to free cholesterol, which then serves as substrate for bile acid synthesis. Finally, cholesterol and bile acids are eliminated from the body via biliary excretion into the feces[59].

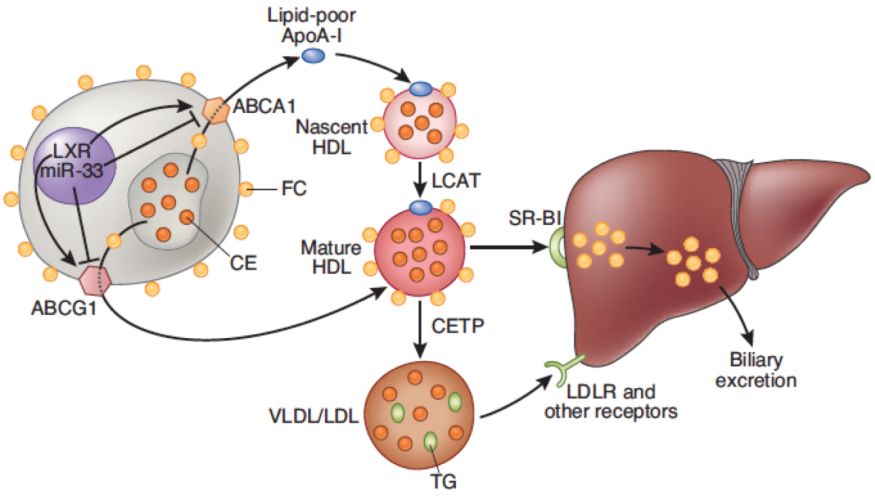

Figure 2-3: Cellular cholesterol efflux and reverse cholesterol transport.

Reverse cholesterol transport describes the process by which excess cellular cholesterol effluxed to HDL particles and transported to the liver for excretion from the body. The cholesterol efflux transporters ABCA1 and ABCG1 transfer cellular cholesterol to lipid-poor ApoA1 or lipid-rich HDL particles, respectively. Effluxed free cholesterol (FC) is converted into cholesterol esters (CE) by LCAT, thereby forming mature HDL particles. CEs in HDL particles are then either transferred by CETP to VLDL and LDL particles that also contain trigylcerides (TG) or directly taken up into the liver via SR-BI for subsequent bile acid synthesis and biliary cholesterol excretion. Figure adapted from Rader and Tall[60] with reprint permission (see appendix).

2.2.5.4 Regulation of cellular cholesterol homeostasis

For maintaining cellular cholesterol homeostasis, cellular cholesterol synthesis, uptake, storage and efflux need to be tightly regulated. Transcriptional regulation of cellular cholesterol homeostasis primarily involves two families of transcription factors, whose activity is controlled by the binding of sterols and oxysterols, and therefore directly depends on the

sterol status of the cell. Cholesterol biosynthesis and uptake are regulated by genes under the control of sterol regulatory element-binding protein (SREBP) transcription factors, which are activated in response to low levels of cellular cholesterol. In contrast, genes involved in cholesterol efflux pathways are under the control of the liver X receptor (LXR) transcription factors, which are activated under conditions of excess cellular cholesterol (Fig. 2-4)[61].

SREBPs

Transcription factors of the SREBP family control the expression of genes that regulate both the cholesterol and fatty acid biosynthesis pathways. While SREBP-1a regulates both pathways and SREBP-1c regulates fatty acid synthesis, SREBP-2 is the main regulator of cholesterol biosynthesis. SREBP precursor proteins reside in the ER as integral membrane proteins, which interact with SREBP cleavage activating protein (SCAP). When cellular cholesterol levels are low, SCAP mediates the transport of SREBP precursors to the Golgi where proteolytic processing produces the mature SREBP transcription factors. Upon translocation to the nucleus, SREBPs bind to sterol-response elements in their target genes thereby activating their transcription[62]. SREBP-2 target genes encode proteins involved in cholesterol uptake and biosynthesis, such as LDLR or HMG-CoA reductase, which is the rate-limiting enzyme for cholesterol synthesis. Therefore, activation of SREBPs results in an increase of cellular cholesterol levels. However, when cellular cholesterol levels are high, cholesterol and its precursor desmosterol cause SREBP/SCAP ER retention by directly binding to SCAP, which prevents SCAP-mediated SREBP trafficking to the Golgi, while oxysterols bind to the ER-retention proteins insulin-induced gene (INSIG) 1 or INSIG2, which promotes their binding to SCAP mediating ER-retention of SREBP[61]. With SREBPs inactive and sequestered in the ER, they are no longer able to activate their gene expression programs.

LXRs

Transcription factors of the LXR nuclear receptor family, namely LXRα and LXRβ, form heterodimers with retinoid X receptor (RXR) transcription factors to bind LXR response elements in their target genes. LXR/RXR heterodimers can both positively and negatively control the transcription of their target genes depending on the presence of endogenous LXR agonists. While SREBPs can be directly regulated by cholesterol, LXRs are solely activated by sterols and oxysterols that accumulate under conditions of high cellular cholesterol. These endogenous LXR agonists include the cholesterol precursor desmosterol and several oxysterols, such as 24(S)-hydroxycholesterol (HC), 25-HC and 27-HC. Therefore, when cellular cholesterol levels are low, no LXR ligand is present and LXR/RXR heterodimers interact with a co-repressor complex resulting in inhibition of target gene expression. But

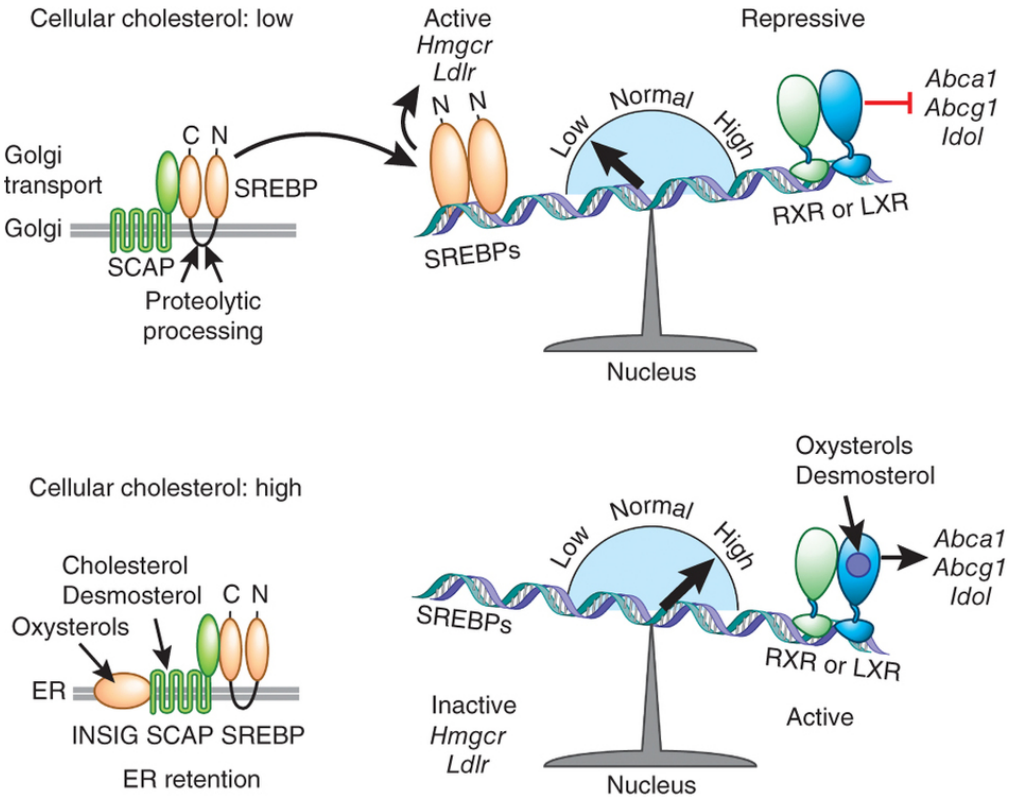

Figure 2-4: Transcriptional regulation of cellular cholesterol homeostasis.

Cellular cholesterol levels control transcriptional regulation of cholesterol homeostasis by SREBPs and LXRs. Low cellular cholesterol levels (top) cause SCAP-mediated transport of SREBP precursors to the Golgi, where proteolytic processing generates mature SREBP transcription factors. Nuclear translocation of SREBP induces the transcription of genes encoding proteins involved in cholesterol synthesis and uptake (e.g. HMG-CoA reductase or LDLR). At the same time LXR/RXR heterodimers repress the transcription of genes encoding proteins involved in cholesterol efflux (e.g. ABCA1 and ABCG1). This cooperative transcriptional regulation causes an increase in cellular cholesterol. High cellular cholesterol levels (bottom) cause the retention of SCAP/SREBP complexes in the ER, which is mediated by desmosterol, cholesterol and oxysterols, and prevents SREBP target gene expression. At the same time desmosterol and oxysterols bind to LXRs thereby activating the transcription of target genes (e.g. Abca1 and Abcg1). This activation of cellular cholesterol efflux pathways results in a decrease in cellular cholesterol. Figure from Spann and Glass[61] with reprint permission (see appendix).

when cellular cholesterol levels are high, endogenous LXR ligands bind LXRs and induce the recruitment of a co-activator complex resulting in activation of target gene expression. LXR target genes encode proteins important for cellular cholesterol efflux, such as ABCA1, ABCG1 and ApoE, but LXRs also activate genes involved in fatty acid biosynthesis, among them SREBP-1c[61]. SREBP-1c in turn activates stearoyl-CoA desaturase-1 (Scd-1), the enzyme producing oleoyl-CoA, which is the preferred substrate for ACAT, resulting in increased esterification of free cholesterol by ACAT[63]. Therefore, LXR activation restores cellular cholesterol homeostasis predominantly by regulating cholesterol efflux, but also by indirectly promoting cholesterol storage. Finally, in addition to regulating cholesterol homeostasis, activated LXR transcription factors can also function as transcriptional repressors of pro-inflammatory responses by transrepression of NF-κB[64].

Oxysterols

Oxysterol production under conditions of excess cellular cholesterol is of particular importance for regulating cellular cholesterol homeostasis, as cholesterol itself is not a ligand for LXR and therefore cannot regulate cholesterol efflux pathways. Instead, oxysterols function as indirect signals of cholesterol excess, which can simultaneously regulate cholesterol efflux pathways by LXR activation and cholesterol biosynthetic pathways by suppression of SREBP processing. Moreover, oxysterols can also promote INSIG1 binding to HMG-CoA reductase resulting in ubiquitination and proteasomal degradation of HMG-CoA reductase, which represents another mechanism of inhibiting cholesterol biosynthesis[65]. In the liver, oxysterols can be further metabolized to bile acids and therefore importantly contribute to cholesterol removal from the body by biliary cholesterol excretion[66]. Oxysterols are generated from cholesterol by specific enzymes. For instance cholesterol 24-hydroxylase (Cyp46a1), cholesterol 25-hydroxylase (Ch25h) and cholesterol 27-hydroxylase (Cyp27a1) catalyze the production of 24(S)-HC, 25-HC and 27-HC, respectively[67]. The hydroxylation at the side-chain of cholesterol makes the oxysterol more hydrophilic, which improves its movement in the aqueous cytoplasmic environment increasing its potential to function as signaling molecule[66]. Furthermore, oxysterols regulate intracellular cholesterol trafficking between internal compartments, such as the ER, where many cholesterol regulatory enzymes reside, and the plasma membrane[65]. This regulation of intracellular cholesterol trafficking is important for adequate cellular responses to changes in cellular cholesterol levels and maintaining of cellular cholesterol homeostasis.

2.2.6 Cholesterol crystals in atherosclerosis

The physical state of cholesterol is greatly influenced by its concentration, but also by several environmental factors such as the surrounding medium, pH, temperature and pressure. Since cholesterol is a hydrophobic molecule with low water solubility, high cholesterol concentrations in aqueous environments result in the crystallization of cholesterol.

The deposition of crystalline cholesterol has long been regarded as a hallmark of advanced atherosclerotic plaques. However, the role of cholesterol crystals (CCs) in the development, progression and clinical outcome of atherosclerosis was underestimated for a long time. Initially, CC deposition was only observed in late stages of the disease, and moreover, CCs were only indirectly detected by the presence of so-called cholesterol crystal clefts, which occur when the organic solvents used for common histological sample preparation dissolve deposited crystalline cholesterol. While both extra- and intracellular cholesterol crystal clefts have been described, the origin of the crystalline material, especially inside the cells, was unclear[68]. Indeed, one hypothesis was that cholesterol crystallization might be a handling artifact arising during tissue preparation, but in the 1970s Small and colleagues confirmed

the presence of monohydrate CCs in intermediate and advanced atherosclerotic plaques[69]. They also already proposed that supersaturation of free cholesterol inside lysosomes induces intracellular cholesterol crystallization followed by lysosome disruption and subsequent cell death, thereby promoting the formation of the lipid-rich necrotic core of advanced atherosclerotic plaques[69]. This concept was proven by *in vitro* studies on macrophage foam cells that showed intracellular cholesterol monohydrate crystal formation upon free cholesterol accumulation in the lysosome[70], which was accompanied by apoptotic and necrotic cell death[71]. The findings of the latter *in vitro* study, which used an ACAT inhibitor to increase free cholesterol in the cells, were confirmed *in vivo*, where ACAT deficiency in atherosclerosis mouse models resulted in extensive accumulation of extracellular CCs and a drastic decrease in macrophage plaque content, presumably due to increased cell death in response to excessive free cholesterol[72]. These studies provided evidence that intra- and extracellular phase transition of free cholesterol to its crystalline form is physically possible *in vivo*, and that this can be triggered by dysregulated cellular cholesterol homeostasis, resulting in high cholesterol concentrations. Therefore, in the atherosclerotic plaque, cholesterol crystallization may occur in response to accumulated cholesterol derived from lipoproteins or dying cells. While increased efferocytosis and phagocytic lipoprotein clearance might overwhelm regulatory mechanisms of cellular cholesterol homeostasis and drive intracellular CC formation, the accumulated cholesterol can also directly crystallize in the extracellular milieu of the atherosclerotic plaque.

2.2.6.1 CCs as contributors to the clinical outcome of atherosclerosis

CCs, which were long-known to be present in late stage atherosclerotic plaques, are also abundantly present at sites of plaque rupture in human atherosclerosis, suggesting an important role for CCs in the clinical manifestations of CVD[73]. In a series of studies, Abela and colleagues elucidated the contribution of CCs in advanced atherosclerotic plaques to plaque rupture and the clinical outcomes of atherosclerosis. First they observed *in vitro* that cholesterol phase transition to crystalline cholesterol results in the formation of large sharp-edged CCs, which can penetrate and thereby damage biological membranes[74]. Therefore, they suggested the contribution of CCs to plaque vulnerability and rupture. Evidence for this was provided by scanning electron microscopical analysis of human coronary arteries of patients with severe atherosclerosis, who had either died from myocardial infarction or other causes. They found that CCs perforated the arterial intima and the fibrous cap of atherosclerotic plaques exclusively in patients who died from acute coronary syndrome, indicating a correlation between mechanical plaque disruption and disease outcome[73]. Furthermore, this vascular injury triggered by CC penetration of the endothelial cell layer might also cause a systemic inflammatory response by local production of IL-6 and subsequent hepatic production of the acute phase protein hsCRP, which is the primary

inflammatory biomarker for the prediction of future acute cardiovascular events[75]. Finally, statin treatment, which inhibits cholesterol biosynthesis, beneficially reduced cholesterol crystallization and promoted CC dissolution in human carotid plaque tissue, thereby promoting plaque stabilization, which might be another of the beneficial pleiotropic effects of statins in atherosclerosis[76]. Together these findings demonstrate that CCs present in advanced atherosclerotic plaques contribute to the clinical outcome of atherosclerosis by promoting plaque rupture and subsequent thrombus formation.

2.2.6.2 CCs as contributors to atherosclerosis progression

Although a pathogenic role for crystalline cholesterol was already suggested in the 1980s[77], the potential contribution of CCs to atherosclerosis progression was largely ignored, most likely because CCs were only observed in late stages of atherosclerosis. However, the application of a novel imaging technique based on the reflective nature of crystalline cholesterol combined with solvent-free sample preparation finally allowed the direct visualization of CCs in atherosclerotic plaques. Indeed crystalline cholesterol was shown to be present in all stages of murine atherosclerosis, even in very early diet-induced atherosclerotic plaques. Moreover, the appearance of CCs in early atherosclerotic plaques coincided with the first appearance of innate immune cells in these plaques[24], indicating that CCs might be inflammatory and directly contributing to atherosclerosis progression.

As an essential molecule, cholesterol was long regarded as a non-immunogenic substance. However, evidence that crystalline cholesterol might have immunostimulatory potential has accumulated over the years. Firstly, CCs were found to activate both the alternative and classical pathways of the complement system, which itself was already suggested to play a role in the pathogenesis of atherosclerosis[78,79]. Furthermore, CCs were shown to induce the production of specific IgG antibodies[80]. In a model of chronic apical periodontitis, another disease characterized by CC accumulation, the recruitment of immune cells to CC implants was observed. While the recruited immune cells were not able to clear the CC implants, the induction of a robust, non-resolving inflammation was observed[81]. Beyond this, deposition of extracellular CCs in the ACAT deficient atherosclerosis mice was also accompanied by a substantial inflammatory response indicating a link between extracellular crystalline cholesterol deposition and cardiovascular inflammation[72]. Ten years later, two independent studies reported that extracellular CCs are abundantly phagocytozed by murine and human macrophages, which causes the damage of lysosomal compartments. In turn the NLRP3 inflammasome becomes activated, which results in caspase-1 mediated processing and secretion of pro-inflammatory and pro-atherogenic cytokines of the IL-1β family: IL-1β and IL-18[24,25].

The finding that crystalline cholesterol, which is present in the vessel wall at all stages of atherosclerosis, activates the NLRP3 inflammasome in macrophages provided a possible

molecular mechanism for IL-1β production in atherosclerotic plaques. Moreover, atherosclerosis development was impaired in LDLR$^{-/-}$ mice transplanted with bone marrow from mice deficient in either NLRP3 or the central inflammasome adaptor molecule ASC, indicating that CC-induced myeloid NLRP3 inflammasome activation mediates the IL-1β-dependent inflammatory response that promotes atherosclerosis progression[24]. While one conflicting study reported that a deficiency in NLRP3 inflammasome components had no influence on atherosclerosis progression in ApoE$^{-/-}$ mice[82], which was most likely due to differences in experimental conditions (e.g. use of mouse model and much stronger atherogenic diet), several other studies supported the importance of NLRP3 inflammasome activation for atherosclerosis development and progression. For example, macrophage-specific ATG5-null mice, a common mouse model for autophagy deficiency, when crossed to ApoE$^{-/-}$ mice developed enlarged atherosclerotic plaques upon high-fat diet feeding, which was attributed to increased CC-mediated inflammasome activation and subsequent IL-1β secretion in autophagy-deficient macrophages[83]. NLRP3 is also highly expressed in the aortas of patients with coronary atherosclerosis and NLRP3 expression levels correlate with disease severity as well as clinical risk factors for CVD, which is further indirect evidence for a role of NLRP3 inflammasome activation in atherosclerosis[84]. Furthermore, lentiviral gene silencing of NLRP3 in ApoE$^{-/-}$ mice reduced atherosclerotic plaque growth, macrophage and lipid plaque content and pro-inflammatory cytokine production, demonstrating impaired atherosclerosis progression in the absence of NLRP3[85].

In vitro, activation of the NLRP3 inflammasome requires an initial priming signal, which induces NRLP3 and pro-IL-1β expression before stimulation with the activating ligands, such as CCs (see section 2.1.3.2). While it was shown that oxLDL particles, which are present in large quantities in early atherosclerotic plaques, can provide this obligatory priming signal for NLRP3 activation in macrophages *in vitro*[24], other factors might mediate macrophage priming in the atherosclerotic plaque *in vivo*. For example, CC-mediated complement activation was shown to prime monocytes in human whole blood while simultaneously promoting CC phagocytosis therefore providing both signal 1 and 2 for NLRP3 activation in this system[86]. Moreover, a recent study demonstrated that CCs trigger the release of neutrophil extracellular traps (NETs), which can in turn prime human monocytes for CC-mediated inflammasome activation and subsequent pro-inflammatory cytokine release. Since NET-deficient mice show impaired atherosclerosis development accompanied with decreased plasma levels of pro-inflammatory cytokines, NET formation might be an essential requirement for inflammasome priming *in vivo*[87].

In summary, these studies showed that cholesterol in its crystalline state is a potent immunogenic DAMP, which stimulates innate immune cells, such as macrophages, by activating the NLRP3 inflammasome. The NLRP3 inflammasome, in turn, was associated

with atherosclerosis progression. Since CCs are already present in early atherosclerotic plaques, they qualify as inducers of this NLRP3-dependent atherogenesis. Therefore, these findings collectively demonstrate that CCs contribute to the non-resolving cardiovascular inflammation that drives disease progression by activating the NLRP3 inflammasome to release pro-atherogenic IL-1β.

2.3 Cyclodextrins

Cyclodextrins are cyclic oligosaccharides of natural origin. They are generated from the enzymatic degradation of starch by cyclodextrin glycosyltransferases. These bacterial enzymes are closely related to α-amylases, but have the unique ability to catalyze the cyclization of six to eight α-(1,4)-linked D-glucopyranose units. This enzymatic reaction produces the three main cyclodextrins: α-, β- and γ-cyclodextrin, which contain six, seven or eight glucose units, respectively (Fig. 2-5A). The circular sugar molecules form cone-shaped 3D-structures, with a central hydrophobic cavity, while the outer part is hydrophilic because of the large number of hydroxyl groups (Fig. 2-5B). Therefore, cyclodextrins are both water-soluble and able to incorporate hydrophobic molecules or hydrophobic moieties of molecules into their central hydrophobic cavity. This reversible, non-covalent incorporation of "guest"

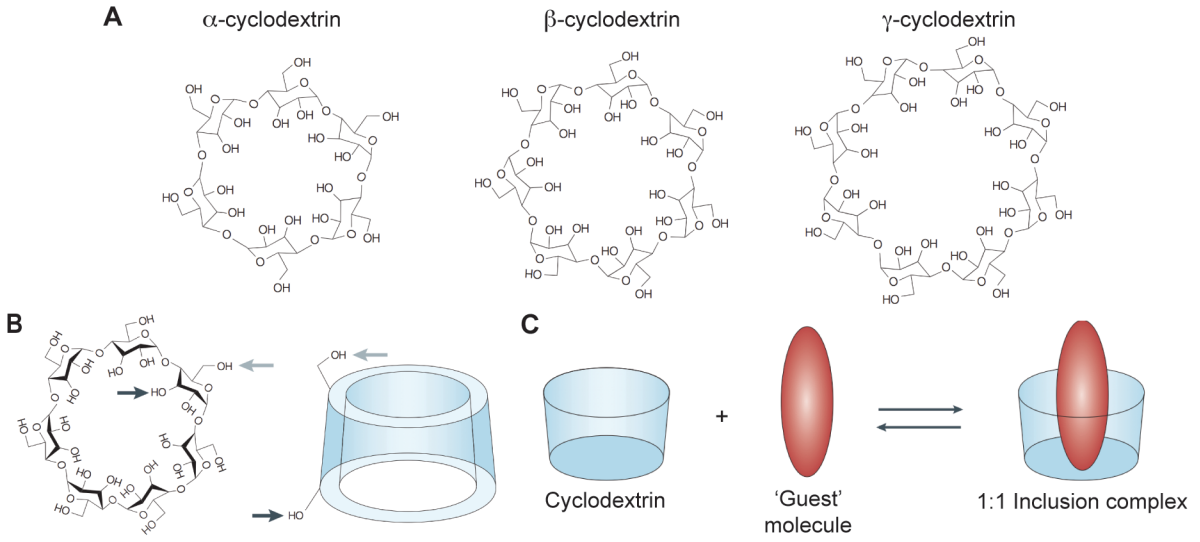

Figure 2-5: Cyclodextrins and formation of cyclodextrin inclusion complexes.

(A) Chemical structures of α-, β- and γ-cyclodextrin with six, seven and eight glucopyranoside units, respectively. (B) Chemical structure and schematic representation of the conical 3D structure of β-cyclodextrin (representative for all cyclodextrins). The cone-like structure is composed of the glucose residues, forming a hydrophobic central cavity, whereas the exterior is hydrophilic due to the presence of the hydroxyl groups. The primary hydroxyl groups (light grey arrow) of the cyclic oligosaccharides reside on the narrow side, while the secondary hydroxyl groups (dark grey arrow) reside on the wider side of the cone. The size of the central cavity varies between α-, β- and γ-cyclodextrins as it is determined by the number of glucopyranoside units. (C) Schematic illustration of the dynamic equilibrium between free cyclodextrins, free "guest" molecules and their formed 1:1 inclusion complex. Figure adapted from Davis and Brewster[88] with reprint permission (see appendix).

molecules into cyclodextrin inclusion complexes is the most important feature of cyclodextrins, because it changes the physicochemical properties (such as solubility, stability and bioavailability) of the incorporated molecule. Cyclodextrins are therefore extensively utilized for various applications including agrochemicals, fragrances, cosmetics, foods and pharmaceuticals[88,89].

The formation of inclusion complexes between cyclodextrins and suitably sized hydrophobic "guest" molecules is a reversible process characterized by a dynamic equilibrium (Fig. 2-5C). The formation and dissociation of these inclusion complexes is determined by the affinity of the "guest" molecule for the cyclodextrin cavity. Although 1:1 inclusion complexes are most common, interactions with more than one cyclodextrin molecule are possible, depending on conformation and size of the "guest" molecule[88,90]. Since cyclodextrin inclusion complexes are in a dynamic equilibrium with the free cyclodextrin and "guest" molecules and no covalent bonds are formed between cyclodextrins and the incorporated molecules, the release from cyclodextrin is mediated by simple dilution and does not affect the nature of the released "guest" molecules. However, the equilibrium can be shifted in the presence of high-affinity acceptors of the incorporated molecules[89]. Furthermore, the release of the "guest" molecule from cyclodextrin might also be triggered by competitive displacement by other molecules with a higher binding affinity[91].

The parent cyclodextrins are water-soluble, but their solubility in aqueous solutions is limited, ranging from only 2% (w/w) in the case of β-cyclodextrin to 26% (w/w) for γ-cyclodextrin[88]. Therefore, several chemically modified cyclodextrin derivatives have been synthesized, where the hydroxyl groups are randomly substituted by other chemical moieties resulting in a drastic increase in water solubility. The most commonly used chemical modifications for increasing the water solubility of cyclodextrins are methylation, hydroxypropylation and sulfobutylation. Hydroxypropylated β-cyclodextrin, for instance, has a water solubility of 60% (w/w). While these cyclodextrin derivatives can still incorporate molecules in their central cavity, the binding affinity will be different compared to the parent cyclodextrins[89,90].

2.3.1 Pharmaceutical use of cyclodextrins

Cyclodextrins have emerged as useful tools for the formulation of (for example) poorly water-soluble drugs. By forming reversible, non-covalent inclusion complexes, they increase both the drug's solubility and its physical or chemical stability without affecting the drug molecule itself. Cyclodextrins can therefore potently improve the bioavailability of these drugs. While this is probably the most important pharmaceutical application of cyclodextrins, they can also have further beneficial effects, such as masking the bitter taste or the bad odor of some drugs.

2.3.1.1 Pharmacokinetics of cyclodextrins

Cyclodextrins are mainly resistant to stomach acid, but can be degraded by α-amylases, which, in humans, are mainly present in pancreatic juice and saliva. However, their susceptibility to enzymatic degradation is reduced when cyclodextrins are complexed with other molecules, and the rate of their hydrolysis also depends on their ring size. While α- and β-cyclodextrins are mainly resistant to α-amylases in the gastrointestinal tract, γ-cyclodextrin is rapidly degraded in pancreatic juice and saliva. Therefore, orally administered γ-cyclodextrin is almost completely degraded in the gastrointestinal tract, while α- and β-cyclodextrin proceed to the colon. Here, they can be digested and metabolized by bacterial and fungal amylases, in which α-cyclodextrin is again less susceptible to enzymatic degradation than β-cyclodextrin[89,91].

The oral bioavailability of pharmaceutically interesting cyclodextrins is generally below 4%, which is mainly due to their high molecular weight and their hydrophilic character, which impedes their ability to cross biological membranes and accordingly their absorption from the gastrointestinal tract. However, once absorbed, any intact cyclodextrin subsequently distributes to various tissues including the kidney, adrenal gland, urinary bladder, liver, but most of it accumulates in the kidney. Cyclodextrins disappear from the tissues quite quickly after administration (within the first few hours) and the intact cyclodextrins are excreted via the urine. Similarly, intravenous administration of cyclodextrins results in rapid renal excretion of the unmetabolized cyclodextrin molecules with nearly 100% recovery in the urine. As such, cyclodextrin clearance from the circulation is dependent on the glomerular filtration rate and renal function[89,91].

2.3.1.2 Toxicity of cyclodextrins

An important determinant for the pharmaceutical application of cyclodextrins is their biocompatibility. Cyclodextrins do not induce immune responses in mammals and show quite low toxicity in animals and humans, although the toxicity of cyclodextrins is highly dependent on the type of cyclodextrin and the route of administration[88].

In vitro studies revealed that cyclodextrins have a hemolytic activity on human erythrocytes, which correlates to their ability to solubilize cholesterol and to extract cholesterol from membranes[89]. Moreover, β-cyclodextrin and its methylated derivative, which have the highest affinity for cholesterol, were shown to induce caspase-dependent apoptotic cell death in human keratinocytes in response to membrane cholesterol depletion, which was not observed with other parent cyclodextrins or hydroxypropylated β-cyclodextrin[92]. However, this hemolytic activity has not been directly shown *in vivo*.

Oral administration of cyclodextrins is mainly nontoxic, presumably because of their low absorption from the gastrointestinal tract. Only at high doses, the hypertonic nature of

cyclodextrins causes side effects like flatulency, soft stool and diarrhea, which are similar to side effects caused by other poorly digestible carbohydrates (e.g. lactose) and osmotically active nutrients or excipients. Therefore, most cyclodextrins are included in the U.S. food and drug administration's (FDA) "generally recognized as safe" (GRAS) list of compounds and are generally accepted as food additives[91].

Parenteral administration of cyclodextrins generally shows more toxic effects. Intravenous, subcutaneous or intramuscular injections of cyclodextrins at high doses or over a long period of time resulted in histopathological changes in laboratory animals. These included vacuolation of the kidney and urinary bladder, as well as the appearance of foamy macrophages in liver, lung and lymph nodes[91]. However, due to the renal excretion of systemically absorbed cyclodextrins, the kidney is typically the most affected organ. While irreversible kidney damage and dysfunction has been reported upon administration of parent α- and β-cyclodextrins, parent γ-cyclodextrin as well as many cyclodextrin derivatives including hydroxypropylated β-cyclodextrin, only induced a reversible vacuolation of the proximal tubular epithelium of the kidney without any manifestation of cell injury, degeneration, or disruption of renal function[89,91]. Similarly, renal toxicity upon parenteral administration of β-cyclodextrin to rats was associated with the accumulation of intracellular needle-like CCs, which was not observed with hydroxypropylated β-cyclodextrin. While both β-cyclodextrin and hydroxypropylated β-cyclodextrin form inclusion complexes with endogenous cholesterol in blood, the water solubility of the two inclusion complexes is very different. Therefore, glomerular filtration of the β-cyclodextrin-cholesterol inclusion complexes most likely results in the dissociation of the complexes due to their limited aqueous solubility followed by cholesterol accumulation and crystallization in the proximal tubular cells of the kidney. In contrast, the considerably more hydrophilic inclusion complexes of hydroxypropylated β-cyclodextrin and cholesterol are less likely to dissociate, and therefore are able to be excreted without cholesterol accumulating and crystallizing in the kidneys, which might explain the lower nephrotoxicity of intravenously administered hydroxypropylated β-cyclodextrin[93].

In summary, while oral administration of most cyclodextrins is well tolerated, the parenteral administration of some cyclodextrins, in particular parent α- and β-cyclodextrins can cause problems like renal toxicity. However, some cyclodextrin derivatives, especially hydroxypropylated β-cyclodextrin, have less toxic side effects and are therefore safer for biomedical use than their parent cyclodextrins[91].

2.3.1.3 Pharmacokinetics and toxicology of 2-hydroxypropyl-β-cyclodextrin

2-Hydroxypropyl-β-cyclodextrin (CD), a hydroxypropylated β-cyclodextrin with improved water solubility and good inclusion complexation, is one of the well-tolerated, non-nephrotoxic cyclodextrin derivatives. Drug-CD complexes rapidly dissociate upon parenteral

administration and can drastically improve the oral bioavailability of poorly water-soluble drugs, while CD's own bioavailability is limited. Together, these properties make CD a perfect oral drug carrier[89,91,94].

In humans, the oral bioavailability of CD ranges from only 0.5 to 3.3%. Approximately half of the orally administered dose is excreted as intact CD via the feces, while the remaining CD is metabolized in the colon by bacterial enzymes. When CD is intravenously administered to humans, it is rapidly excreted from the body as intact, non-metabolized CD molecules into the urine. CD has a small volume of distribution (i.e. the ratio of administered amount to plasma concentration), indicating that CD is not considerably distributed into the tissues. The biological half-life of CD is less than 2 hours and mainly depends on the glomerular filtration rate. Therefore, in individuals with normal kidney function, about 90% of the intravenously administered dose is excreted via the urine within 6 hours, and about 99% within 12 hours post administration (Fig. 2-6). Consequently, parenteral administration of CD will not result in considerable accumulation of CD in individuals with normal kidney function[89].

CD is listed in the FDA's list of inactive pharmaceutical ingredients and is used as an excipient in several commercially available drugs[95]. Amongst these, the most prominent drug is the antifungal agent itraconazole, which is formulated with 40% (w/v) CD solutions for oral and intravenous administration. At this concentration CD increases the solubility of itraconazole by up to six orders of magnitude. During itraconazole treatment, patients receive an oral dose of 8 g CD per day or an intravenous dose of up to 16 g CD per day respectively (8 g twice a day, see Fig. 2-6 for resultant CD plasma concentrations)[88,91]. Therefore, the oral and intravenous administration of CD at these concentrations over approximately 2 weeks are known to be well tolerated with diarrhea being the main side effect of oral administration. Furthermore, even after parenteral administration of up to 24 g CD per day (12 g twice a day) over a period of 15 days no adverse effects were observed[89].

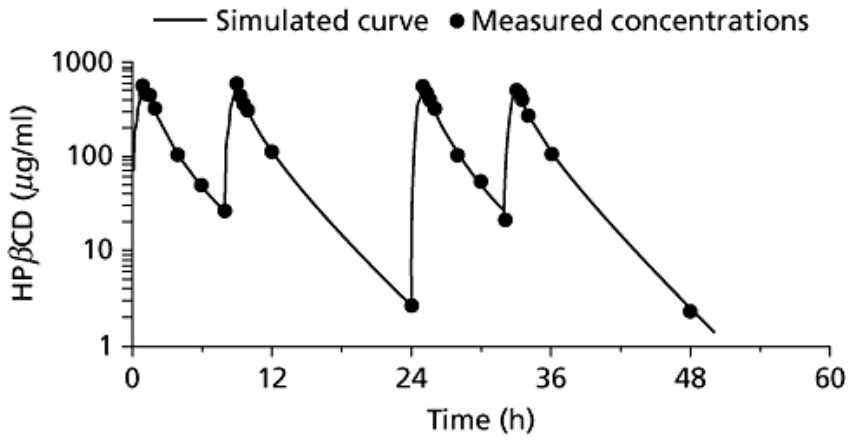

Figure 2-6: Plasma clearance of 2-Hydroxypropyl-β-cyclodextrin.

Plasma concentrations of CD over time in humans, following repeated intravenous administration of 8 g CD twice a day. Figure from Lofftson and Brewster[89] with reprint permission (see appendix).

2.3.2 Cyclodextrins and cellular cholesterol

Cyclodextrins also interact with hydrophilic membrane components, such as phospholipids and cholesterol. While α-cyclodextrin predominantly forms inclusion complexes with phospholipids, β-cyclodextrin has the highest affinity for cholesterol. This feature of β-cyclodextrins prompted the development of several functionalized or conjugated β-cyclodextrins for selective cholesterol binding and detection[96-98]. More importantly, *in vitro* studies revealed that cyclodextrins extract lipid molecules from the cell membranes when forming inclusion complexes with these molecules, which was associated with their hemolytic activity in human erythrocytes[89]. This observation prompted the introduction of cyclodextrins as research tools to manipulate and study cellular membranes. In this regard β-cyclodextrins turned out to be powerful modulators of cellular cholesterol levels in living cells. While cyclodextrins can serve as cholesterol acceptors that remove cholesterol from cells, pre-formed β-cyclodextrin-cholesterol inclusion complexes can also function as cholesterol donors that replenish or even enrich cellular cholesterol[99].

Furthermore, studies on the safety of the parenteral use of β-cyclodextrins and its derivatives in rats and rabbits showed a transient decrease in plasma cholesterol levels accompanied by redistribution of plasma cholesterol to the kidneys, resulting in the urinary excretion of

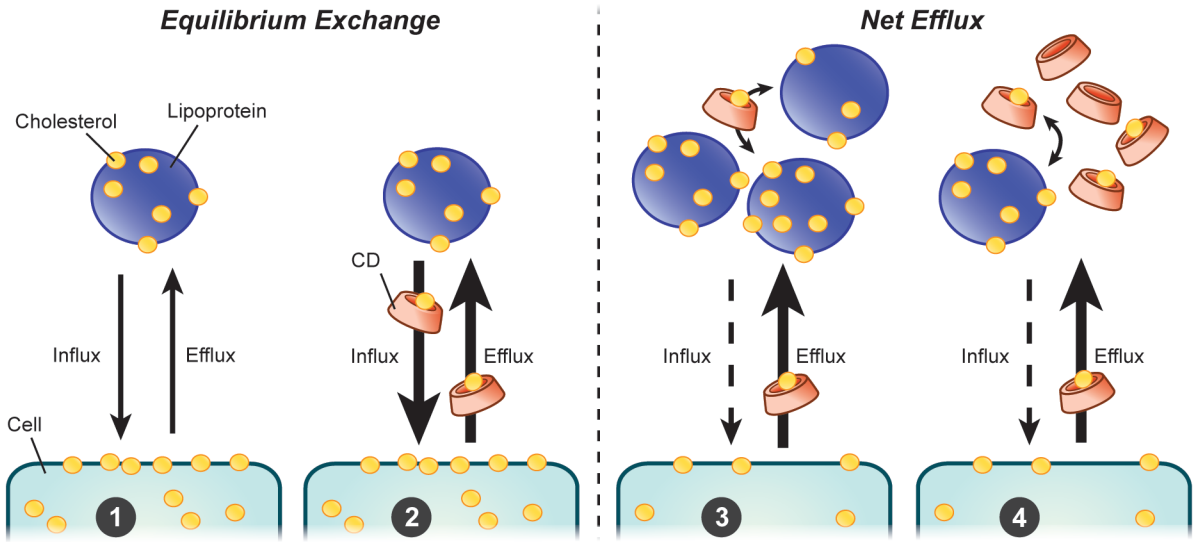

Figure 2-7: 2-Hydroxypropyl-β-cyclodextrin in the shuttle/sink model for cellular cholesterol efflux.

Cholesterol movement between cells and serum lipoproteins is a bidirectional process. Under normal conditions (1), cellular and lipoprotein cholesterol are at equilibrium with a constant exchange between the two cholesterol pools. When low concentrations of CD are present (2), CD functions as cholesterol shuttle which increases cholesterol turnover without affecting the equilibrium condition. When more cholesterol acceptors, such as serum lipoproteins, are present in addition to low concentrations of CD (3), the serum lipoproteins function as extracellular cholesterol sinks, which increases the cholesterol efflux rate and therefore shifts the equilibrium towards net efflux. At high concentrations of CD (4), CD molecules themselves function as extracellular cholesterol sinks mediating the net efflux of cellular cholesterol. Model adapted from Atger *et al.*[100].

cholesterol in inclusion complexes with CD (2-Hydroxypropyl-β-cyclodextrin)[93,101]. These findings indicated that β-cyclodextrin derivatives, such as CD, catalyze the transport of lipids within the organism, and suggested a potential use for manipulating lipid transport and distribution *in vivo*. This idea was further supported by *in vitro* studies, which investigated the ability of CD to move cholesterol from cells to serum cholesterol acceptors, such as lipoproteins, thereby mimicking the first step of RCT *in vivo*. While CD itself depleted cellular cholesterol at high concentrations, low concentrations of CD only induced net cholesterol efflux from cells in the presence of cholesterol acceptors presumably by catalyzing the bidirectional exchange of cholesterol between cells and serum lipoproteins[100]. Based on these findings, a shuttle/sink model for the first step in RCT, which involves the net movement of cellular cholesterol to lipoproteins, was proposed[100]. Importantly, CD can function as both shuttles and sinks for causing net efflux of cellular cholesterol, depending on its concentration (Fig. 2-7). Moreover, CD was also effective in depleting free and esterified cholesterol from mouse and human foam cell macrophages, therefore presenting a potential pharmacological use of CD or CD-like cholesterol shuttles in the treatment of atherosclerosis[100,102].

2.3.3 Use of 2-hydroxypropyl-β-cyclodextrin in NPC disease

While CD is currently extensively used as excipient for poorly water-soluble drugs, the potential of CD itself as an active drug molecule was disregarded for a long time. However, it is currently being tested in clinical trials as a pharmaceutical drug for the treatment of Niemann-Pick type C (NPC) disease.

NPC disease is a rare inherited neurodegenerative disorder. Genetically, it is caused by a mutation in either the NPC1 gene or, in rare cases, the NPC2 gene. The mutations compromise the function of the proteins NPC1 and NPC2 respectively, which regulate intracellular trafficking of cholesterol and other lipids (see section 2.2.5.2). Without functional NPC1/2-mediated trafficking, free cholesterol and sphingolipids accumulate inside the cells of various organs, including the brain. The clinical manifestations of NPC disease are mainly neurological, such as swallowing problems, ataxia, seizures, and progressive impairment of motor and cognitive function. The first signs of disease can appear at different ages, ranging from infancy to adulthood, but they mainly occur in early childhood and patients mostly die in adolescence. So far, there is no adequate therapy available for NPC disease[95].

Cells from NPC patients are unable to release cholesterol from endolysosomal compartments resulting in the detrimental intracellular accumulation of free cholesterol. Since CD is known to mediate cellular cholesterol removal, whether CD treatment could improve cholesterol metabolism and efflux in $NPC^{-/-}$ cells and animal models was tested. Indeed, in $NPC^{-/-}$ cells *in vitro*, CD mobilized cholesterol transport from lysosomal compartments to the

ER and thereby enhanced cellular cholesterol metabolism, esterification and efflux[103,104]**.** Moreover, a plethora of $NPC^{-/-}$ animal studies have revealed that CD administration *in vivo* reverses defective lysosomal transport stimulating cholesterol metabolism, suppressing *de novo* cholesterol synthesis, improving liver dysfunction and neurodegeneration, and markedly prolonging the animal's lifespan[95]. Interestingly, a single subcutaneous CD injection into $NPC^{-/-}$ mice was enough to mediate these effects[105,106]. Several routes of CD administration have been investigated in animals, including parenteral administration and direct injections into the brain (intracerebroventricularly or intrathecally). Injections of CD into the central nervous system (CNS) have proven particularly successful in the prevention of neurodegeneration[95], most likely because of the low blood brain barrier permeability of CD[107]. Based on the evidence from the *in vitro* and *in vivo* studies, CD was considered a promising drug candidate for NPC patients. In 2009, the first Investigational New Drug (IND) application for intravenous CD administration was approved by the FDA, which was extended in 2010 to include intrathecal administration. IND approvals allow the application of a new drug to individual patients with serious life-threatening diseases if there is no alternative therapy and if the possible benefit justifies possible risks. Therefore, the use of CD on an individual basis already indicated the effectiveness and safety of CD administration in NPC patients[95]. However, well-controlled clinical trials with a larger number of NPC patients are needed to properly determine safety and efficacy of CD treatment in NPC disease. The first completed phase 1 clinical trial suggested that intrathecal CD administration in NPC patients is well-tolerated and slows the progression of their neurologic disease, and a phase 2/ phase 3 clinical trial for assessing ideal dosage and efficacy of intrathecal CD treatment in NPC patients is currently recruiting subjects (ClinicalTrials.gov Identifier: NCT02534844).

2.4 Objectives of this study

Atherosclerosis is a progressive inflammatory disease that is linked to increased levels of cholesterol in the blood. Despite ongoing advances in surgical and pharmacological treatment of atherosclerosis, it still accounts for the majority of deaths worldwide. Identifying novel therapeutic targets will improve pharmacological treatment strategies and aid the development of new drugs for treating atherosclerosis.

Several studies have highlighted the contribution of crystalline cholesterol to the development, progression and clinical outcomes of atherosclerosis. CCs play a role in late stages of the disease where they physically disrupt the fibrous cap promoting plaque rupture and thrombus formation, thereby initiating the acute clinical events. Moreover, CCs induce inflammatory responses by activating the NLRP3 inflammasome. This already happens in early atherosclerotic plaques and is likely to contribute to disease progression[108]. However, so far it has not been investigated whether decreasing the amount of CCs in the plaque represents a valuable strategy for pharmaceutical intervention in atherosclerosis. One possible agent for targeting CCs in atherosclerotic plaques is 2-hydroxypropyl-β-cyclodextrin (CD). CD is known to mediate the removal of cholesterol from cells and its potential pharmacological use in atherosclerosis as a shuttle for cholesterol mobilization from atherosclerotic plaque tissue to serum lipoproteins such as HDL for increased RCT was already proposed nearly 20 years ago[100]. However, the ability of CD to clear cholesterol from atherosclerotic plaque tissue in the walls of blood vessels has not yet been investigated.

Therefore, the objective of this study was to investigate whether the cholesterol solubilizing substance CD has the potential to reduce the amount of CCs in atherosclerotic plaques and whether this reduction of crystalline cholesterol in turn impairs atherosclerosis development and progression. In detail, the specific aims of this study were:

1. To evaluate whether CCs present a viable treatment target in atherosclerosis.
2. To investigate whether CD has the potential to decrease CC plaque load in atherosclerosis mouse models.
3. To determine if a reduction of crystalline cholesterol by CD in turn impairs murine atherosclerosis development and progression.
4. To characterize the molecular mechanisms of CD's potentially atheroprotective effects *in vitro* by assessing macrophage cholesterol efflux and metabolism.
5. To determine the effect of CD on CC-induced macrophage inflammatory responses.
6. To evaluate the relevance of the molecular mechanisms identified *in vitro* in atherosclerosis models using gene-specific knockout mice or bone marrow chimeras *in vivo*.

3 Materials and Methods

3.1 Materials

3.1.1 Consumables

4-well microscopy dish (CELLview™ Cell Culture Dish, Glass bottom)	Greiner Bio-One (Frickenhausen)
8-well microscopy dish (Nunc™ Lab-Tek™ Chambered Coverglass)	Thermo Fisher Scientific (Waltham, MA, USA)
96-well microscopy plate (µclear-plate, black)	Greiner Bio-One (Frickenhausen)
96-well V-bottom microplate, clear	Greiner Bio-One (Frickenhausen)
Cell scrapers	Sarstedt (Nümbrecht)
Cell Strainers, 70 µm (Falcon®)	VWR International (Radnor, PA, USA)
Centrifuge Tubes (15 ml/ 50 ml), (CELLSTAR® polypropylene, conical)	Greiner Bio One (Kremsmünster, Austria)
Cover glasses (22x50 cm), thickness no. 1.5	Marienfeld (Lauda Königshofen)
Dako pen (Delimiting pen)	Dako Deutschland (Hamburg)
ELISA plates (Nunc-Immuno™ MaxiSorp™ 96-Well plate)	Nunc (Roskilde, Denmark)
Eppendorf safe-lock tubes (1.5 ml/ 2 ml)	Eppendorf (Hamburg)
FACS tubes	Sarstedt (Nümbrecht)
Glass vials (4 ml) with screw cap	CS - Chromatographie Service (Langerwehe)
MultiScreen-GV Filter Plate, 0.22 µm	Merck (Darmstadt)
Needles	B. Braun (Melsungen)
NuPAGE® Novex 4-12% Bis-Tris Gel 1.5 mm, 10 Well	Novex Life Technologies (Carlsbad, CA, USA)
NuPAGE® Novex 4-12% Bis-Tris Gel 1.5 mm, 15 Well	Novex Life Technologies (Carlsbad, CA, USA)
Opti-Seal	Bioplastics (Landgraaf, Netherlands)
PVDF membrane (Immobilon-FL, 0.45 µm)	Merck (Darmstadt)
qPCR plate (MicroAmp® Optical 384-Well Reaction Plate)	Applied Biosystems Life Technologies (Carlsbad, CA, USA)
Sterile filter tips	Mettler Toledo (Greifensee, Switzerland)
Superfrost™ Plus Microscope Slides	Thermo Fisher Scientific (Waltham, MA, USA)

Syringe filters, 0.2 µm (Whatman® Puradisc 30)	Sigma-Aldrich (Taufkirchen)
Syringes	BD Biosciences (Heidelberg)
Tali Cellular Analysis Slides	Invitrogen Life Technologies (Carlsbad, CA, USA)
Tissue culture flasks (25/ 75/ 175 cm^2)	Labomedic (Bonn)
Tissue culture plates (6-well/ 12-well/ 24-well/ 96-well)	Labomedic (Bonn)
UHU plus schnellfest 2-K-Epoxidharzkleber (5 min)	UHU (Bühl)
Ultrafree-MC Centrifugal Filter, 0.22 µm	Merck (Darmstadt)
Whatman® cellulose chromatography paper	Sigma-Aldrich (Taufkirchen)

3.1.2 Chemicals and reagents

[1,2-^{3}H]-cholesterol	Perkin Elmer (Waltham, MA, USA)
1-Propanol p.a.	AppliChem (Darmstadt)
2 N H_2SO_4	Carl Roth (Karlsruhe)
2-Mercaptoethanol	Sigma-Aldrich (Taufkirchen)
Acridine orange	Thermo Fisher Scientific (Waltham, MA, USA)
Adenosine 5′-triphosphate disodium salt hydrate	Sigma-Aldrich (Taufkirchen) .
Benzonase® Nuclease	Sigma-Aldrich (Taufkirchen)
Bovine Serum Albumin (BSA)	Sigma-Aldrich (Taufkirchen)
Cholera Toxin Subunit B, Alexa Fluor® 488 Conjugate	Molecular Probes Life Technologies (Carlsbad, CA, USA)
Cholera Toxin Subunit B, Alexa Fluor® 647 Conjugate	Molecular Probes Life Technologies (Carlsbad, CA, USA)
Cholesterol, suitable for cell culture	Sigma-Aldrich (Taufkirchen)
complete EDTA-free Protease Inhibitor Cocktail Tablets	Roche (Mannheim) .
CSL111 (reconstituted HDL)	CSL Behring (King of Prussia, PA, USA)
D_6-cholesterol ([26,26,26,27,27,27-$^2H_6$]-cholesterol)	CDN Isotopes (Pointe-Claire, Quebec, Canada) .
Dimethyl sulfoxide (DMSO), cell culture grade	AppliChem (Darmstadt) .
dNTP Mix (10 mM each)	Thermo Fisher Scientific (Waltham, MA, USA)
Ethanol (EtOH) 99% absolute	AppliChem (Darmstadt)

EtOH 99% denatured with 1% MEK	AppliChem (Darmstadt) .
Glycerol, anhydrous	Merck (Darmstadt)
H-Leu-Leu-Ome (LeuLeu)	Chem-Impex International (Wood Dale, IL, USA)
Hoechst 34580 .	Molecular Probes Life Technologies (Carlsbad, CA, USA)
LD540 .	produced and provided by Prof. Dr. Christoph Thiele (LIMES Institute, University of Bonn, Bonn)
Methanol p.a.	AppliChem (Darmstadt)
MIN-U-SIL® 15	US Silica (Frederick, MD, USA)
Monodosium urate (MSU) crystals .	produced and provided by Anne Alfter (Institute of Innate Immunity, University Hospital Bonn, Bonn)
Nigericin, free acid	Invitrogen Life Technologies (Carlsbad, CA, USA)
Oligo(dT)18 Primer	Thermo Fisher Scientific (Waltham, MA, USA)
PageRuler™ Plus Prestained Protein Ladder, 10 to 250 kDa	Thermo Fisher Scientific (Waltham, MA, USA) .
PMSF	AppliChem (Darmstadt)
RBITC-NH2-HPβCD	Cyclolab (Budapest, Hungary)
Saponin from quillaja bark	Sigma-Aldrich (Taufkirchen)
Sodium chloride	Merck (Darmstadt)
Sodium deoxycholate	Sigma-Aldrich (Taufkirchen)
Sodium dodecyl sulfate (SDS)	Sigma-Aldrich (Taufkirchen)
SuperScript® III Reverse Transcriptase	Invitrogen Life Technologies (Carlsbad, CA, USA)
T0901317 (T09)	Tocris R&D Systems (Minneapolis, MN, USA)
Trappsol® Hydroxypropyl Beta Cyclodextrin, pharmaceutical grade	CTD Holdings (Alachua, FL, USA) .
Triton X-100	Carl Roth (Karlsruhe)
TRIzol® Reagent	Ambion Life Technologies (Carlsbad, CA, USA)
Tween-20	Sigma-Aldrich (Taufkirchen)
Ultrapure LPS, E. coli 0111:B4	Invivogen (Toulouse, France)

3.1.3 Buffers and solutions

3.1.3.1 ELISA

ELISA blocking buffer	1x PBS; 1% (w/v) BSA, 0.2 µm filtered
ELISA reagent diluent (mIL-1β)	20 mM Tris-HCl pH7.4, 150 mM NaCl, 0.1% (w/v) BSA, 0.05% (v/v) Tween-20, 0.2 µm filtered
ELISA reagent diluent (mTNF-α)	1x PBS; 1% (w/v) BSA, 0.2 µm filtered
ELISA substrate (BD OptEIA™ TMB Substrate Reagent Set)	BD Biosciences (Heidelberg)

3.1.3.2 Immunohistochemistry

IHC blocking buffer	1x PBS, 5% (v/v) FCS, 5% (w/v) BSA, 10% (v/v) goat serum, 0.1% (w/v) saponin
IHC mounting medium	dd H_2O, 80% (v/v) glycerol
IHC staining buffer	1x PBS, 10% (v/v) goat serum

3.1.3.3 Western blot

NuPAGE® LDS Sample Buffer, 4x	Novex Life Technologies (Carlsbad, CA, USA)
NuPAGE® MES SDS Running Buffer, 20x	Novex Life Technologies (Carlsbad, CA, USA)
NuPAGE® MOPS SDS Running Buffer, 20x	Novex Life Technologies (Carlsbad, CA, USA)
NuPAGE® Sample Reducing Agent, 10x	Novex Life Technologies (Carlsbad, CA, USA)
Pierce™ 10X Tris-Glycine Buffer	Thermo Fisher Scientific (Waltham, MA, USA)
Pierce™ Tris-Glycine Buffer, 10x	Thermo Fisher Scientific (Waltham, MA, USA)
RIPA buffer	20 mM Tris-HCl pH 7.4, 150 mM NaCl, 1 mM EDTA, 1% (v/v) Triton X-100, 10% (v/v) glycerol, 0.1% (w/v) SDS, 0.5% (w/v) sodium deoxycholate
Transfer buffer	1x Tris-Glycine buffer, 15% (v/v) methanol
Tris Buffered Saline (TBS), 20x	Santa Cruz Biotechnology (Heidelberg)
TBS-T	1x TBS; 0.1% (v/v) Tween-20
WB blocking buffer	1x TBS; 3% (w/v) BSA; 0.1% (w/v) Tween-20, 0.2 µm filtered

3.1.3.4 Tissue culture

BMDM dissociation buffer	1x PBS, 2% (v/v) FCS, 2 mM EDTA
Trypan blue solution (0.4%)	Sigma-Aldrich (Taufkirchen)

Trypsin-EDTA (0.05%), phenol red	Gibco Life Technologies (Carlsbad, CA, USA)

3.1.3.5 Others

16% (w/v) Formaldehyde solution, methanol-free	Thermo Fisher Scientific (Waltham, MA, USA)
Ampuwa (*aqua ad iniectabilia*)	Fresenius Kabi (Bad Homburg)
Goat serum	Gibco Life Technologies (Carlsbad, CA, USA)
Nuclease-free water	Invitrogen Life Technologies (Carlsbad, CA, USA)
Phosphate buffered saline (PBS), 10x	Santa Cruz Biotechnology (Heidelberg)
Tris-HCl, pH7.4 (1M)	AppliChem (Darmstadt)
UltraPure™ 0.5M EDTA, pH 8.0	Invitrogen Life Technologies (Carlsbad, CA, USA)

3.1.4 Cell culture media and supplements

Dulbecco's Modified Eagle Medium (DMEM), high glucose	Gibco Life Technologies (Carlsbad, CA, USA)
Dulbecco's PBS	Gibco Life Technologies (Carlsbad, CA, USA)
Fetal calf serum (FCS)	Invitrogen Life Technologies (Carlsbad, CA, USA)
L929 supernatant	*Produced and provided by Gudrun Engels (Institute of innate immunity, University of Bonn)*
M-CSF	R&D Systems (Minneapolis, MN, USA)
Penicillin-Streptomycin (10,000 U/mL)	Gibco Life Technologies (Carlsbad, CA, USA)

3.1.5 Kits

BD OptEIA™ TMB Substrate Reagent Set for ELISA	BD Biosciences (Heidelberg)
CellTiter-Blue® Cell Viability Assay	Promega (Mannheim)
Maxima™ SYBR Green/ROX qPCR Master Mix	Thermo Fisher Scientific (Waltham, MA, USA)
Mouse IL-1 beta/IL-1F2 DuoSet	R&D Systems (Minneapolis, MN, USA)
Mouse TNF-alpha DuoSet	R&D Systems (Minneapolis, MN, USA)
Pierce™ BCA Protein Assay Kit	Thermo Fisher Scientific (Waltham, MA, USA)
RNase-Free DNase Set	Qiagen (Hilden)
RNeasy Mini Kit	Qiagen (Hilden)

3.1.6 Antibodies

Antibodies used in this study are listed in Table 3-1 and Table 3-2 according to the indicated applications.

Table 3-1: List of antibodies used for immunohistochemistry.

Name	Supplier	Antigen	Source	Clone	Conjugate	Dilution
Rat anti mouse CD68	AbD Serotec	mouse CD68	rat	FA-11	-	1:500
Goat anti-Rat IgG (H+L) Secondary Antibody, Alexa Fluor® 647 conjugate	Invitrogen Life Technologies	rat IgG(H+L)	goat	polyclonal	Alexa Fluor 647	1:500

Table 3-2: List of antibodies used for western blot analysis.

Name	Supplier	Antigen	Source	Clone	Conjugate	Dilution
Anti-ABCA1 (MAB10005)	Merck Millipore	mouse ABCA1	mouse	AB.H10	-	1:250
ASC Antikörper (N-15)-R	Santa Cruz Biotechnology	mouse ASC	rabbit	polyclonal	-	1:200
β-Actin Rabbit Monoclonal Antibody	LI-COR Biosciences	mouse b-actin	rabbit	monoclonal	-	1:1,000
β-Tubulin (9F3) Rabbit mAb	Cell Signaling	mouse b-tubulin	rabbit	9F3	-	1:1,000
Anti-NLRP3/NALP3	Adipogen	mouse NLRP3	mouse	Cryo-2	-	1:5,000
Mouse IL-1β Detection Antibody (from Mouse IL-1 beta/IL-1F2 DuoSet Kit)	R&D Systems	mouse pro-IL-1b	goat	polyclonal	biotin	1:1,000
IRDye® 680RD Donkey anti-Rabbit IgG (H + L)	LI-COR Biosciences	rabbit IgG(H+L)	donkey	polyclonal	IRDye 680RD	1:15,000
IRDye® 800CW Donkey anti-Goat IgG (H + L)	LI-COR Biosciences	goat IgG(H+L)	donkey	polyclonal	IRDye 800CW	1:15,000
IRDye® 800CW Donkey anti-Mouse IgG (H + L)	LI-COR Biosciences	mouse IgG(H+L)	donkey	polyclonal	IRDye 800CW	1:15,000

3.1.7 Primers and probes for quantitative PCR

Primers used for quantitative real-time PCR (qPCR) (Table 3-3) were designed for amplification of 100 to 150 base pairs of a specific target gene using Primer3 (http://bioinfo.ut.ee/primer3-0.4.0/). Primers were placed across exon boundaries to avoid amplification of genomic DNA. Oligo7 (http://www.oligo.net) was used to select primer pairs

with minimal possible secondary structures (e.g. primer dimer or hairpin formation). Desalted primers were ordered from Metabion (Martinsried) and resuspended in nuclease-free water to a concentration of 100 µM.

Table 3-3: List of qPCR primers used for amplification of mouse genes.

Gene name, NCBI Reference Sequence (RefSeq) database accession (http://www.ncbi.nlm.nih.gov/refseq/) and primer sequence annotated from 5' to 3' end of the mouse gene of interest.

Gene	RefSeq accession	Sequence 5'-3'	
Abca1	NM_013454.3	fw	GGAAGTTGGCAAGGTTGGTG
		rev	TGGCTGTGGAGAGCTTTCGT
Abcg1	NM_009593.2	fw	ATCCCCGTCCTGCTCTTCTC
		rev	GACCCCCTCAAAGCCGTATC
Cyp27a1	NM_024264.4	fw	TCATCGCACAAGGAGAGCAA
		rev	CCAGCCGGGTGATAAAGTCA
Hprt	NM_013556.2	fw	TGAAGTACTCATTATAGTCAAGGGCA
		rev	CTGGTGAAAAGGACCTCTCG
Insig1	NM_153526.5	fw	ACCACGCCAGTGCCAAATTA
		rev	GCTTCGGGAACGATCAAATG
Lss1	NM_146006.2	fw	AGGCTGGGGAGAGGACTTTG
		rev	TGAGCAGTGATGTCGGGATG
Nr1h3	NM_001177730.1	fw	AGCACGCTATGTCTGCCACA
		rev	CAGCACACACTCCTCCCTCA

Taqman® RT-qPCR assays were performed by Niklas Bode (Medical Clinic and Polyclinic II, University Hospital Bonn, Bonn) using commercially available Taqman probes (Table 3-4) purchased from Applied Biosystems (Life Technologies, Carlsbad, CA, USA).

Table 3-4: List of Taqman probes used for quantitative amplification of mouse genes.

Gene name, NCBI Reference Sequence (RefSeq) database accession (http://www.ncbi.nlm.nih.gov/refseq/) and Taqman probe ID of the mouse gene of interest.

Gene	RefSeq accession	Taqman probe ID
Abca1	NM_013454.3	Mm00442646_m1
Abcg1	NM_009593.2	Mm00437390_m1
Rn18S	NR_003278.3	Mm03928990_g1

3.1.8 Cells

3.1.8.1 Immortalized macrophage cell lines

Immortalized mouse macrophage (iMO) cell lines were previously generated from bone marrow-derived macrophages (BMDMs) of WT C57BL/6 and WT BALB/c mice by infection with a J2 recombinant retrovirus (carrying v-myc and v-raf(mil) oncogenes) as described by Hornung and colleagues[26].

3.1.8.2 Primary BMDMs

Primary BMDMs were generated using either L929 supernatants or recombinant macrophage colony-stimulating factor (M-CSF) as described in section 3.2.5. Unless otherwise indicated, BMDMs were derived from WT C57BL/6 mice using L929 supernatants. Recombinant M-CSF was exclusively used for cell differentiation for microarray analysis.

3.1.9 Mice

WT C57BL/6 mice as well as ApoE$^{-/-}$ and LDLR$^{-/-}$ on C57BL/6J background were purchased from Charles River Laboratories (Wilmington, MA USA). LXRα$^{-/-}$/LXRβ$^{-/-}$ mice on a mixed genetic background based on C57BL/6 and 129/Sv strains were obtained from Jan-Åke Gustaffson (University of Houston, Houston, TX, USA). LysmCreAbca1$^{fl/fl}$Abcg1$^{fl/fl}$ (MAC-ABC^{DKO}) mice on C57BL/6J background were kindly provided by Alan R. Tall (Columbia University, New York, NY, USA).
All animal studies described in this thesis were carried out by Dr. Sebastian Zimmer and colleagues (Medical Clinic and Polyclinic II, University Hospital Bonn, Bonn). Animal handling and all animal experiments were performed in accordance with institutional guidelines and the German animal protection law.

3.2 Methods

3.2.1 2-Hydroxypropyl-β-cyclodextrin

2-Hydroxypropyl-β-cyclodextrin (Trappsol® Hydroxypropyl Beta Cyclodextrin, referred to as CD) was reconstituted in sterile pyrogen-free water (Ampuwa) to a concentration of 100 mM and filtered through a 0.2 µm syringe filter. For long-term storage 1.5 ml aliquots were frozen at -20°C.
Rhodamine-labeled CD (RBITC-NH2-HPβCD) was reconstituted in sterile pyrogen-free water (Ampuwa) to a concentration of 25 mM under sterile conditions.

3.2.2 Cholesterol crystal preparation

Cholesterol crystals (CCs) were prepared under sterile conditions from a sterile-filtered 2 mg/ml cholesterol solution in 1-propanol. Crystallization was induced by addition of 1.5 volumes of sterile pyrogen-free water (Ampuwa) and crystals were allowed to stabilize for at least 30 min. CCs were pelleted by centrifugation (3000 x g, 30 min) before as much liquid as possible was removed without disturbing the loose CC pellet. The remaining CC solution was then transferred into autoclaved 4 ml glass vials and dried in a drying cabinet at 75°C. Dried CCs were resuspended by water bath sonication in sterile PBS containing 0.1% FCS to obtain a stock solution of 20 mg/ml.

3.2.3 Radioactive cholesterol crystal dissolution assay

Radioactive tritium-labeled CCs (^{3}H-CCs) were prepared from a 2 mg/ml cholesterol solution composed of 0.1 mCi [1,2-^{3}H]-cholesterol in a 1:50 (w/w) ratio with unlabeled cholesterol. Crystallization was induced by addition of 1.5 volumes of sterile pyrogen-free water (Ampuwa) and crystals were allowed to stabilize for at least 30 min. The crystal solution was filtered through a 0.22 µm spin filter column to remove free [1,2-^{3}H]-cholesterol. ^{3}H-CCs were recovered from the filter membrane in a total volume of 5 ml PBS containing 0.1% FCS. A defined volume of ^{3}H-CC (50 µl) was added to CD solutions (500 µl) ranging from 100 mM to 0.01 mM and the mixture was incubated overnight, shaking at 37°C in a heating block.

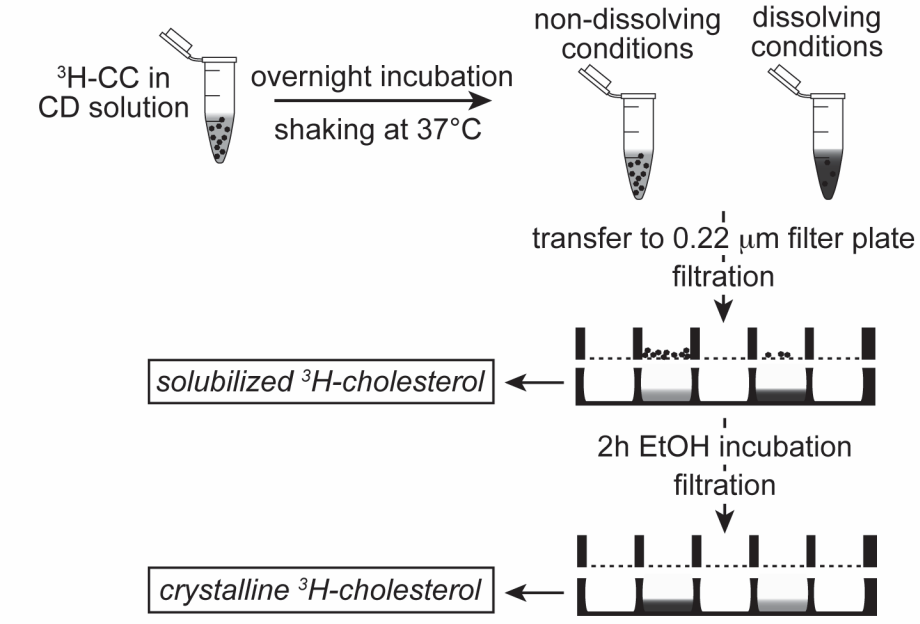

Figure 3-1: Filtration-based CC dissolution assay using radioactive ^{3}H-CCs.

Radiolabeled ^{3}H-CCs were incubated overnight in CD solutions of different concentrations prior to filtration through a 0.22 µm filter plate. The filter holds back the crystalline ^{3}H-cholesterol, whereas solubilized ^{3}H-cholesterol passes the filter and can thus be detected in the filtrate. ^{3}H-CCs on the filter membrane are dissolved by incubation in EtOH for 2 h and subsequent filtration allows the quantification of the previously crystalline ^{3}H-cholesterol in the second filtrate.

The solutions were then transferred to 0.22 µm 96-well filter plates and vacuum filtration was used in order to determine the amount of solubilized [1,2-^{3}H]-cholesterol in the first filtrate (solubilized fraction). For quantification of the amount of total crystalline [1,2-^{3}H]-cholesterol, the retentate was washed with PBS containing 0.1% FCS, dissolved in ethanol for 2 h and subsequently filtered for measurement of radioactivity in the second filtrate (crystalline fraction). A summary of this method is provided in Fig. 3-1. Following filtration, the filtrates were transferred to scintillation tubes, 7 ml of liquid scintillation cocktail was added to each scintillation tube and radioactivity was determined by ^{3}H-counting for 5 min using a liquid scintillation counter (Beckmann LS-6000 Scintillation Counter, Perkin Elmer, Waltham, MA, USA).

3.2.4 Cell culture

Cell culture work was always carried out in tissue culture hoods using sterile and pyrogen-free consumables and reagents. Primary cells and cell lines were cultured at 37°C with 5% CO_2 in a humidified atmosphere. Cells were grown as monolayers in cell culture dishes or in cell culture flasks in DMEM supplemented with 10% (v/v) FCS and 1% (v/v) Penicillin-Streptomycin (10,000 U/ml), referred to as complete DMEM.

Immortalized mouse macrophages (iMOs) were detached by incubation with trypsin-EDTA for 5 min at 37°C. They were passaged every second or third day dependent on actual growth conditions.

The cell number of a cell suspension was usually determined in a Neubauer cell counting chamber. The cell suspension was diluted in adequate amounts of trypan blue solution, which exclusively stains dead cells. Only unstained (living) cells inside the four large squares of the Neubauer counting chamber were counted under a light microscope. The total cell number was calculated using the following formula:

$$\text{Cell number/ ml} = \text{No. of cells counted/ 4} * \text{dilution factor} * 10^4$$

In some occasions cell numbers were determined using the “Quick Count” settings of the Tali Image Cytometer (Life Technologies, Carlsbad, CA, USA).

3.2.5 Generation of primary BMDMs

BMDMs were prepared from male, 6-10 week old WT C57BL/6 mice or from age and sex matched WT and LXRα$^{-/-}$/LXRβ$^{-/-}$ mice. Bone marrow was collected under sterile conditions from femurs and tibiae. Any residual tissue was removed from intact bones by incubation in 70% EtOH and subsequent cleaning. The bones were then flushed with complete DMEM using a 10 ml syringe with a 25G needle. After centrifugation (340 x g, 5 min) pelleted bone marrow cells from one mouse were resuspended in 40 ml of complete DMEM supplemented with 20% (v/v) L929 supernatant as the source of M-CSF or 40 ng/ml recombinant M-CSF.

The cell suspension was separated through a 70 µm nylon cell strainer and split up into two 175 cm tissue-culture flasks. Adherent BMDMs were harvested on day 7 of differentiation by incubation in cold BMDM dissociation buffer for 10 min at 4°C and subsequent scraping. Cells were pelleted by centrifugation (340 x g, 5 min) and resuspended in complete DMEM for further experiments.

3.2.6 CellTiter-Blue Cell Viability Assay

WT BMDMs and BALB/c iMOs were seeded at $0.5x10^5$ cells per well in 96-well plates and treated with different concentrations of CD for different time points. A 1:2 dose titration series starting with 50 mM CD was added in a reversed time course. Some cells were left untreated as positive control or were treated with 70% EtOH for 1 h prior to assessment of cell viability as a negative control (dead cells). Cell viability was determined by measuring the metabolic activity of the cells using the CellTiter-Blue (CTB) Viability Assay according to the manufacturer's instructions. Fluorescence of the metabolized CTB reagent was read on the Spectramax i3 (Molecular Devices, Sunnyvale, CA, USA) using an excitation wavelength of 530-570 nm and detecting emission at a wavelength of 580-620 nm.

3.2.7 Mouse studies

All mouse studies were performed in collaboration with Dr. Sebastian Zimmer (Medical Clinic and Polyclinic II, University Hospital Bonn, Bonn). Catharina Lahrmann, Niklas Bode and Dr. Sebastian Zimmer carried out all animal work described in this section, including animal care, handling, treatment and dissection. Mice were maintained in a 22°C room with a 12 h light/dark cycle and received food pellets and drinking water *ad libitum*.

3.2.7.1 Atherosclerosis mouse models

Atherosclerosis mouse models were carried out with age and sex matched 12-week old $ApoE^{-/-}$ mice on C57BL/6J background. To induce atherosclerosis development, the mice received an atherogenic high-fat, high-cholesterol (HFHC) diet containing 21% fat, 19.5% casein and 1.25% cholesterol (Ssniff, Soest) as indicated in the specific study protocols below.

Body weight, arterial blood pressure and heart rate of the mice were controlled throughout the studies. Mice were fasted overnight and blood was collected from the inferior vena cava using a heparinized syringe directly after sacrifice. Animals were immediately dissected and various organs including liver, spleen and kidneys were snap-frozen and stored at -80°C for potential further analysis. Hearts with ascending aortas were directly embedded in Tissue Tek OCT embedding medium and snap-frozen. A cryostat (Leica, Mannheim) was used to cut 5 µm thick sections, starting at the aortic arch and progressing through the aortic

valve area into the heart. 3-5 tissue sections were placed on microscopy slides and stored at -80°C for further analyses.

Plasma was obtained by centrifugation (3000 x g, 10 min) of the heparinized blood and plasma cholesterol concentrations were determined by gas chromatography-flame ionization detection using 5α-cholestane as internal standard. These measurements were performed by Prof. Dr. Dr. Dieter Lütjohann and colleagues (Institute of Clinical Chemistry and Clinical Pharmacology, University Hospital Bonn, Bonn).

Atherosclerosis prevention study

ApoE$^{-/-}$ mice received a HFHC diet for 8 weeks and were subcutaneously injected with 2 g CD/ kg body weight or vehicle control twice a week.

Atherosclerosis regression studies

ApoE$^{-/-}$ mice received a HFHC diet for 8 weeks to establish advanced atherosclerosis. A control group of mice was sacrificed at this stage (pretreatment control). The remaining mice were either treated with CD or vehicle control as described above for another 4 weeks. During this treatment period the diet of some mice was switched to a normal chow diet (***Regression A***) or the mice were kept on the HFHC diet (***Regression B***).

3.2.7.2 *In vivo* RCT model

BMDMs were prepared from WT or LXRα$^{-/-}$/LXRβ$^{-/-}$ mice and loaded with 100 µg D_6-CCs (see section 3.2.14) per 1x10^6 cells for 3 h to allow for crystal intake. Following 3 washes with PBS containing 0.1% FCS to remove non-internalized D_6-CCs, CC-loaded macrophages were harvested by incubation in cold BMDM dissociation buffer for 10 min at 4°C and subsequent scraping. Cells were pelleted by centrifugation (340 x g, 5 min), resuspended in sterile PBS and handed over to Dr. Sebastian Zimmer and colleagues (Medical Clinic and Polyclinic II, University Hospital Bonn, Bonn). 16-week old WT C57BL/6 mice were then intraperitoneally injected with 15x10^6 D_6-CC-loaded BMDMs from either WT or LXRα$^{-/-}$/LXRβ$^{-/-}$ mice. Subsequently mice were subjected to intraperitoneal treatment with either 2 g CD/ kg body weight or vehicle control. The first treatment injection was given approximately 30 min after application of the D_6-CC-loaded BMDMs, and a second one was given 16 h later. Following the first treatment injection, feces and urine were collected every 3-6 h over a 30 h period. The excrement was analyzed for presence of crystal-derived D_6-cholesterol by gas chromatographic-mass spectrometric-selected ion monitoring (GC-MS-SIM) as described in section 3.2.15. Fecal D_6-cholesterol was determined as the ratio area of D_6-cholesterol to the endogenous cholesterol metabolite 5α-cholestane.

3.2.7.3 Bone marrow transplantation model

Bone marrow of 14- to 18-week old WT, LXRα$^{-/-}$/LXRβ$^{-/-}$ and MAC-ABC^{DKO} (LysmCreAbca1$^{fl/fl}$Abcg1$^{fl/fl}$) mice (see section 3.1.9) was collected under sterile conditions by flushing femurs and tibia with complete DMEM using a 23G needle. The cell suspension was filtered through a 70 µm nylon cell strainer, washed twice with Hank's acid citrate dextrose solution and resuspended in PBS. For full engraftment of donor bone marrow, 8-week old recipient LDLR$^{-/-}$ mice were lethally irradiated with 6x6 Gy over 4 h from a Cs-137 source using an OB 29/4 (STS Steuerungstechnik & Strahlenschutz, Braunschweig). 4 h after irradiation recipient mice were reconstituted with 1x10^7 bone marrow cells from donor mice by intravenous injection into the tail vein. All mice received drinking water containing 0.1 mg/ml Ciprofloxacin for 7 days to prevent systemic infection during neutropenia. The atherosclerosis study was initiated 4 weeks after irradiation following the protocol of the atherosclerosis prevention study described in section 3.2.7.1.

3.2.8 Immunohistochemistry of aortic cryosections

Fluorescent immunohistochemistry (IHC) was performed for microscopical characterization of atherosclerotic lesions. Aortic cryosections were encircled using the hydrophobic Dako Pen prior to fixation for 30 min with 4% (v/v) methanol-free formaldehyde. Tissue sections were then blocked and permeabilized for 60 min with IHC blocking buffer. For detection of macrophages, indirect fluorescent immunolabeling of cluster of differentiation 68 (CD68) was performed. First, the sections were incubated with primary rat anti-mouse CD68 antibody (MCA1957) diluted to 2 µg/ml in IHC staining buffer overnight at 4°C in a humidified chamber. Following three washes with IHC staining buffer, the sections were incubated with the secondary goat anti-rat IgG Alexa647 conjugate diluted to 4 µg/ml in IHC staining buffer for 60 min in the dark. The sections were again washed three times with IHC staining buffer before a final incubation with Hoechst 34580 (nuclear counterstain) diluted to 5 µg/ml in PBS for 2 min in the dark was performed. Subsequently the sections were washed twice with PBS and a final wash was done with double-distilled water (ddH_2O). Coverslips were mounted using 80% glycerol in ddH_2O as mounting medium and the edges were carefully sealed using a solvent-free two-component epoxy resin adhesive (UHU, Bühl).

3.2.9 Confocal laser reflection and fluorescence microscopy

Confocal microscopy was performed using a Leica TCS SP5 II AOBS confocal laser-scanning microscope controlled by the Leica Application Suite Advanced Fluorescence (LAS AF) software. Fluorescence staining was detected using standard confocal imaging techniques. Laser reflection microscopy was used to visualize crystalline material, more precisely crystalline cholesterol, as previously described[24,26]. For detection of the reflected

laser light, the detector was set to cover the wavelength of the laser light (± 5-10 nm) and the acousto-optical beam splitter was set to enhanced transmittance allowing the laser light to be passed to the detector. A combination of fluorescence and laser reflection microscopy allowed the detection of fluorescence and laser reflection signals derived from the same confocal plane.

3.2.10 Quantitative image analysis

Volocity Quantitation (PerkinElmer, Waltham, MA, USA) was used for quantitative image analysis. Measurement protocols were designed for the specific analysis purposes. Between individual experiments measurement protocols were slightly adapted to the respective image properties, but within one experiment identical measurement protocols were applied to every image analyzed to ensure comparability of the quantification results.

Microscopic images of aortic cryosections were examined for atherosclerotic plaque size, CC plaque load, plaque cellularity and plaque macrophage load. For this purpose, regions of interest (ROIs) were manually drawn to assess total vessel wall area (Fig. 3-2A) and

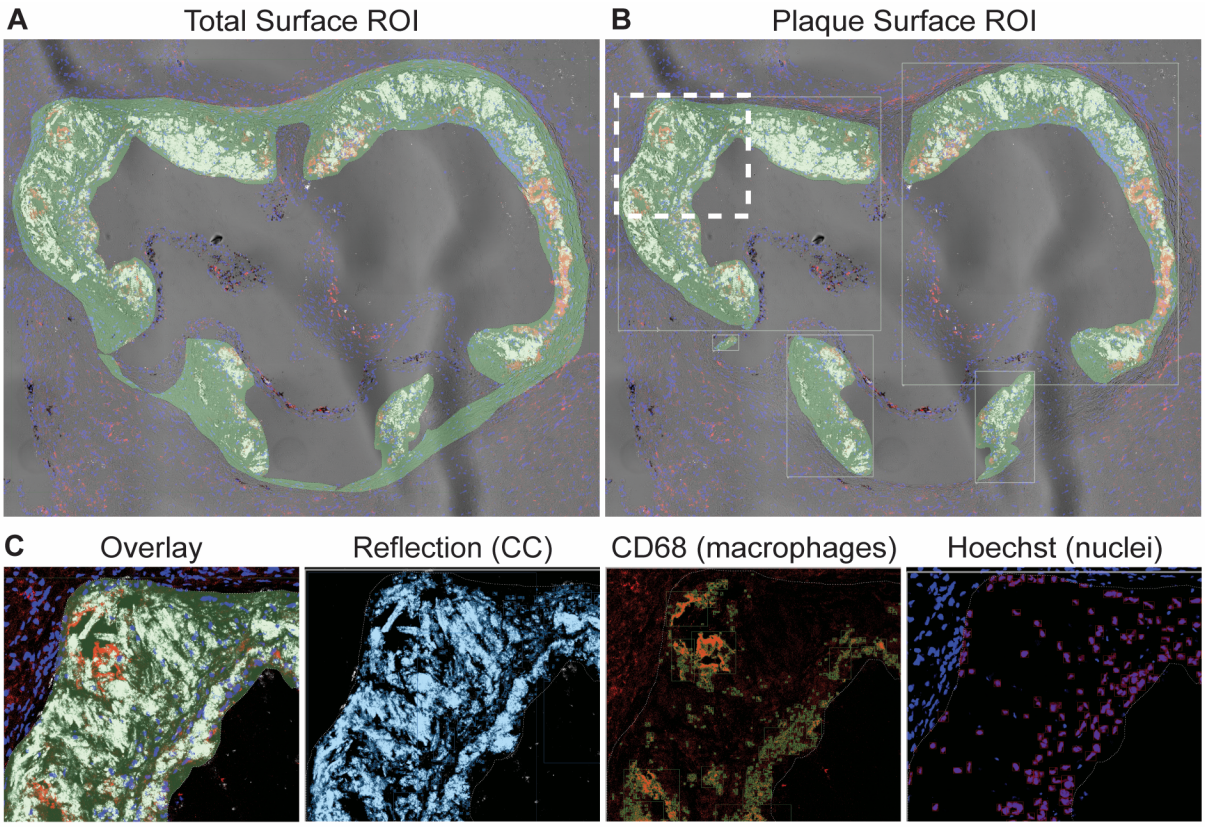

Figure 3-2: Quantitative image analysis of aortic cryosections.

ROIs for (A) total surface area and (B) plaque surface area were manually drawn and are represented by green translucent surfaces. (C) Images represent an overlay image and the separate channels of the enlarged area outlined by the dashed line in (B). The first image illustrates an overlay of fluorescence and reflection signals (CC = white, macrophages = red, nuclei = blue) as well as the plaque surface ROI (green translucent surface). The other three images show the separate channels with the detected objects inside the plaque surface ROI (illustrated by translucent surfaces and outlines in blue for CC, green for macrophages and red for nuclei).

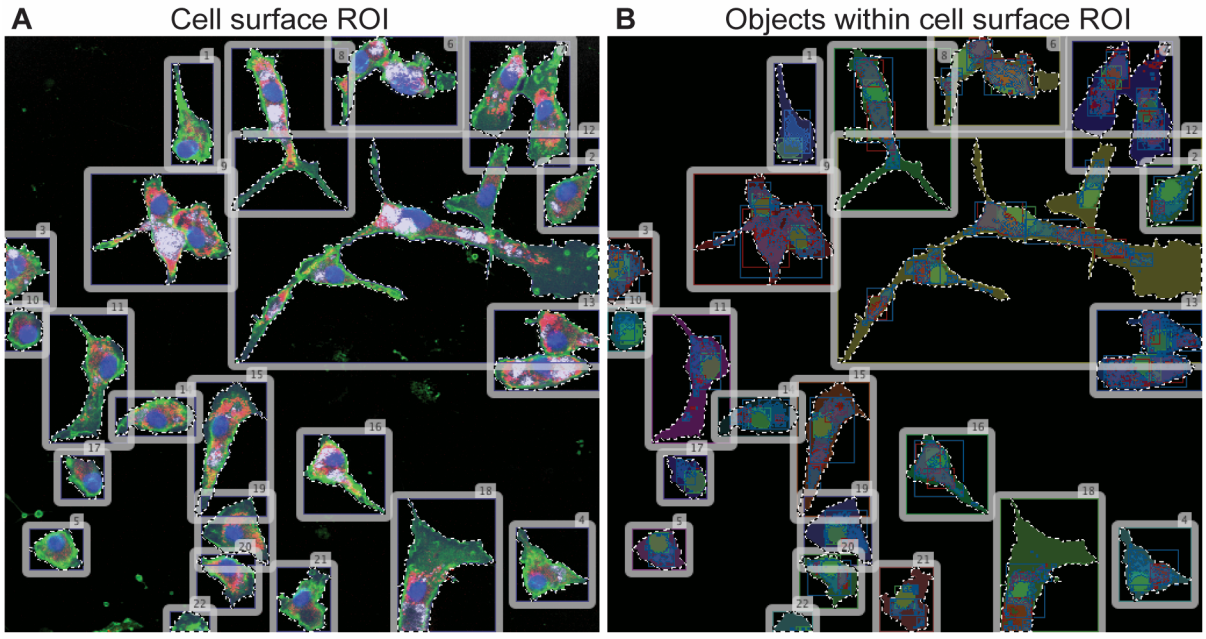

Figure 3-3: Automated intracellular object quantification.

(A) ROIs of cell surfaces were automatically generated from the CtxB signal (green). (B) The obtained cell surface mask was used for quantification of intracellular objects, such as nuclei (green outlines), CC (red outlines) or lipid droplets (blue outlines).

atherosclerotic plaque area (Fig. 3-2B). Measurement protocols were designed to detect and quantify reflection and fluorescence signals as well as single nuclei objects obtained from the Hoechst staining within the ROI representing the atherosclerotic plaque (Fig. 3-2C). Image analysis of the aortic cryosections was performed blinded to the treatment of the respective animals.

Intracellular reflection and fluorescence signals were quantified in fixed, cholera toxin subunit B (CtxB) stained cells (see sections 3.2.12 and 3.2.13). CtxB staining was used for creating a ROI of the cell surfaces (Fig. 3-3A). The area of reflection or fluorescence signals, as well as the number of single nuclei (as obtained with Hoechst staining) were then determined exclusively within this cell surface mask (Fig. 3-3B).

3.2.11 CD binding and uptake assays

Rhodamine-labeled CD (see section 3.2.1) was used to investigate CD binding to CCs and CD uptake into macrophages. Binding and uptake of rhodamine-labeled CD was measured by flow cytometry using a MACSQuant analyzer (Miltenyi Biotec, Bergisch Gladbach) where rhodamine fluorescence was detected in the Y2 channel. In addition confocal microscopy was used to visualize the localization of the fluorescent rhodamine signal.

CD binding to CCs was assessed by incubation of 1 mg CCs in 0.5 mM rhodamine-labeled CD for 6 h shaking at 4°C. Crystals were washed 5 times with PBS prior to confocal microscopic or flow cytometric analyses.

CD uptake into macrophages was investigated in C57BL/6 iMOs and CC-loaded C57BL/6 iMOs. For microscopic analysis 75,000 cells were seeded into a 4-well microscopy dish and 20 µg CCs were added to one of the wells. Cells were left to adhere for 3 h before live cell imaging was started to capture rhodamine-labeled CD uptake. 1 mM rhodamine CD solution (1:10 mixture of rhodamine-labeled CD and unlabeled CD) was added to the wells and the cells were imaged for 6 h. Following 3 washes with PBS, the cells were fixed for 30 min with 4% (v/v) methanol-free formaldehyde and stained for nuclei using Hoechst 34580 (diluted to 5 µg/ml in PBS) and cell membranes using Alexa Fluor 488-conjugated CtxB (diluted to 1 µg/ml in PBS) for 10 min. Cells were again washed 3 times with PBS and confocal microscopy was performed to estimate the localization of rhodamine-labeled CD. For flow cytometry 300,000 cells were seeded into a 24-well plate and 40 µg CCs were added to some of the wells. Cells were left to adhere for 3 h before addition of 1 mM rhodamine CD solution (1:10 mixture of rhodamine-labeled CD and unlabeled CD) or appropriate controls (unlabeled CD only or PBS). Following 3 washes in PBS, cells were trypsinized and transferred to FACS tubes for detection of rhodamine fluorescence on the MACSQuant analyzer.

3.2.12 Intracellular CC dissolution

Intracellular CC dissolution was determined by confocal laser reflection and fluorescence microscopy. For this, $1x10^5$ WT BMDMs were seeded into 8-well microscopy dishes and loaded with 100 µg CC per $1x10^6$ cells for 3 h to allow for crystal intake. Following 3 washes with PBS containing 0.1% FCS to remove non-internalized CCs, BMDMs were incubated with 10 mM CD or medium control for 24 h. Cells were fixed for 30 min with 4% (v/v) methanol-free formaldehyde and stained for nuclei using Hoechst 34580 (diluted to 5 µg/ml in PBS) and cell membranes using Alexa Fluor 647-conjugated CtxB (diluted to 1 µg/ml in PBS) for 10 min. Cells were washed 3 times with PBS and confocal reflection and fluorescence microscopy was performed. 10-15 random images were acquired per sample and analyzed for intracellular CC content as described in section 3.2.10.

3.2.13 Lipid droplet staining

Lipid droplets were stained using the lipid droplet dye LD540[109] which was kindly provided by Prof. Dr. Christoph Thiele (Life & Medical Sciences Institute (LIMES), University of Bonn, Bonn). In detail, $0.5x10^5$ C57BL/6 iMOs were seeded per well into a 96-well microscopy plate. The cells were loaded with 100 µg CCs per $1x10^6$ cells for 3 h to allow for crystal intake. Following 3 washes with PBS containing 0.1% FCS to remove non-internalized CCs, cells were incubated with 10 mM CD or medium control for 24 h. Cells were fixed for 30 min

with 4% (v/v) methanol-free formaldehyde and stained with LD540 (diluted to 0.1 µg/ml in PBS) for 30 min at 37°C. Subsequently nuclei and cell membranes were stained using Hoechst 34580 (diluted to 5 µg/ml in PBS) and Alexa Fluor 647-conjugated CtxB (diluted to 1 µg/ml in PBS) for 10 min. Cells were washed 3 times with PBS and confocal reflection and fluorescence microscopy was performed. Per sample 10 random images were acquired and cellular lipid droplet content was determined as described in section 3.2.10.

3.2.14 Analysis of crystal-derived cholesterol in macrophages

D_6-cholesterol ([26.26.26.27.27.27-2H6]-cholesterol) was used to prepare deuterium-labeled CCs (D_6-CCs) according to the protocol described in section 3.2.2.
$1.5x10^6$ C57BL/6 iMOs were incubated with 200 µg D_6-CCs per $1x10^6$ cells for 3 h to allow for crystal intake. Cells were washed 3 times with PBS containing 0.1% FCS to remove non-internalized D_6-CCs and a control sample was harvested to assess D_6-cholesterol distribution prior to further treatment (0h control). The remaining cells were treated with 10 mM CD for 24 h and 48 h. Where indicated 0.25 mg/ml reconstituted HDL (rHDL) (CSL111) was added together with CD. Supernatants were collected and the cells were harvested by scraping in 1M ethanolic NaOH or PBS depending on downstream analysis. The samples were then transferred to the laboratory of Prof. Dr. Dr. Dieter Lütjohann (Institute of Clinical Chemistry and Clinical Pharmacology, University Hospital Bonn, Bonn) for analysis of crystal-derived sterols and oxysterols by gas chromatographic-mass spectrometric-selected ion monitoring (GC-MS-SIM).

3.2.15 GC-MS-SIM

GC-MS-SIM analyses including GC-MS-SIM-specific sample preparation was entirely performed by the laboratory of Prof. Dr. Dr. Dieter Lütjohann (Institute of Clinical Chemistry and Clinical Pharmacology, University Hospital Bonn, Bonn).
A certain set of sterols was measured in all samples. This set includes cholesterol precursors such as lanosterol, lathosterol and desmosterol, which can be used as surrogate markers of cholesterol synthesis. Epicoprostanol was used as internal standard for detection of these sterols[110,111].
Crystal-derived D_6-cholesterol was analyzed for degree of esterification and oxidation products. Degree of esterification was calculated from the difference of the cholesterol levels with (total D_6-cholesterol) and without (free D_6-cholesterol only) alkaline hydrolysis. D_6-cholesterol was extracted and derivatized to its trimethyl silylether prior to GC-MS-SIM on m/z 464 [M^+] using epicoprostanol as internal standard on m/z 370 [M^+][112]. The oxidized metabolite [26,26,26,27,27-$^2H_5$]-27-hydroxycholesterol (D_5-27-hydroxycholesterol) was

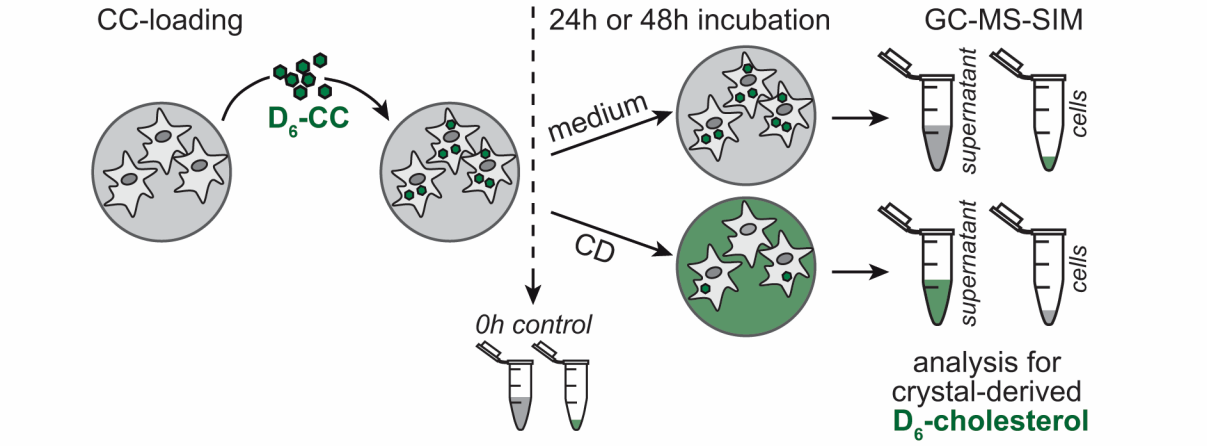

Figure 3-4: Sample preparation for analysis of crystal-derived cholesterol.

Macrophages were loaded with D_6-CCs and a 0 h control was harvested to assess the distribution of D_6-cholesterol right upon crystal loading of the cells. Following incubation with medium or 10 mM CD for 24 h or 48 h, cells and supernatants were harvested for analysis of crystal-derived D_6-cholesterol by GC-MS-SIM. GC-MS-SIM analysis was performed by Prof. Dr. Dr. Dieter Lütjohann and colleagues.

determined by GC-MS-SIM on m/z 461 [M^+-90]. The corresponding normal cellular cholesterol and its oxidation product 27-hydroxycholesterol were measured on m/z 458 [M^+] and m/z 456 [M^+-90], respectively[113].

3.2.16 Western blot analysis

Protein expression was determined by western blot (WB) analysis using protein specific antibodies.

Cholesterol efflux transporter expression was determined in macrophages incubated with 200 µg CCs per $1x10^6$ C57BL/6 iMOs ($0.5x10^6$ cells per sample) or 100 µg CCs per $1x10^6$ BMDMs ($1.5x10^6$ cells per sample) for 3 h to allow for crystal intake. Cells were washed 3 times with PBS containing 0.1% FCS to remove non-internalized CCs and cells were treated for 24 h with 10 mM CD, medium control or 10 µM LXR agonist T0901317 as positive control for LXR activation.

For analysis of NLRP3 inflammasome priming, $1x10^6$ C57BL/6 iMOs or $1.5x10^6$ BMDMs were incubated for 16 h with 10 mM CD, medium control or 10 µM LXR agonist T0901317 as positive control for LXR activation. Subsequently the medium was replaced with complete DMEM containing 200 ng/ml LPS and samples were harvested after 3 h incubation.

3.2.16.1 Preparation of cell lysates

RIPA lysis buffer was made up from a 2x stock solution right before use and supplemented with 0.1 µM PMSF and cOmplete EDTA-free protease inhibitor cocktail. Preparation of cell lysates was performed entirely on ice. Supernatants were removed and cells were washed once with ice-cold PBS before addition of 150 µl RIPA lysis buffer per well. Cells were scraped off and transferred into 1.5 ml centrifuge tubes. Following 30 min incubation on ice,

the cell lysates were cleared by centrifugation at 13,000 x g for 10 min at 4°C and supernatants were collected into new 1.5 ml centrifuge tubes.

3.2.16.2 Determination of protein concentration by BCA assay

Protein concentrations were determined using the BCA protein assay kit according to the manufacturer's instructions. Absorbance at 562 nm was read on the Spectramax i3 (Molecular Devices, Sunnyvale, CA, USA) and protein concentrations were calculated from the blank-corrected BSA standard curve.

3.2.16.3 Sample preparation for SDS-page gel electrophoresis

Cell lysates were diluted to equal protein concentrations in RIPA lysis buffer and mixed with 4x LDS sample buffer and 10x sample reducing agent. For denaturing gel electrophoresis the samples were heated for 10 min at 80°C.

3.2.16.4 SDS-page gel electrophoresis

Equal amounts of protein were leaded on pre-cast 4-12% Bis-Tris gels. PageRuler Plus Prestained protein ladder was used as a size standard ranging from 10 to 250 kDa. Proteins were separated by gel electrophoresis in either MES or MOPS running buffer at 150-200 V for approximately 45 min.

3.2.16.5 Western blotting

Following SDS-page gel electrophoresis proteins were transferred to a methanol-activated PVDF membrane using a semi-wet transfer unit (XCell II Blot Module, Novex Life Technologies, Carlsbad, CA, USA). Protein transfer was performed at 32 V for 1.5 h. For detection of multiple proteins of distinct sizes the membrane was cut with a scalpel using the prestained protein ladder as orientation. Membranes were blocked for 1h in WB blocking buffer prior to overnight incubation at 4°C with the specific primary antibodies (see section 3.1.6, Table 3-2) diluted as indicated in 1% BSA in TBS-T. Following three washes in TBS-T the membranes were incubated with the respective IRDye secondary antibodies (see section 3.1.6, Table 3-2) diluted 1:10,000 1% BSA in TBS-T for 45 min in the dark. Following two washes in TBS-T and 1 final wash in TBS the infrared fluorescent signals on the membranes were visualized using the Odyssey Imager (LI-COR, Lincoln, NE, USA). Quantification of western blot images was performed using Image Studio 3.1.4 (LI-COR, Lincoln, NE, USA).

3.2.17 Reverse transcription quantitative real-time PCR

Reverse transcription quantitative real-time PCR (RT-qPCR) was used to quantify the abundance of messenger RNA (mRNA) transcripts in a sample. For analysis of gene expression changes upon CD treatment, $2x10^6$ BMDMs were incubated with 100 µg CCs per

$1x10^6$ cells overnight. Cells were washed 3 times with PBS containing 0.1% FCS to remove non-internalized CCs and where indicated a 0 h control sample was harvested to assess cellular gene expression right after crystal loading of the cells. The remaining cells were incubated for the indicated times (usually 4 h, 8 h or 24 h) in medium or 10 mM CD. Where indicated BMDMs were incubated with 10 µM LXR agonist T0901317 for 24 h as positive control for LXR activation.

3.2.17.1 RNA preparation

Plates were placed on ice, cells were washed once with PBS and 350 µl Buffer RLT (RNeasy mini kit) supplemented with 1% (v/v) β-mercaptoethanol was added per well. Cells were scraped off and the lysates were transferred into 1.5 ml centrifuge tubes, where they were homogenized using a 20G needle fitted to an RNase-free syringe. Total RNA was isolated using the RNeasy mini kit with on-column DNase digestion according to the manufacturer's instructions. RNA concentration and purity were determined by measuring the absorbance at 260 nm, 280 nm (indicating protein contamination) and 230 nm (indicating contamination with organic compounds). Absorbance readings were performed using the SpectraDrop Micro-Volume Microplate on the Spectramax i3 (Molecular Devices, Sunnyvale, CA, USA).

3.2.17.2 cDNA synthesis

Approximately 1 µg of isolated total RNA was used as starting material for complementary DNA (cDNA) synthesis by reverse transcription PCR (RT-PCR). $Oligo(dT)_{18}$ primers, which hybridize to the poly(A) tail of mRNAs, were used for specific amplification of mRNA. The RT-PCR reaction was set up in a final volume of 20 µl containing RNA (approx. 1 µg), 5 µM $Oligo(dT)_{18}$ primer, 0.1 µl (20 U) SuperScript III reverse transcriptase with associated first-strand buffer, 5 mM DTT and 0.5 mM dNTPs. A control reaction without reverse transcriptase was included to control for genomic DNA contamination. In detail, the appropriate volume of RNA was diluted in nuclease-free water, mixed with $Oligo(dT)_{18}$ primer and heated to 65 °C for 5 min. Upon incubation on ice for at least 1 min, SuperScript III reverse transcriptase, first-strand buffer, DTT and dNTPs were added. RT-PCR was performed for 50 min at 50°C and the reaction was inactivated by heating to 85°C for 5 min. The cDNA was finally diluted 1:20 in nuclease-free water and stored at -20°C.

3.2.17.3 SYBR green based quantitative real-time PCR

Quantitative real-time PCR was performed using SYBR Green, a fluorescent DNA intercalating dye, which allows for double-stranded DNA detection and quantification. To determine the amount of specific mRNA transcripts, cDNA was mixed with 0.4 µM gene-specific primers (see section 3.1.7, Table 3-3) and 10x Maxima SYBR Green/ROX qPCR master mix containing SYBR Green, ROX as a passive reference dye as well as Maxima Hot

Start Taq DNA Polymerase and dNTPs in an optimized PCR buffer. A control without any template was included to control for DNA contaminations in the qPCR reaction mix. The qPCR reaction was performed in 384-well plates in a total reaction volume of 10 µl on the QuantStudio 6 Flex Real-Time PCR System (Applied Biosystems Life Technologies, Carlsbad, CA, USA) using the following program: 95°C 10 min; 40x [95°C, 15 sec; 60°C, 1 min]. Subsequent melt curve analysis was performed to control for primer specificity (indicative) and presence of primer-dimers. The $\Delta\Delta C_T$ method (Applied Biosystems) was used to calculate relative mRNA expression to the reference gene hypoxanthine-guanine phosphoribosyltransferase (Hprt).

3.2.18 NLRP3 inflammasome activation

BALB/c iMOs or BMDMs were plated at $0.1x10^6$ cells per well into a 96-well tissue culture plate. Macrophages were pretreated for 16 h with 10 mM CD, medium control or 10 µM LXR agonist T0901317 as positive control for LXR activation. Cells were primed with 100 µl complete DMEM containing 200 ng/ml LPS for 3 h prior to addition of 25 µl 5-fold concentrated NLRP3 stimuli. Ultimately cells were stimulated with 5 mM ATP or 10 µM nigericin for 1 h, with 1 mM H-Leu-Leu-Ome (LeuLeu) for 4 h, 0.5 mg/ml silica crystals or 1.5 mg/ml CCs for 6 h. Upon centrifugation (340 x g, 5 min) cell-free culture supernatants were collected and cytokine production was measured by enzyme-linked immunosorbent assay (ELISA).

3.2.19 ELISA

Cytokine secretion was quantified using commercial ELISA kits for the detection of murine IL-1β and murine TNF-α (see section 3.1.5). ELISAs were performed according to the manufacturer's instructions, but all volumes were halved. In brief, 96-well ELISA plates were coated overnight with the respective coating antibody diluted in PBS. The wells were blocked for 2 h with ELISA blocking buffer before samples and standards were added to the plates. Cell culture supernatants were used undiluted for detection of mIL-1β or diluted 1:4 in ELISA reagent diluent (TNF-α) for mTNF-α detection. Samples and standards were incubated for 2 h, plates were washed 3 times using ELISA wash buffer and the respective biotinylated detection antibody diluted in the respective ELISA reagent diluent was added for 2 h. Following 3 washes with ELISA wash buffer, streptavidin-conjugated horseradish-peroxidase was diluted in the respective ELISA reagent diluent and incubated for 20 min. The TMB substrate solution was prepared according to the manufacturer's instructions and ELISAs were developed in the dark for approximately 15-20 min. The reaction was stopped with 2 N Sulfuric Acid (H_2SO_4) and the absorbance at 450 nm and 570 nm was read on the

Spectramax i3 (Molecular Devices, Sunnyvale, CA, USA). Cytokine concentrations were calculated from the blank-corrected standard curves.

3.2.20 Lysosomal damage and crystal uptake assay

Lysosomal integrity can be measured by flow cytometry using acridine orange. Acridine orange is a cationic nucleic acid binding fluorescent dye that emits green light in its monomeric state when it is bound to nucleic acids and red light upon dimerization when it accumulates in acidic compartments, such as lysosomes[26]. As the amount of red fluorescence of acridine orange stained cells directly correlates to the amount of acidic lysosomes, lysosomal damage can be measured by a loss of red acridine orange fluorescence.

BALB/c iMOs or BMDMs were plated at $0.1x10^6$ cells per well in a 96-well tissue culture plate. Macrophages were pretreated for 16 h with 10 mM CD or medium control prior to staining with 5 µg/ml acridine orange for 15 min at 37°C. Following 3 washes with PBS, the cells were incubated for 6 h with 1 mM H-Leu-Leu-Ome (LeuLeu), 0.5 mg/ml silica crystals, 1.5 mg/ml CCs or medium control. The cells were subsequently washed once with PBS containing 0.1% FCS, incubated with trypsin for 5 min at 37°C and detached from the plate

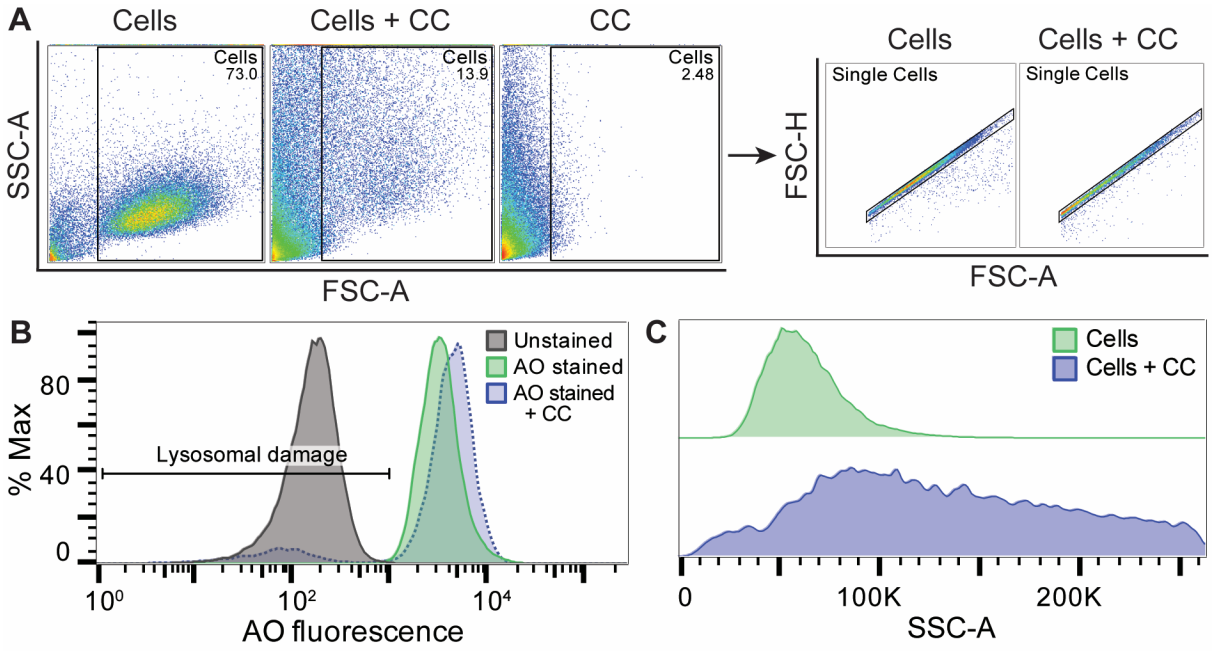

Figure 3-5: Gating strategy for measuring lysosomal damage and crystal uptake.

(A) The cell population gate was set according to the forward scatter (FSC) and side scatter (SSC) properties of a sample containing cells only (Cells) and crystal-loaded cells (Cells + CC). In addition, a control with 0.1 mg/ml CC only (CC) was used to ensure exclusion of free crystals present in the samples with crystal-loaded cells from the cell population. Subsequently doublet discrimination was performed on the cell population. (B) Histograms of the acridine orange fluorescence detected in the B2 channel. Gating for loss of acridine orange fluorescence on the single cell populations as measure of lysosomal damage. (C) SSC histograms of the single cell populations. The SSC median was analyzed as measure of cellular crystal uptake.

by pipetting up and down several times. Complete DMEM was added to the wells and the cell suspension was transferred into v-shape bottom 96-well plates. Upon centrifugation (340 x g, 5 min) cells were resuspended in 50 µl PBS and applied to the MACS Quant Analyzer (Miltenyi Biotec, Bergisch Gladbach). For quantification of lysosomal damage the red acridine orange fluorescence was detected in the B2 channel (Fig 3-5B). At the same time crystal uptake was analyzed using the side scatter signal (Fig 3-5C).

3.2.21 Genome-wide transcriptome analysis by microarray

For genome-wide transcriptome analysis by microarray, BMDMs of WT and LXRα$^{-/-}$/LXRβ$^{-/-}$ mice were generated as described in section 3.2.5 using recombinant M-CSF for macrophage differentiation. 3x10^6 cells per well were plated into a 6-well dish and left to adhere overnight. Some wells were incubated with 100 µg CCs per 1x10^6 cells for 3 h to allow for crystal intake. 3 wash steps with PBS containing 0.1% FCS were performed to remove non-internalized CCs. Cells were then incubated for 6 h with 10 mM CD or medium control. Plates were placed on ice, cells were washed once with PBS, and scraped off in 1 ml Trizol per well. Samples were then handed over to Prof. Dr. Joachim Schultze and colleagues (Life & Medical Sciences Institute (LIMES), University of Bonn, Bonn) for further processing for array-based gene expression profiling. In brief, total RNA was purified using the MinElute Reaction Cleanup Kit (Qiagen, Hilden). Prior to further RNA processing for microarray analysis, sample quality was controlled by Taqman RT-qPCR performed by Niklas Bode (Medical Clinic and Polyclinic II, University Hospital Bonn, Bonn). For this, about 300 ng RNA was reverse transcribed to cDNA using the Omniscript RT Kit (Qiagen, Hilden) according to the manufactures protocol and expression of cholesterol efflux transporters was determined using commercially available Taqman probes (see section 3.1.7, Table 3-4). Abca1 and Abcg1 mRNA expression was normalized to the abundance of 18S RNA. For subsequent microarray analysis biotin-labeled cRNA was produced using the TargetAmp Nano-g Biotin-cRNA Labeling Kit for the Illumina System (Epicentre, Madison, WI, USA). The biotin-labeled cRNA (1.5 µg) was subsequently hybridized to Illumina MouseWG-6 v2.0 Beadchips and scanned on an Illumina iScan or HiScanSQ system (Illumina, San Diego, CA, USA). Raw intensity data were processed and exported with Genome Studio V2011.1 (Illumina, San Diego, CA, USA).

3.2.22 Bioinformatic analysis of microarray data

Bioinformatic analyses were performed by or with the help of Dr. Thomas Ulas (Life & Medical Sciences Institute (LIMES), University of Bonn, Bonn). Array data was imported into Partek Genomics Suite 6.6 (Partek, St. Louis, MO, USA). Quality control analyses including principle component analyses and box-whisker plots to visualize

expression distribution were applied to the data set. Non-normalized data (log2) were quantile normalized and transcripts with variable expression within the dataset as well as differentially expressed (DE) genes between the different conditions were calculated using two-way analysis of variance (ANOVA) models including batch correction for sentrix bar code and gender where applicable.

For analyses of the microarray data on *in vitro* treated BMDMs derived from WT or LXRα$^{-/-}$/LXRβ$^{-/-}$ mice, DE genes were defined by a fold change (FC) greater 2 and p-value < 0.05. Gene set enrichment analysis (GSEA) was used to determine whether induction of a defined set of genes was statistically significant between two different states. A set of genes was statistically significant enriched when the p-value was ≤ 0.05 and the false discovery rate (FDR) was ≤ 0.25 comparing two different states. GSEA was performed with 1000 permutations against a list of LXR target genes generated from the LXR target genes identified by Heinz and colleagues[114]. FCs of genes involved in the steroid biosynthesis pathway (KEGG pathway mmu00100, http://www.genome.jp/kegg/pathway.html) were visualized in a heat map.

For analyses of the microarray data on descending aortas of mice from the bone-marrow transplantation model, DE genes were defined by a FC greater 1.5 and p-value < 0.05. Gene expression of genes relevant for the NLRP3 inflammasome was visualized using Partek Pathway (KEGG pathway mmu04621: NOD-like receptor signaling pathway, http://www.genome.jp/kegg/pathway.html).

3.2.23 Data processing and statistical analysis

Unless otherwise indicated at least three individual experiments with duplicates were performed and data is presented as mean ± standard error of the mean (SEM). Statistical differences were assessed by Student's t-test and one-way ANOVA with appropriate post test for multiple comparisons (as indicated) where applicable. Values of $p < 0.05$ were considered significant. All statistical hypothesis testing was performed using GraphPad Prism 6 (GraphPad Software, San Diego, CA, USA). For graphical representation significance levels were grouped by p-value: *** = p<0.001, ** = p<0.01, * = p<0.05, ns = not significant.

Basic data processing was performed with Microsoft Excel (Microsoft Corporation, Redmond, WA, USA). Unless otherwise indicated data visualization was performed using GraphPad Prism 6 (GraphPad Software, San Diego, CA, USA). Heat maps of sterol measurements were plotted in R version 3.1.0 (RStudio, Boston, MA, USA) using the package "pheatmap" version 1.0.2. Volocity Quantitation (PerkinElmer, Waltham, MA, USA) was used for quantitative microscopy image analysis, WB images were quantified using Image Studio 3.1.4 (LI-COR, Lincoln, NE, USA) and flow cytometry data was processed with FlowJo vX.0.7 (Tree Star. Ashland, OR, USA). Gene expression data was analyzed with

Partek Genomics Suite 6.6 (Partek, St. Louis, MO, USA) using ANOVA models and GSEA results were plotted by Dr. Thomas Ulas (Life & Medical Sciences Institute (LIMES), University of Bonn, Bonn) using Sigmaplot 12.2 (Systat Software, San Jose, CA, USA).

4 Results

4.1 Targeting cholesterol crystal deposition in atherosclerosis mouse models

Cholesterol crystals (CCs) potently stimulate innate immune cells, such as macrophages, by activating the NLRP3 inflammasome[24,25]. In atherosclerosis mouse models, CCs were found in early atherosclerotic plaques and their presence coincided with the first appearance of innate immune cells in these plaques[24]. Therefore, CC-induced inflammatory responses might contribute to the underlying inflammation that promotes atherosclerosis development and progression. Based on this assumption, it was hypothesized that reducing crystalline cholesterol deposition in atherosclerotic plaques might impede atherogenesis by lowering inflammation.

4.1.1 Genetic deletion of oxLDL uptake receptor CD36

Atherosclerotic plaque formation starts with the accumulation of lipids and lipoproteins in the vessel wall, which causes the infiltration of immune cells such as monocytes. Due to continuous lipid uptake these cells develop into cholesterol-laden macrophage foam cells[115]. CC formation in macrophage foam cells was observed upon accumulation of intracellular free cholesterol *in vitro*[71,116]. However, until recently, the origin of free cholesterol that crystallizes in plaque macrophage foam cells was unknown.

The scavenger receptor CD36 mediates the uptake of oxLDL into macrophages[117]. Furthermore, recognition of oxLDL by CD36 induces the assembly of a TLR heterodimer consisting of TLR4 and TLR6 which subsequently induces an NFκB-mediated inflammatory response[8]. Hence, as CD36 promotes intracellular lipid accumulation and regulates an inflammatory response to modified endogenous ligands, it was linked to the pathogenesis of atherosclerosis. A recent study performed in collaboration with Dr. Frederick Sheedy and Dr. Kathryn J. Moore (New York University School of Medicine, New York, NY, USA) demonstrated that excess cholesterol crystallized in macrophage lysosomes following CD36-mediated uptake of oxLDL[118]. The relevance of this finding for atherosclerosis development was assessed in an atherosclerosis mouse model. $ApoE^{-/-}$ mice and $ApoE^{-/-}$ mice lacking CD36 ($ApoE^{-/-}/CD36^{-/-}$) or one of its signaling partners TLR4 ($ApoE^{-/-}/TLR4^{-/-}$) or TLR6 ($ApoE^{-/-}/TLR6^{-/-}$) were fed a modified Western diet for 12 weeks to induce atherosclerosis. I received aortic root cryosections from these mice for analysis of atherosclerotic plaque size and plaque CC deposition by confocal laser reflection and fluorescence microscopy (Fig. 4-1A). Although the mice had similar serum cholesterol levels[118], $ApoE^{-/-}/CD36^{-/-}$, but also $ApoE^{-/-}/TLR4^{-/-}$and $ApoE^{-/-}/TLR6^{-/-}$ mice had significantly

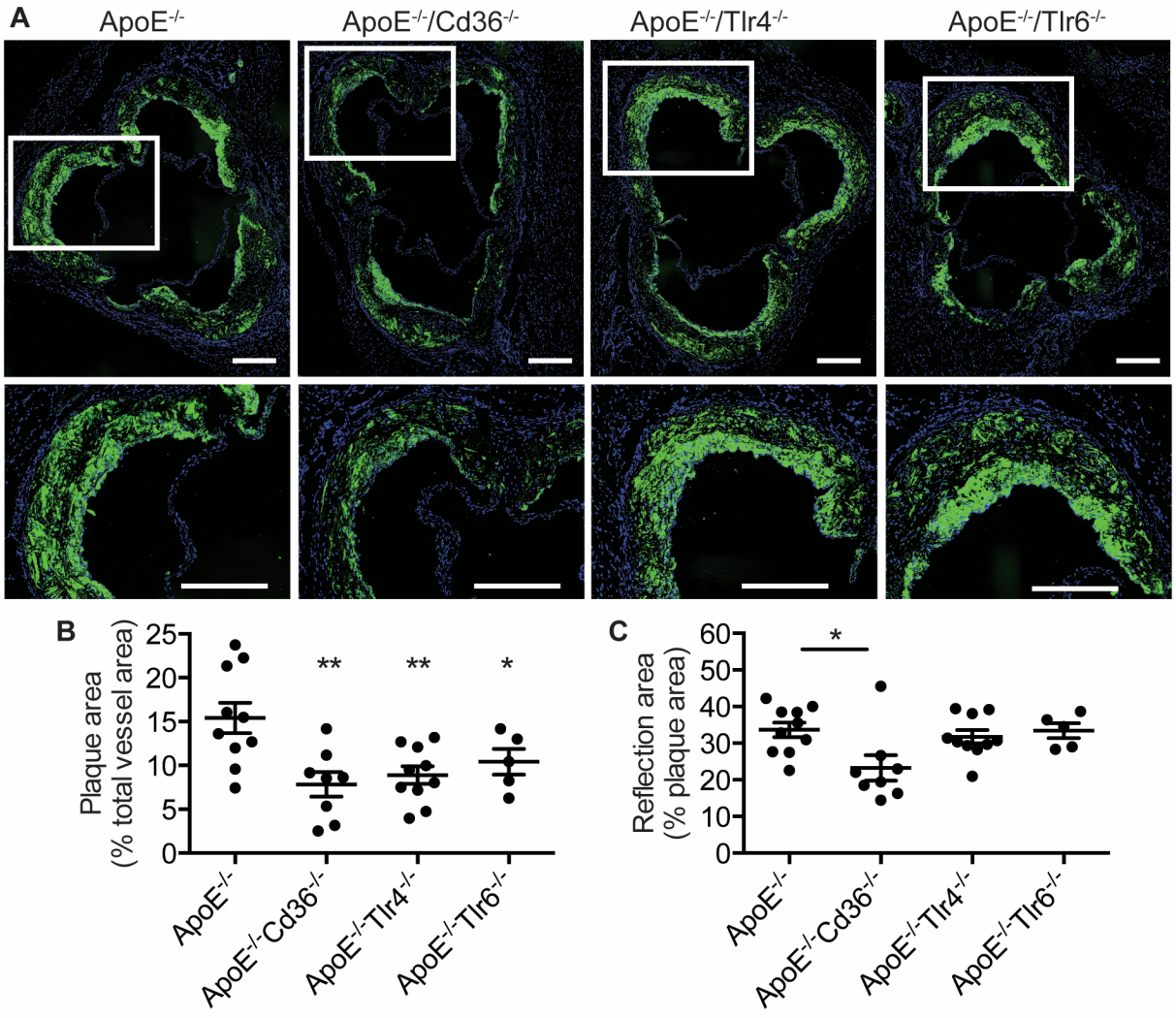

Figure 4-1: Genetic deletion of CD36 reduces plaque CC deposition and impairs murine atherosclerosis development.

ApoE$^{-/-}$ (n=10), ApoE$^{-/-}$/Cd36$^{-/-}$ (n=8), ApoE$^{-/-}$/Tlr4$^{-/-}$ (n=10) and ApoE$^{-/-}$/Tlr6$^{-/-}$ (n=5) mice received a modified Western diet (containing 3 g cholesterol per kg chow; DYET#100244; Dyets) for 12 weeks. All animal work was performed in the laboratory of Dr. Kathryn J. Moore (New York University School of Medicine, New York, NY, USA). Serial aortic root sections were analyzed by confocal laser reflection and fluorescence microscopy. (A) Representative images of each study group with enlarged plaque area in bottom panels; Hoechst 34580 staining for nuclei (blue) and laser reflection signal for CCs (green). Scale bars indicate 200 µm. (B) Quantification of atherosclerotic plaque size depicted as plaque area as percentage of total vessel wall area. (C) Quantification of CC plaque load depicted as reflection area as percentage of plaque area. Data in (B) and (C) are shown as mean ± SEM of two to three individual sections per mouse. Significance was determined by one-way ANOVA comparing each group against the ApoE$^{-/-}$ control group applying Sidak's post test for multiple comparisons (** = p<0.01, * = p<0.05).

smaller atherosclerotic plaques than the ApoE$^{-/-}$ control mice (Fig. 4-1B). Furthermore, these mice had reduced aortic pro-inflammatory cytokine expression as well as reduced pro-inflammatory cytokine levels in the serum[118]. However, a significant reduction of CC deposition was exclusively observed in the plaques of ApoE$^{-/-}$/CD36$^{-/-}$ mice (Fig. 4-1C), which also showed the greatest reduction in atherosclerotic plaque size.

In summary, these data showed that the genetic deletion of CD36, the receptor mediating intracellular cholesterol crystallization, causes a reduction in crystalline cholesterol deposition

in atherosclerotic plaques while limiting inflammation and atherosclerosis development. Hence, these findings supported the working hypothesis of this thesis that CCs represent a valuable therapeutic treatment target in atherosclerosis.

4.1.2 Effects of CD treatment on atherosclerosis development

Since 2-Hydroxypropyl-β-cyclodextrin (CD) has been described to mediate cholesterol depletion from cells, and especially from macrophage foam cells[100,102], the therapeutic potential of CD in murine atherosclerosis was investigated with a particular focus on whether CD affected the amount of CCs present in atherosclerotic plaques. First, the effect of CD treatment on the development and progression of atherosclerosis was assessed in an $ApoE^{-/-}$ mouse model in collaboration with Dr. Sebastian Zimmer and colleagues (see section 3.2.7). $ApoE^{-/-}$ mice were put on a HFHC diet for eight weeks while one group of mice was treated subcutaneously with 2 g CD per kg bodyweight twice a week, whereas the other group was injected with a vehicle control (Fig. 4-2A). For each mouse, parameters like body weight, arterial blood pressure and heart rate were controlled throughout the study period. No differences in these parameters were observed between the two treatment groups (data not shown, personal communication with Dr. Sebastian Zimmer). Serum cholesterol levels of the mice determined at the end of the study revealed a minimal decrease of serum cholesterol in CD-treated mice compared to vehicle-treated mice (Fig. 4-2B).

For assessment of atherosclerosis development, cryosections of the aortic roots of the mice were examined by confocal laser reflection and fluorescence microscopy. Fig. 4-2C shows representative images of aortic roots of three vehicle-treated (left) and three CD-treated (right) mice. Both atherosclerotic plaque size, which is a measure of disease progression, and the abundance of laser reflection signal (green) representing CCs were visually reduced upon CD treatment. Quantitative analysis for atherosclerotic plaque size, CC plaque load, plaque cellularity and plaque macrophage load was performed on three to four sections per mouse. As indicated by the images in Fig. 4-2C, atherosclerotic plaque size (Fig. 4-2D) as well as the amount of CCs inside the plaques (Fig. 4-2E) were significantly reduced upon CD treatment. Although overall plaque cellularity (total number of all cells as determined by nuclear stain) was not changed by CD treatment (Fig. 4-2G), the amount of plaque macrophages was clearly reduced (Fig. 4-2F).

These results indicated that CD treatment effectively impaired atherosclerosis development and progression in mice. Notably, crystalline cholesterol and CD68-positive macrophages were reduced upon CD treatment, suggesting a less inflammatory state of the arterial tissue. In line with this assumption, pro-inflammatory serum cytokines, such as IL-6, TNF-α and IL-1β were also decreased in CD-treated mice (data not shown, Zimmer and Grebe *et al.*, in press).

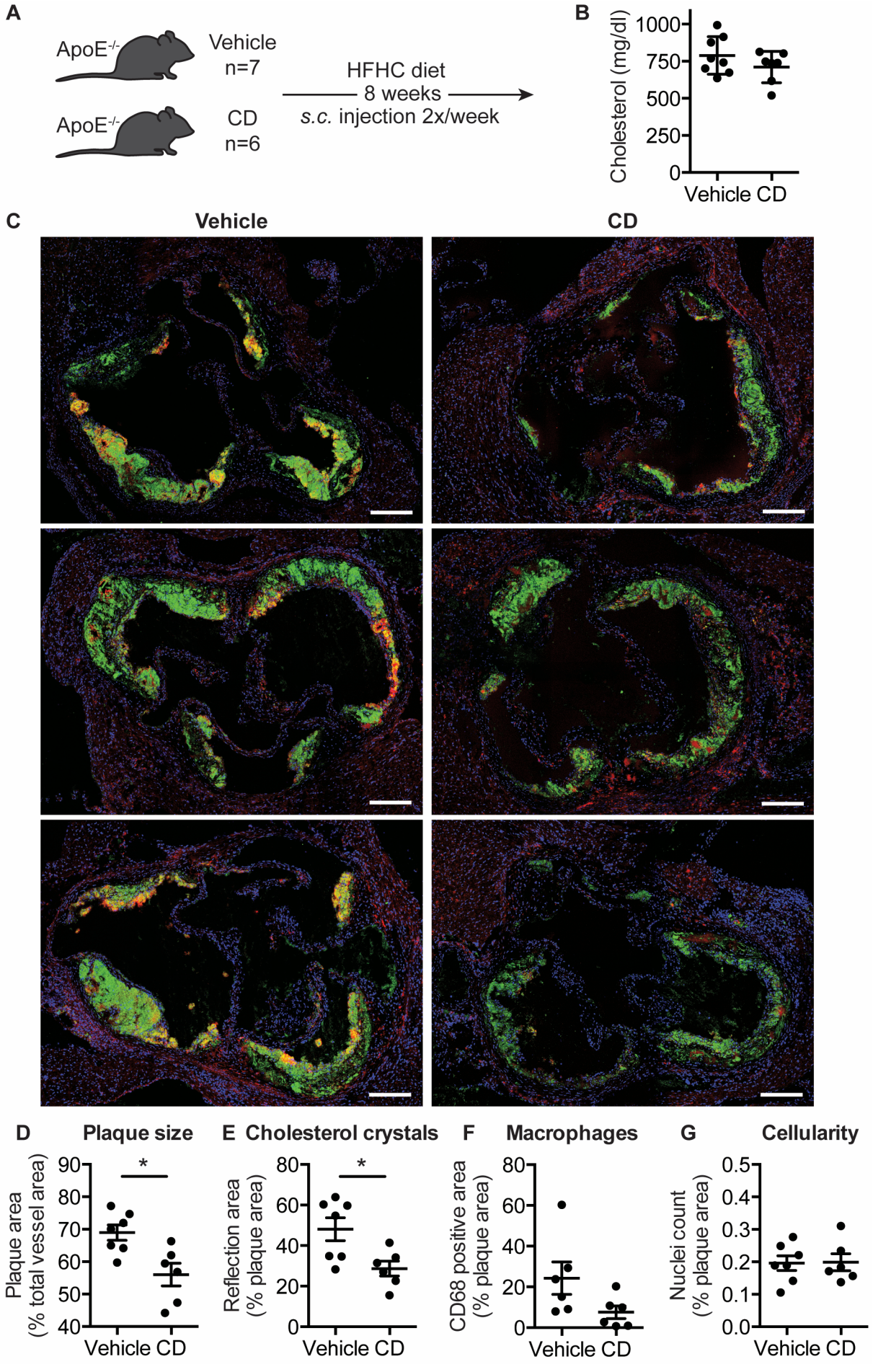
A
ApoE-/-
Vehicle
n=7
ApoE-/-
CD
n=6
HFHC diet
8 weeks
s.c. injection 2x/week
B
Cholesterol (mg/dl)
1000
750
500
250
0
Vehicle CD
C
Vehicle
CD
D
Plaque size
Plaque area (% total vessel area)
90
80
70
60
50
40
*
Vehicle CD
E
Cholesterol crystals
Reflection area (% plaque area)
80
60
40
20
0
*
Vehicle CD
F
Macrophages
CD68 positive area (% plaque area)
80
60
40
20
0
Vehicle CD
G
Cellularity
Nuclei count (% plaque area)
0.5
0.4
0.3
0.2
0.1
0.0
Vehicle CD

Figure 4-2: CD treatment impairs atherosclerosis development and progression in mice.

(A) Schematic of study protocol for the atherosclerosis prevention model. ApoE$^{-/-}$ mice received a HFHC diet for eight weeks accompanied by subcutaneous injections with CD (n=6) or vehicle control (n=7) twice a week. All animal work was performed by Dr. Sebastian Zimmer and colleagues. (B) Serum cholesterol levels after eight weeks of atherogenic diet determined by gas chromatography-flame ionization detection (performed by Prof. Dr. Dr. Dieter Lütjohann and colleagues). Data is shown as mean ± SD. (C-G) Serial aortic root sections were analyzed by confocal laser reflection and fluorescence microscopy. (C) Representative images of both study groups; Hoechst 34580 staining for nuclei (blue), CD68 staining for macrophages (red) and laser reflection signal for CCs (green). Scale bars indicate 200 µm. (D) Quantification of atherosclerotic plaque size depicted as plaque area as percentage of total vessel wall area. (E) Quantification of CC plaque load depicted as reflection area as percentage of plaque area. (F) Quantification of macrophage plaque load depicted as CD68 positive area as percentage of plaque area. (G) Quantification of plaque cellularity depicted as nuclei counts as percentage of plaque area. Data in (D-G) are shown as mean ± SEM of three to four individual sections per mouse. Significance was determined by unpaired two-tailed Student's t-tests with Welch's correction (* = $p<0.05$).

4.1.3 Effects of CD treatment on atherosclerosis regression

In the atherosclerosis prevention model it was observed that CD treatment impairs murine atherosclerosis development and progression. However, atherosclerosis in humans is usually only diagnosed and treated in the advanced stages of the disease. Hence a clinically relevant therapeutic treatment should be efficient in regressing already established atherosclerosis. To investigate whether CD treatment also possesses this important potential of mediating plaque reversion, two mouse models of atherosclerosis regression were performed in collaboration with Dr. Sebastian Zimmer and colleagues (see section 3.2.7). The study protocols of these atherosclerosis regression models are illustrated in Fig 4-3A. In an eight-week pretreatment phase all mice received a HFHC diet to induce advanced atherosclerosis. A pretreatment control group (Ctrl) was sacrificed at this stage to control for the development of advanced atherosclerotic plaques. In the subsequent four-week treatment phase the remaining mice were subcutaneously treated with 2 g CD per kg bodyweight or vehicle control twice a week. During this treatment period, the diet was either switched to a chow diet (Regression A), because patients with diagnosed atherosclerosis are typically advised to reduce their cholesterol intake as well, or the atherogenic HFHC diet was continued (Regression B).

Again, for each mouse, parameters like body weight, arterial blood pressure and heart rate were controlled throughout the study period. Within one regression study group (Regression A or Regression B) no differences in these parameters were observed between CD-treated or vehicle-treated animals (data not shown, personal communication with Dr. Sebastian Zimmer). Serum cholesterol levels of the mice were measured in serum collected from a final blood draw right before sacrifice (Fig. 4-3B). In Regression A (upper panel) a highly significant drop in serum cholesterol levels was observed when comparing the pretreatment control mice (Ctrl) with the two treatment groups (Vehicle and CD). This reduction was caused by the change of diet during the treatment phase. However, within the

two treatment groups, only a minimal decrease of serum cholesterol in CD-treated mice compared to vehicle-treated mice was observed. In Regression B (lower panel) serum cholesterol levels remained unchanged besides the previously observed insignificant decrease of serum cholesterol in CD-treated animals.

Atherosclerosis parameters were assessed by confocal laser reflection and fluorescence microscopy of three to four aortic root cryosections. Representative images are displayed in Fig. 4-3C, demonstrating the induction of advanced atherosclerotic plaques upon 8 weeks of HFHC diet in sections obtained from the pretreatment control group (Ctrl). Furthermore, for both regression models (Regression A and Regression B), a prominent reduction in atherosclerotic plaque size was visually apparent upon CD treatment. This was confirmed by quantitative image analysis where atherosclerotic plaque size was significantly decreased upon CD treatment when compared to the vehicle treatment and the pretreatment control (Ctrl) groups in both regression models (Fig. 4-3D). Analysis of CC plaque load (Fig. 4-3E) revealed that the switch of diets in Regression A already resulted in significantly lower amounts of CCs within the plaques when comparing pretreatment control (Ctrl) and vehicle treatment groups. This change in CC plaque load was not observed under continued HFHC diet (Regression B). However, when comparing CC plaque loads of CD-treated animals to vehicle-treated animals, a significant reduction upon CD treatment was found in both regression models, even in Regression A despite the already decreased basal level of CC plaque content. The data on plaque macrophage load (Fig. 4-3F) looked similar to the data on CC plaque load although this reduction was not statistically significant. In detail, in Regression A, a decrease in the amount of CD68-positive macrophages in the plaques was observed between pretreatment control (Ctrl) and both treatment groups, and thus coincided

Figure 4-3: CD treatment mediates atherosclerosis regression in mice.

(A) Schematic of study protocol for atherosclerosis regression models. ApoE$^{-/-}$ mice received a HFHC diet for eight weeks to induce advanced atherosclerosis. A pretreatment control group (Ctrl; n=8) was sacrificed at this stage; the remaining mice were subcutaneously treated for another four weeks with CD or vehicle control twice a week. During this treatment period, the diet was either switched to a chow diet (Regression A; Vehicle n=7, CD n=7) or the HFHC diet was continued (Regression B; Vehicle n=8, CD n=7). All animal work was performed by Dr. Sebastian Zimmer and colleagues.(B) Serum cholesterol levels determined by gas chromatography-flame ionization detection (performed by Prof. Dr. Dr. Dieter Lütjohann and colleagues). Data is shown as mean ± SD. (C-G) Serial aortic root sections were analyzed by confocal laser reflection and fluorescence microscopy. (C) Representative images of pretreatment control as well as CD and vehicle treatment of both regression models; Hoechst 34580 staining for nuclei (blue), CD68 staining for macrophages (red) and laser reflection signal for CCs (green). Scale bars indicate 200 µm. (D) Quantification of atherosclerotic plaque size depicted as plaque area as percentage of total vessel wall area. (E) Quantification of CC plaque load depicted as reflection area as percentage of plaque area. (F) Quantification of macrophage plaque load depicted as CD68 positive area as percentage of plaque area. (G) Quantification of plaque cellularity depicted as nuclei counts as percentage of plaque area. Data in (D-G) are shown as mean ± SEM of three to four individual sections per mouse. Significance was determined by one-way ANOVA with Tukey's post test for multiple comparisons (*** = $p<0.001$, ** = $p<0.01$, * = $p<0.05$, ns = not significant).

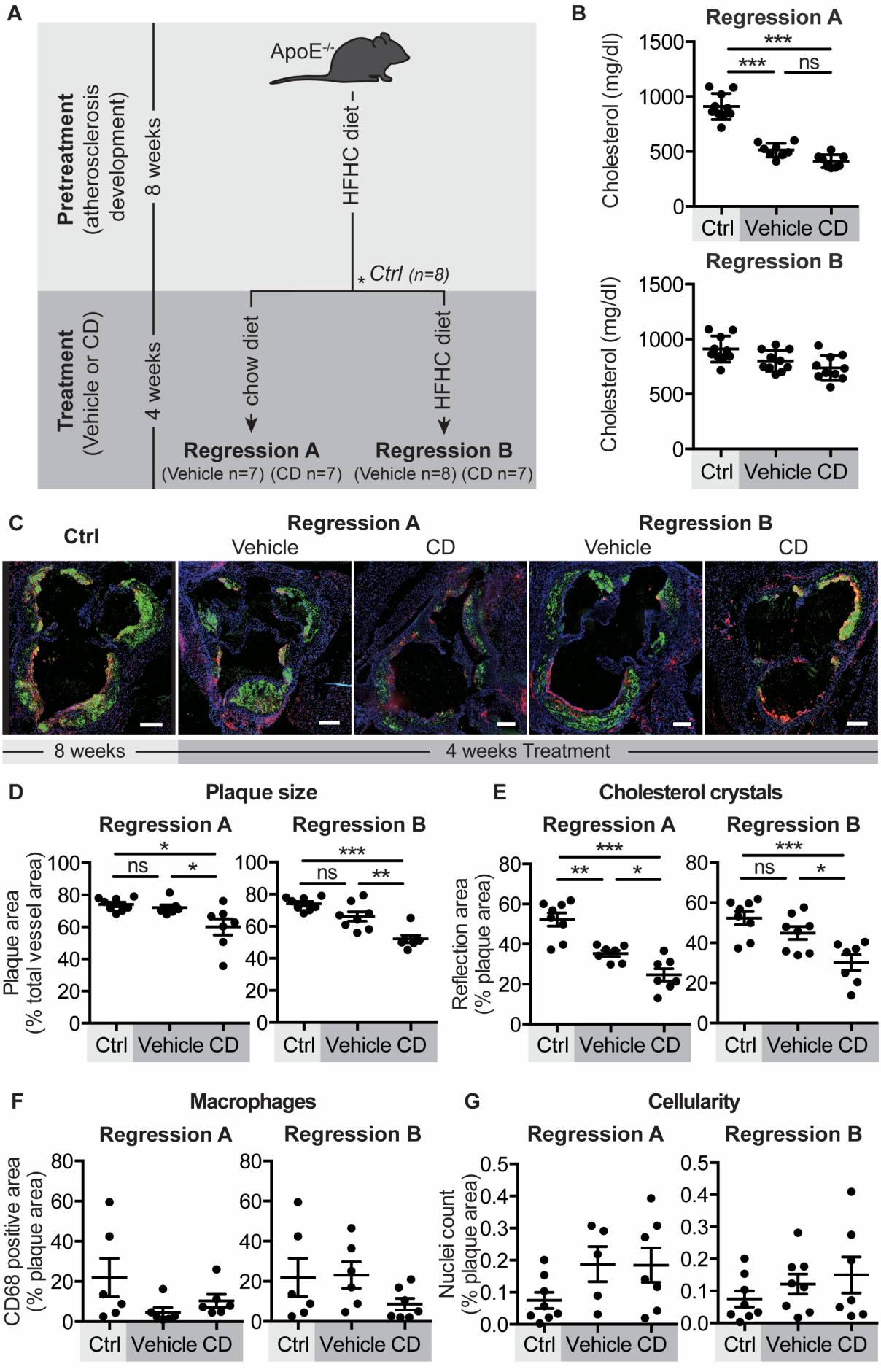
A
ApoE-/-
Pretreatment
(atherosclerosis development)
8 weeks
HFHC diet
* Ctrl (n=8)
Treatment
(Vehicle or CD)
4 weeks
chow diet
HFHC diet
Regression A
(Vehicle n=7) (CD n=7)
Regression B
(Vehicle n=8) (CD n=7)
B
Regression A
Cholesterol (mg/dl)
1500
1000
500
0
***
***
ns
Ctrl
Vehicle CD
Regression B
Cholesterol (mg/dl)
1500
1000
500
0
Ctrl
Vehicle CD
C
Ctrl
Regression A
Vehicle
CD
Regression B
Vehicle
CD
8 weeks
4 weeks Treatment
D
Plaque size
Regression A
Regression B
Plaque area
(% total vessel area)
100
80
60
40
20
0
*
ns
*
***
ns
**
Ctrl
Vehicle CD
E
Cholesterol crystals
Regression A
Regression B
Reflection area
(% plaque area)
80
60
40
20
0
***
**
*
***
ns
*
Ctrl
Vehicle CD
F
Macrophages
Regression A
Regression B
CD68 positive area
(% plaque area)
80
60
40
20
0
Ctrl
Vehicle CD
G
Cellularity
Regression A
Regression B
Nuclei count
(% plaque area)
0.5
0.4
0.3
0.2
0.1
0.0
Ctrl
Vehicle CD

with the change of diet. Here, CD treatment did not reduce but rather slightly increased macrophage plaque load compared to vehicle treatment. In Regression B, where the HFHC diet was continued throughout the treatment phase, the amount of plaque macrophages was not altered in the vehicle treatment group compared to the pretreatment control (Ctrl) group. However, CD treatment reduced the amount of macrophages inside the plaque. Although overall plaque cellularity increased during the 4-week treatment phase, this was not further affected by CD treatment (Fig. 4-3G).

These results confirmed that advanced atherosclerosis was established upon eight weeks of HFHC diet feeding. Beyond that, CD treatment was found to be efficient in mediating the regression of atherosclerotic plaques in mice even under continued administration of the atherogenic diet.

4.2 2-Hydroxypropyl-β-cyclodextrin and cholesterol crystals

The atherosclerosis mouse models showed that CD has beneficial effects on atherosclerosis development and is even efficient in mediating the regression of atherosclerotic plaques. However, the underlying molecular mechanisms of CD-mediated atheroprotection remained unclear. The finding that decreased murine atherosclerosis was accompanied with a reduction in crystalline cholesterol in the plaques supported the hypothesis that CD's cholesterol solubilizing capacities might contribute to its anti-atherogenic properties. Moreover, the fact that CD treatment did not affect serum cholesterol levels, but decreased the amount of CCs in plaques indicated that CD might have more direct effects on plaque CCs than just lowering CC deposition through reduced serum cholesterol levels. While it is well described in the literature that CD molecules can interact with and solubilize cholesterol molecules[99], it was unknown whether CD can also interact with cholesterol in a crystalline state. Therefore, the potential of CD to interact with and potentially mediate the dissolution of crystalline cholesterol was investigated.

4.2.1 Interaction of CD with cholesterol crystals

To test whether CD can interact with cholesterol in a crystalline state, CCs were incubated for 6 hours in fluorescent rhodamine-labeled CD. Incubation was performed at 4°C to allow for binding of rhodamine-labeled CD to crystalline cholesterol while reducing the chance of potential crystal dissolution. The crystals were vigorously washed to remove any unbound rhodamine-labeled CD prior to detection of rhodamine fluorescence by confocal laser reflection and fluorescence microscopy (Fig. 4-4A) as well as flow cytometry (Fig. 4-4B). Both methods confirmed the binding of fluorescent CD molecules to CCs as seen by a strong fluorescence increase in the rhodamine signal (Fig. 4-4B) as well as a clear encapsulation of the crystals by rhodamine-labeled CD (Fig. 4-4A).

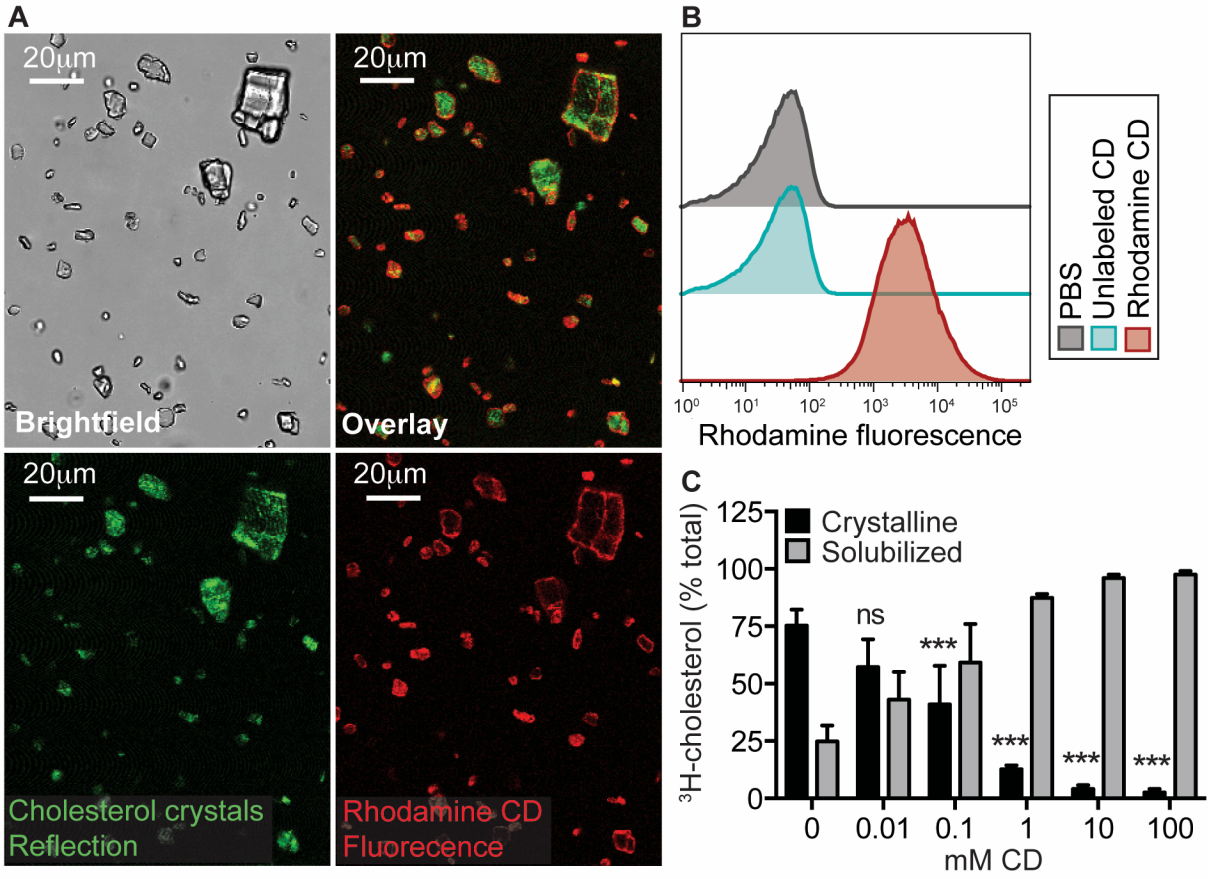

Figure 4-4: CD binds to extracellular CCs and dose-dependently mediates their dissolution.

(A,B) 1 mg CCs were incubated for 6 h shaking at 4°C in 0.5 mM rhodamine-labeled CD, unlabeled CD or PBS as control. (A) Representative images of CCs incubated in rhodamine-labeled CD obtained by confocal laser reflection and fluorescence microscopy. (n=2) (B) Flow cytometric analysis of CCs. Histogram of rhodamine fluorescence is representative of 2 independent experiments. (C) Radioactive ^{3}H-CC were incubated overnight shaking at 37°C in CD solutions of indicated concentrations. The solutions were filtered through 0.22 µm filter plates and ^{3}H-cholesterol was measured in filtrate (solubilized ^{3}H-cholesterol) and retentate (crystalline ^{3}H-cholesterol). Data are shown as mean + SEM of four independent experiments with duplicates. Significance was determined by one-way ANOVA of the crystalline cholesterol fraction comparing each sample with the 0 mM CD control applying Dunnett's post test for multiple comparisons (*** = $p<0.001$, ns = not significant).

To further investigate whether CD can also mediate the dissolution of crystalline cholesterol, a filtration-based dissolution assay with radioactively labeled ^{3}H-CCs was established (see section 3.2.3, Fig. 3-1). First, ^{3}H-CCs were incubated overnight shaking in CD solutions of different concentrations ranging from 0.01 mM to 100 mM. Then the samples were filtered through a 0.22 µm filter to separate the crystalline cholesterol, which is unable to pass through the filter, from the solubilized cholesterol. Hence, subsequent detection of crystal-derived ^{3}H-cholesterol in the filtrate (soluble fraction) as well as in the retentate (crystalline fraction) allowed quantification of CC dissolution. The results revealed that CD dose-dependently dissolved CCs where significant CC dissolution was observed with CD concentrations of 0.1 mM or higher (Fig. 4-4C). In addition, dissolution of extracellular CCs by CD could also be observed by general cell counting methods (Neubauer cell counting

chamber, Tali Image Cytometer), where the crystals simply disappeared upon incubation in concentrated CD solutions (data not shown).

These results demonstrated CD binding to crystalline cholesterol as well as dissolution of extracellular CCs incubated in CD. However, beyond extracellular CCs, atherosclerotic plaques also contain intracellular CCs, mainly inside macrophages[24,119]. Therefore, the capacity of CD to dissolve intracellular CCs was investigated next. Beforehand, the cytotoxicity of CD on murine macrophages in *in vitro* experiments was tested in a time- and dose-dependent manner. Both normocholesterolemic immortalized macrophages (iMOs) (Fig. 4-5A) and CC-loaded hypercholesterolemic iMOs (Fig. 4-5B) were incubated for up to 48 hours with increasing CD concentrations up to 50 mM CD. CD incubation showed dose- and time-dependent effects on macrophage viability under both conditions. Cell viability was drastically decreased upon incubation with CD concentrations higher than 10 mM (dashed lines), especially in normocholesterolemic macrophages. Similar results were obtained when cell viability was determined in normo- or hypercholesterolemic bone marrow-derived macrophages (BMDMs) (data not shown). Here, even a slight improvement of cell viability was observed with low CD concentrations between1.5 and 10 mM. Since macrophage viability was not considerably impaired upon incubation with 10 mM CD for up to 48 hours in both macrophage cell types, this concentration (10 mM) was used for all further *in vitro* experiments in macrophages.

Next, the uptake of CD into macrophages as a prerequisite for intracellular CC dissolution by CD was investigated. CC-loaded macrophages were incubated with fluorescent rhodamine-

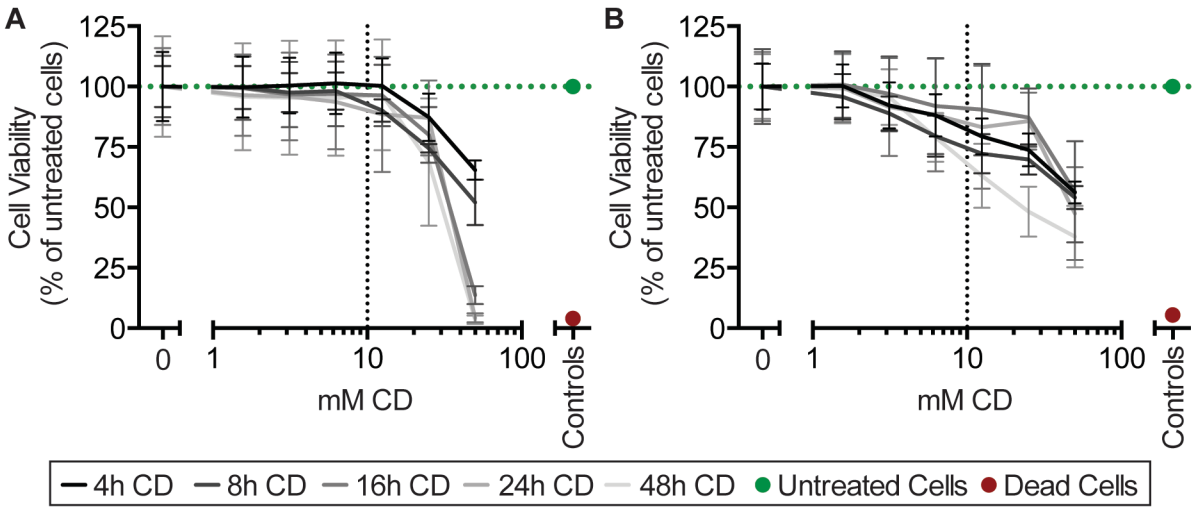

Figure 4-5: Dose- and time-dependent effects of CD incubation on macrophage viability.

(A) Normocholesterolemic BALB/c iMOs or (B) BALB/c iMOs loaded with 200 µg CCs per $1x10^6$ cells overnight were treated for indicated times with different concentrations of CD ranging from 50 mM to 1.5625 mM. Cell viability was determined by CTB Viability Assay. Untreated cells served as positive control and 70% EtOH-treated cells were used as negative control. Dashed line indicates commonly used CD concentration (10 mM). Data are shown as mean ± SEM of three independent experiments with duplicates.

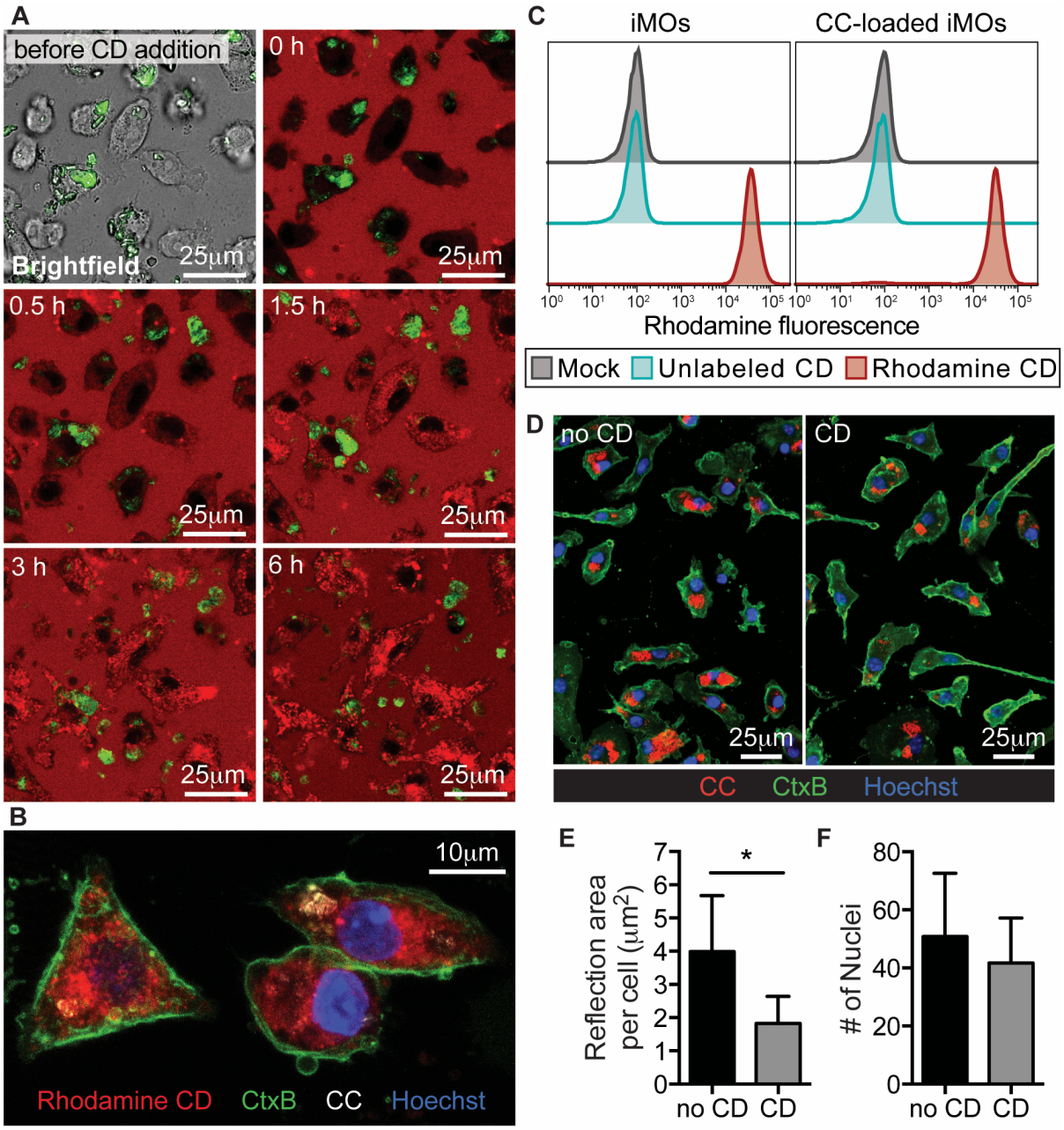

Figure 4-6: CD is internalized by macrophages and mediates intracellular CC dissolution.

(A-C) Untreated or CC-loaded C57BL/6 iMOs were incubated for 6 h in a 1 mM CD solution containing one-tenth rhodamine-labeled CD. (A) Representative images of rhodamine-labeled CD accumulation in CC-loaded macrophages over time obtained by confocal live cell imaging. (n=2) (B) Representative Z-stack image (maximum intensity projection) of CC-loaded macrophages obtained by confocal laser reflection and fluorescence microscopy following 6h rhodamine-labeled CD incubation; rhodamine-labeled CD (red), Hoechst 34580 staining for nuclei (blue), CtxB A488 staining for cell membranes (green) and laser reflection signal for CCs (white). (n=2) (C) Flow cytometric analysis of macrophages treated with rhodamine-labeled CD, unlabeled CD or medium control. (n=1) (D-F) WT BMDMs were loaded with 100 µg CC per $1x10^6$ cells for 3 h prior to 24 h incubation with 10 mM CD or medium control. (D) Representative images obtained by confocal laser reflection and fluorescence microscopy; Hoechst 34580 staining for nuclei (blue), CtxB A647 staining for cell membranes (green) and laser reflection signal for CCs (red). (E) Quantification of intracellular crystal reflection area per cell. (F) Number of analyzed cells indicated by number of counted nuclei. Data presented in (E) and (F) are shown as mean + SEM of four independent experiments where 10-15 individual fields of view were analyzed. Significance was determined using (E) a ratio paired one-tailed t-test or (F) a ratio paired two-tailed t-test (* = $p<0.05$).

labeled CD and confocal live cell imaging was performed to track CD uptake (Fig. 4-6A). The brightfield image acquired right before addition of rhodamine-labeled CD was used as a reference for macrophage localization. Thus, upon addition of rhodamine-labeled CD (0 h) a negative representation of the cells (black areas within red background stain) can be observed. The cells accumulated rhodamine-labeled CD over time as seen by an increase of rhodamine fluorescence in the previously black areas. The fluorescent signal shows a cytoplasmic, dotted pattern leaving a black spot representing the nucleus, which indicated uptake of rhodamine-labeled CD into cytoplasmic cellular compartments. Following live cell imaging the cells were washed and stained with CtxB for visualization of the cell membranes as well as Hoechst for visualization of the nuclei. Examination of maximum intensity projections of Z-stack images obtained by confocal laser reflection and fluorescence microscopy confirmed the uptake and the previously observed cellular distribution of rhodamine-labeled CD (Fig. 4-6B). Some overlap with the intracellular CC reflection signal was observed, particularly in 3D reconstructions of the Z-stack images (data not shown), but image resolution was not good enough to unequivocally prove interaction between CD and intracellular crystalline cholesterol. Flow cytometric analysis of CC-loaded macrophages or resting macrophages revealed a strong fluorescence increase in the rhodamine signal upon incubation with rhodamine-labeled CD (Fig. 4-6C) verifying that CD was efficiently taken up into macrophages.

Intracellular CC dissolution by CD in macrophages was finally investigated by confocal laser reflection and fluorescence microscopy of CC-loaded BMDMs following 24 hours of CD or control treatment. A reduction in the crystal reflection signal (CC) upon CD treatment was clearly visible (Fig. 4-6D), already indicating the dissolution of intracellular CCs by CD. To quantify this, the amount of intracellular reflection signal representing crystalline cholesterol was determined by quantitative image analysis from 10-15 randomly acquired fields of view (see section 3.2.10, Fig. 3-3). CD treatment significantly decreased the amount of intracellular CCs (Fig. 4-6E) while the amount of analyzed cells was not considerably different (Fig. 4-6F). Similar results were observed in a single experiment using C57BL/6 iMOs, although intracellular CC dissolution by CD was slightly more efficient in BMDMs (data not shown). In summary, these results indicated that CD has the capacity to mediate the dissolution of intracellular CCs in macrophages.

4.2.2 Fate of crystal-derived cholesterol in macrophages

In the previous section it was demonstrated that CD mediates intracellular CC dissolution. However, CC uptake and subsequent dissolution by CD presumably cause excessive accumulation of free cholesterol inside the macrophages. Intracellular accumulation of free cholesterol is known to be cytotoxic[57], but no cytotoxic effects were observed in CC-loaded

macrophages upon treatment with 10 mM CD for 24 hours (see Fig. 4-5B). This suggested that the cholesterol derived from the crystals must either be converted into cholesterol esters, the nontoxic storage form of cholesterol that is deposited in lipid droplets, or it must be eliminated from the cells[58]. Therefore, the fate of the crystal-derived cholesterol inside the macrophages upon CD treatment was investigated.

Firstly, the potential of CD to promote esterification and storage of crystal-derived cholesterol was examined. The formation of lipid droplets in CC-loaded macrophages following 24 hours of CD incubation was microscopically assessed using the lipid droplet dye LD540[109]. The representative microscopy images in Fig. 4-7A demonstrate that upon CD treatment the

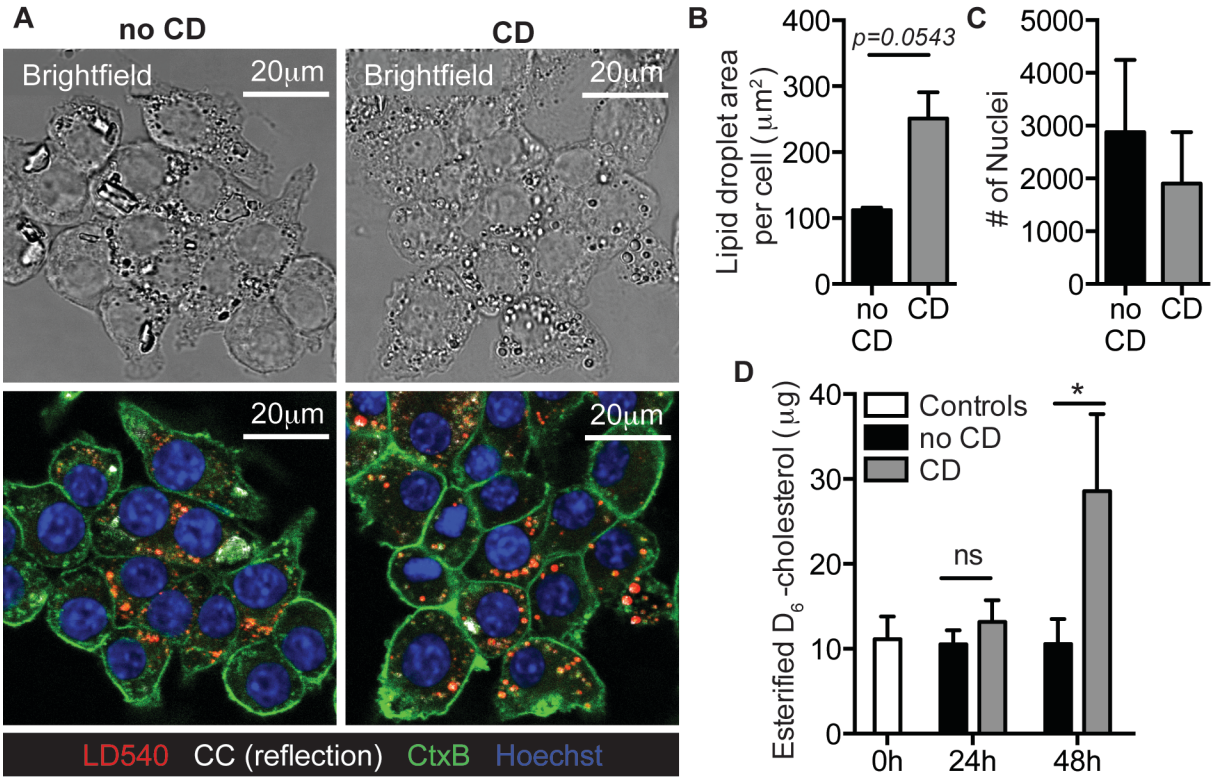

Figure 4-7: CD increases lipid droplet formation in CC-loaded macrophages and promotes esterification of crystal-derived cholesterol.

(A-C) C57BL/6 iMOs were loaded with 100 µg CC per 1x10^6 cells for 3 h prior to 24 h incubation with 10 mM CD or medium control. (A) Representative images obtained by confocal laser reflection and fluorescence microscopy; Hoechst 34580 staining for nuclei (blue), CtxB A647 staining for cell membranes (green), laser reflection signal for CCs (white) and LD540 staining for lipid droplets (red). (B) Quantification of lipid droplets depicted as LD540 positive area per cell. (C) Number of analyzed cells indicated by number of counted nuclei. Data presented in (B) and (C) are shown as mean + SEM of three independent experiments where 10 individual fields of view were analyzed. P-values were calculated using a ratio paired two-tailed t-test. (D) C57BL/6 iMOs were loaded with 200 µg D_6-CC per 1x10^6 cells for 3 h prior to 24 h or 48 h incubation with 10 mM CD or medium control. Before addition of CD a 0 h control sample was harvested. Degree of esterification of D_6-cholesterol was determined by GC-MS-SIM (performed by Prof. Dr. Dr. Dieter Lütjohann and colleagues) and used to calculate the amount of esterified D_6-cholesterol. Data are shown as mean + SEM of four independent experiments with duplicates. Significance was determined by one-way ANOVA comparing no CD versus CD with Sidak's post test for multiple comparisons (* = $p<0.05$, ns = not significant).

square-edged intracellular structures in the brightfield representing CCs (see laser reflection signal) disappear, whereas the spherical structures in the brightfield, representing lipid droplets as confirmed by LD540 staining, accumulate inside the cells. Quantitative image analysis of the intracellular LD540 stain showed an increase in lipid droplet area per cell following CD treatment (Fig. 4-7B), while the number of cells analyzed was not considerably different (Fig. 4-7C).

However, although this experiment showed that CD treatment increased lipid droplet formation, the origin of esterified cholesterol inside the lipid droplets was not clear. Therefore, to monitor the esterification of crystal-derived cholesterol in particular, macrophages were loaded with stable isotope-labeled D_6-CCs. This allows the discrimination of crystal-derived D_6-cholesterol from unlabeled endogenous cholesterol by GC-MS-SIM. Thus, D_6-CC-loaded macrophages were treated for 24 hours or 48 hours with CD or medium as control and the amount and degree of esterification of crystal-derived D_6-cholesterol were determined by GC-MS-SIM (see section 3.2.15), which was then used to back calculate the amount of esterified D_6-cholesterol per sample. CD treatment of D_6-CC-loaded macrophages for 48 hours significantly increased the esterification of D_6-cholesterol compared to non-CD treated cells (Fig. 4-7D). Taken together, these data indicated that CD treatment of CC-loaded macrophages promotes the intracellular esterification and storage of crystal-derived cholesterol.

Next, it was investigated whether crystal-derived cholesterol is eliminated from the macrophages upon CD treatment. For this, macrophages loaded with D_6-CCs were incubated with CD or medium control for 24 hours or 48 hours and the distribution of crystal-derived D_6-cholesterol was determined in the cells and the cell culture supernatants (Fig. 4-8A). The 0 hour control bars show the distribution of D_6-cholesterol right after loading the cells with D_6-CCs. Comparing the medium control samples to the 0 hour control sample, a decrease of D_6-cholesterol was observed in the cells and consequently D_6-cholesterol increased in the supernatants over time. This indicated that macrophages alone are able to dissolve CCs to a low extent and to export the crystal-derived cholesterol out of the cells. This basal efflux of crystal-derived cholesterol was significantly increased at 24 hours when macrophages were treated with CD. However, longer CD treatment did not further increase D_6-cholesterol efflux from the macrophages suggesting that the maximum CD-mediated cholesterol efflux capacity is reached at 24 hours.

Unexpectedly, analysis of unlabeled cholesterol in the same samples showed no effect of CD treatment on unlabeled, cellular cholesterol levels (Fig. 4-8B). A non-significant reduction of cellular cholesterol was observed upon incubation with CD for 24 hours, but no change was visible upon 48 hours. This suggested that CD specifically depletes crystal-derived cholesterol, but in contrast to D_6-cholesterol, which can only be derived from D_6-CCs, the

origin of the unlabeled cholesterol measured by GC-MS-SIM is unknown. Thus, the lack of CD-mediated depletion of unlabeled, cellular cholesterol might be due to cellular cholesterol being replenished by *de novo* synthesis or by uptake of excess cholesterol from the FCS-containing cell culture medium.

Export of free cholesterol from macrophages is primarily mediated by the cholesterol efflux transporters ABCA1 and ABCG1, which transfer the cholesterol to ApoA-1 or HDL particles, respectively[58]. To determine whether the addition of HDL as cholesterol acceptor can

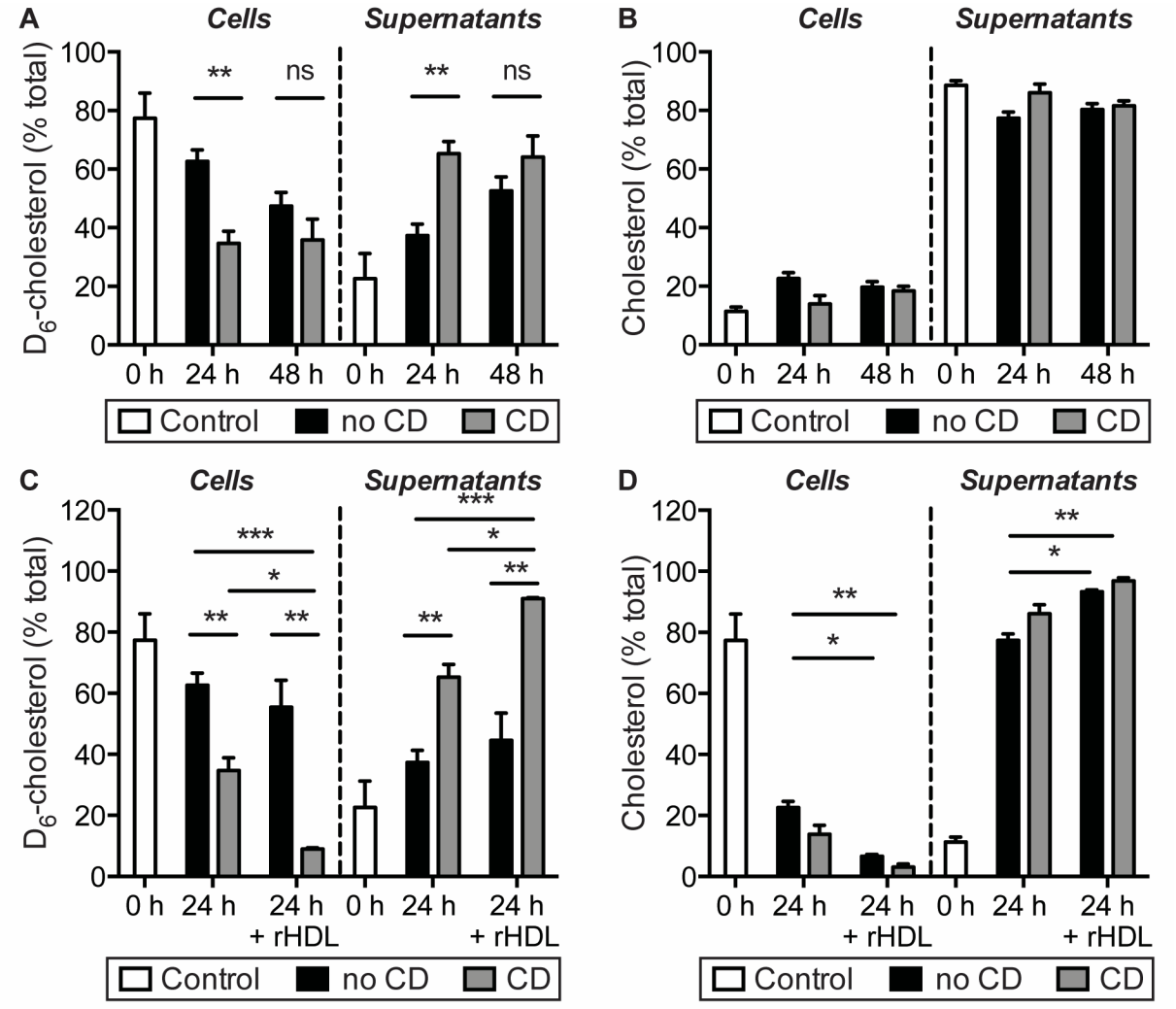

Figure 4-8: CD mediates efflux of crystal-derived cholesterol from macrophages, which is augmented by addition of rHDL.

C57BL/6 iMOs were loaded with 200 µg D_6-CC per $1x10^6$ cells for 3 h prior to incubation with 10 mM CD or medium control for indicated times. Cells and supernatants were harvested and analyzed for the presence of crystal-derived D_6-cholesterol and unlabeled cholesterol determined by GC-MS-SIM (performed by Prof. Dr. Dr. Dieter Lütjohann and colleagues). Before addition of CD a 0 h control sample was harvested to assess the distribution of D_6-cholesterol right after D_6-CC loading of the cells. (A) D_6-cholesterol and (B) cholesterol distribution following CD or control treatment. Data are shown as mean + SEM of four independent experiments with duplicates. (C) D_6-cholesterol and (D) cholesterol distribution upon 24 h CD or control treatment along with 0.25 mg/ml rHDL. Data are shown as mean + SEM of two independent experiments with duplicates. Significance was determined by one-way ANOVA with Tukey's post test for multiple comparisons (*** = $p<0.001$, ** = $p<0.01$, * = $p<0.05$, ns = not significant).

enhance the CD-mediated efflux of crystal-derived cholesterol, reconstituted HDL (rHDL) with low cholesterol content was added together with CD to D_6-CC-loaded macrophages. While rHDL incubation for 24 hours did not mediate the efflux of D_6-cholesterol by itself, it significantly reduced cellular D_6-cholesterol when added in combination with CD (Fig. 4-8C). These results confirmed that the addition of rHDL as cholesterol acceptor could boost CD-mediated efflux of crystal-derived cholesterol. However, while on initial observation this data conflicts with the current literature, where HDL is described to deplete cellular cholesterol[120,121], when analyzing unlabeled, cellular cholesterol in these cells, rHDL treatment alone and in combination with CD did indeed significantly reduce total cellular cholesterol levels (Fig. 4-8D). This indicated that CD is required for mobilizing the crystalline D_6-cholesterol for HDL-mediated efflux out of the macrophages.

The previous results demonstrated that CD mediates the dissolution of intracellular CCs and subsequently promotes esterification for intracellular storage as well as efflux of crystal-derived cholesterol. Free cholesterol can be further metabolized to other bioactive derivatives, such as oxysterols including 27-hydroxcholesterol (HC), 24(S)-HC and 25-HC. To assess whether CD treatment affects oxysterol production, crystal-derived and cellular 24(S)-HC and 27-HC were also analyzed by GC-MS-SIM. While both oxysterols were similarly regulated by CD treatment (data not shown), only the production of 27-HC, which was more efficiently produced in macrophages, was significantly affected by CD treatment. Therefore, the effects of CD treatment on crystal-derived and cellular 27-HC production were further investigated.

For detection of D_6-CC-derived 27-HC by GC-MS-SIM it needs to be considered that hydroxylation at the 27-position of the D_6-cholesterol molecule removes one deuterium atom, resulting in D_5-27-HC. When measuring this crystal-derived metabolite in D_6-CC-loaded macrophages (Fig. 4-9A), no crystal-derived D_5-27-HC was detectable right after macrophage loading with D_6-CC (0 h Ctrl), but the production of small amounts of D_5-27-HC was observed over time in control-treated cells (no CD). This again indicated that macrophages themselves are able to dissolve some crystalline cholesterol to a low extent, subsequently allowing the enzymatic conversion of crystal-derived cholesterol to oxysterols. However, when D_6-CC-loaded macrophages were incubated with CD for 24 hours or 48 hours, D_5-27-HC production was significantly increased compared to the respective control-treated (no CD) samples. The majority of D_5-27-HC was found in the supernatants of the cells, but as cholesterol 27-hydroxylase, the enzyme responsible for the conversion of cholesterol to 27-HC, is a mitochondrial enzyme[122], 27-hydroxylation must happen inside the cells followed by efflux of the resultant oxysterols.

The conversion of unlabeled, cellular cholesterol to 27-HC was also analyzed in the same samples (Fig. 4-9B). CD treatment also promoted 27-HC production from unlabeled, cellular

cholesterol in D_6-CC-loaded macrophages. Taken together, these data suggested that CD treatment promotes 27-hydroxylation of cholesterol in general, rather than just increasing the total pool of cellular cholesterol available for enzymatic conversion into 27-HC by dissolution of intracellular CCs. To assess whether these observations could be explained by a general induction of cholesterol 27-hydroxylase (encoded by the gene Cyp27a1) by CD treatment, expression of this enzyme was analyzed in CC-loaded macrophages at the transcriptional

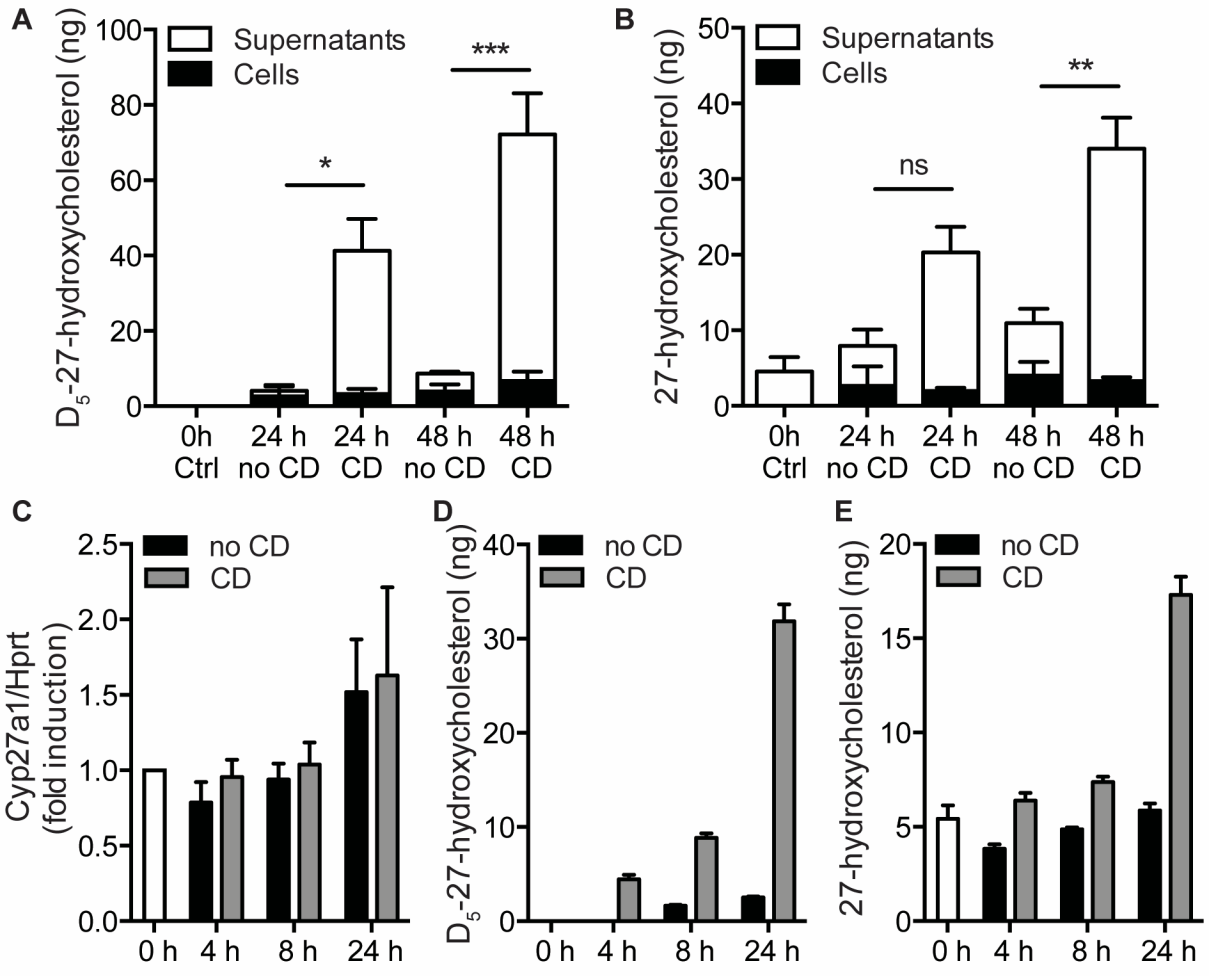

Figure 4-9: CD induces the production of 27-HC independent of Cyp27a1 expression levels.

(A,B) C57BL/6 iMOs were loaded with 200 µg D_6-CC per $1x10^6$ cells for 3 h prior to 24 h or 48 h incubation with 10 mM CD or medium control. Cells and supernatants were harvested and analyzed for the presence of (A) crystal-derived D_5-27-HC and (B) cellular 27-HC by GC-MS-SIM (performed by Prof. Dr. Dr. Dieter Lütjohann and colleagues). Before addition of CD a 0 h control sample was harvested. Data are shown as mean + SEM of three independent experiments with duplicates. Significance was determined by one-way ANOVA with Tukey's post test for multiple comparisons (*** = $p<0.001$, ** = $p<0.01$, * = $p<0.05$, ns = not significant). (C-E) WT BMDMs were loaded with 100 µg CC per $1x10^6$ cells overnight prior to incubation with 10 mM CD or medium control for 4 h, 8 h or 24 h. (C) Cyp27a1 mRNA levels relative to the reference gene Hprt assessed by RT-qPCR and presented as fold induction of the 0 h control. Data are shown as mean + SEM of three independent experiments with technical duplicates. (D,E) Cells and supernatants were harvested and analyzed for the presence of (D) crystal-derived D_5-27-HC and (E) cellular 27-HC by GC-MS-SIM (performed by Prof. Dr. Dr. Dieter Lütjohann and colleagues). Before addition of CD a 0 h control sample was harvested. Data are shown as mean + SD of one experiment with triplicates.

level (Fig. 4-9C). However, no changes in Cyp27a1 mRNA abundance were observed upon CD treatment compared to the respective untreated cells (Fig. 4-9C). As the expression of cholesterol 27-hydroxylase was analyzed in CC-loaded BMDMs, whereas the 27-hydroxylation product was determined in D_6-CC-loaded iMOs, a single experiment was performed to confirm that CD also promotes 27-hydroxylation of crystal-derived and cellular cholesterol in BMDMs. A slight time-dependent increase in D_5-27-HC (Fig. 4-9D) and 27-HC (Fig. 4-9E) was observed in control cells. However, CD treatment again strongly increased the production of both, crystal-derived D_5-27-HC and unlabeled, cellular 27-HC, thus confirming the observations in iMOs in primary BMDMs. Protein expression of cholesterol 27-hydroxylase was also assessed in one experiment using CC-loaded iMOs, but no changes were observed following CD treatment (data not shown) matching the findings on Cyp27a1 mRNA expression in BMDMs. These results indicated that CD promotes 27-hydroxylation of crystal-derived and cellular cholesterol independent of cholesterol 27-hydroxylase expression levels, which was confirmed in both iMOs and primary BMDMs.

In summary, the data presented in this section showed that CD treatment of CC-loaded macrophages mediates the dissolution of intracellular CCs and subsequently promotes the esterification, metabolism to oxysterols such as 27-HC and efflux of crystal-derived cholesterol. CD-mediated efflux of crystal-derived cholesterol could also be further enhanced by addition of rHDL indicating active export of crystal-derived cholesterol via the cholesterol efflux transporters ABCA1 and ABCG1.

4.3 Induction of LXR gene expression by 2-hydroxypropyl-β-cyclodextrin

The observation that CD mediated extra- and intracellular CC dissolution and subsequently promoted cellular efflux of crystal-derived cholesterol strongly supported the working hypothesis that lowering plaque CC loads, presumably through CC dissolution and cholesterol elimination from the tissue, might contribute to CD's anti-atherogenic properties. Moreover, the finding that CD promoted the production of 27-HC in CC-loaded, hypercholesterolemic macrophages provided further insight into the potential molecular mechanisms of the beneficial effects of CD treatment on murine atherosclerosis.

27-HC is one of the oxysterols known to activate LXR transcription factors[123]. LXR transcription factors in turn activate gene expression programs controlling cholesterol efflux and negatively regulating inflammatory responses[64]. Both, cholesterol efflux and inflammation play a critical role in atherosclerosis and activation of LXR transcription factors by synthetic LXR agonists was shown to be protective against atherosclerosis development[116,124]. Therefore, it was hypothesized that the increased production of the

endogenous LXR ligand 27-HC in response to CD treatment might contribute to the observed anti-atherogenic effects of CD in mice.

4.3.1 Regulation of cholesterol efflux transporters by CD

Macrophages mainly export free cholesterol via the cholesterol efflux transporters ABCA1 and ABCG1[58]. As these transporters were previously described as LXR target genes[125-127] and CD was found to promote the production of the endogenous LXR agonist 27-HC, the expression of ABCA1 and ABCG1 was investigated as an indication of CD-mediated LXR transcription factor activation.

First, changes in the abundance of Abca1 and Abcg1 mRNA transcripts were determined by RT-qPCR in BMDMs treated with CD or medium control for 8 hours (Fig. 4-10A). Treatment with the synthetic LXR agonist T09 confirmed the LXR-induced upregulation of both cholesterol efflux transporter genes. CD treatment of normocholesterolemic BMDMs did not affect Abca1 and Abcg1 gene expression, while CC-loading of the macrophages already resulted in increased Abca1 and Abcg1 expression levels, presumably as normal cellular response to cholesterol overload[128,129]. However, CD treatment of CC-loaded macrophages clearly resulted in a further upregulation of Abca1 and Abcg1 gene expression. Furthermore,

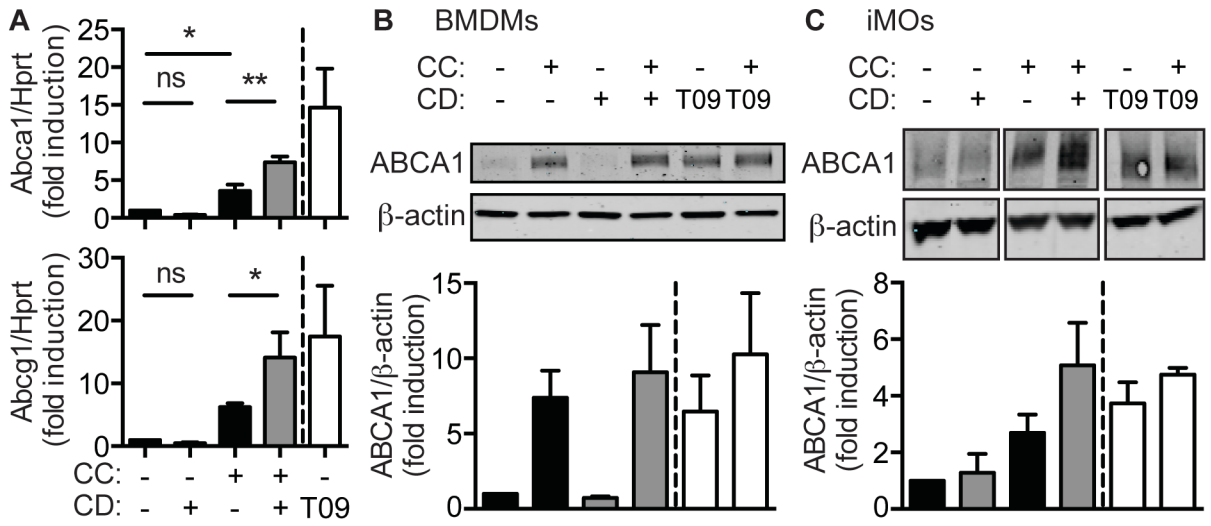

Figure 4-10: CD induces expression of cholesterol efflux transporters in macrophages.

(A) WT BMDMs were partially loaded with 100 µg CC per $1x10^6$ cells overnight prior to 8 h incubation with 10 mM CD or medium control. Incubation with 10 µM T0901317 (T09) for 24 h was used as positive control. Abca1 and Abcg1 mRNA levels relative to the reference gene Hprt assessed by RT-qPCR and presented as fold induction of the untreated cells. (B, C) ABCA1 protein expression was analyzed by western blot in (B) WT BMDMs partially loaded with 100 µg CC per $1x10^6$ cells and (C) C57BL/6 iMOs partially loaded with 200 µg CC per $1x10^6$ cells for 3h prior to 24 h incubation with 10 mM CD, 10 µM T0901317 (T09) or medium control. β-actin expression was used as loading control. Data are presented as representative blot and densitometry analysis of (A) two and (B) four independent experiments (mean + SD). Data are shown as mean + SEM of four independent experiments with technical duplicates. Significance was determined by one-way ANOVA with Tukey's post test for multiple comparisons (** = $p<0.01$, * = $p<0.05$, ns = not significant).

ABCA1 protein expression was analyzed upon 24h CD treatment in normocholesterolemic or CC-loaded, hypercholesterolemic BMDMs (Fig. 4-10B). Again, CC-loading already enhanced ABCA1 protein expression, which was significantly enhanced upon CD treatment of CC-loaded BMDMs. ABCA1 protein levels in CD-treated, CC-loaded macrophages were comparable to ABCA1 induction by the synthetic LXR agonist T09. As most of the GC-MS-SIM analyses were performed in samples derived from iMOs, CD-mediated effects on ABCA1 protein expression were also confirmed in these cells (Fig. 4-10C). In summary, CD treatment of CC-loaded macrophages, similar to LXR agonist treatment, resulted in increased expression of the cholesterol efflux transporters ABCA1 and ABCG1.

4.3.2 Genome-wide analysis of LXR target gene expression in macrophages following CD treatment

To further confirm whether CD promotes LXR activation, global LXR target gene expression in macrophages following CD treatment was investigated using genome-wide gene expression analysis, which was performed in collaboration with Prof. Dr. Joachim Schultze and colleagues (see sections 3.2.21 and 3.2.22). For this, BMDMs prepared from bone marrow of WT and LXRα$^{-/-}$/LXRβ$^{-/-}$ mice were either loaded with CCs or left untreated before incubation in CD or medium alone for six hours.

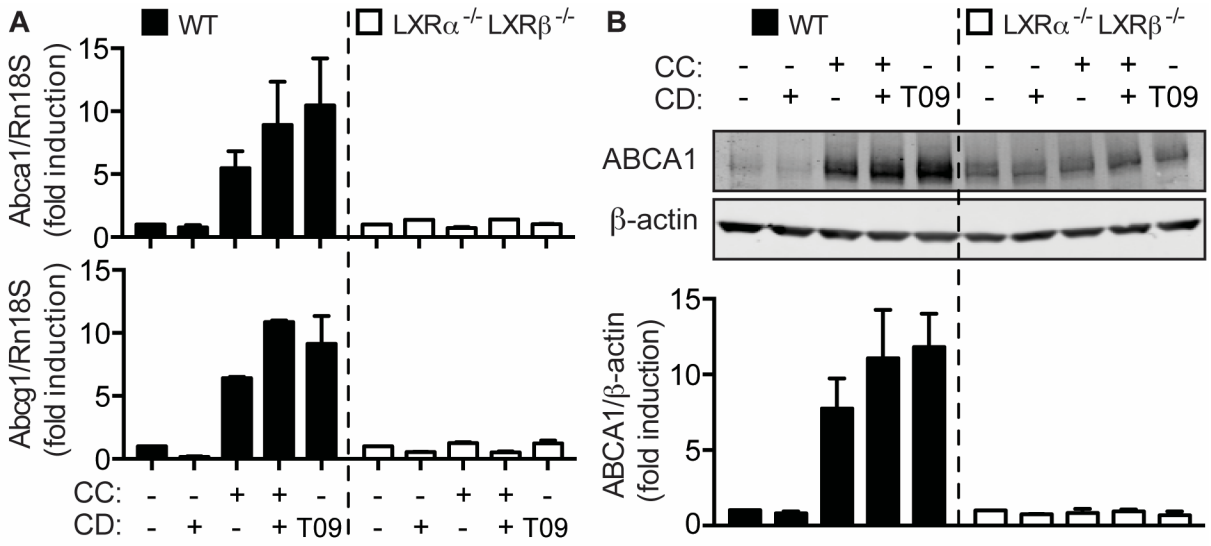

Figure 4-11: CD-mediated upregulation of cholesterol efflux transporters is LXR-dependent.

BMDMs generated from WT and LXRα$^{-/-}$/LXRβ$^{-/-}$ mice were partially loaded with 100 µg CC per 1x10^6 cells overnight prior to (A) 6 h or (B) 24 h incubation with 10 mM CD or medium control. Incubation with 10 µM T0901317 (T09) for 24 h was used as positive control. (A) Abca1 and Abcg1 mRNA levels relative to the reference gene Rn18S assessed by Taqman RT-qPCR and presented as fold induction of untreated cells of the respective genotype. Taqman RT-qPCR was run by Niklas Bode. Data are shown as mean + SEM of one experiment with two individual mice per genotype and technical duplicates. (B) ABCA1 protein expression analyzed by western blot. β-actin expression was used as loading control. Data are presented as representative blot and densitometry analysis of one experiment with three individual mice per genotype (mean + SD).

Prior to microarray analysis, quality controls of the cells and isolated RNAs were performed. The RNA isolated for microarray analysis was examined for Abca1 and Abcg1 gene expression (Fig. 4-11A), and in parallel to microarray sample preparation, some WT and LXRα$^{-/-}$/LXRβ$^{-/-}$ BMDMs were also analyzed for ABCA1 protein expression following 24 hours of CD treatment (Fig. 4-11B). The results of both these quality control analyses confirmed the previously observed induction of cholesterol efflux transporter expression at both the mRNA and protein level following CD treatment of WT BMDMs. Furthermore, despite basally higher levels of ABCA1 and ABCG1 expression (due to normalization to respective untreated control only visible in ABCA1 WB in Fig. 4-11B), no changes in cholesterol efflux transporter expression were observed in LXRα$^{-/-}$/LXRβ$^{-/-}$ BMDMs, either upon CD or upon T09 incubation. The lack of ABCA1 and ABCG1 induction with the synthetic LXR agonist T09 validated that LXRα$^{-/-}$/LXRβ$^{-/-}$ BMDMs were indeed knockout cells. Furthermore, the finding that CC-loading and CD treatment also failed to induce cholesterol efflux transporter expression, confirmed that the regulation of ABCA1 and ABCG1 by cholesterol overloading as well as by CD treatment was dependent on LXR transcription factors.

To assess whether CD treatment of macrophages particularly changed LXR target gene expression, gene set enrichment analysis (GSEA) was performed for a set of 533 previously described LXR target genes[114] that were contained in the microarray. GSEA reveals whether the induction of a defined set of genes is statistically different between two different states. In LXRα$^{-/-}$/LXRβ$^{-/-}$ BMDMs none of the treatments resulted in a significant enrichment of LXR target gene sets (Fig 4-12). In contrast, LXR target gene sets were significantly enriched

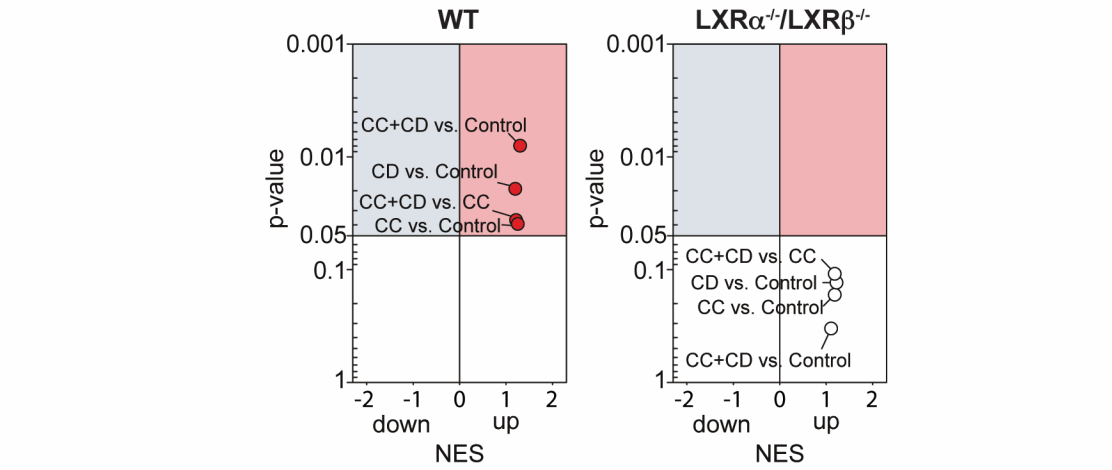

Figure 4-12: GSEA for LXR target genes in CD-treated WT and LXRα$^{-/-}$/LXRβ$^{-/-}$ macrophages.

M-CSF-derived BMDMs generated from WT mice (n=3) and LXRα$^{-/-}$/LXRβ$^{-/-}$ mice (n=4) were partially loaded with 100 µg CC per 1x10^{6} cells overnight prior to incubation with 10 mM CD or medium control for 6 h. Array-based gene expression profiling of these samples was performed by Prof. Dr. Joachim Schultze and colleagues. GSEA for LXR target genes was performed for both genotypes comparing all conditions against the untreated cells (Control) and CC-loaded and CD-treated samples against CC-loaded cells (CC+CD vs. Control). Results are presented in volcano plots showing the normalized enrichment score (NES) and the enrichment p-value. Dr. Thomas Ulas performed the GSEA and graphed the resultant data.

upon loading of WT BMDMs with CCs, which was in line with the observations on ABCA1 and ABCG1 expression following CC-loading (see Fig. 4-10 and Fig. 4-11) and is presumably caused by cholesterol overloading of the macrophages. Furthermore, CD treatment of CC-loaded WT BMDMs resulted in a highly significant enrichment of LXR target gene sets when compared to normocholesterolemic WT BMDMs, and furthermore significant enrichment was even observed when compared to CC-loaded hypercholesterolemic WT BMDMs (Fig 4-12). This result reflected the ABCA1 and ABCG1 expression patterns observed in Fig. 4-10 and Fig. 4-11, and supported the concept that CD-mediated production of 27-HC in CC-loaded macrophages (see Fig. 4-9) results in the induction of LXR gene expression programs. However, a significant enrichment of LXR target gene sets was also observed in CD-treated normocholesterolemic WT BMDMs (Fig 4-12). This finding was counterintuitive considering that LXR-meditated gene expression is involved in regulation of cholesterol homeostasis, mainly by regulating cellular cholesterol efflux mechanisms[130], while CD is known to deplete normocholesterolemic cells from cholesterol[131]. Therefore, the effects of CD treatment on normocholesterolemic macrophages were examined more closely.

4.3.3 Oxysterol production and LXR gene expression in CD-treated normocholesterolemic macrophages

In collaboration with Prof. Dr. Dr. Dieter Lütjohann GC-MS-SIM was performed on normocholesterolemic iMOs treated with CD or medium control for 24 hours and 48 hours. The results confirmed the removal of cholesterol from normocholesterolemic macrophages

Figure 4-13: CD removes cholesterol and induces cholesterol biosynthesis in normocholesterolemic macrophages, but still mediates oxysterols production and LXRα upregulation.

(A,B) C57BL/6 iMOs were incubated with 10 mM CD or medium control for indicated times. A 0 h control sample was harvested before addition of CD. Samples were analyzed by GC-MS-SIM (performed by Prof. Dr. Dr. Dieter Lütjohann and colleagues). (A) Cholesterol distribution in cells and supernatants Data are shown as mean + SEM of three independent experiments with duplicates. (B) 27-HC and cholesterol synthesis markers. Data combined from three individual experiments with duplicates are presented in a heatmap showing the fold induction of the 0 h control. (C,D) M-CSF derived BMDMs generated from WT and LXRα$^{-/-}$/LXRβ$^{-/-}$ mice were partially loaded with 100 µg CC per 1x10^6 cells overnight prior to incubation with 10 mM CD or medium control for 6h. Array-based gene expression profiling was performed by Prof. Dr. Joachim Schultze and colleagues. (C) Graphical representation of the slightly adapted KEGG steroid biosynthesis reference pathway (KEGG mmu00100). Genes in grey boxes were not included in microarray analysis; green circles indicate cholesterol and the cholesterol synthesis markers measured by GC-MS-SIM. (D) Heatmap shows fold changes of genes included in the steroid biosynthesis pathway (KEGG mmu00100) ordered as they appear in the pathway in (C). (E) WT BMDMs were incubated with 10 mM CD or medium control for 8 h. 27-HC and cholesterol synthesis markers determined by GC-MS-SIM (performed by Prof. Dr. Dr. Dieter Lütjohann and colleagues). Results of one experiment with triplicates are presented in a heatmap showing the fold induction of the 0 h control. (F-H) WT BMDMs were partially loaded with 100 µg CC per 1x10^6 cells overnight prior to incubation with 10 mM CD or medium control for 8 h. (F) Lss1, (G) Insig1, and (H) Nr1h3 mRNA levels relative to the reference gene Hprt assessed by RT-qPCR and presented as fold induction of the untreated cells. Data are shown as mean + SEM of three independent experiments with technical duplicates.

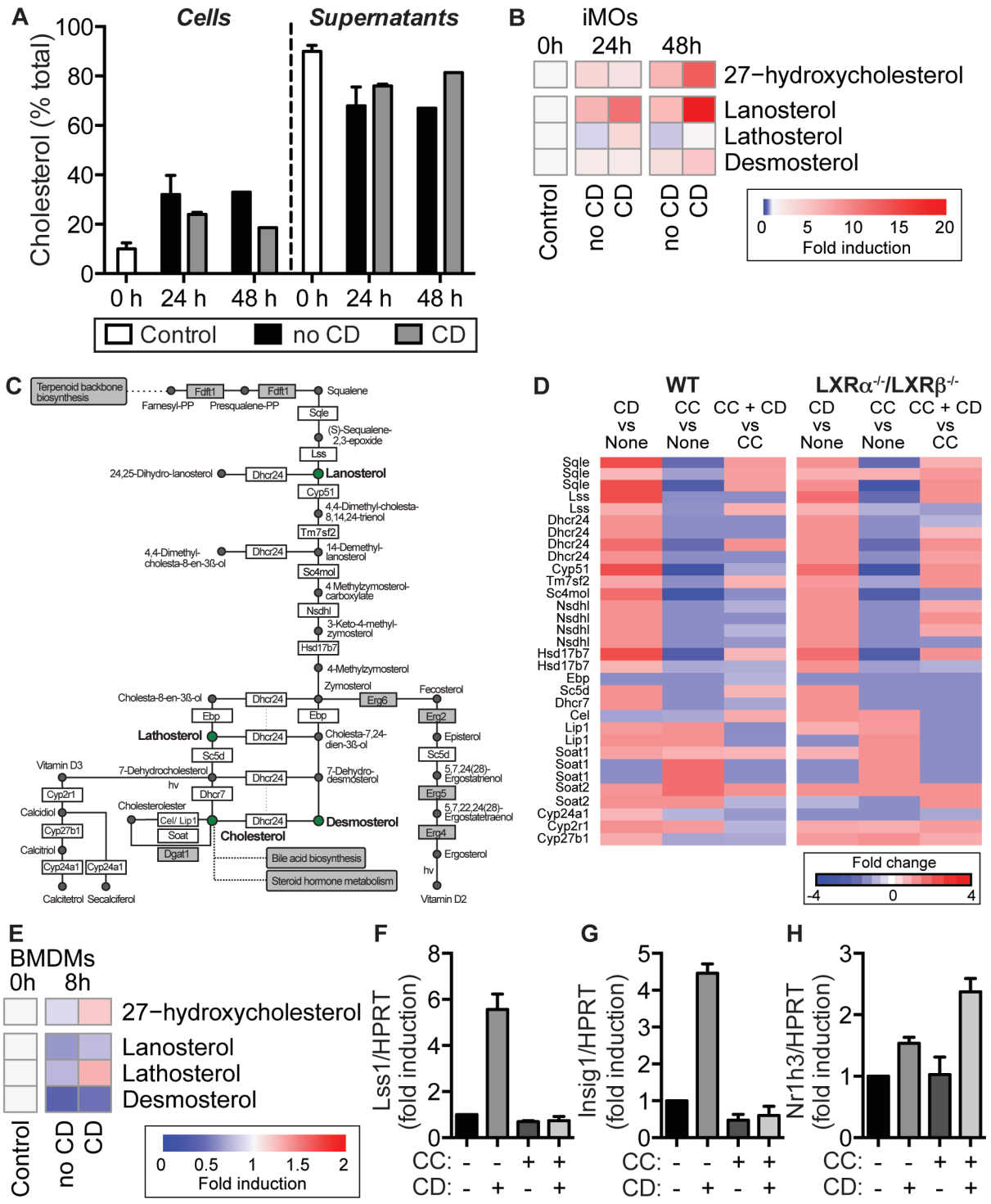

upon CD treatment (Fig. 4-13A). In addition, CD-mediated cholesterol depletion from these cells was accompanied by the induction of cholesterol biosynthesis markers lanosterol, lathosterol and desmosterol (Fig. 4-13B).

To confirm that CD also resulted in cholesterol depletion and subsequent induction of cholesterol biosynthesis in the samples analyzed by microarray, gene expression changes of genes contained in the steroid biosynthesis pathway (KEGG pathway mmu00100) were evaluated. Fig. 4-13C shows a slightly adapted graphical representation of this pathway,

indicating the position of the cholesterol precursors that were analyzed as cholesterol synthesis markers by GC-MS-SIM (green circles). All genes in white boxes were contained in the microarray analysis and their expression levels are represented as fold changes in Fig. 4-13D. Indeed, CD treatment of BMDMs for 6 hours upregulated genes involved in cholesterol biosynthesis regardless of the genotype, indicating that cholesterol depletion from normocholesterolemic macrophages and transcriptional regulation of the cholesterol biosynthesis pathway is independent of LXR activation. Furthermore, while macrophage loading with CCs resulted in the downregulation of cholesterol biosynthesis genes, additional treatment with CD partially reversed these effects, presumably by facilitating CC dissolution and efflux of crystal-derived cholesterol. However, of importance, the GC-MS-SIM data of iMOs treated with CD for 24 and 48 hours not only revealed the induction of cholesterol biosynthesis markers, but also production of 27-HC in response to CD treatment (Fig. 4-13B).

To gain better insight into the status of the cells used for microarray analysis, production of 27-HC and induction of cholesterol precursors were also analyzed in BMDMs treated with CD for 8 hours. This analysis confirmed that CD increased the levels of cholesterol biosynthesis markers, but at the same time mediated the production of 27-HC (Fig 4-13E). In addition, gene expression analysis of normocholesterolemic or CC-loaded BMDMs treated with CD for 8 hours confirmed the induction of genes involved in SREBP-mediated regulation of cholesterol biosynthesis, namely lanosterol synthase (Lss1) (Fig. 4-13F) and Insig1 (Fig. 4-13G), but also revealed the simultaneous induction of the LXR target gene Nr1h3, which encodes for the LXRα receptor (Fig. 4-13H). Although the induction of Nr1h3 was higher in CC-loaded BMDMs, presumably due to greater amounts of the LXR ligand 27-HC (about 5 ng in normocholesterolemic BMDMs opposed to 8.8 ng crystal-derived plus 7.3 ng cellular 27-HC in CC-loaded BMDMs (Fig. 4-9D and Fig. 4-9E), the finding that Nr1h3 expression was also induced in normocholesterolemic WT BMDMs confirmed the results of the GSEA (Fig. 4-12).

In summary these results indicated that CD mediates the activation of LXR gene expression via the production of endogenous LXR ligands such as 27-HC in CC-loaded hypercholesterolemic, but also normocholesterolemic macrophages.

4.3.4 CD-mediated reverse cholesterol transport of crystal-derived cholesterol

It was observed that CD treatment results in LXR-dependent upregulation of macrophage cholesterol efflux transporters and facilitates the export of crystal-derived cholesterol from macrophages *in vitro*. To determine whether this could also occur *in vivo*, RCT and excretion of crystal-derived cholesterol was monitored in mice (see section 3.2.7.2). Therefore,

BMDMs generated from WT and LXRα$^{-/-}$/LXRβ$^{-/-}$ mice were loaded with D_6-CCs. These D_6-CC-loaded macrophages were then injected into the peritoneum of WT mice. 30 minutes after injection of the D_6-CC-loaded BMDMs the mice were treated intraperitoneally with CD or vehicle control, which was repeated 16 hours later because of the fast clearance of CD upon parenteral administration (see section 2.3.1.3). Feces and urine were collected in three to six hour intervals over a 30 hours period and analyzed for presence of crystal-derived D_6-cholesterol using GC-MS-SIM. A schematic of the experimental workflow is provided in Fig. 4-14A.

Almost no D_6-cholesterol was detected in the feces of vehicle-treated mice (Fig. 4-14B and Fig. 4-14C). In contrast, large amounts of crystal-derived D_6-cholesterol were excreted via the feces six hours after the first CD treatment of mice injected with D_6-CC-loaded WT BMDMs. This CD-mediated fecal excretion of crystal-derived D_6-cholesterol, appeared to be LXR-dependent as only comparatively small amounts of D_6-cholesterol were measured in the feces of CD-treated mice injected with D_6-CC-loaded LXRα$^{-/-}$/LXRβ$^{-/-}$ BMDMs, and even this was only apparent 24 hours after the first CD treatment.

Besides fecal cholesterol excretion, which is the conventional route of cholesterol excretion from the body[132], urinary excretion of crystal-derived D_6-cholesterol was also examined. This was done as CD is mainly secreted from the body via the urine[91], and it was shown that cholesterol can exit the body in complex with CD molecules via the urine[101]. Indeed, the analysis of crystal-derived D_6-cholesterol revealed the excretion via the urine upon CD treatment (Fig. 4-14D and Fig. 4-14E). Urinary excretion of crystal-derived D_6-cholesterol from CD-treated mice injected with D_6-CC-loaded WT BMDMs peaked at approximately nine hours after the first CD injection and again at approximately 18 hours after the first CD injection (two hours after the second CD injection). Smaller amounts of crystal-derived D_6-cholesterol were found in the urine of CD-treated mice injected with D_6-CC-loaded LXRα$^{-/-}$/LXRβ$^{-/-}$ BMDMs. Here, D_6-cholesterol was only excreted approximately 24 hours after the first CD injection (about six hours after the second CD injection). Similarly, very little D_6-cholesterol was also detected in the urine of vehicle-treated mice injected with D_6-CC-loaded LXRα$^{-/-}$/LXRβ$^{-/-}$ BMDMs. For vehicle-treated animals injected with D_6-CC-loaded WT BMDMs almost no urinary excretion of crystal-derived D_6-cholesterol was observed.

In summary, this experiment showed that CD mediates the RCT of crystal-derived cholesterol from WT macrophages as well as subsequent excretion via both urine and feces. Some crystal-derived cholesterol was also removed from LXRα$^{-/-}$/LXRβ$^{-/-}$ BMDMs upon CD treatment. However, RCT from these cells and subsequent excretion was considerably impaired, as less crystal-derived cholesterol was excreted and excretion was delayed. These findings indicated that CD-mediated RCT and excretion of crystal-derived cholesterol is at least partially dependent on LXR activation.

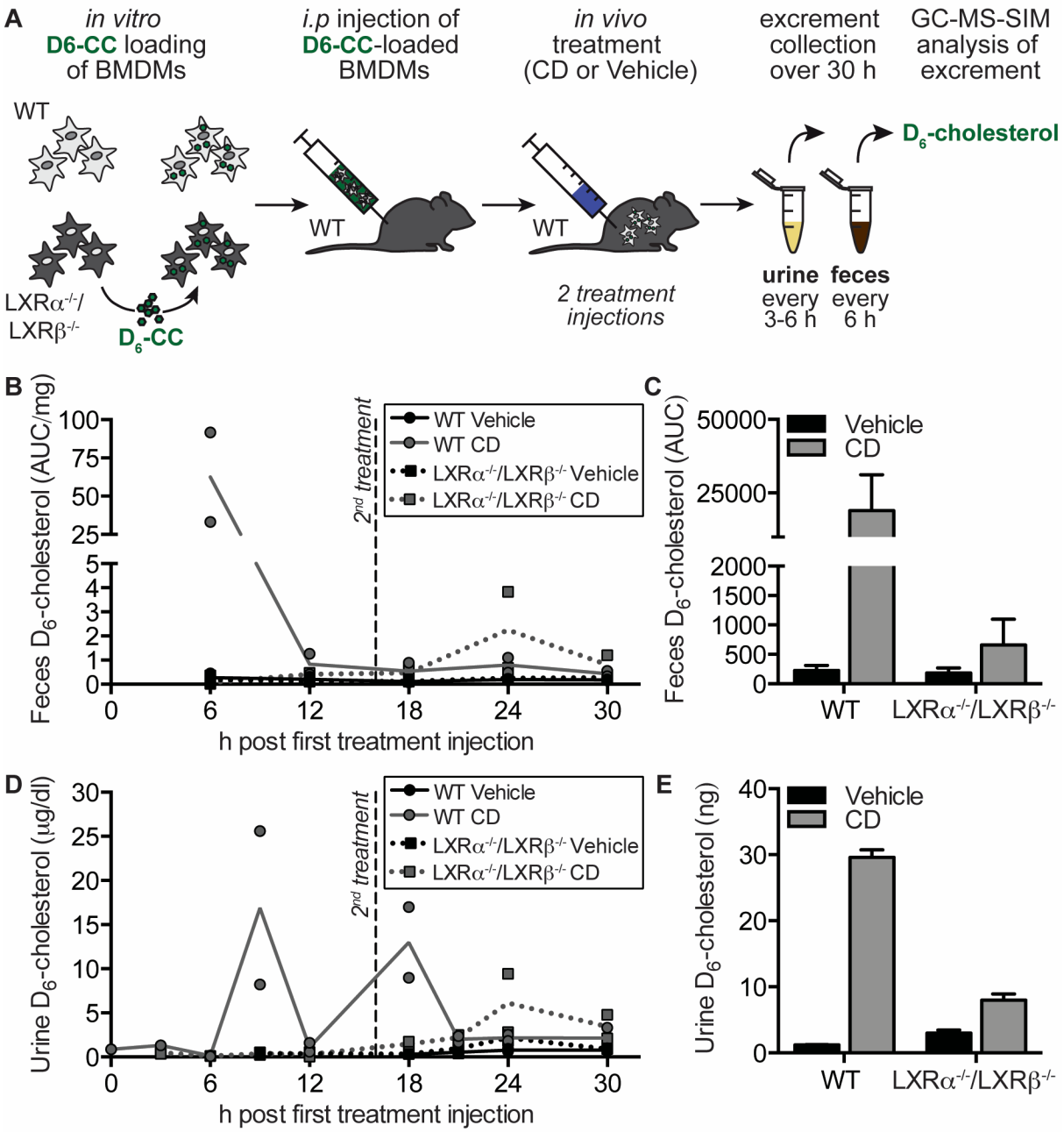

Figure 4-14: CD mediates RCT of crystal-derived cholesterol *in vivo* in a partially LXR-dependent manner.

(A) Schematic of experimental setup for assessing RCT and excretion of crystal-derived cholesterol *in vivo*. BMDMs generated from WT and LXRα$^{-/-}$/LXRβ$^{-/-}$ mice were loaded for 3 h with 100 µg D_6-CC per 1x10^6 cells. WT mice were intraperitoneally injected with 15x10^6 D_6-CC-loaded BMDMs and subsequently treated with CD or vehicle control twice. The first treatment injection was given 30 min after application of the D_6-CC-loaded BMDMs, the second one was given 16 h later. Feces and urine were collected every 3-6 h over a 30 h period and analyzed for presence of crystal-derived D_6-cholesterol by GC-MS-SIM (performed by Prof. Dr. Dr. Dieter Lütjohann and colleagues). All animal work was carried out by Dr. Sebastian Zimmer and colleagues. Excretion kinetics of D_6-cholesterol in (B) feces presented as area under the curve (AUC) of D_6-cholesterol per mg feces and (D) urine presented as µg D_6-cholesterol per dl urine. Data are presented as individual replicates with lines connecting the means; WT = solid lines with circles, LXRα-/-/LXRβ-/- = dotted lines with squares, Vehicle = black, CD = grey. Dashed vertical line illustrates time of second treatment injection. Total D_6-cholesterol excreted via (C) feces and (E) urine. Data are shown as mean + SD of two replicates.

4.4 Role of cholesterol efflux transporters and LXR transcription factor activation in 2-hydroxypropyl-β-cyclodextrin-mediated atherosclerosis protection

The findings presented in the previous chapters led to the hypothesis that CD might exert its beneficial effects on murine atherosclerosis by dissolving plaque CCs and promoting the production of the endogenous LXR agonist 27-HC. Subsequent activation of LXR transcription factors would induce the expression of cholesterol efflux transporters and thus facilitate removal of cholesterol from the tissue and ultimately the whole body. The first evidence supporting this hypothesis was provided by Taqman RT-qPCR analysis of Abca1 and Abcg1 gene expression in the descending aortas of the mice from the atherosclerosis prevention model, which was performed by Sebastian Zimmer and colleagues. This analysis revealed that Abca1 and Abcg1 expression was significantly increased in the aortic tissue of CD-treated animals compared to vehicle-treated animals (data not shown, Zimmer and Grebe *et al.*, in press).

To further test this hypothesis, it was investigated, whether LXR activation and subsequent induction of ABCA1 and ABCG1 expression contribute to the anti-atherogenic effects of CD treatment in murine atherosclerosis. Therefore, a bone marrow transplantation atherosclerosis model was performed in collaboration with Sebastian Zimmer and colleagues (see section 3.2.7). $LDLR^{-/-}$ mice were transplanted with WT, MAC-ABC^{DKO} or $LXR\alpha^{-/-}/LXR\beta^{-/-}$ bone marrow. Four weeks after transplantation the atherosclerosis study was initiated according to the protocol of the atherosclerosis prevention study presented in Fig. 4-2A. The mice received a HFHC diet for eight weeks accompanied by subcutaneous injections with CD or vehicle control twice a week (Fig. 4-15A). Atherosclerosis parameters were analyzed by confocal laser reflection and fluorescence microscopy of three to five aortic root cryosections. Two representative images of vehicle-treated (left) and CD-treated (right) mice per transplantation group are displayed in Fig. 4-15B. First, it was observed that the plaques of $LDLR^{-/-}$ mice fed a HFHC diet for eight weeks were not as pronounced and advanced as the plaques of equally treated $ApoE^{-/-}$ mice in the previous atherosclerosis studies (Fig. 4-2 and Fig. 4-3). However, this difference between these two mouse models of atherosclerosis is well described in the literature[38]. Nevertheless, the representative images demonstrate that atherosclerotic plaque size was visibly reduced upon CD treatment of mice transplanted with WT and MAC-ABC^{DKO}, but not $LXR\alpha^{-/-}/LXR\beta^{-/-}$ bone marrow. Quantitative image analysis confirmed this visual observation, as CD treatment resulted in significantly smaller atherosclerotic plaques in mice transplanted with WT and MAC-ABC^{DKO} bone marrow, whereas plaque size of $LXR\alpha^{-/-}/LXR\beta^{-/-}$ bone marrow-transplanted mice was unchanged by CD treatment (Fig. 4-15C). Analysis of CC plaque load did not reveal

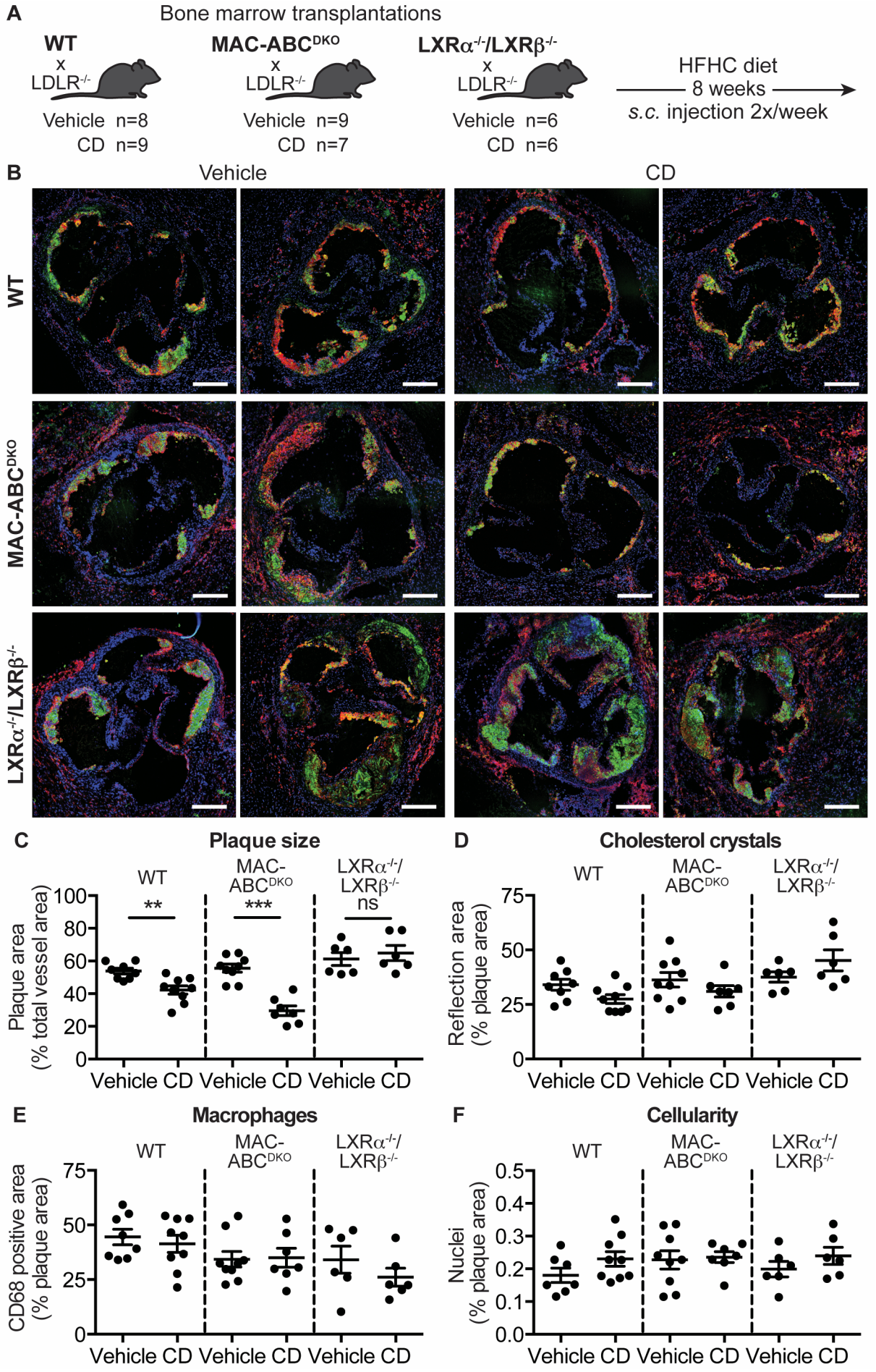
A
Bone marrow transplantations
WT x LDLR-/-
Vehicle n=8
CD n=9
MAC-ABCDKO x LDLR-/-
Vehicle n=9
CD n=7
LXRα-/-/LXRβ-/- x LDLR-/-
Vehicle n=6
CD n=6
HFHC diet
8 weeks
s.c. injection 2x/week
B
Vehicle
CD
WT
MAC-ABCDKO
LXRα-/-/LXRβ-/-
C
Plaque size
Plaque area (% total vessel area)
WT
MAC-ABCDKO
LXRα-/-/LXRβ-/-
**
***
ns
Vehicle CD Vehicle CD Vehicle CD
D
Cholesterol crystals
Reflection area (% plaque area)
Vehicle CD Vehicle CD Vehicle CD
E
Macrophages
CD68 positive area (% plaque area)
Vehicle CD Vehicle CD Vehicle CD
F
Cellularity
Nuclei (% plaque area)
Vehicle CD Vehicle CD Vehicle CD

Figure 4-15: The anti-atherogenic effects of CD are dependent on the presence of LXRs but not cholesterol efflux transporters.

(A) Schematic of study protocol for bone marrow transplantation atherosclerosis model. $LDLR^{-/-}$ mice were transplanted with WT, MAC-ABC^{DKO} or $LXR\alpha^{-/-}/LXR\beta^{-/-}$ bone marrow. They received a HFHC diet for eight weeks accompanied by subcutaneous injections with CD or vehicle control twice a week (n numbers indicated for each group). All animal work was performed by Dr. Sebastian Zimmer and colleagues. (B-F) Serial aortic root sections were analyzed by confocal laser reflection and fluorescence microscopy. (B) Representative images of all study groups; Hoechst 34580 staining for nuclei (blue), CD68 staining for macrophages (red) and laser reflection signal for CCs (green). Scale bars indicate 250 µm. (C) Quantification of atherosclerotic plaque size depicted as plaque area as percentage of total vessel wall area. (D) Quantification of CC plaque load depicted as reflection area as percentage of plaque area. (E) Quantification of macrophage plaque load depicted as CD68 positive area as percentage of plaque area. (F) Quantification of plaque cellularity depicted as nuclei counts as percentage of plaque area. Data in (C-F) are shown as mean ± SEM of three to five individual sections per mouse. Significance was determined by unpaired two-tailed Student's t-tests with Welch's correction comparing Vehicle and CD per genotype (*** = $p<0.001$, ** = $p<0.01$, ns = not significant).

significant changes between vehicle-treated and CD-treated mice (Fig. 4-15D). Nevertheless, a clear trend towards reduced amounts of CCs inside the plaques was observed in CD-treated mice transplanted with WT and MAC-ABC^{DKO} bone marrow, whereas in $LXR\alpha^{-/-}/LXR\beta^{-/-}$ bone marrow-transplanted mice CC plaque load rather increased upon CD treatment. In contrast to the observations from the $ApoE^{-/-}$ atherosclerosis models (Fig. 4-2 and Fig. 4-3), the amount of CD68-positive macrophages in the plaques (Fig. 4-15E) as well as overall plaque cellularity (Fig. 4-15F) was almost unaffected by CD treatment in this $LDLR^{-/-}$ bone marrow transplantation atherosclerosis model.

In summary, the results of the bone marrow transplantation atherosclerosis study indicated that CD treatment still impairs atherosclerosis development and progression in mice lacking macrophage ABCA1 and ABCG1, whereas this atheroprotective function is lost in the absence of LXR transcription factors in hematopoietic-derived cells.

As for the other atherosclerosis mouse models, serum cholesterol levels of the mice were determined at the end of the study using gas chromatography-flame ionization detection. This analysis revealed that serum cholesterol levels differed between the individual transplant groups, but no changes were induced by CD treatment (Fig. 4-16A). Besides serum cholesterol levels, serum 27-HC levels were also measured. No significant changes were observed in WT bone marrow-transplanted $LDLR^{-/-}$ mice (Fig. 4-16B). However, serum 27-HC was significantly increased upon CD treatment in MAC-ABC^{DKO}-transplanted $LDLR^{-/-}$ mice, and an almost significant increase was also observed in $LXR\alpha^{-/-}/LXR\beta^{-/-}$ bone marrow-transplanted $LDLR^{-/-}$ mice. To determine whether CD treatment changed the distribution of cholesterol across the various lipoproteins, serum was fractionated by size exclusion chromatography followed by enzymatic cholesterol quantification (performed by the laboratory of Dr. Michael L. Fitzgerald (Center for Computational and Integrative Biology, Boston, MA, USA)). No significant changes in the lipoprotein profiles were observed in WT

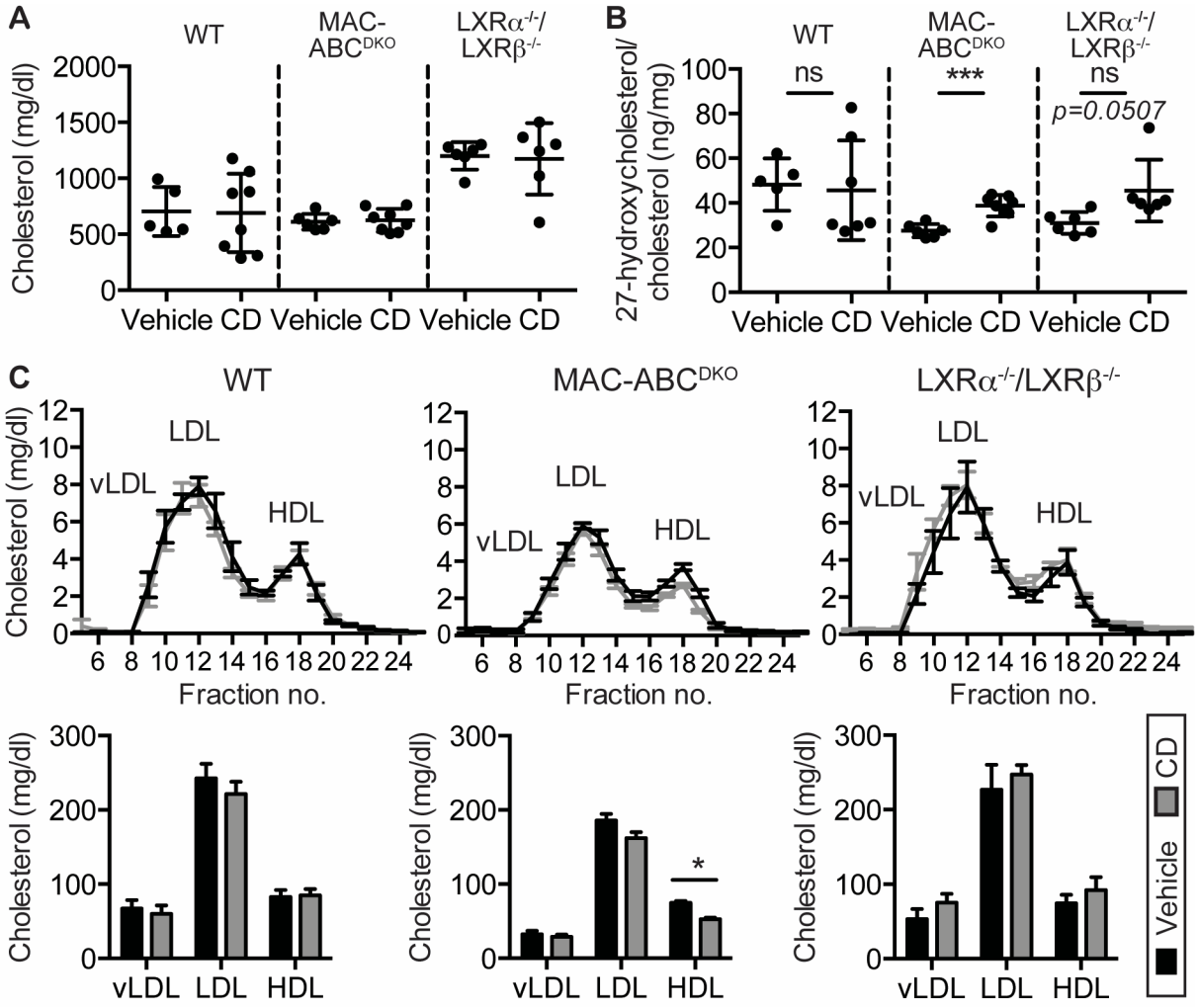

Figure 4-16: CD treatment does not change serum cholesterol distribution on lipoproteins, but increases serum 27-HC levels in bone marrow transplantation atherosclerosis model.

LDLR$^{-/-}$ mice transplanted with WT, MAC-ABC^{DKO} or LXRα$^{-/-}$/LXRβ$^{-/-}$ bone marrow received a HFHC diet for eight weeks accompanied by subcutaneous injections with CD or vehicle control twice a week. Serum (A) cholesterol and (B) 27-HC levels after eight weeks of atherogenic diet. Measurements were done using gas chromatography-flame ionization detection by Prof. Dr. Dr. Dieter Lütjohann and colleagues. Data are shown as mean ± SD. Significance was determined by unpaired two-tailed Student's t-tests with Welch's correction comparing Vehicle and CD per genotype (** = p<0.01, * = p<0.05, ns = not significant). (C) Serum was fractionated by size exclusion chromatography and cholesterol concentration of the fractions was quantified using an enzymatic assay (performed by Michael L. Fitzgerald and colleagues (Harvard Medical School, Boston MA, USA)). Results are presented as lipoprotein profiles (upper panels) and resultant cholesterol distribution on lipoproteins calculated from the lipoprotein profiles (lower panels). Data are shown as mean ± SEM of technical duplicates. Significance was determined by unpaired two-tailed Student's t-tests with Welch's correction comparing Vehicle and CD (* = p<0.05).

and LXRα$^{-/-}$/LXRβ$^{-/-}$ bone marrow-transplanted LDLR$^{-/-}$ mice comparing serum of CD- and vehicle-treated animals, while HDL cholesterol was significantly reduced following CD treatment of MAC-ABC^{DKO} bone marrow-transplanted LDLR$^{-/-}$ mice (Fig. 4-16C). Together, these data confirmed the previous finding that CD treatment did not alter serum cholesterol levels and further suggested that lipoprotein profiles in the LDLR$^{-/-}$ atherosclerosis mouse model are also mostly unaffected by CD treatment.

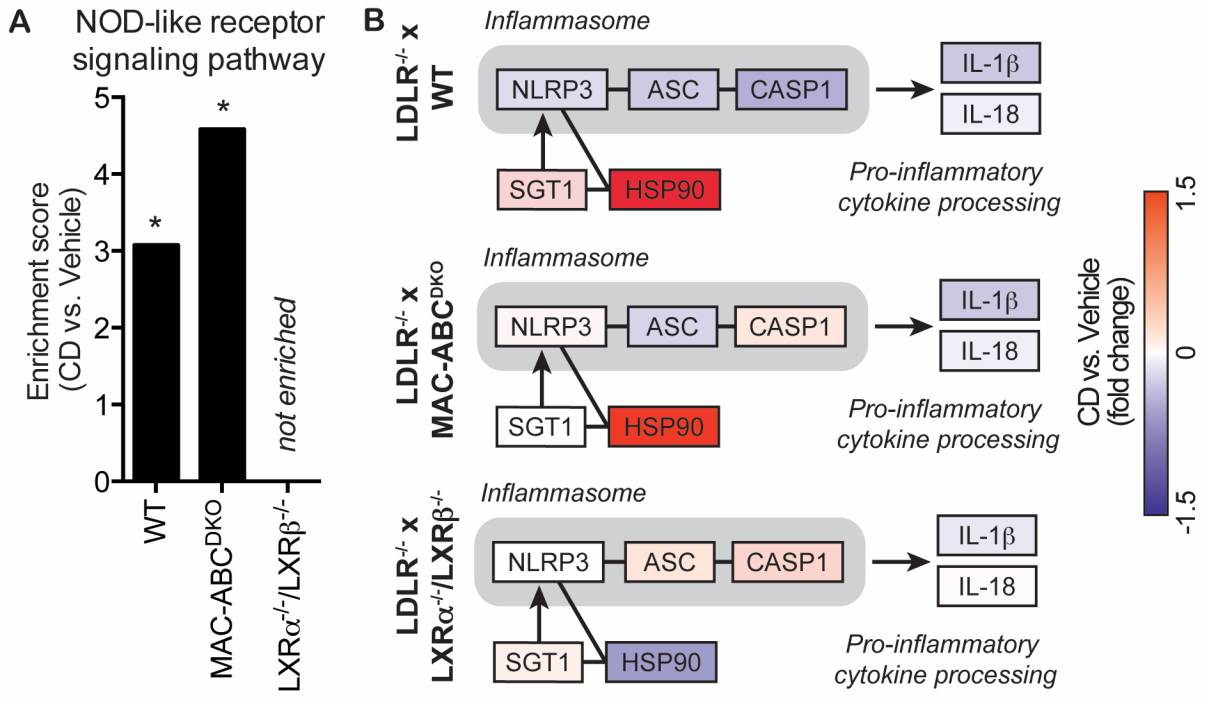

Figure 4-17: NLRP3 inflammasome genes are negatively regulated by CD treatment in atherosclerotic aortic tissue in an LXR dependent manner.

LDLR$^{-/-}$ mice transplanted with WT, MAC-ABC^{DKO} or LXRα$^{-/-}$/LXRβ$^{-/-}$ bone marrow received a HFHC diet for eight weeks accompanied by subcutaneous injections with CD or vehicle control twice a week. Array-based gene expression profiling of the descending aortas was performed by Prof. Dr. Joachim Schultze and colleagues. (n=6 per treatment group) (A) Enrichment score and significance level for NOD-like receptor signaling pathway (KEGG mmu04621) obtained from pathway enrichment analysis comparing CD vs. vehicle treatment. (B) Graphical representation of genes involved in NLRP3 inflammasome activation (extract of KEGG NOD-like receptor signaling reference pathway (KEGG mmu04621)). Colors indicate fold changes in gene expression in aortas of CD-treated versus vehicle-treated mice.

Based on the *in vitro* observation that CD increased the production of the endogenous LXR agonist 27-HC, the potential effects of LXR transcription factor activation in atherosclerotic plaque tissue were investigated. For this, gene expression in descending aortas of the mice was analyzed by microarray (see sections 3.2.21 and 3.2.22). Pathway enrichment analysis of the differentially expressed genes in the aortas of CD-treated mice compared to aortas of vehicle-treated mice revealed a significant enrichment of genes in the NOD-like receptor signaling pathway (KEGG pathway mmu04621) (Fig. 4-17A). However, this enrichment was only observed in WT and MAC-ABC^{DKO} bone marrow-transplanted LDLR$^{-/-}$ mice, but not in mice transplanted with LXRα$^{-/-}$/LXRβ$^{-/-}$ bone marrow. A closer analysis of the individual genes in the NOD-like receptor-signaling pathway showed that genes involved in NLRP3 inflammasome activation were negatively regulated by CD treatment in aortas of mice transplanted with WT and MAC-ABC^{DKO} bone marrow (Fig. 4-17B). In particular, the genes encoding for NLRP3 inflammasome components NLRP3, ASC and caspase-1 as well as the pro-inflammatory inflammasome effector cytokines IL-1β and IL-18 were downregulated upon CD treatment. At the same time CD treatment induced the expression of SGT1 and HSP90, which are described to inhibit NLRP3 inflammasome function by retaining NLRP3 in

an inactive state[32]. All these genes were either much less or inversely regulated in aortas of LDLR$^{-/-}$ mice transplanted with LXRα$^{-/-}$/LXRβ$^{-/-}$ bone marrow. This suggested that the activation of LXR transcription factors in hematopoietic-derived cells is required for the observed CD-mediated inhibitory gene expression changes of genes involved in NLRP3 inflammasome activation.

4.5 Effects of 2-hydroxypropyl-β-cyclodextrin treatment on cholesterol crystal-induced NLRP3 inflammasome activation

The NLRP3 inflammasome was shown to play a critical role in murine atherosclerosis by contributing to the inflammatory response that drives disease progression[24,85]. LXR transcription factor activation is known to repress macrophage pro-inflammatory gene expression programs in general[133,134], and interestingly, NLRP3 was found to be a primary LXR target gene in ChIP-sequencing analysis of human macrophages treated with a synthetic LXR agonist[135]. Therefore, based on the above observations that CD treatment downregulated NLRP3 inflammasome component expression in aortic plaque tissues in an LXR-dependent manner, the potentially LXR-dependent effects of CD on NLRP3 inflammasome activation were investigated *in vitro.*

All experiments assessing the effects of CD on the NLRP3 inflammasome were performed in immortalized WT BALB/c macrophages, as they respond much better to crystalline NLRP3 stimuli than immortalized WT C57BL/6 macrophages. However, as all the previously performed *in vitro* experiments were done in immortalized or bone marrow-derived macrophages obtained from WT C57BL/6 mice, and as the ApoE$^{-/-}$ and LDLR$^{-/-}$ mice used for the atherosclerosis mouse models were also on a C57BL/6 background, the assays were also performed in BMDMs generated from bone marrow of WT C57BL/6 mice.

As a first measure of CD effects on the NLRP3 inflammasome in macrophages, the basal and LPS-induced expression of NLRP3 inflammasome components was determined by WB analysis. Macrophages were pretreated with CD for 16 hours prior to LPS priming, which is characterized by induction of NLRP3 and pro-IL-1β expression. It was hypothesized that during this pretreatment period CD would augment the production of 27-HC to subsequently induce LXR-mediated gene expression. Pretreatment with the synthetic LXR agonist T09 was used as a positive control for the effects of LXR transcription factor activation on NLRP3 inflammasome priming and ABCA1 expression levels were assessed as control for LXR activation in response to T09. Indeed, an increase in ABCA1 expression was observed in T09-pretreated BALB/c iMOs (Fig. 4-18A) and BMDMs (Fig. 4-18B) regardless of the LPS treatment. In line with previous data presented in this thesis, CD treatment in the absence of

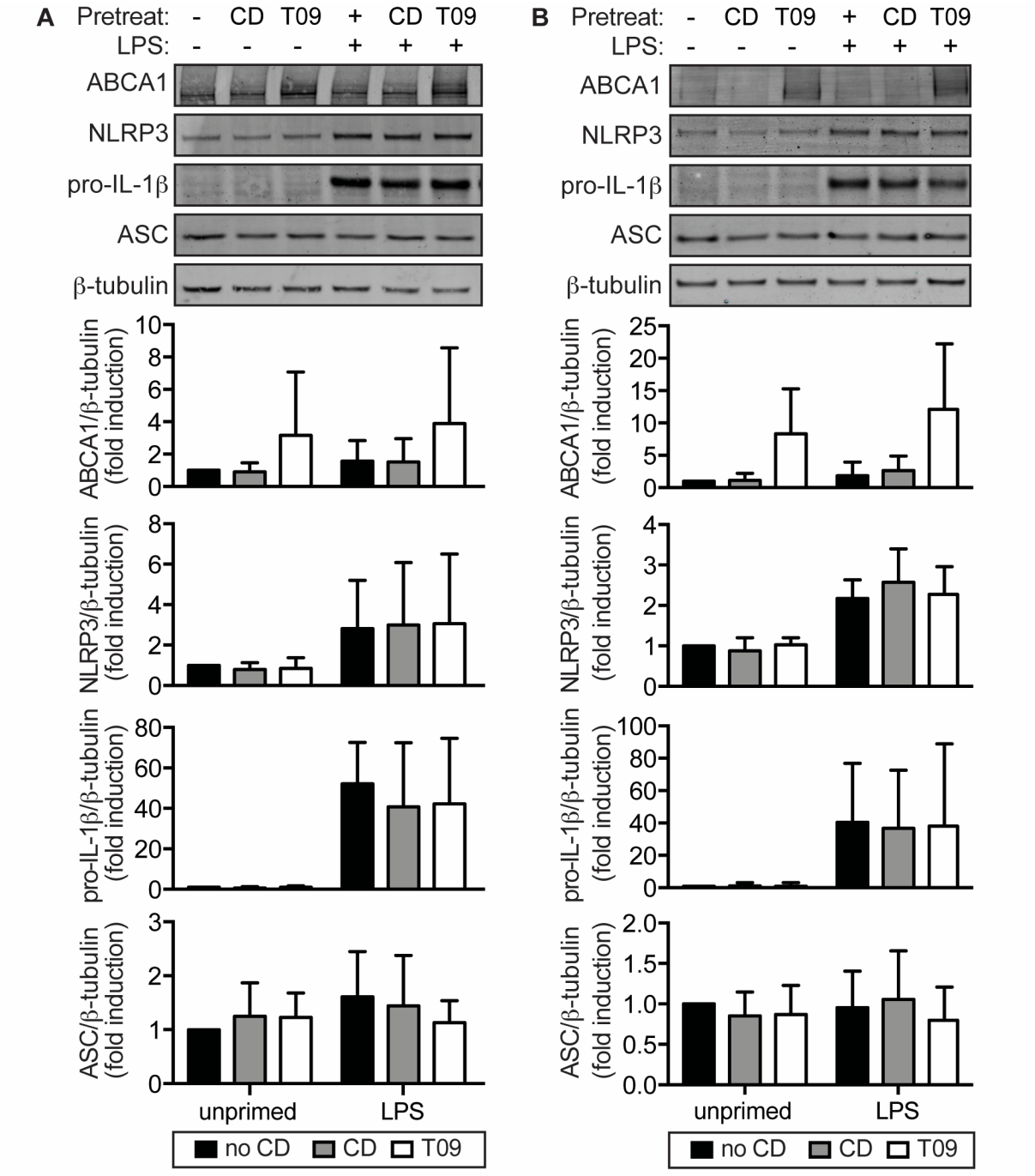

Figure 4-18: Priming of the NLRP3 inflammasome is not affected upon CD pretreatment *in vitro*.

(A) BALB/c iMOs or (B) WT BMDMs were pretreated for 16 h with 10 mM CD, 10 µM T0901317 (T09) or medium control. Subsequently cells were primed for 3 h with 200 ng/ml LPS or left unprimed. ABCA1, NLRP3, pro-IL-1 β and ASC protein expression was analyzed by western blot. β-tubulin expression was used as loading control. Data are presented as representative blot and densitometry analyses for each protein graphed as mean + SD of four independent experiments.

CC-loading did not increase ABCA1 protein expression, presumably due to simultaneous cholesterol depletion of the cells. Concerning NLRP3 priming, protein expression of the NLRP3 inflammasome components NLRP3, pro-IL-1β and ASC was determined. No major differences were observed between BALB/c iMOs (Fig. 4-18A) and BMDMs (Fig. 4-18B). LPS stimulation increased NLRP3 and pro-IL-1β expression, while ASC expression was

mainly unaffected. However, neither CD nor T09 pretreatment had an influence on basal expression of NLRP3 inflammasome components. Likewise, the LPS-induced upregulation of NLRP3 and pro-IL-1β expression was not influenced by macrophage pretreatment with CD or T09. These results indicated that neither basal expression of NLRP3 inflammasome components nor LPS-mediated NLRP3 inflammasome priming was affected by CD treatment and LXR activation in macrophages.

In order to assess whether CD treatment nevertheless affects NLRP3 inflammasome activation with regard to the potential influence of CD-mediated production of endogenous LXR ligands, macrophages were pretreated with CD or T09 for 16 hours prior to

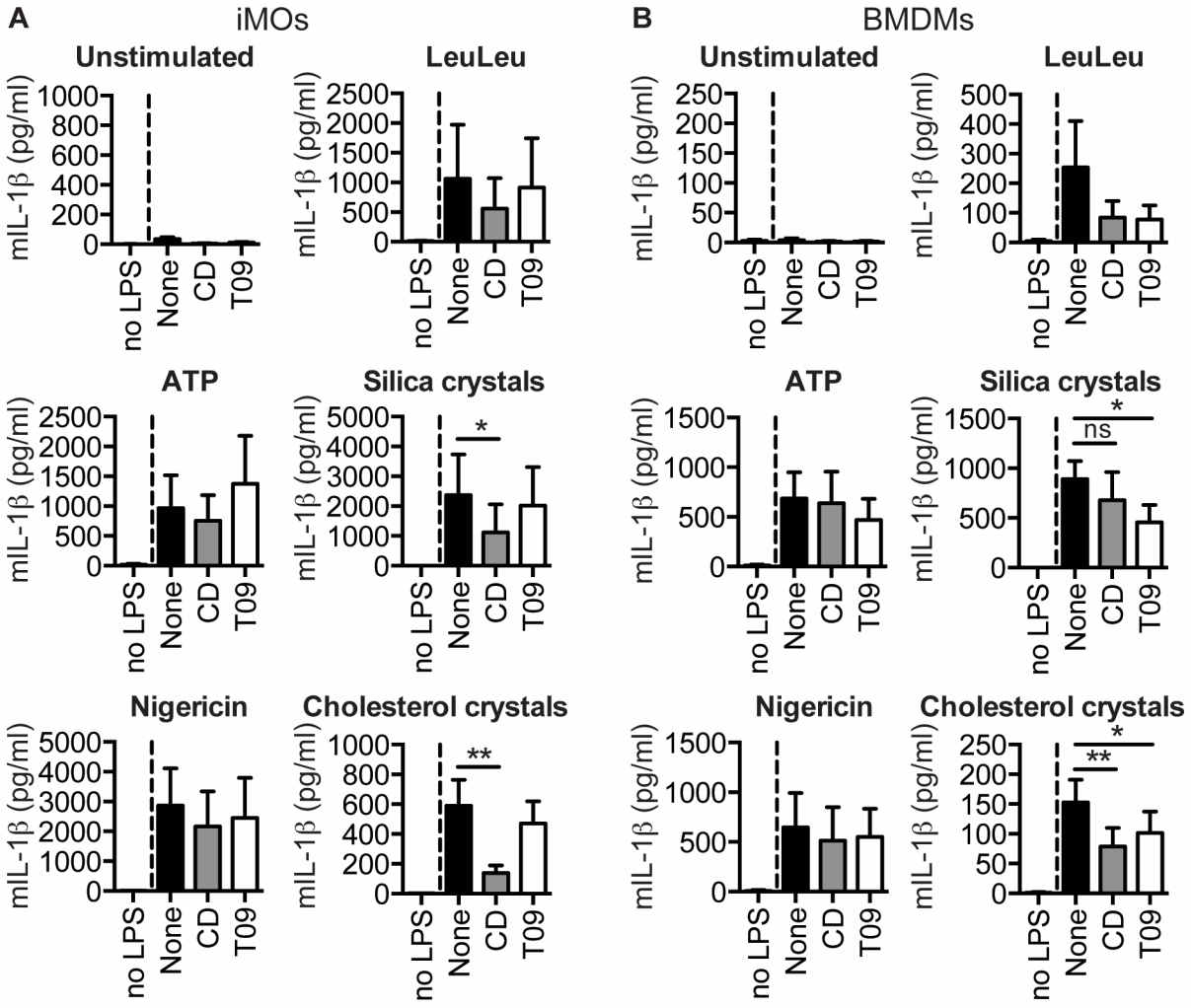

Figure 4-19: NLRP3 inflammasome activation by crystalline stimuli is decreased following CD pretreatment of normocholesterolemic macrophages.

(A) BALB/c iMOs or (B) WT BMDMs were pretreated for 16 h with 10 mM CD, 10 µM T0901317 (T09) or medium control. Subsequently cells were primed for 3 h with 200 ng/ml LPS prior to stimulation with various NLRP3 stimuli: 5 mM ATP or 10 µM nigericin for 1 h, 1 mM LeuLeu for 4 h, 0.5 mg/ml silica crystals or 1.5 mg/ml CC for 6 h. Secretion of mIL-1β was determined by ELISA. Data are shown as mean + SEM of four independent experiments with duplicates. Significance was determined by paired one-way ANOVA comparing each sample with the unstimulated control (None) applying Dunnett's post test for multiple comparisons (** = $p<0.01$, * = $p<0.05$, ns = not significant).

LPS-induced NLRP3 inflammasome priming and subsequent stimulation with various NLRP3inflammasome ligands. Overall the results obtained from the two different cell types were pretty similar. The only major difference was observed with the LXR agonist T09, which showed no effects in BALB/c iMOs (Fig. 4-19A), whereas it did affect NLRP3 inflammasome activation by certain ligands in BMDMs (Fig. 4-19B). CD pretreatment significantly reduced IL-1β secretion in response to silica and cholesterol crystals. Additionally, the response to LeuLeu was also consistently diminished in CD-treated cells. However, due to great variation in the LeuLeu response of non-pretreated cells, this reduction in IL-1β secretion was not significant. In BMDMs, IL-1β secretion in response to LeuLeu and crystalline stimuli was additionally decreased upon pretreatment with T09. In contrast, responses to ATP and nigericin were mainly unaffected by both pretreatments.

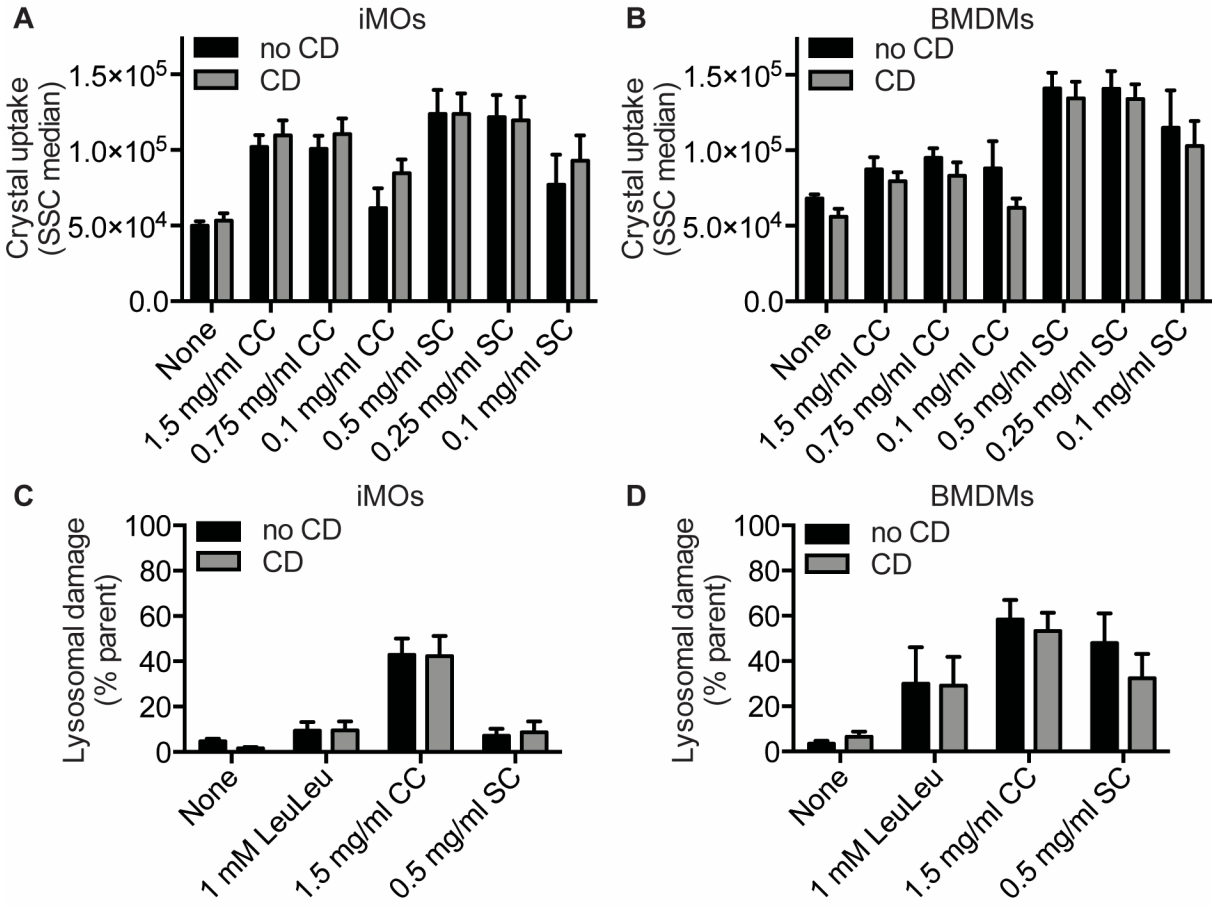

Figure 4-20: CD pretreatment has no effects on crystal uptake and subsequent lysosomal damage in normocholesterolemic macrophages.

(A,C) BALB/c iMOs or (B,D) WT BMDMs were pretreated for 16 h with 10 mM CD or medium control and stained with 5 µg/ml acridine orange for 15 min. Cells were incubated for 6 h with indicated concentrations of H-Leu-Leu-Ome (LeuLeu), silica crystals (SC), CCs or medium control prior to analysis by flow cytometry. (A,B) Median of SSC signal as measure of cellular crystal uptake. (C,D) Loss of acridine orange fluorescence was determined as measure of lysosomal damage presented as percentage of the parent single cell population (see 3.2.20, Fig. 3-5). Data are shown as mean + SEM of six independent experiments with duplicates.

Significant inhibition of NLRP3 inflammasome activation by CD pretreatment was observed exclusively in response to crystalline stimuli. Therefore, it was speculated that CD might affect macrophage membranes by extraction of membrane cholesterol, which in turn might impair crystal uptake, a prerequisite for NLRP3 inflammasome activation. To test this hypothesis, macrophages were pretreated for 16 hours with CD or medium control and subsequently incubated with different amounts of cholesterol or silica crystals. Crystal uptake into the macrophages was quantified using flow cytometry by analyzing the side scatter (SSC) signal, which increases when cells become more granular. As such, the SSC signal increases upon uptake of crystalline material (see Fig 3-5C). Indeed, crystal uptake into BALB/c iMOs (Fig. 4-20A) and BMDMs (Fig. 4-20B) could be determined in a dose-dependent manner, but was unaffected by CD pretreatment.

Besides crystal uptake, cholesterol depletion from macrophage membranes could also impact intracellular membranes and therefore impair crystal-mediated lysosomal damage. According to current knowledge, lysosomal damage plays an important role in the activation of the NLRP3 inflammasome in response to crystalline stimuli[31], but also in response to LeuLeu[136]. As CD pretreatment had an effect on both crystalline stimuli and LeuLeu, it was investigated whether CD might reduce NLRP3 inflammasome activation by affecting lysosomal damage. Lysosomal damage occurred in both BALB/c iMOs (Fig. 4-20C) and BMDMs (Fig. 4-20D) in response to the same ligand concentrations that activated the NLRP3 inflammasome (see Fig 4-19). However, no differences in lysosomal damage were observed upon CD pretreatment compared to medium control pretreatment.

In summary, these data showed that NLRP3 inflammasome activation was reduced upon CD pretreatment (and in BMDMs also upon LXR agonist pretreatment) when macrophages were stimulated with LeuLeu or crystalline stimuli. However, LPS-induced NLRP3 priming, uptake of crystalline stimuli and lysosomal damage were not influenced by CD pretreatment of normocholesterolemic macrophages, suggesting that CD is mediating its inhibitory effects on NLRP3 inflammasome activation by an as yet undefined mechanism.

5 Discussion

While elevated blood cholesterol levels have long been considered a risk factor for atherosclerosis, the pathogenic role of crystalline cholesterol, which accumulates in the arterial intima during atherogenesis, has only recently been identified. CCs potently induce innate inflammatory responses, and are considered responsible for the underlying vascular inflammation driving atherosclerosis development and progression. However, so far it has not been investigated whether decreasing the amount of CCs in atherosclerotic plaques is a valuable strategy for pharmaceutical intervention in atherosclerosis. Therefore, this study investigated the potential of the cholesterol solubilizing and mobilizing compound 2-hydroxypropyl-β-cyclodextrin (CD) to remove vascular CCs and thereby prevent murine atherosclerosis development and progression.

5.1 Cholesterol crystal deposition as therapeutic target in atherosclerosis

This study aimed at evaluating the potential of CCs as primary treatment target, by means of removing the trigger of inflammation[24,25] and plaque instability[73,74], rather than directly manipulating CC-induced inflammation as is currently being investigated in several clinical trials[42]. Theoretically, therapeutically targeting CCs can be achieved by dissolving and thereby removing existing CCs from atherosclerotic plaques or by preventing the formation of CCs in the vessel wall. The first evidence that prevention of CC formation might reduce CC-mediated inflammation and be atheroprotective originated from the genetic deletion of the oxLDL uptake receptor CD36 in murine diet-induced atherosclerosis. This study demonstrated that intracellular cholesterol crystallization upon oxLDL uptake into macrophages is dependent on CD36[118]. In turn, mice lacking CD36 developed smaller atherosclerotic plaques with significantly less CC deposits, which was accompanied by reduced aortic and systemic inflammation (section 4.1.1)[118].

CD was then tested for its capacity to prevent CC formation and potentially mediate the dissolution and removal of CCs from atherosclerotic plaque tissue *in vivo*. Of note, CD treatment did not affect general parameters like body weight, arterial blood pressure and heart rate, excluding the possibility of unequal intake of the atherogenic diet or differences in the general health of the animals throughout the study. In the atherosclerosis prevention model (section 4.1.2), CD treatment was effective in impairing atherosclerosis development and the deposition of CCs during atherogenesis. This was accompanied by reduced local and systemic inflammation as determined by decreased numbers of inflammatory macrophages inside the plaque and lower levels of circulating cytokines. Moreover, CD treatment was also effective in mediating the regression of already established

atherosclerotic plaques (section 4.1.3). Simply switching from atherogenic to chow diet significantly reduced the amount of CCs in the plaques as compared to the pretreatment control. This diet-induced CC reduction could be directly correlated to a reduction of serum cholesterol levels upon diet change and indicates the reversibility of CC deposition in diet-induced murine atherosclerotic plaques. However, the diet change did not reverse atherosclerotic plaque size. In contrast, CD treatment in both regression models (with or without diet change) reduced the amount of existing CCs in the plaques while also mediating a reduction in plaque size, even under continuous feeding of the atherogenic diet.

Interestingly, although parenteral CD administration was previously described to transiently decrease serum cholesterol levels in animal models and humans[93,101], in this study CD did not change overall serum cholesterol levels determined at the end of each atherosclerosis model. This indicates that CD does not reduce CC plaque loads by lowering blood cholesterol levels and thereby removing the trigger for vascular CC deposition. While the prevention model suggests that CC deposition is impaired upon CD treatment, the regression studies moreover indicate that CD also actively removes existing CCs from atherosclerotic plaques. This feature distinguishes CD from other pharmacological substances, which have been recently identified to also reduce CC formation, improve plaque stability and improve clinical outcomes in patients with CVD, such as statins[76], ezetimibe[137] and inhibitors of proprotein convertase subtilisin/kexin type 9 (PCSK9)[138,139]. All these substances lower serum cholesterol levels, in particular LDL cholesterol, thereby reducing cholesterol deposition in the vessel wall, resulting in a diminished pool of free cholesterol in the atherosclerotic plaque and thus preventing CC formation.

Altogether these studies indicate that CCs represent a viable treatment target in atherosclerosis and that reducing the amount of CCs in atherosclerotic plaques by genetic or pharmacological means can indeed impede atherogenesis. CD in particular was able to both prevent vascular CC deposition and remove preexisting CCs from atherosclerotic plaque tissues, and was therefore effective in mediating atherosclerosis regression.

Recently, the presence of CCs was also shown in nonalcoholic steatohepatitis (NASH), a chronic metabolic liver disease characterized by hepatic lipid accumulation (known as hepatic steatosis), inflammation and fibrosis, which can lead to cirrhosis, liver failure, and hepatocellular carcinoma. NASH shares several disease characteristics of atherosclerosis, such as dysregulated cholesterol homeostasis resulting in cholesterol accumulation, intracellular CC deposition and macrophage inflammation. In addition, a growing body of evidence suggests that NLRP3 inflammasome activation also contributes to NASH-related liver inflammation[140,141]. As in atherosclerosis, NASH can be induced by excess dietary cholesterol in animal models, and as such cholesterol-lowering therapies, such as statin treatment, were protective against steatosis, inflammation, and fibrosis in patients with

nonalcoholic fatty liver disease and NASH[141]. In this context, the dissolution of preexisting hepatic CCs was observed in mouse models of diet-induced NASH upon combinational treatment of statins and ezetimibe[142]. Furthermore, in a collaboration study, we have also demonstrated the potential of CD treatment to promote cholesterol transport from lysosomes to the cytoplasm and to prevent the accumulation of hepatic CCs in diet-induced NASH[143]. The livers of the mice from the atherosclerosis prevention model (section 4.1.2.) were also controlled for signs of hepatic toxicity, and CD treatment reduced common markers of liver damage and fibrosis which are commonly increased by HFHC feeding of ApoE$^{-/-}$ mice (data not shown, personal communication with Dr. Sebastian Zimmer). Consequently, pharmaceutical targeting of CCs might also represent a beneficial treatment approach for other cholesterol-related metabolic diseases in which CC deposition is observed.

5.2 2-Hydroxypropyl-β-cyclodextrin and cholesterol crystals

The ability of β-cyclodextrins to form inclusion complexes with cholesterol is well described in the literature[89,99]. CD, as a hydroxypropylated β-cyclodextrin derivative, has a slightly lower cholesterol affinity than its parent β-cyclodextrin, but due to its increased water solubility CD has a greater potential to bring cholesterol into aqueous solution[89]. While the solubilizing interaction between CD and cholesterol molecules is well described, this study demonstrated that CD also interacts with and binds to crystalline cholesterol. Moreover, CD dose-dependently mediated the dissolution of CCs in an aqueous solution (Fig. 4-4). These findings indicate that CD can form inclusion complexes with the cholesterol molecules in CCs, thereby triggering the release of cholesterol molecules from the crystals, which are usually quite inert in aqueous environment.

In atherosclerosis CCs accumulate within the atherosclerotic plaque tissue. They are abundantly present in the extracellular space, for example in the lipid-rich necrotic core region of advanced atherosclerotic plaques. However, intracellular CCs are also present, mainly inside plaque macrophages[24,119], and the general consensus is that these intracellular CCs are either formed inside the cells in response to free cholesterol accumulation or acquired by phagocytosis of extracellular CCs[144]. Therefore, for CD to mediate the removal of existing CCs from atherosclerotic plaque tissue, which was observed in the atherosclerosis regression models (section 4.1.3), it must be able to enter the plaque tissue and possibly also intracellular compartments. Cyclodextrins generally have a poor ability to cross biological membranes[91], however, this study found that CD was efficiently taken up into macrophages and the cellular distribution of the internalized CD (dotted perinuclear pattern) (Fig. 4-6A-C), indicated CD uptake via endocytotic pathways. Accordingly, a recent study showed the uptake of fluorescently labeled randomly methylated β-cyclodextrin into intestinal epithelial cells via macropinocytosis[145]. This suggests that CD might be taken up into the

macrophages by random pinocytosis. However, since macrophages express several surface receptors which recognize carbohydrates or glucose-modified proteins, such as CLRs and scavenger receptors, which mediate ligand uptake[146,147], CD could also be taken up into macrophages via receptor-mediated phagocytosis. Regardless of which pathway CD utilizes to enter macrophages, the fact that CD is taken up into macrophages provides the basis for CD-mediated dissolution of intracellular CCs. It is also likely that CD, if it is taken up by one of these endocytic pathways, will end up in the same subcellular compartments as CCs, which are either taken up by phagocytosis or form in phagolysosomal compartments due to free cholesterol accumulation, for example upon phagocytic uptake of oxLDL or apoptotic bodies. Although colocalization of CD and phagocytozed CCs could not be examined in the presented experiments due to insufficient image resolution, CD did mediate the dissolution of phagocytozed, intracellular CCs (Fig. 4-6D-E) at concentrations that did not affect macrophage morphology (Fig. 4-6D) or viability (Fig. 4-5). Further evidence for the dissolution of intracellular CCs was obtained from studies using CCs prepared from stable isotope-labeled D_6-cholesterol (section 4.2.2). These studies revealed increased efflux and enzymatic metabolism of crystal-derived D_6-cholesterol upon CD treatment of D_6-CC-loaded macrophages. Since CCs are quite inert, this is only possible after D_6-cholesterol is released from the crystals.

Consequently, this study demonstrates the potential of the cholesterol solubilizing substance CD to interact with and dissolve crystalline cholesterol. The dissolution is not restricted to extracellular CCs, but also applies to intracellular CCs that had been phagocytozed by macrophages. In addition, intracellular CC formation upon uptake of oxLDL via CD36 in macrophages was able to be reversed upon CD treatment[118]. *In vivo*, CD is known to accumulate in various tissues for a short time after administration prior to renal excretion[91,106]. This transient tissue accumulation might allow CD to mediate the dissolution and removal of preexisting CCs from atherosclerotic plaques.

5.3 2-Hydroxypropyl-β-cyclodextrin-mediated modification of macrophage cholesterol homeostasis

Excessive accumulation of intracellular free cholesterol is known to be toxic for cells[57]. The dissolution of intracellular CCs by CD would be expected to increase intracellular pool of free cholesterol to detrimental levels, but interestingly no considerable cytotoxic effect of CD incubation on CC-loaded macrophages was observed (Fig. 4-5B). This already indicated that the cells are able to eliminate and/or detoxify this crystal-derived cholesterol, which was confirmed by more detailed investigations into the metabolism and efflux of crystal-derived cholesterol. CD treatment resulted in the dissolution of stable isotope-labeled D_6-CCs and

promoted the cellular efflux, storage and enzymatic metabolism to oxysterols of the crystal-derived D_6-cholesterol (section 4.2.2).

The effects of CD on cholesterol efflux and metabolism have been extensively studied in $NPC^{-/-}$cells and animal models. Here, it was demonstrated that CD overcomes the lysosomal cholesterol efflux defect of $NPC^{-/-}$cells and thereby promotes cellular cholesterol metabolism, storage and efflux[103-106]. Liu *et al.* suggested that cholesterol, which is trapped in lysosomes of $NPC^{-/-}$ cells, becomes mobilized by CD for lysosomal escape and is thereby shifted into the cell's metabolically active cholesterol pool. In turn, this liberated cholesterol is rapidly esterified for nontoxic cholesterol storage and eliminated from the cells and ultimately the whole body in $NPC^{-/-}$ mice[105,106]. This study suggests that CD mobilizes cholesterol in a similar manner in CC-loaded macrophages, where the sequestered pool of free cholesterol resulting from NPC-deficiency in NPC disease is instead represented by the naturally quite inert CCs. A summary of the hypothesized functions of CD on CC-loaded macrophages is given in Fig. 5-1 and will be discussed in detail in the following sections.

5.3.1 CD-mediated cellular storage of crystal-derived cholesterol

CD treatment of D_6-CC-loaded macrophages induced the formation of lipid droplets and increased the amount of esterified D_6-cholesterol, indicating the nontoxic intracellular storage of the liberated crystal-derived cholesterol in lipid droplets (Fig. 4-7). Similarly, a decrease in intracellular CCs along with increased cholesterol ester storage was also observed in the livers of CD-treated hyperlipidemic mice in a NASH model, which is similar to the atherosclerosis models presented in this study[143]. Furthermore, increased cholesterol ester storage was also observed upon CD treatment of hypercholesterolemic $NPC^{-/-}$ mice, in almost every organ except the lungs[106]. Together these data indicate that CD treatment also promotes nontoxic cholesterol storage *in vivo*.

This CD-induced esterification is most likely to occur because CD liberates the crystal-derived D_6-cholesterol and promotes its intracellular movement to cellular compartments, such as the ER, where cholesterol can be enzymatically converted to its esters by ACAT for nontoxic storage in lipid droplets. CD treatment however also induced LXR target gene expression. One of these LXR target genes is Srebp-1c, which in turn activates the expression of Scd-1. Scd-1 catalyzes the production of oleoyl-CoA, which is the preferred substrate for ACAT-mediated cholesterol esterification[63]. Therefore, besides mobilizing crystal-derived D_6-cholesterol to the metabolically active cholesterol pool, CD might also indirectly improve cholesterol ester storage by activating LXRs and subsequently promoting ACAT activity.

5.3.2 CD-mediated metabolism of crystal-derived cholesterol

27-HC is a bioactive, oxygenated cholesterol metabolite and is a key regulator of cellular and systemic cholesterol homeostasis, for example by serving as an endogenous LXR ligand[123] and a substrate for bile acid synthesis in the liver[66]. Interestingly, some crystal-derived D_5-27-HC was detected in D_6-CC loaded macrophages alongside unlabeled 27-HC from endogenous cholesterol, even in the absence of CD (Fig. 4-9). This confirms earlier studies showing that macrophages themselves can at least partially degrade CCs, since crystal-derived cholesterol is demonstrably integrated into macrophage cholesterol metabolism[148]. However, CD treatment significantly increased the production of 27-HC from both crystal-derived and endogenous cellular cholesterol in macrophages (Fig. 4-9). No changes in mRNA and protein expression levels of cholesterol 27-hydroxylase (Cyp27a1), which is the enzyme catalyzing the hydroxylation of cholesterol at the 27-position were observed upon CD treatment of hypercholesterolemic macrophages. This observation is in line with earlier studies, which also found increased 27-HC production upon cholesterol loading of macrophages without changes in 27-hydroxylase expression[149]. Therefore, it is more likely that CD promotes 27-HC production in CC-loaded macrophages in two steps: Firstly, CD-mediated dissolution of CCs increases the intracellular pool of free cholesterol thereby providing more substrate for mitochondrial 27-hydroxylase. This hypothesis is supported by the strong increase in crystal-derived D_5-27-HC following CD treatment. Secondly, similar to what is described for NPC disease[106], CD treatment presumably increases the turnover of intracellular cholesterol pools, thereby promoting cholesterol trafficking to mitochondrial membranes where it can be enzymatically converted to 27-HC. The latter scenario could also explain the unexpected increase in 27-HC production upon CD treatment seen in normocholesterolemic macrophages, where CD also reduces the total amount of cellular cholesterol (Fig. 4-13).

Intriguingly, the majority of the 27-HC was actually found in the cell culture supernatants. Since 27-hydroxylase is a mitochondrial enzyme[122], 27-HC must be generated inside the macrophages and then subsequently effluxed from the cell. Rapid efflux of 27-HC from macrophages in the presence of a lipophilic cholesterol acceptor such as β-cyclodextrin or HDL has indeed been previously described[150]. Moreover, β-cyclodextrin was shown to desorb the more polar oxysterols from model membranes much faster than cholesterol[151], indicating that CD might more efficiently deplete oxysterols from macrophages than cholesterol. This suggests that an increase in 27-HC production in CD-treated macrophages contributes to the depletion of cellular cholesterol pools.

Furthermore, oxysterols themselves were also found to increase cholesterol solubility *in vitro* and even mediated the dissolution of subcutaneous cholesterol implants in rats, which are comparable to crystalline cholesterol in atherosclerotic plaques[77,152]. Therefore, the

production of 27-HC might also aid in dissolving intracellular CCs, which explains the capacity of macrophages to partially degrade CCs and suggests a positive feedback loop for CD-mediated macrophage cholesterol metabolism and efflux.

The production of oxysterols upon CD treatment was also observed in NPC patients, and indeed plasma 24(S)-HC levels are often used as biomarkers for the effectiveness of intracerebroventricular and intrathecal CD treatment[153]. 24(S)-HC levels were also determined in this study and while 24(S)-HC showed a similar trend to 27-HC induction by CD, this was not significant. This is presumably because 24(S)-HC is mainly produced by neurons in the CNS[67], while 27-HC is the major oxysterol produced in response to cholesterol loading in macrophages[123], and therefore maybe the most relevant oxysterol in atherosclerosis.

5.3.3 Transcriptional macrophage reprogramming by CD-mediated LXR activation

A key finding of this study was that CD treatment significantly increased the production of 27-HC in macrophages, which is known to activate LXR transcription factors[123]. LXR transcription factor activation is important for regulating cellular cholesterol homeostasis, mainly by regulating cholesterol efflux pathways[130]. In this context, the major LXR target genes include the cholesterol efflux transporters ABCA1 and ABCG1[125-127]. CC loading of macrophages increased gene and protein expression of both cholesterol efflux transporters, which was considerably increased upon CD treatment (Fig. 4-10). Both the CC-mediated and the CD-amplified increase in ABCA1 and ABCG1 expression was LXR-dependent (Fig. 4-11). Earlier studies demonstrated that cholesterol loading of macrophages induces ABCA1 and ABCG1 expression in a dose-dependent manner[128,129], and that the cholesterol dose applied correlated with 27-HC production and LXR activation in these cells[123]. Therefore, by simply dissolving intracellular CCs and increasing the intracellular metabolically active pool of free cholesterol, CD most likely triggers increased 27-HC production, subsequent LXR activation and induction of cholesterol efflux pathways. In keeping with this model, LXR target gene expression was also observed upon CD treatment of $NPC^{-/-}$ mice[105].

Genome-wide gene expression analysis of CD-treated normocholesterolemic and CC-loaded macrophages revealed that CD treatment led to a significant enrichment of previously published LXR target gene sets[114] compared to untreated macrophages. These data confirmed LXR activation upon CC loading and even stronger LXR activation upon CD treatment of CC loaded macrophages on a genome wide scale. Interestingly, this analysis also showed that LXR target gene expression was induced in CD-treated normocholesterolemic macrophages. This finding was unexpected as CD removed

cholesterol from normocholesterolemic macrophages and induced genes in the cholesterol biosynthesis pathway, which was also confirmed by an increase in cholesterol synthesis markers (Fig. 4-13), and, consistent with the idea of the cells restoring cholesterol homeostasis in response to depletion, a decrease in cholesterol efflux gene expression would have been expected. However, as observed with mass spec analysis, CD treatment of normocholesterolemic macrophages also increased 27-HC production, which might be sufficient to mediate the observed increase in LXR target gene expression. Furthermore, CD treatment of normocholesterolemic macrophages also increased intracellular levels of desmosterol, which is a cholesterol precursor that has also been described as a potent endogenous LXR agonist in macrophages[154,155]. In general, the data presented in this study indicate a direct link between increased 27-HC production and LXR activation in response to CD treatment. However, it cannot be excluded that CD treatment also induces the production of other endogenous LXR ligands, such as other naturally occurring oxysterols with proposed LXR agonistic function including 20(S)-HC, 22(R)-HC, 24(S)-HC, 25-HC and 24(S), 25-epoxycholesterol[154], which contribute to the LXR-mediated transcriptional macrophage reprogramming upon CD treatment. In macrophages, however, of the oxysterols that were measured, 27-HC was the only oxysterol that was significantly regulated by CD, therefore presumably it is mediating many of the effects observed *in vitro* in macrophages.

5.3.4 CD-mediated efflux of crystal-derived cholesterol

It is well described that CD promotes the efflux of cholesterol from macrophages and other cells[99,102,131]. This study demonstrated that CD also increases the efflux of crystal-derived D_6-cholesterol from D_6-CC-loaded macrophages, which can be significantly increased by the addition of a cholesterol acceptor (Fig. 4-8).

CC-loaded macrophages appeared to readily efflux some of the crystal-derived D_6-cholesterol in a time-dependent manner after replenishment of fresh medium, confirming that they have mechanisms for partially degrading crystalline cholesterol themselves, thus making it available for cellular cholesterol efflux mechanisms (and cholesterol metabolism, see section 5.3.2)[25,148]. Free cholesterol is usually eliminated from macrophages via the cholesterol efflux transporters ABCA1 and ABCG1, which transfer the free cholesterol to lipid-free ApoA1 and HDL particles, respectively[156]. Since ABCA1 and ABCG1 were both upregulated upon CC-loading of macrophages (Fig. 4-10) and the cell culture medium used for these experiments was supplemented with FCS containing lipoproteins including HDL, it is likely that the macrophages effluxed the liberated crystal-derived D_6-cholesterol via these cholesterol efflux transporters.

This basal macrophage efflux of crystal-derived D_6-cholesterol was significantly increased after 24 hours of CD treatment, indicating a more rapid dissolution of the CCs followed by

increased elimination of free cholesterol from the cells. The greater elimination might be explained by the LXR-dependent upregulation of ABCA1 and ABCG1 expression following CD treatment of CC-loaded macrophages (Fig. 4-11, section 5.3.3.), which could therefore more efficiently remove the liberated crystal-derived cholesterol. Furthermore, at the concentration used in these experiments, CD is also expected to function as cholesterol acceptor[100] and could therefore also increase the removal of crystal-derived cholesterol. CD has been proposed to mediate cellular cholesterol depletion by desorbing cholesterol from the plasma membrane and bringing it into aqueous solution by forming a 2:1 CD-cholesterol inclusion complex[157,158]. However, CD might also affect the overall distribution of intracellular cholesterol by promoting the movement of cholesterol from intracellular membranes to the plasma membrane[99], similar to what has been suggested for NPC disease, where CD overcomes the cholesterol transport defect that prevents cholesterol transport from the endolysosomal compartment to other cellular membranes[105]. Therefore, a CD-mediated increase in intracellular cholesterol turnover might cause more rapid incorporation of the liberated crystal-derived cholesterol into the plasma membrane and therefore increase CD-mediated desorption of crystal-derived cholesterol from these membranes.

Prolonged CD treatment (48 hours) did not result in a further decrease of intracellular D_6-cholesterol, indicating that the maximum CD-mediated cholesterol efflux capacity was already reached after 24 hours. Given that cyclodextrin inclusion complexes are known to be in a dynamic equilibrium with the free cyclodextrin and guest molecules[89], it is possible that after 24 hours there are not enough free cyclodextrin molecules left to form further inclusion complexes, impeding further CC dissolution and cholesterol desorption from the membranes. Moreover, since CD enhances the bidirectional cholesterol flux between cells and the extracellular environment[100] and pre-formed cyclodextrin-cholesterol inclusion complexes can also be used to enrich cells with cholesterol[99], the effluxed D_6-cholesterol might even be returned to the cells again. Another possible explanation is that some of the crystal-derived D_6-cholesterol, which was liberated by CD, might already be esterified at 48 hours (Fig. 4-7), and thus can't be removed by ABCA1- and ABCG1-mediated cholesterol efflux without prior hydrolysis by CEH[58,156]. CD was shown to be effective in removing both free and esterified cholesterol from macrophage foam cells[100,102], which most likely works by improving intracellular cholesterol turnover, thus increasing CEH-mediated hydrolysis of esterified cholesterol and its subsequent efflux or desorption. However, this only works in the presence free cyclodextrin molecules, which is a further indication that CD's capacity to remove liberated crystal-derived cholesterol is reached after 24 hours at this concentration, promoting the esterification of liberated free D_6-cholesterol for nontoxic intracellular cholesterol storage. Whether the addition or replenishment of fresh CD would induce further

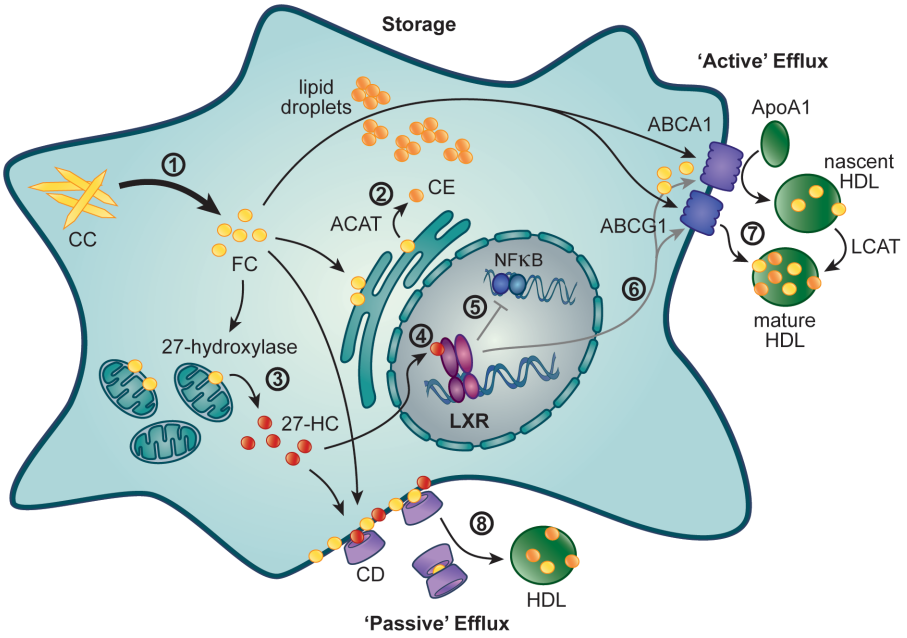

Figure 5-1: Model of CD function on CC-loaded macrophages.

CD promotes the dissolution of intracellular CCs, resulting in an increased cellular free cholesterol (FC) pool (1). Furthermore, CD increases the turnover of intracellular cholesterol pools, which leads to increases in cellular cholesterol storage, cholesterol metabolism, and "active" and "passive" cholesterol efflux. Liberated crystal-derived FC is esterified by ACAT in the ER resulting in subsequent nontoxic storage of cholesterol esters (CE) in cytoplasmic lipid droplets (2). Furthermore, FC is metabolized into oxysterols, e.g. 27-HC by mitochondrial 27-hydroxylase (3). 27-HC activates LXR-transcription factors resulting in transcriptional reprogramming of the macrophages (4). LXR activation mediates the repression of NF-κB-mediated inflammatory responses (5) and induction of cellular cholesterol efflux pathways, including the upregulation of cholesterol efflux transporters ABCA1 and ABCG1 (6). ABCA1 transfers cellular FC to lipid-poor ApoA1 particles generating nascent HDL particles (7). Esterification of FC in HDL particles by LCAT generates mature HDL particles, which accept cellular FC from ABCG1 (7). Furthermore, CD can remove cellular FC and oxysterols by desorption from the plasma membrane, with subsequent formation of 2:1 inclusion complexes (CD as "cholesterol sink") and transfer to cholesterol acceptors, such as HDL (CD as "cholesterol shuttle") (8).

removal of crystal-derived cholesterol as well as a reduction in cellular cholesterol ester pools has not yet been investigated.

The addition of lipid-poor reconstituted HDL (rHDL) particles significantly improved the crystal-derived D_6-cholesterol efflux mediated by CD (Fig. 4-8). rHDL itself was shown to mediate the depletion of cellular cholesterol[121] and indeed significantly removed unlabeled endogenous cholesterol from D_6-CC loaded macrophages. However, rHDL alone was not able to mediate the depletion of crystal-derived D_6-cholesterol, demonstrating that the presence of CD was required for the improved removal of crystal-derived D_6-cholesterol, potentially by dissolving the crystals and making the liberated free cholesterol available for subsequent cellular cholesterol efflux mechanisms. In this setting rHDL most likely functioned as an extracellular cholesterol acceptor for ABCA1- and ABCG1-mediated active cholesterol efflux, but also for cyclodextrin-mediated cholesterol depletion according to the "shuttle/sink model" proposed by Atger *et al.* (Fig. 2-7)[100]. In this model, CD supposedly transfers

cholesterol molecules desorbed from the plasma membranes to lipid-poor rHDL particles and therefore functions as shuttle between the cells and the cholesterol acceptors (where the lipid-poor rHDL is the “sink”).

In summary, this study indicated that CD might improve the removal of crystal-derived cholesterol from macrophages by several mechanisms (Fig. 5-1). CD enhances CC dissolution and potentially mobilizes intracellular crystal-derived cholesterol for active cellular cholesterol efflux via ABCA1 and ABCG1, but also for direct CD-mediated desorption from the plasma membranes and potential shuttling of cellular cholesterol to lipoproteins (extracellular cholesterol acceptors/ “sinks”). Moreover, increased oxysterol production by CD, subsequent LXR transcription factor activation and transcriptional upregulation of cholesterol efflux transporters might indirectly contribute to the improved removal of crystal-derived cholesterol from macrophages upon CD treatment.

5.4 RCT and alternative cholesterol excretion by 2-hydroxypropyl-β-cyclodextrin

Besides promoting macrophage efflux of crystal-derived cholesterol *in vitro*, CD also enabled the RCT of crystal-derived D_6-cholesterol from D_6-CC-loaded macrophages *in vivo* in a partially LXR-dependent manner (section 4.3.4). Macrophage cholesterol efflux is the first step of RCT, and is therefore a crucial event for the elimination of cholesterol from the body[60]. Since CD is excreted from the body via the urine[89], and co-secretion of cholesterol with CD was observed in in animal models[101] and also upon intravenous CD treatment of NPC patients (Zimmer and Grebe *et al.*, in press), the commonly used macrophage-to-feces approach for assessing RCT was extended to include a macrophage-to-urine analysis. Indeed, CD treatment of mice injected with D_6-CC-loaded WT macrophages induced the rapid elimination of crystal-derived D_6-cholesterol from the body via both biliary and renal excretion.

CD treatment increases the efficiency of cholesterol elimination from the body by providing an alternative pathway for cholesterol excretion into the urine in addition to HDL-mediated RCT to the liver for subsequent fecal excretion. Therefore, according to the “shuttle/sink model” proposed for CD-mediated cholesterol efflux *in vitro* (Fig. 2-7)[100], CD facilitates macrophage cholesterol efflux and serves as cholesterol “shuttle” between cells and serum lipoproteins for biliary cholesterol excretion, while also serving as “sink” for directly removing cholesterol complexed to CD by renal excretion.

CD-mediated excretion of crystal-derived cholesterol into both the feces and the urine was delayed and compromised in the *in vivo* RCT experiment with LXR-deficient macrophages. This indicates that the rapid RCT and elimination of crystal-derived cholesterol by CD is dependent on LXR transcription factor activation, presumably by LXR-mediated regulation of

cholesterol efflux pathways, including the upregulation of ABCA1 and ABCG1 expression. However, since the excretion of crystal-derived cholesterol is so quick (within 6-9 hours after CD treatment), it is most likely mediated by the LXR-dependent upregulation of the cholesterol efflux transporters in response to CC loading of the macrophages, rather than the secondary LXR-dependent increase in ABCA1 and ABCG1 expression upon CD treatment of CC-loaded macrophages (Fig. 4-11). Therefore, the LXR-dependency of this process is most likely independent of CD treatment. Nevertheless, since no fecal or urinary D_6-cholesterol was detected in vehicle treated animals, CD treatment is definitely required for the RCT and excretion of crystal-derived cholesterol, where it presumably mediates intracellular CC dissolution and thereby enabling the efflux of the liberated crystal-derived cholesterol.

5.5 Atheroprotective effects of 2-hydroxypropyl-β-cyclodextrin

Chronic subcutaneous CD treatment was found to be atheroprotective in two different models of murine diet-induced atherosclerosis (sections 4.1.2 and 4.4). Analysis of CD treatment of hypercholesterolemic, CC loaded macrophages indicated that CD treatment might be atheroprotective by dissolving CCs, thus increasing macrophage cholesterol metabolism and production of endogenous LXR agonists, such as 27-HC, and thereby promoting macrophage cholesterol efflux and subsequent RCT (sections 4.2 and 4.3). However, these mechanistic data only provide insight into the effects of CD on hypercholesterolemic macrophages, which represent an important cell type of atherosclerotic plaques, but do not reflect the *in vivo* situation, where CD affects the whole body, including various organs and tissues with mixed cell populations. Therefore, the bone marrow transplantation atherosclerosis model was performed to evaluate whether CD's atheroprotective effects *in vivo* were primarily due to changes in the cholesterol metabolism of macrophage foam cells. This model revealed that the cholesterol efflux transporters ABCA1 and ABCG1 were dispensable for CD-mediated atheroprotectivity, while the presence of LXR transcription factors in hematopoietic-derived cells was essentially required. However, CD-mediated atheroprotection is most likely multifactorial and not solely dependent on either LXR activation or enhanced RCT alone.

5.5.1 Importance of CC dissolution for CD-mediated atheroprotection

As discussed in section 5.1, prevention of vascular CC deposition as well as the pharmacological reduction of already existing plaque CCs was found to impede atherogenesis. Since CD-mediated atheroprotection was always associated with a reduction in plaque CC loads throughout this study, it is likely that the dissolution and removal of plaque CCs is one of the mechanisms involved in CD-mediated atheroprotectivity. Moreover, CD treatment either had no effect or even increased CC quantities in atherosclerotic plaques

of LDLR$^{-/-}$ mice transplanted with LXRα$^{-/-}$/LXRβ$^{-/-}$ bone marrow, and in these mice CD was also not atheroprotective.

Since LXR transcription factors are involved in the regulation of cholesterol efflux pathways, including ABCA1 and ABCG1 cholesterol efflux transporters[130], and given the defect in CD-mediated RCT from LXRα$^{-/-}$/LXRβ$^{-/-}$ macrophages, a plausible explanation would be that the LXR transcription factor absence impairs ABCA1- and ABCG1-mediated macrophage cholesterol efflux and therefore cholesterol removal from the atherosclerotic plaque tissue. However, CD treatment efficiently reduced the amounts of CCs in LDLR$^{-/-}$ mice transplanted with bone marrow of MAC-ABC^{DKO} mice, which supposedly have a defect in macrophage cholesterol efflux. This indicates that CD can dissolve plaque CCs and subsequently remove the crystal-derived cholesterol independently of the cholesterol efflux transporters ABCA1 and ABCG1. It also indicates that other LXR-mediated processes, beyond ABCA1- and ABCG1-mediated cholesterol efflux, such as the suppression of cholesterol biosynthesis under conditions of high cellular cholesterol[61], might be more important in this context, especially since CD treatment of LXRα$^{-/-}$/LXRβ$^{-/-}$ bone marrow transplanted mice even slightly increased CC plaque loads. This increase could be explained by the following scenario: CD treatment results in the dissolution of plaque CCs, resulting in increased amounts of free cholesterol, which cannot be efficiently removed and detoxified due to the lack of LXR transcription factors. Moreover, without LXR-mediated repression of cellular cholesterol biosynthesis, CD treatment might even further increase the cellular pool of free cholesterol. Subsequent cell death and increased inflammation might also promote the build-up of free cholesterol in the plaques and consequently favor cholesterol (re)crystallization.

The findings of the bone marrow transplantation model suggested a direct link between the amount of plaque CCs and atherosclerosis progression, and indicated that the CD-mediated dissolution and removal of plaque CCs might contribute to its atheroprotectivity. Plaque CC dissolution in atherosclerosis might be important to mobilize this inert pool of free cholesterol for increased metabolism and efflux from plaque tissue, similar to the proposed effects of CD in NPC disease[106]. However, this study does not prove the requirement of CD-mediated CC dissolution for its atheroprotective effects.

5.5.2 CD-mediated 27-HC production and atheroprotection

The observation that CD treatment significantly induced 27-HC production in CC-loaded macrophages (Fig. 4-9), was the impetus to investigate whether LXR transcription factors were also activated in this system. That CD treatment might also promote the production of the endogenous LXR agonist 27-HC in murine atherosclerosis *in vivo* was inferred from the bone marrow transplantation atherosclerosis model (Fig. 4-16), where LXR transcription factor activation was required for CD-mediated atheroprotectivity, and increased serum

levels of 27-HC upon CD treatment were observed. Significantly increased serum 27-HC levels were only observed in $LDLR^{-/-}$ mice reconstituted with $MAC\text{-}ABC^{DKO}$ and $LXR\alpha^{-/-}/LXR\beta^{-/-}$ bone marrow (almost significant), but not in $LDLR^{-/-}$ mice transplanted with WT bone marrow. This could be explained by impaired macrophage cholesterol efflux due to ABCA1/ABCG1- and LXRα/LXRβ-deficiency of the hematopoietic derived cells, which might cause increased cellular cholesterol levels compared to WT cells, which consequently provides more substrate for the enzymatic conversion to 27-HC. This could also explain the lack of increased 27-HC serum levels upon CD treatment in the first atherosclerosis mouse models.

While increased amounts of 27-HC are suggested be atheroprotective by activating LXR transcription factors and subsequent anti-atherogenic gene expression programs, a recent study suggested pro-atherogenic activities of 27-HC. 27-HC was recently identified to be an endogenous selective estrogen receptor modulator[159] and as such 27-HC was found to promote pro-inflammatory processes via estrogen receptor α and thus inhibiting estrogen-related atheroprotection[160]. These results were obtained from $Cyp7b1^{-/-}$ mice, where 27-HC accumulates because it cannot be further metabolized to 7α-hydroxycholesterol, a precursor of bile acid synthesis. Conversely, in Cyp7b1 competent animals, such as those used in our study, increased amounts of 27-HC could theoretically be efficiently converted to 7α-hydroxycholesterol, and therefore promote bile acid synthesis and cholesterol removal via biliary excretion. Consequently, it is likely that prolonged accumulation of 27-HC is pro-atherogenic by activating estrogen receptors, while moderately or transiently increased 27-HC might be anti-atherogenic via the activation of atheroprotective LXR transcriptional programs and an increase in bile acid synthesis and excretion. To properly evaluate whether increased 27-HC production is integral to the mechanism of CD-induced LXR-mediated atheroprotection, the effectiveness of CD treatment would need to be assessed in an atherosclerosis model with Cyp27a1 knockout mice or bone marrow chimeras. However, $Cyp27a1^{-/-}/ApoE^{-/-}$ mice, which do not produce any 27-HC, already show decreased atherosclerosis development, which is supposedly due to changes in lipoprotein profiles, with decreased LDL/VLDL cholesterol and increased HDL cholesterol, as well as compensatory mechanisms such as increased Cyp7a1-mediated conversion of cholesterol to 7α-hydroxycholesterol[161]. In contrast, heterozygous $Cyp27a1^{+/-}/ApoE^{-/-}$ mice develop more severe atherosclerotic lesions, which is assumed to be caused by decreased production of 27-HC and missing compensatory mechanisms resulting in impaired cholesterol efflux from plaque macrophages[161]. Therefore, the role of Cyp27a1 in atherogenesis is not fully understood and seems to be quite complex due to different functions of Cyp27a1 in hepatic and extrahepatic cells. Maybe a bone marrow transplantation model with $Cyp27a1^{-/-}$ donor bone marrow might overcome this complexity, as only hematopoietic derived cells would

carry the Cyp27a1 deficiency. Therefore, if 27-HC is crucially involved in CD-mediated LXR activation *in vivo*, these mice should show the same CD treatment phenotype than LDLR$^{-/-}$ mice transplanted with LXRα$^{-/-}$/LXRβ$^{-/-}$ bone marrow. Furthermore, as already discussed in section 5.3.3, 27-HC was the only significantly induced endogenous LXR agonist analyzed in this study, but it cannot be excluded that CD induces the production of other sterol-based endogenous LXR agonists *in vivo*. Therefore, it is possible that other CD-induced endogenous LXR agonists might compensate for a lack in 27-HC or might generally be more important than 27-HC, or alternatively, that several CD-induced endogenous LXR agonists act in concert to mediate the atheroprotective LXR transcription factor activation in response to CD treatment.

5.5.3 Potential mechanisms of LXR-mediated atheroprotection

Mice lacking LXR transcription factors develop enhanced atherosclerosis, suggesting a protective role for these transcription factors, and complementary to this, administration of synthetic LXR agonists was shown to be atheroprotective in mice[116,124,162]. The atheroprotective effects of LXR agonists have been attributed to the two main functions of LXR transcription factors: upregulation of genes involved in macrophage cholesterol efflux such as ABCA1 and ABCG1 and the subsequent regulation of RCT[116,163] and suppression of inflammation via transrepression of NF-κB target genes[164].

CD activated LXR transcription factors in hypercholesterolemic macrophages *in vitro* (section 4.3), and promoted macrophage cholesterol efflux (Fig. 4-8) as well as RCT of crystal-derived cholesterol from macrophages in a partially LXR-dependent manner (Fig. 4-14). Moreover, CD treatment mediated the upregulation of cholesterol efflux transporter ABCA1 and ABCG1 expression in aortic tissue of CD-treated animals (Zimmer and Grebe *et al.*, in press). Although, these results indicated that CD might be atheroprotective by LXR-mediated upregulation of the cholesterol efflux transporters ABCA1 and ABCG1 in macrophages, which are important for macrophage cholesterol efflux and subsequent RCT[165], CD was still atheroprotective in LDLR$^{-/-}$ mice transplanted with MAC-ABC^{DKO} bone marrow. Nevertheless, LXR transcription factor activation in hematopoietic-derived cells was required for CD-mediated atheroprotection, indicating that LXR-mediated processes other than the upregulation of macrophage cholesterol efflux and RCT might be responsible for CD-mediated atheroprotection. This is in line with current literature demonstrating that synthetic LXR agonist treatment is atheroprotective in LDLR$^{-/-}$ mice transplanted with MAC-ABC^{DKO} bone marrow, which suggests a key role for the LXR-mediated anti-inflammatory effects in atheroprotection[166]. However, this study with synthetic LXR agonists did not definitively prove that LXR activation induces anti-inflammatory pathways *in vivo*, rather only reported a reduction of inflammatory cells

(macrophages) in the atherosclerotic plaques of LXR agonist-treated mice. In addition to reducing macrophage plaque loads in the ApoE$^{-/-}$ mouse models CD treatment also decreased circulating pro-inflammatory cytokine levels (section 4.1.2, Zimmer and Grebe *et al.*, in press). However, this decrease in macrophage plaque loads was not observed upon CD treatment of the LDLR$^{-/-}$ mice in the bone marrow transplantation atherosclerosis models (Fig. 4-15), probably because of the less advanced atherosclerotic plaques in the latter mouse model. Nevertheless, gene expression analysis of the aortic tissue of these mice revealed that CD treatment induced inhibitory gene expression changes of genes involved in NLRP3 inflammasome activation *in vivo*, which was dependent on LXR transcription factor activation in hematopoietic-derived cells (Fig. 4-17). In particular, CD treatment downregulated genes encoding for the NLRP3 inflammasome components NLRP3, ASC and caspase-1 as well as the pro-inflammatory inflammasome effector cytokines IL-1β and IL-18, while upregulating SGT1 and HSP90, which have been described as inhibitors of NLRP3 inflammasome function. Similar, but even stronger inhibitory effects of CD treatment on genes involved in NLRP3 inflammasome activation were also observed in *ex vivo* cultures of human atherosclerotic plaque tissue (Zimmer and Grebe *et al.*, in press). Indeed, NLRP3 and HSP90 have both been identified as LXR target genes by ChIP sequencing analysis of human macrophages treated with a synthetic LXR agonist[135]. Furthermore, NLRP3 expression is upregulated in response to NF-κB transcription factor activation[28], which is inhibited by transrepression mechanisms of activated LXRs[164]. This data indicated that CD might be atheroprotective by LXR-dependent inhibition of NLRP3 inflammasome activation in atherosclerotic plaque tissue, which would in turn decrease CC-mediated pro-atherogenic inflammatory responses.

The effect of CD treatment and potential subsequent LXR activation on NLRP3 inflammasome activation, in particular in response to CCs, was assessed *in vitro* in murine macrophages (section 4.5). In contrast to the genetic changes in *in vivo*-treated murine or *ex vivo*-treated human atherosclerotic plaque tissue, CD treatment of normocholesterolemic macrophages did not affect basal or LPS-induced protein expression of NLRP3 inflammasome components, but neither did LXR agonist treatment (Fig. 4-18). However, NLRP3 was identified as an LXR target gene in human macrophages[135], but currently there is no evidence in the literature that NLRP3 is an LXR target gene in murine macrophages. Nevertheless, NLRP3 inflammasome activation by LeuLeu or crystalline stimuli was reduced upon both CD pretreatment and LXR agonist pretreatment (Fig. 4-19), indicating that LXR activation might be important for this inhibition. Furthermore, this finding suggested that CD treatment and LXR activation might affect the uptake of crystalline material or subsequent lysosomal damage, which is hypothesized to be part of the NLRP3 inflammasome activation mechanism in response to these ligands (see section 2.1.3.2)[28], but neither of these

mechanisms were influenced by CD treatment in this experimental setup (Fig. 4-20). Therefore, these data suggest that CD treatment can indeed inhibit CC-mediated NLRP3 inflammasome activation in macrophages by an as yet undefined mechanism. This unidentified mechanism is possibly mediated by CD-induced LXR activation, since the same NLRP3 inflammasome inhibition was observed in response to LXR agonist treatment. In conclusion, the gene expression analysis of human and murine aortic plaque tissue as well as the *in vitro* data on macrophage NLRP3 inflammasome activation indicate that CD inhibits NLRP3 inflammasome activation in an LXR-dependent manner and that this might contribute to CD's atheroprotective effects by decreasing CC-mediated pro-atherogenic inflammatory responses in atherosclerotic plaques.

Another potential mechanism of LXR-mediated atheroprotection is the regulation of efferocytosis. Upon phagocytic uptake of apoptotic cells, LXR transcription factors become activated, presumably in response to intracellular cholesterol accumulation (section 2.2.5.4)[61]. While LXR activation upregulates the expression of the TAM receptor tyrosine kinase Mer, which has a crucial role in phagocytosis and therefore promotes apoptotic cell clearance, LXR activation can also simultaneously suppress inflammatory pathways that might be induced by phagocytozed apoptotic cells[167]. Consequently, LXR-deficient macrophages also have a defect in phagocytosis of apoptotic cells and induce abnormal pro-inflammatory responses. Effective phagocytic clearance of apoptotic cells by macrophages without activation of inflammatory responses is important for keeping immune homeostasis and defective efferocytosis is thought to promote atherosclerosis plaque development and formation of a lipid-rich necrotic core[35]. Therefore, activation of LXR transcription factors upon CD treatment might also be atheroprotective by promoting effective efferocytosis and thereby inhibiting atherosclerosis plaque development.

Of note, CD treatment did not only prevent the development and progression of murine atherosclerosis, but was also effective in mediating the regression of already established atherosclerotic plaques (section 4.1.3). This might be the most important feature of CD-mediated atheroprotection for human disease, because atherosclerosis patients are usually only diagnosed in advanced disease stages with established atherosclerotic plaques. LXR activation was also implicated in mediating the regression of already established atherosclerotic plaques by inducing the expression of chemokine receptor CCR7, which promotes maximal egress of monocyte-derived cells from murine aortic plaques[168,169]. Although the gene expression data of the aortas from the bone marrow transplantation model did not show any significant upregulation of CCR7 by CD treatment, this may be because whole aortic tissue was analyzed, while the published studies analyzed monocyte-derived cell populations isolated from atherosclerotic plaques by laser capture microscopy. The slightly decreased amounts of plaque macrophages in the regression models however

indicate a potential involvement of LXR-mediated monocyte-derived cell egress. Moreover, CD treatment *in vitro* strongly increased the expression of CCR7 induction in bone marrow derived DCs and also slightly in BMDMs, which correlated with LXRα expression levels (data not shown, results from single preliminary experiment). These data indicate that LXR-dependent, CCR7-mediated egress of monocyte-derived cells might be important for atherosclerosis regression upon CD treatment and might therefore also contribute to the LXR-dependent atheroprotective effects of CD.

5.5.4 Indications of atherogenic adaptive immune response inhibition by β-cyclodextrin derivatives

The data presented in this thesis suggest that there is significant therapeutic potential in cholesterol solubilizing β-cyclodextrins, in particular CD, for the treatment of atherosclerosis. This was confirmed by a study published last year, which demonstrated the atheroprotective effects of KLEPTOSE® CRYSMEB (Roquette, France) treatment in diet-induced atherosclerosis in ApoE$^{-/-}$ mice[170]. Unlike CD (hydroxypropylated β-cyclodextrin), KLEPTOSE® CRYSMEB is a patented low methylated β-cyclodextrin developed for pharmaceutical formulations, which (similar to CD) possesses improved safety compared to highly methylated β-cyclodextrins[*].

Similar to CD, methyl β-cyclodextrin was found to decrease atherosclerotic plaque size without changing total serum cholesterol levels. However, Montecucco *et al.* observed that methyl β-cyclodextrin treatment increased HDL cholesterol levels in ApoE$^{-/-}$ mice, and suggested that improving the serum lipoprotein profile contributes to the atheroprotective effects of methyl β-cyclodextrin. In contrast, CD treatment did not induce any changes HDL cholesterol levels in LDLR$^{-/-}$ mice (Fig. 4-16). This discrepancy is most likely due to the different mouse models used, which possess different lipoprotein profiles. The lipoprotein profile of the LDLR$^{-/-}$ mouse model most closely resembles that of dyslipidemic humans[36] and might therefore be more relevant with regard to human disease. Moreover, these discrepancies might be due the different types of modified β-cyclodextrin as well as differences in treatment time and dosage. However, as CD was protective in the LDLR$^{-/-}$model without modulation of serum lipoprotein profiles, this suggests that the increase in HDL seen with methyl β-cyclodextrin might be negligible for its atheroprotectivity.

Montecucco *et al.* observed reduced plaque T lymphocyte numbers and a reduction in genetic markers for type 1 T helper cell (Th1)-mediated immune responses. Their data indicated that methyl β-cyclodextrin reduced proliferation of CD4-positive Th1 cells and

[*] ROQUETTE website: http://www.roquette-pharma.com/crysmeb-beta-cyclodextrin-pharmaceutical-excipient-injectable-dosage-forms/ - 19th March, 2016, 5:08 pm

subsequent IFNγ production. IFNγ exerts various pro-atherogenic effects, which promote plaque development and contribute to plaque destabilization[171], and IFNγ-producing Th1 cells are therefore considered main drivers of disease progression[44]. Consequently they concluded that methyl β-cyclodextrin is atheroprotective by reducing adaptive Th1-mediated immune responses[170].

The work presented in this thesis was focused on the effects of cholesterol solubilizing CD on plaque CCs and subsequent CC-mediated innate immune responses elicited by plaque macrophages. The detailed analysis of macrophage cholesterol metabolism indicated that LXR transcription factor activation was important for CD's atheroprotective effects (section 4.2.2 and 4.3), and this was confirmed *in vivo* in the bone marrow transplantation atherosclerosis mouse models (section 4.4), which suggests that hematopoietic LXR transcription factor activation is required for CD's atheroprotectivity. Interestingly, LXR activation was shown to inhibit Th1-type pro-inflammatory cytokine expression in human CD4-positive lymphocytes[172], indicating that methyl β-cyclodextrin might reduce Th1-mediated immune responses by activating LXR-mediated transcriptional programs. Conversely, reduced adaptive Th1-mediated immune responses resulting from LXR activation might also contribute to CD's atheroprotectivitiy. Moreover, the pro-atherogenic character of IL-18[171], which is the major cytokine promoting Th1 differentiation and subsequent IFNγ production[44], is a pro-inflammatory IL-1β family cytokine produced upon CC-mediated NLRP3 inflammasome activation[24]. This might represent another connection between the findings on the atheroprotective effects of CD in this study and methyl β-cyclodextrin in the study of Montecucco and colleagues respectively. Both the CD-mediated reduction in plaque CCs (Fig. 4-2 and Fig. 4-15) and the LXR-dependent transcriptional deactivation of the NLRP3 inflammasome (Fig. 4-17) might decrease CC-mediated inflammasome activation and subsequent IL-18 production, Th1 differentiation and adaptive Th1-mediated immune responses.

Combining the findings of the presented study and the study of Montecucco and colleagues, β-cyclodextrin-mediated atheroprotective effects might be triggered by plaque CC dissolution, increased production of endogenous LXR agonists and subsequent activation of LXR-mediated transcriptional programs, which might improve aortic cholesterol homeostasis and suppress both innate and adaptive inflammatory responses.

5.6 Potential clinical application of 2-hydroxypropyl-β-cyclodextrin for treatment of atherosclerosis

Atherosclerosis treatment currently relies on pharmacological lowering of blood LDL cholesterol levels to decelerate disease progression and surgical intervention to bypass narrowed arteries or remove atherosclerotic plaque tissue[33]. However, no appropriate

pharmacological treatment for mediating atherosclerotic plaque regression is currently available, although evidence for the possibility of atherosclerosis plaque regression in humans, for example by long-term high-dose statin treatment, has accumulated over the last years[173]. Current studies on human plaque regression suggest that regression requires large reductions in LDL cholesterol levels and concurrent great enhancements in HDL function in RCT[173]. The work in this thesis identified that CD treatment prevented the development and progression of murine atherosclerosis, but also effectively mediated the regression of already established murine atherosclerotic plaques (section 4.1.3). Although CD treatment in mice did not alter serum cholesterol levels and serum lipoprotein profiles, it was found to significantly increase RCT from macrophages and subsequent fecal and renal cholesterol excretion (section 4.3.4), thus providing an additional mechanism for cholesterol removal from the body. Moreover, CD promoted the production of endogenous LXR agonists and thereby mediated the activation of LXR transcription factors. Macrophage LXR transcription factor activation by synthetic LXR agonists, such as T0901317 and GW3965, was shown to inhibit murine atherosclerosis development and promote atherosclerotic plaque regression[124,162]. Based on these findings, there was great interest in developing synthetic LXR-activating molecules as anti-atherogenic drugs in humans. However, initial clinical trials uncovered unwanted side effects, such as fatty liver disease and liver toxicity in response to LXR-mediated hepatic lipogenesis[174]. In contrast, CD treatment potentially induces LXR-mediated transcriptional reprogramming via the production of endogenous LXR agonists, such as 27-HC, as was also observed in *ex vivo* cultures of human atherosclerotic plaque tissue (Zimmer and Grebe *et al.*, in press). Moreover, CD treatment did not induce signs of hepatic toxicity in the presented ApoE$^{-/-}$atherosclerosis mouse models, but it rather decreased common markers of liver damage and fibrosis (data not shown, personal communication with Dr. Sebastian Zimmer), and which was also shown in studies of CD treatment in murine NASH[143].

The following mechanism of action for CD efficacy in atherosclerosis is therefore proposed: CD mediates LXR activation by promoting CC dissolution, thereby increasing intracellular free cholesterol and providing more substrate for cholesterol metabolism to bioactive oxysterols, which can function as LXR agonists. A similar mechanism of action was proposed for CD treatment in NPC disease, where CD is thought to mobilize cholesterol sequestered in lysosomes and shift it into the cell's metabolically active cholesterol pool and thereby improving cholesterol efflux, storage and metabolism[105,106]. These changes in cholesterol metabolism were absent in CD-treated non-NPC mice, indicating that CD treatment only induced these changes in the presence of a large sequestered pool of cholesterol[105,106]. While such sequestered cholesterol pools are present throughout the body in NPC patients, in atherosclerosis they are predominantly present in the arterial plaque tissue, including

hypercholesterolemic cells such as macrophage foam cells and inert cholesterol crystals. Hypothetically, the effects of CD in atherosclerosis might therefore be more or less restricted to atherosclerotic tissues. Such a directed and specific treatment might prevent undesired side effects. For example, LXR-mediated anti-inflammatory effects would be mainly exerted locally, therefore circumventing the detrimental risks of inhibiting systemic inflammation.

The atheroprotective effects of CD have so far only been demonstrated in mice, but *ex vivo* cultures of human atherosclerotic plaque tissue incubated with CD showed that CD can also induce the proposed atheroprotective pathways in human disease, with cholesterol efflux, production of endogenous LXR agonists and LXR transcriptional reprogramming all being upregulated upon CD treatment (Zimmer and Grebe *et al.*, in press). Collectively, these findings suggest that CD might be a promising compound for the treatment of human atherosclerosis. Moreover, the use of CD as an active drug in NPC disease with FDA IND approval and a first completed phase 1 clinical trial provides evidence for the safety of long-term intravenous (and intrathecal) CD administration in humans (section 2.3.3)[95]. However, there are several possible limitations to the pharmaceutical use of CD in the treatment of human atherosclerosis. The most substantial limitation might be the bad oral bioavailability of CD[89,91], which would require the parenteral (most likely intravenous) administration of CD. While this might be suitable for short-term treatments, which could be effective in temporarily stabilizing rupture-prone plaques in patients at high risk for cardiovascular events, it is impractical for long-term treatment, which might be required for mediating atherosclerosis regression. Furthermore, the pharmacokinetics of intravenously administered CD in humans demonstrate the rapid tissue and plasma clearance of CD in individuals with normal kidney function (section 2.3.1.3)[89]. Even the highest doses of CD currently applied to humans intravenously in the context of high-dose itraconazole treatment (8 g CD twice a day) only yield plasma CD levels of up to approximately 700 µg/ml (equals about 0.5 mM) (Fig. 2-6), which is 20-fold less to the concentration used in the presented *in vitro* studies. The pharmacokinetics of CD are similar in mice[106], where CD administration twice a week was sufficient for atheroprotection. However, it remains to be determined whether a subtoxic and well-tolerated CD dose is sufficient to prevent and or indeed reverse human atherosclerosis.

Combinational therapies with CD and other pharmacological substances that simultaneously lower LDL cholesterol levels (e.g. statins, ezetimibe, PCSK9 inhibitors) or increase HDL-mediated reverse cholesterol transport (e.g. phosphatidylcholine liposomes, ApoA1 mimetic peptides, rHDL)[173], might augment the therapeutic efficacy of CD to impair atherosclerosis progression and mediate atherosclerotic plaque regression. A combinational therapy with CD and rHDL seems particularly promising, considering the improved crystal-derived cholesterol efflux from macrophages upon combined treatment with CD and rHDL

observed in this study (Fig. 4-8). Moreover, CSL112, a new formulation of the rHDL used in this study (CSL111), was recently evaluated in a phase 2a clinical trial, which revealed a rapid and strong increase in RCT while being well tolerated in patients with stable atherosclerosis[175]. Considering the "shuttle/sink" model proposed for CD-mediated cellular cholesterol efflux (Fig. 2-7)[100], CD might act as a cholesterol shuttle for further improving the rHDL-mediated RCT. Moreover, CD might also facilitate macrophage cholesterol efflux by LXR-mediated transcriptional reprogramming. Vice versa, a complementation of CD treatment with rHDL might even be required for ensuring adequate RCT in humans, since mice have naturally much higher HDL cholesterol levels than humans[36]. Beyond these potential advantages, rHDL induces the expression of activating transcription factor 3 (ATF3) which mediates dramatic anti-inflammatory effects on macrophages[121] and could therefore complement the LXR-mediated anti-inflammatory pathways induced by CD treatment.
In summary, CD is a promising candidate for treating human atherosclerosis. However, the potential of CD mono- or combinational therapies for mediating atheroprotection or atherosclerosis regression in humans remains to be determined. Therefore, clinical studies are required to evaluate the safety and efficacy of CD treatment in atherosclerosis patients.

5.7 Conclusion

CC deposition in atherosclerotic plaques is well established as a histopathological feature of late stage disease but was for a long time regarded merely as a result of disease progression. However, CCs are already present in early atherosclerotic plaques, where they importantly contribute to the underlying vascular inflammation driving atherosclerosis development and progression.
This study investigated whether decreasing the amount of CCs in the plaque represents a valuable strategy for pharmaceutical intervention in atherosclerosis and whether the cholesterol solubilizing substance CD (2-hydroxypropyl-β-cyclodextrin) has the potential to mediate vascular CC removal and impair murine atherosclerosis development and progression. The genetic and pharmacological reduction of vascular CC deposits was associated with decreased atherosclerosis and therefore this study identified that CCs represent a viable treatment target in atherosclerosis. CD treatment effectively decreased murine atherosclerosis development and progression, and was moreover even effective in mediating the regression of already established atherosclerotic plaques. CD treatment reduced the deposition of vascular CCs and mediated the removal of existing CCs from already established plaques. *In vitro*, CD treatment of CC-loaded macrophages mediated the dissolution of intracellular CCs and subsequently promoted crystal-derived cholesterol efflux, storage and metabolism to bioactive oxysterols, which can function as endogenous LXR agonists. Accordingly, CD treatment also resulted in the LXR-dependent transcriptional

reprogramming of macrophages towards increased cholesterol efflux, which promoted reverse cholesterol transport and cholesterol excretion *in vivo*. Moreover, LXR transcription factor activation was required for the atheroprotective and anti-inflammatory effects of CD *in vivo* in murine atherosclerosis.

This study demonstrates that CD is atheroprotective in mice by dissolving and removing CCs from atherosclerotic plaques and by promoting the production of cholesterol-derived endogenous LXR agonists that activate anti-atherogenic transcriptional processes. Since CD treatment is already in clinical use as drug excipient and active drug for NPC disease, it could be directly tested in clinical trials for the prevention or treatment of human atherosclerosis.

List of Abbreviations

ABCA1	ATP-binding cassette transporter A1
ABCG1	ATP-binding cassette transporter G1
ACAT	Acyl-CoA cholesterol acyltransferase
AIM	Absent in melanoma
ALR	AIM-like receptor
ANOVA	Analysis of variance
Apo	Apolipoprotein
ASC	Apoptosis associated speck-like protein containing a CARD
ATP	Adenosine triphosphate
AUC	Area under the curve
BMDM	Bone marrow-derived macrophage
BSA	Bovine serum albumin
CARD	Caspase activation and recruitment domain
CC	Cholesterol crystal
CD	2-Hydroxypropyl-β-cyclodextrin
CD14	Cluster of differentiation 14
CD36	Cluster of differentiation 36
CD68	Cluster of differentiation 68
cDNA	Complementary DNA
CEH	Cholesterol ester hydrolase
CETP	Cholesterol ester transfer protein
CLR	C-type lectin receptor
CNS	Central nervous system
CoA	Coenzyme A
CTB	CellTiter-Blue
CtxB	Cholera toxin subunit B
CVD	Cardiovascular disease
D_6-CC	Deuterium-labeled CC
DAMP	Damage-associated molecular pattern
DC	Dendritic cell
ddH_2O	Double-distilled water
DE	Differentially expressed
DMEM	Dulbecco's Modified Eagle Medium
DNA	Deoxyribonucleic acid
ELISA	Enzyme-linked immunosorbent assay
ER	Endoplasmic reticulum
EtOH	Ethanol
FC	Fold change
FCS	Fetal calf serum
FDA	U.S. food and drug administration
FSC	Forward scatter
GC-MS-SIM	Gas chromatographic-mass spectrometric-selected ion monitoring
GSEA	Gene set enrichment analysis
^{3}H-CC	Tritium-labeled CC
HC	Hydroxycholesterol

HDL	High-density lipoprotein
HFHC	High fat, high cholesterol
Hprt	Hypoxanthine-guanine phosphoribosyltransferase
hsCRP	High sensitivity C-reactive protein
HSP	heat shock protein
IFN	Interferon
IHC	Immunohistochemistry
IL	Interleukin
IL-1R	IL-1 receptor
iMO	Immortalized mouse macrophage
IND	Investigational New Drug
INSIG	Insulin-induced gene
IRF	IFN regulatory factor
LCAT	Lecithin-cholesterol acyltransferase
LDL	Low-density lipoprotein
LDLR	LDL receptor
LeuLeu	H-Leu-Leu-Ome
LPS	Lipopolysaccharide
LRR	Leucine-rich repeat
Lss1	Lanosterol synthase
LXR	Liver X receptor
M-CSF	macrophage colony-stimulating factor
MAP	Mitogen-activated protein
MCP	Monocyte chemotactic protein
mRNA	Messenger RNA
MSU	Monodosium urate
MyD88	Myeloid differentiation factor 88
NASH	Nonalcoholic steatohepatitis
NET	Neutrophil extracellular trap
NF-κB	Nuclear factor kappa B
NK	Natural killer
NLR	NOD-like receptor
NLRC	NOD, LRR and CARD containing
NLRP	NOD, LRR and PYD containing
NOD	Nucleotide-binding and oligomerization domain
NPC	Niemann-Pick type C
oxLDL	Oxidized LDL
PAMP	Pathogen-associated molecular pattern
PBS	Phosphate buffered saline
PCR	Polymerase chain reaction
PCSK9	Proprotein convertase subtilisin/kexin type 9
PRR	Pattern recognition receptor
PYD	Pyrin domain
qPCR	Quantitative real-time PCR
R	Resistance
RCT	Reverse cholesterol transport
rHDL	Reconstituted HDL
RIG	Retinoc acid-inducible gene

RLR	RIG-I-like receptor
RNA	Ribonucleic acid
ROI	Region of interest
ROS	Reactive oxygen species
RT-PCR	Reverse transcription PCR
RT-qPCR	Reverse transcription quantitative real-time PCR
RXR	Retinoid X receptor
SARM	Sterile-α and HEAT-Armadillo motifs (SARM)
SCAP	SREBP cleavage activationg protein
Scd-1	Stearoyl-CoA desaturase-1
SD	Standard deviation
SDS	Sodium dodecyl sulfate
SEM	Standard error of the mean
SGT1	Suppressor of G2 allele of S-phase kinase-associated protein 1
SR-B1	Scavenger receptor B1
SREBP	Sterol regulatory element-binding protein
SSC	Side scatter
T09	T0901317
TBS	Tris buffered saline
Th1	Type 1 T helper cell
TIR	Toll/IL-1 receptor
TIRAP	TIR-associated protein
TLR	Toll-like receptor
TNF	Tumor necrosis factor
TRAM	TRIF-related adaptor molecule
TRIF	TIR domain-containing adaptor protein-inducing IFN-β
WB	Western blot
WT	Wild type

List of Figures

List of Tables

References

1. Iwasaki, A. & Medzhitov, R. Control of adaptive immunity by the innate immune system. *Nat. Immunol.* **16,** 343–353 (2015).
2. Medzhitov, R. Origin and physiological roles of inflammation. *Nature* **454,** 428–435 (2008).
3. Medzhitov, R. Recognition of microorganisms and activation of the immune response. *Nature* (2007). doi:10.1038/nature06246
4. Matzinger, P. The Danger Model: A Renewed Sense of Self. *Science* **296,** 301–305 (2002).
5. Brubaker, S. W., Bonham, K. S., Zanoni, I. & Kagan, J. C. Innate immune pattern recognition: a cell biological perspective. *Annual review of immunology* **33,** 257–290 (2015).
6. Creagh, E. M. & O'Neill, L. A. J. TLRs, NLRs and RLRs: a trinity of pathogen sensors that co-operate in innate immunity. *Trends Immunol.* **27,** 352–357 (2006).
7. Kawai, T. & Akira, S. The role of pattern-recognition receptors in innate immunity: update on Toll-like receptors. *Nat. Immunol.* **11,** 373–384 (2010).
8. Stewart, C. R. *et al.* Nat Immunol 2009 Stewart. *Nat. Immunol.* **11,** 155–161 (2009).
9. O'Neill, L. A. J., Fitzgerald, K. A. & Bowie, A. G. The Toll-IL-1 receptor adaptor family grows to five members. *Trends Immunol.* **24,** 286–290 (2003).
10. Takeuchi, O. & Akira, S. Pattern recognition receptors and inflammation. *Cell* **140,** 805–820 (2010).
11. Kawai, T. & Akira, S. Toll-like Receptors and Their Crosstalk with Other Innate Receptors in Infection and Immunity. *Immunity* **34,** 637–650 (2011).
12. Carty, M. *et al.* The human adaptor SARM negatively regulates adaptor protein TRIF–dependent Toll-like receptor signaling. *Nat. Immunol.* **7,** 1074–1081 (2006).
13. Latz, E., Xiao, T. S. & Stutz, A. Activation and regulation of the inflammasomes. *Nat Rev Immunol* **13,** 397–411 (2013).
14. Zhong, Y., Kinio, A. & Saleh, M. Functions of NOD-Like Receptors in Human Diseases. *Front Immunol* **4,** 333 (2013).
15. Kawai, T. & Akira, S. The roles of TLRs, RLRs and NLRs in pathogen recognition. *Int. Immunol.* **21,** 317–337 (2009).
16. Jones, J. D. G. & Dangl, J. L. The plant immune system. *Nature* **444,** 323–329 (2006).
17. Ting, J. P.-Y. *et al.* The NLR gene family: a standard nomenclature. *Immunity* **28,** 285–287 (2008).
18. Barbé, F., Douglas, T. & Saleh, M. Advances in Nod-like receptors (NLR) biology. *Cytokine Growth Factor Rev.* **25,** 681–697 (2014).
19. Hoffman, H. M., Mueller, J. L., Broide, D. H., Wanderer, A. A. & Kolodner, R. D. Mutation of a new gene encoding a putative pyrin-like protein causes familial cold autoinflammatory syndrome and Muckle-Wells syndrome. *Nat. Genet.* **29,** 301–305 (2001).
20. Agostini, L. *et al.* NALP3 forms an IL-1beta-processing inflammasome with increased activity in Muckle-Wells autoinflammatory disorder. *Immunity* **20,** 319–325 (2004).
21. Martinon, F., Pétrilli, V., Mayor, A., Tardivel, A. & Tschopp, J. Gout-associated uric acid crystals activate the NALP3 inflammasome. *Nature* **440,** 237–241 (2006).
22. Halle, A. *et al.* The NALP3 inflammasome is involved in the innate immune response to amyloid-β. *Nat. Immunol.* **9,** 857–865 (2008).
23. Masters, S. L. *et al.* Activation of the NLRP3 inflammasome by islet amyloid polypeptide provides a mechanism for enhanced IL-1[beta] in type 2 diabetes. *Nature Publishing Group* **11,** 897–904 (2010).
24. Duewell, P. *et al.* NLRP3 inflammasomes are required for atherogenesis and activated by cholesterol crystals. *Nature* **464,** 1357–1361 (2010).

25. Rajamäki, K. *et al.* Cholesterol crystals activate the NLRP3 inflammasome in human macrophages: a novel link between cholesterol metabolism and inflammation. *PLoS ONE* **5,** e11765 (2010).
26. Hornung, V. *et al.* Silica crystals and aluminum salts activate the NALP3 inflammasome through phagosomal destabilization. *Nat. Immunol.* **9,** 847–856 (2008).
27. Dostert, C. *et al.* Innate immune activation through Nalp3 inflammasome sensing of asbestos and silica. *Science* **320,** 674–677 (2008).
28. Horvath, G. L., Schrum, J. E., De Nardo, C. M. & Latz, E. Intracellular sensing of microbes and danger signals by the inflammasomes. *Immunol Rev* **243,** 119–135 (2011).
29. Bauernfeind, F. G. *et al.* Cutting edge: NF-kappaB activating pattern recognition and cytokine receptors license NLRP3 inflammasome activation by regulating NLRP3 expression. *J Immunol* **183,** 787–791 (2009).
30. Vanaja, S. K., Rathinam, V. A. K. & Fitzgerald, K. A. Mechanisms of inflammasome activation: recent advances and novel insights. *Trends in Cell Biology* **25,** 308–315 (2015).
31. Hornung, V. & Latz, E. Critical functions of priming and lysosomal damage for NLRP3 activation. *Eur. J. Immunol.* **40,** 620–623 (2010).
32. Mayor, A., Martinon, F., De Smedt, T., Pétrilli, V. & Tschopp, J. A crucial function of SGT1 and HSP90 in inflammasome activity links mammalian and plant innate immune responses. *Nat. Immunol.* **8,** 497–503 (2007).
33. Task Force Members *et al.* 2013 ESC guidelines on the management of stable coronary artery disease: the Task Force on the management of stable coronary artery disease of the European Society of Cardiology. *European Heart Journal* **34,** 2949–3003 (2013).
34. Moore, K. J. & Tabas, I. Macrophages in the pathogenesis of atherosclerosis. *Cell* **145,** 341–355 (2011).
35. Moore, K. J., Sheedy, F. J. & Fisher, E. A. Nature Reviews Immunology 2013 Moore. *Nat Rev Immunol* **13,** 709–721 (2013).
36. Kapourchali, F. R. *et al.* Animal models of atherosclerosis. *World J Clin Cases* **2,** 126–132 (2014).
37. Getz, G. S. & Reardon, C. A. Animal models of atherosclerosis. *Arterioscler Thromb Vasc Biol* **32,** 1104–1115 (2012).
38. Whitman, S. C. A practical approach to using mice in atherosclerosis research. *Clin Biochem Rev* **25,** 81–93 (2004).
39. Mayerl, C. *et al.* Atherosclerosis research from past to present—on the track of two pathologists with opposing views, Carl von Rokitansky and Rudolf Virchow. *Virchows Arch* **449,** 96–103 (2006).
40. Methe, H. & Weis, M. Atherogenesis and inflammation - was Virchow right? *Nephrology Dialysis Transplantation* **22,** 1823–1827 (2007).
41. Tedgui, A. Cytokines in Atherosclerosis: Pathogenic and Regulatory Pathways. *Physiological Reviews* **86,** 515–581 (2006).
42. Ridker, P. M. & Lüscher, T. F. Anti-inflammatory therapies for cardiovascular disease. *European Heart Journal* **35,** 1782–1791 (2014).
43. Shalhoub, J., Falck-Hansen, M. A., Davies, A. H. & Monaco, C. Innate immunity and monocyte-macrophage activation in atherosclerosis. *Journal of inflammation (London, England)* **8,** 9 (2011).
44. Hansson, G. K. & Hermansson, A. The immune system in atherosclerosis. *Nature Publishing Group* **12,** 204–212 (2011).
45. Zimmer, S., Grebe, A. & Latz, E. Danger Signaling in Atherosclerosis. *Circulation Research* **116,** 323–340 (2015).
46. Wright, S. D. *et al.* Infectious agents are not necessary for murine atherogenesis. *J. Exp. Med.* **191,** 1437–1441 (2000).
47. Galea, J. *et al.* Interleukin-1 beta in coronary arteries of patients with ischemic heart

disease. *Arterioscler Thromb Vasc Biol* **16,** 1000–1006 (1996).

48. Kirii, H. *et al.* Lack of interleukin-1beta decreases the severity of atherosclerosis in ApoE-deficient mice. *Arterioscler Thromb Vasc Biol* **23,** 656–660 (2003).
49. Elhage, R. *et al.* Differential effects of interleukin-1 receptor antagonist and tumor necrosis factor binding protein on fatty-streak formation in apolipoprotein E-deficient mice. *Circulation* **97,** 242–244 (1998).
50. Devlin, C. M., Kuriakose, G., Hirsch, E. & Tabas, I. Genetic alterations of IL-1 receptor antagonist in mice affect plasma cholesterol level and foam cell lesion size. *Proc Natl Acad Sci USA* **99,** 6280–6285 (2002).
51. Isoda, K. *et al.* Lack of interleukin-1 receptor antagonist modulates plaque composition in apolipoprotein E-deficient mice. *Arterioscler Thromb Vasc Biol* **24,** 1068–1073 (2004).
52. Ridker, P. M., Thuren, T., Zalewski, A. & Libby, P. Interleukin-1β inhibition and the prevention of recurrent cardiovascular events: rationale and design of the Canakinumab Anti-inflammatory Thrombosis Outcomes Study (CANTOS). *Am. Heart J.* **162,** 597–605 (2011).
53. Elshourbagy, N. A., Meyers, H. V. & Abdel-Meguid, S. S. Cholesterol: the good, the bad, and the ugly - therapeutic targets for the treatment of dyslipidemia. *Med Princ Pract* **23,** 99–111 (2014).
54. Gordon, T., Castelli, W. P., Hjortland, M. C., Kannel, W. B. & Dawber, T. R. High density lipoprotein as a protective factor against coronary heart disease. The Framingham Study. *Am. J. Med.* **62,** 707–714 (1977).
55. Khera, A., Cuchel, M. & La Llera-Moya, De, M. Cholesterol efflux capacity, high-density lipoprotein function, and atherosclerosis. *New England Journal …* (2011).
56. Eren, E., Ellidag, H. Y., Aydin, O. & Yilmaz, N. HDL functionality and crystal-based sterile inflammation in atherosclerosis. *Clinica Chimica Acta* **439,** 18–23 (2015).
57. Tabas, I. Free cholesterol-induced cytotoxicity - A possible contributing factor to macrophage foam cell necrosis in advanced atherosclerotic lesions. *Trends Cardiovasc. Med.* **7,** 256–263 (1997).
58. Chang, T.-Y., Chang, C. C., Ohgami, N. & Yamauchi, Y. Cholesterol Sensing, Trafficking, and Esterification. *Annu. Rev. Cell Dev. Biol.* **22,** 129–157 (2006).
59. Heinecke, J. W. The not-so-simple HDL story: A new era for quantifying HDL and cardiovascular risk? *Nat. Med.* **18,** 1346–1347 (2012).
60. Rader, D. J. & Tall, A. R. The not-so-simple HDL story: Is it time to revise the HDL cholesterol hypothesis? *Nat. Med.* **18,** 1344–1346 (2012).
61. Spann, N. J. & Glass, C. K. Sterols and oxysterols in immune cell function. *Nature Publishing Group* **14,** 893–900 (2013).
62. Shao, W. & Espenshade, P. J. Expanding Roles for SREBP in Metabolism. *Cell metabolism* **16,** 414–419 (2012).
63. Repa, J. J., Liang, G., Ou, J. & Bashmakov, Y. Regulation of mouse sterol regulatory element-binding protein-1c gene (SREBP-1c) by oxysterol receptors, LXRα and LXRβ. *Genes & …* (2000).
64. Im, S.-S. & Osborne, T. F. Liver x receptors in atherosclerosis and inflammation. *Circulation Research* **108,** 996–1001 (2011).
65. Olsen, B. N., Schlesinger, P. H., Ory, D. S. & Baker, N. A. Side-chain oxysterols: from cells to membranes to molecules. *Biochim. Biophys. Acta* **1818,** 330–336 (2012).
66. Ikonen, E. Cellular cholesterol trafficking and compartmentalization. *Nat. Rev. Mol. Cell Biol.* **9,** 125–138 (2008).
67. Brown, A. J. & Jessup, W. Oxysterols: Sources, cellular storage and metabolism, and new insights into their roles in cholesterol homeostasis. *Molecular Aspects of Medicine* **30,** 111–122 (2009).
68. Geer, J. C., McGill, H. C. & Strong, J. P. The fine structure of human atherosclerotic lesions. *Am J Pathol* **38,** 263–287 (1961).
69. Small, D. M. George Lyman Duff memorial lecture. Progression and regression of

atherosclerotic lesions. Insights from lipid physical biochemistry. *Arteriosclerosis* **8,** 103–129 (1988).

70. Tangirala, R. K. *et al.* Formation of Cholesterol Monohydrate Crystals in Macrophage-Derived Foam Cells. *The Journal of Lipid Research* **35,** 93–104 (1994).
71. Kellner-Weibel, G. *et al.* Effects of intracellular free cholesterol accumulation on macrophage viability: a model for foam cell death. *Arterioscler Thromb Vasc Biol* **18,** 423–431 (1998).
72. Accad, M. *et al.* Massive xanthomatosis and altered composition of atherosclerotic lesions in hyperlipidemic mice lacking acyl CoA:cholesterol acyltransferase 1. *J. Clin. Invest.* **105,** 711–719 (2000).
73. Abela, G. S. *et al.* Effect of cholesterol crystals on plaques and intima in arteries of patients with acute coronary and cerebrovascular syndromes. *Am. J. Cardiol.* **103,** 959–968 (2009).
74. Abela, G. S. & Aziz, K. Cholesterol crystals cause mechanical damage to biological membranes: a proposed mechanism of plaque rupture and erosion leading to arterial thrombosis. *Clin Cardiol* **28,** 413–420 (2005).
75. Abela, G. S. Cholesterol crystals piercing the arterial plaque and intima trigger local and systemic inflammation. *J Clin Lipidol* **4,** 156–164 (2010).
76. Abela, G. S. *et al.* Effect of statins on cholesterol crystallization and atherosclerotic plaque stabilization. *Am. J. Cardiol.* **107,** 1710–1717 (2011).
77. Krut, L. H. Clearance of subcutaneous implants of cholesterol in the rat promoted by oxidation products of cholesterol. A postulated role for oxysterols in preventing atherosclerosis. *Atherosclerosis* **43,** 105–118 (1982).
78. Hasselbacher, P. & Hahn, J. L. Activation of the alternative pathway of complement by microcrystalline cholesterol. *Atherosclerosis* **37,** 239–245 (1980).
79. Hammerschmidt, D. E., Greenberg, C. S., Yamada, O., Craddock, P. R. & Jacob, H. S. Cholesterol and atheroma lipids activate complement and stimulate granulocytes. *Translational Research* **98,** 68–77 (1981).
80. Swartz, G. M., Gentry, M. K., Amende, L. M., Blanchette-Mackie, E. J. & Alving, C. R. Antibodies to cholesterol. *Proc Natl Acad Sci USA* **85,** 1902–1906 (1988).
81. Nair, P. N., Sjögren, U. & Sundqvist, G. Cholesterol crystals as an etiological factor in non-resolving chronic inflammation: an experimental study in guinea pigs. *Eur J Oral Sci* **106,** 644–650 (1998).
82. Menu, P. *et al.* Atherosclerosis in ApoE-deficient mice progresses independently of the NLRP3 inflammasome. *Cell Death Dis* **2,** e137 (2011).
83. Razani, B. *et al.* Autophagy links inflammasomes to atherosclerotic progression. *Cell metabolism* **15,** 534–544 (2012).
84. Zheng, F., Xing, S., Gong, Z. & Xing, Q. NLRP3 inflammasomes show high expression in aorta of patients with atherosclerosis. *Heart Lung Circ* **22,** 746–750 (2013).
85. Zheng, F., Xing, S., Gong, Z., Mu, W. & Xing, Q. Silence of NLRP3 suppresses atherosclerosis and stabilizes plaques in apolipoprotein E-deficient mice. *Mediators Inflamm.* **2014,** 507208 (2014).
86. Samstad, E. O. *et al.* Cholesterol crystals induce complement-dependent inflammasome activation and cytokine release. *J Immunol* **192,** 2837–2845 (2014).
87. Warnatsch, A., Ioannou, M., Wang, Q. & Papayannopoulos, V. Neutrophil extracellular traps license macrophages for cytokine production in atherosclerosis. *Science* **349,** 316–320 (2015).
88. Davis, M. E. & Brewster, M. E. Cyclodextrin-based pharmaceutics: past, present and future. *Nat Rev Drug Discov* **3,** 1023–1035 (2004).
89. Loftsson, T. & Brewster, M. E. Pharmaceutical applications of cyclodextrins: basic science and product development. *J. Pharm. Pharmacol.* **62,** 1607–1621 (2010).
90. Bilensoy, E. *Cyclodextrins in Pharmaceutics, Cosmetics, and Biomedicine*. (John Wiley & Sons, 2011).

91. Stella, V. J. & He, Q. Cyclodextrins. *Toxicologic Pathology* **36,** 30–42 (2008).

92. Schönfelder, U., Radestock, A., Elsner, P. & Hipler, U.-C. Cyclodextrin-induced apoptosis in human keratinocytes is caspase-8 dependent and accompanied by mitochondrial cytochrome c release. *Exp. Dermatol.* **15,** 883–890 (2006).

93. Frijlink, H. W. *et al.* The effect of parenterally administered cyclodextrins on cholesterol levels in the rat. *Pharm Res* **8,** 9–16 (1991).

94. Gould, J. C., Luna, R. E. & Vogel, D. L. Nat Immunol 2014 Gould. *Nature Publishing Group* **15,** 695–697 (2014).

95. Ottinger, E. A. *et al.* Collaborative development of 2-hydroxypropyl-β-cyclodextrin for the treatment of Niemann-Pick type C1 disease. *Curr Top Med Chem* **14,** 330–339 (2014).

96. Li, H., El-Dakdouki, M. H., Zhu, D. C., Abela, G. S. & Huang, X. Synthesis of β-cyclodextrin conjugated superparamagnetic iron oxide nanoparticles for selective binding and detection of cholesterol crystals. *Chem. Commun.* – (2012).

97. Mondal, A. & Jana, N. R. Fluorescent detection of cholesterol using β-cyclodextrin functionalized graphene. *Chemical Communications* **48,** 7316–7318 (2012).

98. Sinha, A., Basiruddin, S., Chakraborty, A. & Jana, N. R. β-Cyclodextrin functionalized magnetic mesoporous silica colloid for cholesterol separation. *ACS Appl Mater Interfaces* **7,** 1340–1347 (2015).

99. Zidovetzki, R. & Levitan, I. Use of cyclodextrins to manipulate plasma membrane cholesterol content: evidence, misconceptions and control strategies. *Biochim. Biophys. Acta* **1768,** 1311–1324 (2007).

100. Atger, V. M. *et al.* Cyclodextrins as catalysts for the removal of cholesterol from macrophage foam cells. *The Journal of Clinical Investigation* **99,** 773–780 (1997).

101. Irie, T. *et al.* Hydroxypropylcyclodextrins in parenteral use. II: effects on transport and disposition of lipids in rabbit and humans. *Journal of pharmaceutical sciences* **81,** 524–528 (1992).

102. Liu, S. M. Cyclodextrins differentially mobilize free and esterified cholesterol from primary human foam cell macrophages. *The Journal of Lipid Research* **44,** 1156–1166 (2003).

103. Abi-Mosleh, L., Infante, R. E., Radhakrishnan, A., Goldstein, J. L. & Brown, M. S. Cyclodextrin overcomes deficient lysosome-to-endoplasmic reticulum transport of cholesterol in Niemann-Pick type C cells. *Proc Natl Acad Sci USA* **106,** 19316–19321 (2009).

104. Peake, K. B. & Vance, J. E. Defective cholesterol trafficking in Niemann-Pick C-deficient cells. *FEBS Lett.* **584,** 2731–2739 (2010).

105. Liu, B. *et al.* Reversal of defective lysosomal transport in NPC disease ameliorates liver dysfunction and neurodegeneration in the npc1(-/-) mouse. *Proc Natl Acad Sci USA* **106,** 2377–2382 (2009).

106. Liu, B. *et al.* Cyclodextrin overcomes the transport defect in nearly every organ of NPC1 mice leading to excretion of sequestered cholesterol as bile acid. *The Journal of Lipid Research* **51,** 933–944 (2010).

107. Pontikis, C. C., Davidson, C. D., Walkley, S. U., Platt, F. M. & Begley, D. J. Cyclodextrin alleviates neuronal storage of cholesterol in Niemann-Pick C disease without evidence of detectable blood-brain barrier permeability. *J. Inherit. Metab. Dis.* **36,** 491–498 (2013).

108. Grebe, A. & Latz, E. Cholesterol Crystals and Inflammation. *Curr Rheumatol Rep* **15,** 313 (2013).

109. Spandl, J., White, D. J., Peychl, J. & Thiele, C. Live Cell Multicolor Imaging of Lipid Droplets with a New Dye, LD540. *Traffic* **10,** 1579–1584 (2009).

110. Lütjohann, D. *et al.* Profile of cholesterol-related sterols in aged amyloid precursor protein transgenic mouse brain. *The Journal of Lipid Research* **43,** 1078–1085 (2002).

111. Lütjohann, D. *et al.* Influence of rifampin on serum markers of cholesterol and bile acid synthesis in men. *Int J Clin Pharmacol Ther* **42,** 307–313 (2004).

112. Lütjohann, D. *et al.* High doses of simvastatin, pravastatin, and cholesterol reduce brain

cholesterol synthesis in guinea pigs. *Steroids* **69,** 431–438 (2004).

113. Lütjohann, D. *et al.* Cholesterol homeostasis in human brain: evidence for an age-dependent flux of 24S-hydroxycholesterol from the brain into the circulation. *Proc Natl Acad Sci USA* **93,** 9799–9804 (1996).
114. Heinz, S. *et al.* Simple combinations of lineage-determining transcription factors prime cis-regulatory elements required for macrophage and B cell identities. *Mol. Cell* **38,** 576–589 (2010).
115. Lusis, A. J. Atherosclerosis. *Nature* **407,** 233–241 (2000).
116. Tangirala, R. K. *et al.* Identification of macrophage liver X receptors as inhibitors of atherosclerosis. *Proc Natl Acad Sci USA* **99,** 11896–11901 (2002).
117. Kunjathoor, V. V. Scavenger Receptors Class A-I/II and CD36 Are the Principal Receptors Responsible for the Uptake of Modified Low Density Lipoprotein Leading to Lipid Loading in Macrophages. *Journal of Biological Chemistry* **277,** 49982–49988 (2002).
118. Sheedy, F. J. *et al.* CD36 coordinates NLRP3 inflammasome activation by facilitating intracellular nucleation of soluble ligands into particulate ligands in sterile inflammation. *Nat. Immunol.* **14,** 812–820 (2013).
119. Lim, R. S. *et al.* Identification of cholesterol crystals in plaques of atherosclerotic mice using hyperspectral CARS imaging. *The Journal of Lipid Research* **52,** 2177–2186 (2011).
120. Lewis, G. F. & Rader, D. J. New insights into the regulation of HDL metabolism and reverse cholesterol transport. *Circulation Research* **96,** 1221–1232 (2005).
121. De Nardo, D. *et al.* High-density lipoprotein mediates anti-inflammatory reprogramming of macrophages via the transcriptional regulator ATF3. *Nat. Immunol.* (2013). doi:10.1038/ni.2784
122. Cali, J. J. & Russell, D. W. Characterization of human sterol 27-hydroxylase. A mitochondrial cytochrome P-450 that catalyzes multiple oxidation reaction in bile acid biosynthesis. *J Biol Chem* **266,** 7774–7778 (1991).
123. Fu, X. *et al.* 27-hydroxycholesterol is an endogenous ligand for liver X receptor in cholesterol-loaded cells. *J Biol Chem* **276,** 38378–38387 (2001).
124. Joseph, S. B. *et al.* Synthetic LXR ligand inhibits the development of atherosclerosis in mice. *Proc Natl Acad Sci USA* **99,** 7604–7609 (2002).
125. Schwartz, K., Lawn, R. M. & Wade, D. P. ABC1 gene expression and ApoA-I-mediated cholesterol efflux are regulated by LXR. *Biochem. Biophys. Res. Commun.* **274,** 794–802 (2000).
126. Costet, P., Luo, Y., Wang, N. & Tall, A. R. Sterol-dependent transactivation of theABC1 promoter by the liver X receptor/retinoid X receptor. *Journal of Biological Chemistry* (2000).
127. Venkateswaran, A. *et al.* Human white/murine ABC8 mRNA levels are highly induced in lipid-loaded macrophages - A transcriptional role for specific oxysterols. *J Biol Chem* **275,** 14700–14707 (2000).
128. Lawn, R. M. *et al.* The Tangier disease gene product ABC1 controls the cellular apolipoprotein-mediated lipid removal pathway. *J. Clin. Invest.* **104,** R25–31 (1999).
129. Langmann, T. *et al.* Molecular cloning of the human ATP-binding cassette transporter 1 (hABC1): evidence for sterol-dependent regulation in macrophages. *Biochem. Biophys. Res. Commun.* **257,** 29–33 (1999).
130. Hu, Y.-W., Zheng, L. & Wang, Q. Regulation of cholesterol homeostasis by liver X receptors. *Clinica Chimica Acta* **411,** 617–625 (2010).
131. Rothblat, G. H. *et al.* Cell cholesterol efflux: integration of old and new observations provides new insights. *The Journal of Lipid Research* **40,** 781–796 (1999).
132. Cuchel, M. & Rader, D. J. Macrophage reverse cholesterol transport - Key to the regression of atherosclerosis? *Circulation* **113,** 2548–2555 (2006).
133. Joseph, S. B., Castrillo, A., Laffitte, B. A., Mangelsdorf, D. J. & Tontonoz, P. Reciprocal

regulation of inflammation and lipid metabolism by liver X receptors. *Nat. Med.* **9,** 213–219 (2003).

134. Ogawa, S. *et al.* Molecular determinants of crosstalk between nuclear receptors and toll-like receptors. *Cell* **122,** 707–721 (2005).

135. Pehkonen, P. *et al.* Genome-wide landscape of liver X receptorchromatin binding and gene regulation in humanmacrophages. *BMC Genomics* **13,** 50 (2012).

136. Thiele, D. L. & Lipsky, P. E. Mechanism of L-leucyl-L-leucine methyl ester-mediated killing of cytotoxic lymphocytes: dependence on a lysosomal thiol protease, dipeptidyl peptidase I, that is enriched in these cells. *Proc Natl Acad Sci USA* **87,** 83–87 (1990).

137. Patel, R. *et al.* Plaque rupture and thrombosis are reduced by lowering cholesterol levels and crystallization with ezetimibe and are correlated with fluorodeoxyglucose positron emission tomography. *Arterioscler Thromb Vasc Biol* **31,** 2007–2014 (2011).

138. Blom, D. J. *et al.* A 52-week placebo-controlled trial of evolocumab in hyperlipidemia. *N. Engl. J. Med.* **370,** 1809–1819 (2014).

139. Robinson, J. G. *et al.* Efficacy and safety of alirocumab in reducing lipids and cardiovascular events. *N. Engl. J. Med.* **372,** 1489–1499 (2015).

140. Hendrikx, T., Walenbergh, S. M. A., Hofker, M. H. & Shiri-Sverdlov, R. Lysosomal cholesterol accumulation: driver on the road to inflammation during atherosclerosis and non-alcoholic steatohepatitis. *Obes Rev* **15,** 424–433 (2014).

141. Ioannou, G. N. The Role of Cholesterol in the Pathogenesis of NASH. *Trends Endocrinol. Metab.* **27,** 84–95 (2016).

142. Ioannou, G. N. *et al.* Cholesterol-lowering drugs cause dissolution of cholesterol crystals and disperse Kupffer cell crown-like structures during resolution of NASH. *J. Lipid Res.* **56,** 277–285 (2015).

143. Walenbergh, S. M. A. *et al.* Weekly Treatment of 2-Hydroxypropyl-β-cyclodextrin Improves Intracellular Cholesterol Levels in LDL Receptor Knockout Mice. *Int J Mol Sci* **16,** 21056–21069 (2015).

144. Tall, A. R. & Yvan-Charvet, L. Cholesterol, inflammation and innate immunity. *Nat Rev Immunol* **15,** 104–116 (2015).

145. Fenyvesi, F. *et al.* Fluorescently labeled methyl-beta-cyclodextrin enters intestinal epithelial Caco-2 cells by fluid-phase endocytosis. *PLoS ONE* **9,** e84856 (2014).

146. Kerrigan, A. M. & Brown, G. D. C-type lectins and phagocytosis. *Immunobiology* **214,** 562–575 (2009).

147. de Winther, M. P., van Dijk, K. W., Havekes, L. M. & Hofker, M. H. Macrophage scavenger receptor class A: A multifunctional receptor in atherosclerosis. *Arterioscler Thromb Vasc Biol* **20,** 290–297 (2000).

148. McConathy, W. J., Koren, E. & Stiers, D. L. Cholesterol crystal uptake and metabolism by P388D1 macrophages. *Atherosclerosis* **77,** 221–225 (1989).

149. Lund, E. *et al.* Importance of a Novel Oxidative Mechanism for Elimination of Intracellular Cholesterol in Humans. *Arterioscler Thromb Vasc Biol* **16,** 208–212 (1996).

150. Babiker, A. *et al.* Elimination of cholesterol in macrophages and endothelial cells by the sterol 27-hydroxylase mechanism. Comparison with high density lipoprotein-mediated reverse cholesterol transport. *J Biol Chem* **272,** 26253–26261 (1997).

151. Ohvo, H. & Slotte, J. P. Cyclodextrin-mediated removal of sterols from monolayers: effects of sterol structure and phospholipids on desorption rate. *Biochemistry* **35,** 8018–8024 (1996).

152. Krut, L. H. Solubility of cholesterol in vitro promoted by oxidation products of cholesterol. *Atherosclerosis* **43,** 95–104 (1982).

153. Tortelli, B. *et al.* Cholesterol homeostatic responses provide biomarkers for monitoring treatment for the neurodegenerative disease Niemann-Pick C1 (NPC1). *Hum. Mol. Genet.* **23,** 6022–6033 (2014).

154. Yang, C. *et al.* Sterol intermediates from cholesterol biosynthetic pathway as liver X receptor ligands. *J Biol Chem* **281,** 27816–27826 (2006).

155. Spann, N. J. *et al.* Regulated Accumulation of Desmosterol Integrates Macrophage Lipid Metabolism and Inflammatory Responses. *Cell* **151,** 138–152 (2012).

156. Phillips, M. C. Molecular mechanisms of cellular cholesterol efflux. *J Biol Chem* **289,** 24020–24029 (2014).

157. Ramirez, C. M. *et al.* Quantitative role of LAL, NPC2, and NPC1 in lysosomal cholesterol processing defined by genetic and pharmacological manipulations. *The Journal of Lipid Research* **52,** 688–698 (2011).

158. Lopez, A. M. *et al.* Systemic administration of 2-hydroxypropyl-β-cyclodextrin to symptomatic Npc1-deficient mice slows cholesterol sequestration in the major organs and improves liver function. *Clin. Exp. Pharmacol. Physiol.* **41,** 780–787 (2014).

159. Umetani, M. & Shaul, P. W. 27-Hydroxycholesterol: the first identified endogenous SERM. *Trends Endocrinol. Metab.* **22,** 130–135 (2011).

160. Umetani, M. *et al.* The Cholesterol Metabolite 27-Hydroxycholesterol Promotes Atherosclerosis via Proinflammatory Processes Mediated by Estrogen Receptor Alpha. *Cell metabolism* **20,** 172–182 (2014).

161. Zurkinden, L. *et al.* Effect of Cyp27A1 gene dosage on atherosclerosis development in ApoE-knockout mice. *The FASEB Journal* **28,** 1198–1209 (2014).

162. Levin, N. *et al.* Macrophage liver X receptor is required for antiatherogenic activity of LXR agonists. *Arterioscler Thromb Vasc Biol* **25,** 135–142 (2005).

163. Zanotti, I. *et al.* The LXR agonist T0901317 promotes the reverse cholesterol transport from macrophages by increasing plasma efflux potential. *The Journal of Lipid Research* **49,** 954–960 (2008).

164. Ghisletti, S. *et al.* Parallel SUMOylation-dependent pathways mediate gene-and signal-specific transrepression by LXRs and PPARγ. *Mol. Cell* **25,** 57–70 (2007).

165. Wang, X. *et al.* Macrophage ABCA1 and ABCG1, but not SR-BI, promote macrophage reverse cholesterol transport in vivo. *J. Clin. Invest.* **117,** 2216–2224 (2007).

166. Kappus, M. S. *et al.* Activation of Liver X Receptor Decreases Atherosclerosis in Ldlr-/- Mice in the Absence of ATP-Binding Cassette Transporters A1 and G1 in Myeloid Cells. *Arterioscler Thromb Vasc Biol* **34,** 279–284 (2014).

167. A-Gonzalez, N. *et al.* Apoptotic cells promote their own clearance and immune tolerance through activation of the nuclear receptor LXR. *Immunity* **31,** 245–258 (2009).

168. Trogan, E. *et al.* Gene expression changes in foam cells and the role of chemokine receptor CCR7 during atherosclerosis regression in ApoE-deficient mice. *Proc Natl Acad Sci USA* **103,** 3781–3786 (2006).

169. Feig, J. E. *et al.* LXR promotes the maximal egress of monocyte-derived cells from mouse aortic plaques during atherosclerosis regression. *J. Clin. Invest.* **120,** 4415–4424 (2010).

170. Montecucco, F. *et al.* Treatment with KLEPTOSE® CRYSMEB reduces mouse atherogenesis by impacting on lipid profile and Th1 lymphocyte response. *Vascular pharmacology* **72,** 197–208 (2015).

171. Witztum, J. L. & Lichtman, A. H. The Influence of Innate and Adaptive Immune Responses on Atherosclerosis. *Annu Rev Pathol* **9,** 73–102 (2014).

172. Walcher, D. *et al.* LXR activation reduces proinflammatory cytokine expression in human CD4-positive lymphocytes. *Arterioscler Thromb Vasc Biol* **26,** 1022–1028 (2006).

173. Feig, J. E. Regression of atherosclerosis: insights from animal and clinical studies. *Ann Glob Health* **80,** 13–23 (2014).

174. Hong, C. & Tontonoz, P. Liver X receptors in lipid metabolism: opportunities for drug discovery. *Nat Rev Drug Discov* **13,** 433–444 (2014).

175. Tricoci, P. *et al.* Infusion of Reconstituted High-Density Lipoprotein, CSL112, in Patients With Atherosclerosis: Safety and Pharmacokinetic Results From a Phase 2a Randomized Clinical Trial. *J Am Heart Assoc* **4,** e002171 (2015).

Acknowledgement

Mein besonderer Dank gilt meinem Doktorvater **Prof. Dr. Eicke Latz**, der mir für meine Doktorarbeit ein unglaubliches Arbeitsumfeld mit nahezu unbegrenzten Möglichkeiten zur freien wissenschaftlichen Entfaltung geboten hat. Insbesondere möchte ich mich aber für seine kontinuierliche Unterstützung, Geduld und gleichzeitig unablässige Motivation und wissenschaftliche Inspiration bedanken. Darüber hinaus bedanke ich mich dafür, dass ich die Möglichkeit hatte an zahlreichen Konferenzen teilzunehmen und im Rahmen meiner Forschungsarbeit diverse internationale Reisen zu unternehmen.

Prof. Dr. Waldemar Kolanus danke ich herzlich für seine Bereitschaft meine Arbeit als Zweitgutachter zu beurteilen.

Danken möchte ich außerdem allen Personen, die einen wichtigen wissenschaftlichen Beitrag zu meiner Arbeit geleistet haben, und ohne die dieses Projekt in dieser Form nicht möglich gewesen wäre. Dabei geht mein Dank zunächst an **Chris Hempel**, die uns die initiale Idee für dieses Projekt gegeben hat. **Dr. Sebastian Zimmer**, sowie seinen Mitarbeitern **Niklas Bode** und **Catharina Lahrmann** danke ich für die enge Zusammenarbeit und die Durchführung der Mausmodelle. Besonderer Dank geht an **Prof. Dr. Dr. Dieter Lütjohann**, der durch intensive Diskussionen, konstruktive Kritik und seinen Fachkenntnissen über Lipidstoffwechsel und Lipidanalytik maßgeblich zur Entwicklung dieses Projektes beigetragen hat. In diesem Zusammenhang möchte ich auch **Anja Kerksiek** für die Probenaufbereitung und Durchführung der vielzähligen GC-MS-SIM Analysen danken. Ich danke **Dr. Thomas Ulas**, **Michael Kraut** und **Prof. Dr. Joachim Schultze** für die Durchführung der Microarrays und die anschließende bioinformatischen Datenanalyse. Zudem danke ich **Prof. Dr. Michael Fitzgerald** für die Erstellung der Lipoproteinprofile, sowie **Prof. Dr. Alan Tall**, **Prof. Dr. Michael Heneka** und **Prof. Dr. Jan-Åke Gustaffson** für die Bereitstellung von Knockoutmäusen.

Natürlich möchte ich mich auch bei all meinen **Kollegen der AG Latz** für die jahrelange Unterstützung sowie eine angenehme und inspirierende Arbeitsatmosphäre bedanken. Wirklich jeder stand mir bei Bedarf mit Rat und Tat zur Seite - ihr seid einfach unglaublich!
Mein besonderer Dank gilt jedoch **Dr. Dominic De Nardo** und **Dr. Larisa Labzin** für unzählige konstruktive Diskussionen, regelmäßigen Ideenaustausch, ihre unermüdliche Hilfsbereitschaft und ihre stetigen Ermutigungen. Ein zusätzliches, riesiges Dankeschön an Larisa für das kritische Korrekturlesen dieser Arbeit. Außerdem danke ich **Dr. Anette Christ** für diverse aufschlussreiche Gespräche über die Atherosklerosеforschung im Mausmodell, sowie **Gudrun Engels** und **Olivia van Ray** für ihre stete Hilfsbereitschaft und praktische Unterstützung im Labor.

Meiner Familie und meinen Freunden danke ich für all die schönen Stunden mit euch, die mein Leben enorm bereichert haben. Danke, dass ihr Freud und Leid mit mir geteilt habt und immer für mich da gewesen seid.
Mein tiefster Dank gilt dabei **meinen Eltern** für ihre endlose Unterstützung und immerzu aufmunternden Worte. Ohne euch hätte ich das hier nicht geschafft!
Stefan, danke dass du immer für mich da bist!

Appendix

Overview of appendix content

- Reprint permissions for the following figures:
  - Fig. 2-1: NLRP3 inflammasome activation. (p.11)
  - Fig. 2-2: Atherosclerosis plaque development and progression. (p.13)
  - Fig. 2-3: Cellular cholesterol efflux and reverse cholesterol transport. (p.18)
  - Fig. 2-4: Transcriptional regulation of cellular cholesterol homeostasis. (p.20)
  - Fig. 2-5: Cyclodextrins and formation of cyclodextrin inclusion complexes. (p.25)
  - Fig. 2-6: Plasma clearance of 2-Hydroxypropyl-β-cyclodextrin. (p.29)
- World Health Organization (WHO) - Fact sheet N°317 on CVDs
  source: http://www.who.int/mediacentre/factsheets/fs317/en/ (14th March, 2016)

JOHN WILEY AND SONS LICENSE TERMS AND CONDITIONS

Mar 28, 2016

This Agreement between Alena Grebe ("You") and John Wiley and Sons ("John Wiley and Sons") consists of your license details and the terms and conditions provided by John Wiley and Sons and Copyright Clearance Center.

License Number	3837590771533
License date	Mar 28, 2016
Licensed Content Publisher	John Wiley and Sons
Licensed Content Publication	Immunological Reviews
Licensed Content Title	Intracellular sensing of microbes and danger signals by the inflammasomes
Licensed Content Author	Gabor L. Horvath,Jacob E. Schrum,Christine M. De Nardo,Eicke Latz
Licensed Content Date	Aug 26, 2011
Pages	17
Type of Use	Dissertation/Thesis
Requestor type	University/Academic
Format	Print and electronic
Portion	Figure/table
Number of figures/tables	1
Original Wiley figure/table number(s)	Figure 2
Will you be translating?	No
Title of your thesis / dissertation	Targeting cholesterol crystals in atherosclerosis with cholesterol solubilizing 2-hydroxypropyl-β-cyclodextrin
Expected completion date	Apr 2016
Expected size (number of pages)	150
Requestor Location	Alena Grebe WInzerstr. 6-8 None None Bonn, Germany 53129 Attn: Alena Grebe
Billing Type	Invoice
Billing Address	Alena Grebe WInzerstr. 6-8 None None Bonn, Germany 53129 Attn: Alena Grebe
Total	**0.00 EUR**
Terms and Conditions	

TERMS AND CONDITIONS

This copyrighted material is owned by or exclusively licensed to John Wiley & Sons, Inc. or one of its group companies (each a"Wiley Company") or handled on behalf of a society with which a Wiley Company has exclusive publishing rights in relation to a particular work (collectively "WILEY"). By clicking "accept" in connection with completing this licensing transaction, you agree that the following terms and conditions apply to this transaction (along with the billing and payment terms and conditions established by the Copyright Clearance Center Inc., ("CCC's Billing and Payment terms and conditions"), at the time that you opened your RightsLink account (these are available at any time at http://myaccount.copyright.com).

Terms and Conditions

- The materials you have requested permission to reproduce or reuse (the "Wiley Materials") are protected by copyright.
- You are hereby granted a personal, non-exclusive, non-sub licensable (on a stand-alone basis), non-transferable, worldwide, limited license to reproduce the Wiley Materials for the purpose specified in the licensing process. This license, **and any CONTENT (PDF or image file) purchased as part of your order,** is for a one-time use only and limited to any maximum distribution number specified in the license. The first instance of republication or reuse granted by this license must be completed within two years of the date of the grant of this license (although copies prepared before the end date may be distributed thereafter). The Wiley Materials shall not be used in any other manner or for any other purpose, beyond what is granted in the license. Permission is granted subject to an appropriate acknowledgement given to the author, title of the material/book/journal and the publisher. You shall also duplicate the copyright notice that appears in the Wiley publication in your use of the Wiley Material. Permission is also granted on the understanding that nowhere in the text is a previously published source acknowledged for all or part of this Wiley Material. Any third party content is expressly excluded from this permission.
- With respect to the Wiley Materials, all rights are reserved. Except as expressly granted by the terms of the license, no part of the Wiley Materials may be copied, modified, adapted (except for minor reformatting required by the new Publication), translated, reproduced, transferred or distributed, in any form or by any means, and no derivative works may be made based on the Wiley Materials without the prior permission of the respective copyright owner.**For STM Signatory Publishers clearing permission under the terms of the STM Permissions Guidelines only, the terms of the license are extended to include subsequent editions and for editions in other languages, provided such editions are for the work as a whole in situ and does not involve the separate exploitation of the permitted figures or extracts,** You may not alter, remove or suppress in any manner any copyright, trademark or other notices displayed by the Wiley Materials. You may not license, rent, sell, loan, lease, pledge, offer as security, transfer or assign the Wiley Materials on a stand-alone basis, or any of the rights granted to you hereunder to any other person.
- The Wiley Materials and all of the intellectual property rights therein shall at all times remain the exclusive property of John Wiley & Sons Inc, the Wiley Companies, or their respective licensors, and your interest therein is only that of having possession of and the right to reproduce the Wiley Materials pursuant to Section 2 herein during the continuance of this Agreement. You agree that you own no right, title or interest in or to the Wiley Materials or any of the intellectual property rights therein. You shall have no rights hereunder other than the license as provided for above in Section 2. No right, license or interest to any trademark, trade name, service mark or other branding ("Marks") of WILEY or its licensors is granted hereunder, and you agree that you shall not assert any such right, license or interest with respect thereto

- NEITHER WILEY NOR ITS LICENSORS MAKES ANY WARRANTY OR REPRESENTATION OF ANY KIND TO YOU OR ANY THIRD PARTY, EXPRESS, IMPLIED OR STATUTORY, WITH RESPECT TO THE MATERIALS OR THE ACCURACY OF ANY INFORMATION CONTAINED IN THE MATERIALS, INCLUDING, WITHOUT LIMITATION, ANY IMPLIED WARRANTY OF MERCHANTABILITY, ACCURACY, SATISFACTORY QUALITY, FITNESS FOR A PARTICULAR PURPOSE, USABILITY, INTEGRATION OR NON-INFRINGEMENT AND ALL SUCH WARRANTIES ARE HEREBY EXCLUDED BY WILEY AND ITS LICENSORS AND WAIVED BY YOU.

- WILEY shall have the right to terminate this Agreement immediately upon breach of this Agreement by you.

- You shall indemnify, defend and hold harmless WILEY, its Licensors and their respective directors, officers, agents and employees, from and against any actual or threatened claims, demands, causes of action or proceedings arising from any breach of this Agreement by you.

- IN NO EVENT SHALL WILEY OR ITS LICENSORS BE LIABLE TO YOU OR ANY OTHER PARTY OR ANY OTHER PERSON OR ENTITY FOR ANY SPECIAL, CONSEQUENTIAL, INCIDENTAL, INDIRECT, EXEMPLARY OR PUNITIVE DAMAGES, HOWEVER CAUSED, ARISING OUT OF OR IN CONNECTION WITH THE DOWNLOADING, PROVISIONING, VIEWING OR USE OF THE MATERIALS REGARDLESS OF THE FORM OF ACTION, WHETHER FOR BREACH OF CONTRACT, BREACH OF WARRANTY, TORT, NEGLIGENCE, INFRINGEMENT OR OTHERWISE (INCLUDING, WITHOUT LIMITATION, DAMAGES BASED ON LOSS OF PROFITS, DATA, FILES, USE, BUSINESS OPPORTUNITY OR CLAIMS OF THIRD PARTIES), AND WHETHER OR NOT THE PARTY HAS BEEN ADVISED OF THE POSSIBILITY OF SUCH DAMAGES. THIS LIMITATION SHALL APPLY NOTWITHSTANDING ANY FAILURE OF ESSENTIAL PURPOSE OF ANY LIMITED REMEDY PROVIDED HEREIN.

- Should any provision of this Agreement be held by a court of competent jurisdiction to be illegal, invalid, or unenforceable, that provision shall be deemed amended to achieve as nearly as possible the same economic effect as the original provision, and the legality, validity and enforceability of the remaining provisions of this Agreement shall not be affected or impaired thereby.

- The failure of either party to enforce any term or condition of this Agreement shall not constitute a waiver of either party's right to enforce each and every term and condition of this Agreement. No breach under this agreement shall be deemed waived or excused by either party unless such waiver or consent is in writing signed by the party granting such waiver or consent. The waiver by or consent of a party to a breach of any provision of this Agreement shall not operate or be construed as a waiver of or consent to any other or subsequent breach by such other party.

- This Agreement may not be assigned (including by operation of law or otherwise) by you without WILEY's prior written consent.

- Any fee required for this permission shall be non-refundable after thirty (30) days from receipt by the CCC.

- These terms and conditions together with CCC's Billing and Payment terms and conditions (which are incorporated herein) form the entire agreement between you and WILEY concerning this licensing transaction and (in the absence of fraud) supersedes all prior agreements and representations of the parties, oral or written. This Agreement may not be amended except in writing signed by both parties. This Agreement shall be binding upon and inure to the benefit of the parties' successors, legal representatives, and authorized assigns.

- In the event of any conflict between your obligations established by these terms and conditions and those established by CCC's Billing and Payment terms and conditions, these terms and conditions shall prevail.

- WILEY expressly reserves all rights not specifically granted in the combination of (i) the license details provided by you and accepted in the course of this licensing transaction, (ii) these terms and conditions and (iii) CCC's Billing and Payment terms and conditions.

- This Agreement will be void if the Type of Use, Format, Circulation, or Requestor Type was misrepresented during the licensing process.

- This Agreement shall be governed by and construed in accordance with the laws of the State of New York, USA, without regards to such state's conflict of law rules. Any legal action, suit or proceeding arising out of or relating to these Terms and Conditions or the breach thereof shall be instituted in a court of competent jurisdiction in New York County in the State of New York in the United States of America and each party hereby consents and submits to the personal jurisdiction of such court, waives any objection to venue in such court and consents to service of process by registered or certified mail, return receipt requested, at the last known address of such party.

WILEY OPEN ACCESS TERMS AND CONDITIONS

Wiley Publishes Open Access Articles in fully Open Access Journals and in Subscription journals offering Online Open. Although most of the fully Open Access journals publish open access articles under the terms of the Creative Commons Attribution (CC BY) License only, the subscription journals and a few of the Open Access Journals offer a choice of Creative Commons Licenses. The license type is clearly identified on the article.

The Creative Commons Attribution License

The Creative Commons Attribution License (CC-BY) allows users to copy, distribute and transmit an article, adapt the article and make commercial use of the article. The CC-BY license permits commercial and non-

Creative Commons Attribution Non-Commercial License

The Creative Commons Attribution Non-Commercial (CC-BY-NC)License permits use, distribution and reproduction in any medium, provided the original work is properly cited and is not used for commercial purposes.(see below)

Creative Commons Attribution-Non-Commercial-NoDerivs License

The Creative Commons Attribution Non-Commercial-NoDerivs License (CC-BY-NC-ND) permits use, distribution and reproduction in any medium, provided the original work is properly cited, is not used for commercial purposes and no modifications or adaptations are made. (see below)

Use by commercial "for-profit" organizations

Use of Wiley Open Access articles for commercial, promotional, or marketing purposes requires further explicit permission from Wiley and will be subject to a fee.
Further details can be found on Wiley Online Library http://olabout.wiley.com/WileyCDA/Section/id-410895.html

Other Terms and Conditions:

v1.10 Last updated September 2015

Questions? customercare@copyright.com or +1-855-239-3415 (toll free in the US) or +1-978-646-2777.

ELSEVIER LICENSE
TERMS AND CONDITIONS

Mar 28, 2016

This is an Agreement between Alena Grebe ("You") and Elsevier ("Elsevier"). It consists of your order details, the terms and conditions provided by Elsevier, and the payment terms and conditions.

All payments must be made in full to CCC. For payment instructions, please see information listed at the bottom of this form.

Supplier	Elsevier Limited The Boulevard,Langford Lane Kidlington,Oxford,OX5 1GB,UK
Registered Company Number	1982084
Customer name	Alena Grebe
Customer address	WInzerstr. 6-8 Bonn, None 53129
License number	3837591358800
License date	Mar 28, 2016
Licensed content publisher	Elsevier
Licensed content publication	Cell
Licensed content title	Macrophages in the Pathogenesis of Atherosclerosis
Licensed content author	Kathryn J. Moore,Ira Tabas
Licensed content date	29 April 2011
Licensed content volume number	145
Licensed content issue number	3
Number of pages	15
Start Page	341
End Page	355
Type of Use	reuse in a thesis/dissertation
Intended publisher of new work	other
Portion	figures/tables/illustrations
Number of figures/tables/illustrations	1
Format	both print and electronic
Are you the author of this Elsevier article?	No
Will you be translating?	No
Original figure numbers	Figure 1
Title of your thesis/dissertation	Targeting cholesterol crystals in atherosclerosis with cholesterol solubilizing 2-hydroxypropyl-β-cyclodextrin
Expected completion date	Apr 2016
Estimated size (number of pages)	150
Elsevier VAT number	GB 494 6272 12
Price	0.00 EUR
VAT/Local Sales Tax	0.00 EUR / 0.00 GBP
Total	**0.00 EUR**
Terms and Conditions	

INTRODUCTION

1. The publisher for this copyrighted material is Elsevier. By clicking "accept" in connection with completing this licensing transaction, you agree that the following terms and conditions apply to this transaction (along with the Billing and Payment terms and conditions established by Copyright Clearance Center, Inc. ("CCC"), at the time that you opened your Rightslink account and that are available at any time at http://myaccount.copyright.com).

GENERAL TERMS

2. Elsevier hereby grants you permission to reproduce the aforementioned material subject to the terms and conditions indicated.
3. Acknowledgement: If any part of the material to be used (for example, figures) has appeared in our publication with credit or acknowledgement to another source, permission must also be sought from that source. If such permission is not obtained then that material may not be included in your publication/copies. Suitable acknowledgement to the source must be made, either as a footnote or in a reference list at the end of your publication, as follows:
"Reprinted from Publication title, Vol /edition number, Author(s), Title of article / title of chapter, Pages No., Copyright (Year), with permission from Elsevier [OR APPLICABLE SOCIETY COPYRIGHT OWNER]." Also Lancet special credit - "Reprinted from The Lancet, Vol. number, Author(s), Title of article, Pages No., Copyright (Year), with permission from Elsevier."
4. Reproduction of this material is confined to the purpose and/or media for which permission is hereby given.
5. Altering/Modifying Material: Not Permitted. However figures and illustrations may be altered/adapted minimally to serve your work. Any other abbreviations, additions, deletions and/or any other alterations shall be made only with prior written authorization of Elsevier Ltd. (Please contact Elsevier at permissions@elsevier.com)
6. If the permission fee for the requested use of our material is waived in this instance, please be advised that your future requests for Elsevier materials may attract a fee.
7. Reservation of Rights: Publisher reserves all rights not specifically granted in the combination of (i) the license details provided by you and accepted in the course of this licensing transaction, (ii) these terms and conditions and (iii) CCC's Billing and Payment terms and conditions.
8. License Contingent Upon Payment: While you may exercise the rights licensed immediately upon issuance of the license at the end of the licensing process for the transaction, provided that you have disclosed complete and accurate details of your proposed use, no license is finally effective unless and until full payment is received from you (either by publisher or by CCC) as provided in CCC's Billing and Payment terms and conditions. If full payment is not received on a timely basis, then any license preliminarily granted shall be deemed automatically revoked and shall be void as if never granted. Further, in the event that you breach any of these terms and conditions or any of CCC's Billing and Payment terms and conditions, the license is automatically revoked and shall be void as if never granted. Use of materials as described in a revoked license, as well as any use of the materials beyond the scope of an unrevoked license, may constitute copyright infringement and publisher reserves the right to take any and all action to protect its copyright in the materials.
9. Warranties: Publisher makes no representations or warranties with respect to the licensed material.
10. Indemnity: You hereby indemnify and agree to hold harmless publisher and CCC, and their respective officers, directors, employees and agents, from and against any and all claims arising out of your use of the licensed material other than as specifically authorized pursuant to this license.
11. No Transfer of License: This license is personal to you and may not be sublicensed, assigned, or transferred by you to any other person without publisher's written permission.
12. No Amendment Except in Writing: This license may not be amended except in a writing signed by both parties (or, in the case of publisher, by CCC on publisher's behalf).
13. Objection to Contrary Terms: Publisher hereby objects to any terms contained in any purchase order, acknowledgment, check endorsement or other writing prepared by you, which terms are inconsistent with these terms and conditions or CCC's Billing and Payment terms and conditions. These terms and conditions, together with CCC's Billing and Payment terms and conditions (which are incorporated herein), comprise the entire agreement between you and publisher (and CCC) concerning this licensing transaction. In the event of any conflict between your obligations established by these terms and conditions and those established by CCC's Billing and Payment terms and conditions, these terms and conditions shall control.
14. Revocation: Elsevier or Copyright Clearance Center may deny the permissions described in this License at their sole discretion, for any reason or no reason, with a full refund payable to you. Notice of such denial will be made using the contact information provided by you. Failure to receive such notice will not alter or invalidate the denial. In no event will Elsevier or Copyright Clearance Center be responsible or liable for any costs, expenses or damage incurred by you as a result of a denial of your permission request, other than a refund of the amount(s) paid by you to Elsevier and/or Copyright Clearance Center for denied permissions.

LIMITED LICENSE

The following terms and conditions apply only to specific license types:
15. **Translation**: This permission is granted for non-exclusive world **English** rights only unless your license was granted for translation rights. If you licensed translation rights you may only translate this content into the languages you requested. A professional translator must perform all translations and reproduce the content word for word preserving the integrity of the article.
16. **Posting licensed content on any Website**: The following terms and conditions apply as follows: Licensing material from an Elsevier journal: All content posted to the web site must maintain the copyright information line on the bottom of each image; A hyper-text must be included to the Homepage of the journal from which you are licensing at http://www.sciencedirect.com/science/journal/xxxxx or the Elsevier homepage for books at http://www.elsevier.com; Central Storage: This license does not include permission for a scanned version of the material to be stored in a central repository such as that provided by Heron/XanEdu.
Licensing material from an Elsevier book: A hyper-text link must be included to the Elsevier homepage at http://www.elsevier.com . All content posted to the web site must maintain the copyright information line on the bottom of each image.

Posting licensed content on Electronic reserve: In addition to the above the following clauses are applicable: The web site must be password-protected and made available only to bona fide students registered on a relevant course. This permission is granted for 1 year only. You may obtain a new license for future website posting.
17. **For journal authors:** the following clauses are applicable in addition to the above:
Preprints:
A preprint is an author's own write-up of research results and analysis, it has not been peer-reviewed, nor has it had any other value added to it by a publisher (such as formatting, copyright, technical enhancement etc.).
Authors can share their preprints anywhere at any time. Preprints should not be added to or enhanced in any way in order to appear more like, or to substitute for, the final versions of articles however authors can update their preprints on arXiv or RePEc with their Accepted Author Manuscript (see below).
If accepted for publication, we encourage authors to link from the preprint to their formal publication via its DOI. Millions of researchers have access to the formal publications on ScienceDirect, and so links will help users to find, access, cite and use the best available version. Please note that Cell Press, The Lancet and some society-owned have different preprint policies. Information on these policies is available on the journal homepage.
Accepted Author Manuscripts: An accepted author manuscript is the manuscript of an article that has been accepted for publication and which typically includes author-incorporated changes suggested during submission, peer review and editor-author communications.
Authors can share their accepted author manuscript:

- immediately
  - via their non-commercial person homepage or blog
  - by updating a preprint in arXiv or RePEc with the accepted manuscript
  - via their research institute or institutional repository for internal institutional uses or as part of an invitation-only research collaboration work-group
  - directly by providing copies to their students or to research collaborators for their personal use
  - for private scholarly sharing as part of an invitation-only work group on commercial sites with which Elsevier has an agreement
- after the embargo period
  - via non-commercial hosting platforms such as their institutional repository
  - via commercial sites with which Elsevier has an agreement

In all cases accepted manuscripts should:

- link to the formal publication via its DOI
- bear a CC-BY-NC-ND license - this is easy to do
- if aggregated with other manuscripts, for example in a repository or other site, be shared in alignment with our hosting policy not be added to or enhanced in any way to appear more like, or to substitute for, the published journal article.

Published journal article (JPA): A published journal article (PJA) is the definitive final record of published research that appears or will appear in the journal and embodies all value-adding publishing activities including peer review co-ordination, copy-editing, formatting, (if relevant) pagination and online enrichment.
Policies for sharing publishing journal articles differ for subscription and gold open access articles:
Subscription Articles: If you are an author, please share a link to your article rather than the full-text. Millions of researchers have access to the formal publications on ScienceDirect, and so links will help your users to find, access, cite, and use the best available version.
Theses and dissertations which contain embedded PJAs as part of the formal submission can be posted publicly by the awarding institution with DOI links back to the formal publications on ScienceDirect.
If you are affiliated with a library that subscribes to ScienceDirect you have additional private sharing rights for others' research accessed under that agreement. This includes use for classroom teaching and internal training at the institution (including use in course packs and courseware programs), and inclusion of the article for grant funding purposes.
Gold Open Access Articles: May be shared according to the author-selected end-user license and should contain a CrossMark logo, the end user license, and a DOI link to the formal publication on ScienceDirect.
Please refer to Elsevier's posting policy for further information.
18. **For book authors** the following clauses are applicable in addition to the above: Authors are permitted to place a brief summary of their work online only. You are not allowed to download and post the published electronic version of your chapter, nor may you scan the printed edition to create an electronic version. **Posting to a repository:** Authors are permitted to post a summary of their chapter only in their institution's repository.
19. **Thesis/Dissertation**: If your license is for use in a thesis/dissertation your thesis may be submitted to your institution in either print or electronic form. Should your thesis be published commercially, please reapply for permission. These requirements include permission for the Library and Archives of Canada to supply single copies, on demand, of the complete thesis and include permission for Proquest/UMI to supply single copies, on demand, of the complete thesis. Should your thesis be published commercially, please reapply for permission. Theses and dissertations which contain embedded PJAs as part of the formal submission can be posted publicly by the awarding institution with DOI links back to the formal publications on ScienceDirect.

Elsevier Open Access Terms and Conditions
You can publish open access with Elsevier in hundreds of open access journals or in nearly 2000 established subscription journals that support open access publishing. Permitted third party re-use of these open access articles is defined by the author's choice of Creative Commons user license. See our open access license policy for more information.
Terms & Conditions applicable to all Open Access articles published with Elsevier:
Any reuse of the article must not represent the author as endorsing the adaptation of the article nor should the article be modified in such a way as to damage the author's honour or reputation. If any changes have been made, such changes must be clearly indicated.
The author(s) must be appropriately credited and we ask that you include the end user license and a DOI link to the formal publication on ScienceDirect.
If any part of the material to be used (for example, figures) has appeared in our publication with credit or acknowledgement to another source it is the responsibility of the user to ensure their reuse complies with the terms and conditions determined by the rights holder.
Additional Terms & Conditions applicable to each Creative Commons user license:
CC BY: The CC-BY license allows users to copy, to create extracts, abstracts and new works from the Article, to alter and revise the Article and to make commercial use of the Article (including reuse and/or resale of the Article by commercial entities), provided the user gives appropriate credit (with a link to the formal publication through the relevant DOI), provides a link to the license, indicates if changes were made and the licensor is not represented as endorsing the use made of the work. The full details of the license are available at http://creativecommons.org/licenses/by/4.0.
CC BY NC SA: The CC BY-NC-SA license allows users to copy, to create extracts, abstracts and new works from the Article, to alter and revise the Article, provided this is not done for commercial purposes, and that the user gives appropriate credit (with a link to the formal publication through the relevant DOI), provides a link to the license, indicates if changes were made and the licensor is not represented as endorsing the use made of the work. Further, any new works must be made available on the same conditions. The full details of the license are available at http://creativecommons.org/licenses/by-nc-sa/4.0.
CC BY NC ND: The CC BY-NC-ND license allows users to copy and distribute the Article, provided this is not done for commercial purposes and further does not permit distribution of the Article if it is changed or edited in any way, and provided the user gives appropriate credit (with a link to the formal publication through the relevant DOI), provides a link to the license, and that the licensor is not represented as endorsing the use made of the work. The full details of the license are available at http://creativecommons.org/licenses/by-nc-nd/4.0. Any commercial reuse of Open Access articles published with a CC BY NC SA or CC BY NC ND license requires permission from Elsevier and will be subject to a fee.
Commercial reuse includes:

- Associating advertising with the full text of the Article
- Charging fees for document delivery or access
- Article aggregation
- Systematic distribution via e-mail lists or share buttons

Posting or linking by commercial companies for use by customers of those companies.

20. **Other Conditions**:

v1.8

Questions? customercare@copyright.com or +1-855-239-3415 (toll free in the US) or +1-978-646-2777.

NATURE PUBLISHING GROUP LICENSE TERMS AND CONDITIONS

Mar 28, 2016

This is an Agreement between Alena Grebe ("You") and Nature Publishing Group ("Nature Publishing Group"). It consists of your order details, the terms and conditions provided by Nature Publishing Group, and the payment terms and conditions.

All payments must be made in full to CCC. For payment instructions, please see information listed at the bottom of this form.

License Number	3837600047380
License date	Mar 28, 2016
Licensed Content Publisher	Nature Publishing Group
Licensed Content Publication	Nature Medicine
Licensed Content Title	The not-so-simple HDL story: Is it time to revise the HDL cholesterol hypothesis?
Licensed Content Author	Daniel J Rader, Alan R Tall
Licensed Content Date	Sep 7, 2012
Volume number	18
Issue number	9
Type of Use	reuse in a dissertation / thesis
Requestor type	academic/educational
Format	print and electronic
Portion	figures/tables/illustrations
Number of figures/tables/illustrations	1
High-res required	no
Figures	Figure 1
Author of this NPG article	no
Your reference number	None
Title of your thesis / dissertation	Targeting cholesterol crystals in atherosclerosis with cholesterol solubilizing 2-hydroxypropyl-β-cyclodextrin
Expected completion date	Apr 2016
Estimated size (number of pages)	150
Total	**0.00 EUR**
Terms and Conditions	

Terms and Conditions for Permissions

Nature Publishing Group hereby grants you a non-exclusive license to reproduce this material for this purpose, and for no other use,subject to the conditions below:

1. NPG warrants that it has, to the best of its knowledge, the rights to license reuse of this material. However, you should ensure that the material you are requesting is original to Nature Publishing Group and does not carry the copyright of another entity (as credited in the published version). If the credit line on any part of the material you have requested indicates that it was reprinted or adapted by NPG with permission from another source, then you should also seek permission from that source to reuse the material.

2. Permission granted free of charge for material in print is also usually granted for any electronic version of that work, provided that the material is incidental to the work as a whole and that the electronic version is essentially equivalent to, or substitutes for, the print version.Where print permission has been granted for a fee, separate permission must be obtained for any additional, electronic re-use (unless, as in the case of a full paper, this has already been accounted for during your initial request in the calculation of a print run).NB: In all cases, web-based use of full-text articles must be authorized separately through the 'Use on a Web Site' option when requesting permission.

3. Permission granted for a first edition does not apply to second and subsequent editions and for editions in other languages (except for signatories to the STM Permissions Guidelines, or where the first edition permission was granted for free).

4. Nature Publishing Group's permission must be acknowledged next to the figure, table or abstract in print. In electronic form, this acknowledgement must be visible at the same time as the figure/table/abstract, and must be hyperlinked to the journal's homepage.

5. The credit line should read:
   Reprinted by permission from Macmillan Publishers Ltd: [JOURNAL NAME] (reference citation), copyright (year of publication)
   For AOP papers, the credit line should read:
   Reprinted by permission from Macmillan Publishers Ltd: [JOURNAL NAME], advance online publication, day month year (doi: 10.1038/sj.[JOURNAL ACRONYM].XXXXX)

   Note: For republication from the *British Journal of Cancer,* the following credit lines apply.
   Reprinted by permission from Macmillan Publishers Ltd on behalf of Cancer Research UK: [JOURNAL NAME] (reference citation), copyright (year of publication)For AOP papers, the credit line should read:
   Reprinted by permission from Macmillan Publishers Ltd on behalf of Cancer Research UK: [JOURNAL NAME], advance online publication, day month year (doi: 10.1038/sj.[JOURNAL ACRONYM].XXXXX)

6. Adaptations of single figures do not require NPG approval. However, the adaptation should be credited as follows:

   Adapted by permission from Macmillan Publishers Ltd: [JOURNAL NAME] (reference citation), copyright (year of publication)

   Note: For adaptation from the *British Journal of Cancer,* the following credit line applies.
   Adapted by permission from Macmillan Publishers Ltd on behalf of Cancer Research UK: [JOURNAL NAME] (reference citation), copyright (year of publication)

7. Translations of 401 words up to a whole article require NPG approval. Please visit http://www.macmillanmedicalcommunications.com for more information.Translations of up to a 400 words do not require NPG approval. The translation should be credited as follows:

   Translated by permission from Macmillan Publishers Ltd: [JOURNAL NAME] (reference citation), copyright (year of publication).

   Note: For translation from the *British Journal of Cancer,* the following credit line applies.
   Translated by permission from Macmillan Publishers Ltd on behalf of Cancer Research UK: [JOURNAL NAME] (reference citation), copyright (year of publication)

We are certain that all parties will benefit from this agreement and wish you the best in the use of this material. Thank you.
Special Terms:
v1.1

Questions? customercare@copyright.com or +1-855-239-3415 (toll free in the US) or +1-978-646-2777.

NATURE PUBLISHING GROUP LICENSE TERMS AND CONDITIONS

Mar 28, 2016

This is an Agreement between Alena Grebe ("You") and Nature Publishing Group ("Nature Publishing Group"). It consists of your order details, the terms and conditions provided by Nature Publishing Group, and the payment terms and conditions.

All payments must be made in full to CCC. For payment instructions, please see information listed at the bottom of this form.

License Number	3837600193874
License date	Mar 28, 2016
Licensed Content Publisher	Nature Publishing Group
Licensed Content Publication	Nature Immunology
Licensed Content Title	Sterols and oxysterols in immune cell function
Licensed Content Author	Nathanael J Spann, Christopher K Glass
Licensed Content Date	Aug 20, 2013
Volume number	14
Issue number	9
Type of Use	reuse in a dissertation / thesis
Requestor type	academic/educational
Format	print and electronic
Portion	figures/tables/illustrations
Number of figures/tables/illustrations	1
High-res required	no
Figures	Figure 1
Author of this NPG article	no
Your reference number	None
Title of your thesis / dissertation	Targeting cholesterol crystals in atherosclerosis with cholesterol solubilizing 2-hydroxypropyl-β-cyclodextrin
Expected completion date	Apr 2016
Estimated size (number of pages)	150
Total	**0.00 EUR**
Terms and Conditions	

Terms and Conditions for Permissions

Nature Publishing Group hereby grants you a non-exclusive license to reproduce this material for this purpose, and for no other use,subject to the conditions below:

1. NPG warrants that it has, to the best of its knowledge, the rights to license reuse of this material. However, you should ensure that the material you are requesting is original to Nature Publishing Group and does not carry the copyright of another entity (as credited in the published version). If the credit line on any part of the material you have requested indicates that it was reprinted or adapted by NPG with permission from another source, then you should also seek permission from that source to reuse the material.

2. Permission granted free of charge for material in print is also usually granted for any electronic version of that work, provided that the material is incidental to the work as a whole and that the electronic version is essentially equivalent to, or substitutes for, the print version.Where print permission has been granted for a fee, separate permission must be obtained for any additional, electronic re-use (unless, as in the case of a full paper, this has already been accounted for during your initial request in the calculation of a print run).NB: In all cases, web-based use of full-text articles must be authorized separately through the 'Use on a Web Site' option when requesting permission.

3. Permission granted for a first edition does not apply to second and subsequent editions and for editions in other languages (except for signatories to the STM Permissions Guidelines, or where the first edition permission was granted for free).

4. Nature Publishing Group's permission must be acknowledged next to the figure, table or abstract in print. In electronic form, this acknowledgement must be visible at the same time as the figure/table/abstract, and must be hyperlinked to the journal's homepage.

5. The credit line should read:
   Reprinted by permission from Macmillan Publishers Ltd: [JOURNAL NAME] (reference citation), copyright (year of publication)
   For AOP papers, the credit line should read:
   Reprinted by permission from Macmillan Publishers Ltd: [JOURNAL NAME], advance online publication, day month year (doi: 10.1038/sj.[JOURNAL ACRONYM].XXXXX)

   Note: For republication from the *British Journal of Cancer,* the following credit lines apply.
   Reprinted by permission from Macmillan Publishers Ltd on behalf of Cancer Research UK: [JOURNAL NAME] (reference citation), copyright (year of publication)For AOP papers, the credit line should read:
   Reprinted by permission from Macmillan Publishers Ltd on behalf of Cancer Research UK: [JOURNAL NAME], advance online publication, day month year (doi: 10.1038/sj.[JOURNAL ACRONYM].XXXXX)

6. Adaptations of single figures do not require NPG approval. However, the adaptation should be credited as follows:

   Adapted by permission from Macmillan Publishers Ltd: [JOURNAL NAME] (reference citation), copyright (year of publication)

   Note: For adaptation from the *British Journal of Cancer,* the following credit line applies.
   Adapted by permission from Macmillan Publishers Ltd on behalf of Cancer Research UK: [JOURNAL NAME] (reference citation), copyright (year of publication)

7. Translations of 401 words up to a whole article require NPG approval. Please visit http://www.macmillanmedicalcommunications.com for more information.Translations of up to a 400 words do not require NPG approval. The translation should be credited as follows:

   Translated by permission from Macmillan Publishers Ltd: [JOURNAL NAME] (reference citation), copyright (year of publication).

   Note: For translation from the *British Journal of Cancer,* the following credit line applies.
   Translated by permission from Macmillan Publishers Ltd on behalf of Cancer Research UK: [JOURNAL NAME] (reference citation), copyright (year of publication)

We are certain that all parties will benefit from this agreement and wish you the best in the use of this material. Thank you.
Special Terms:
v1.1

Questions? customercare@copyright.com or +1-855-239-3415 (toll free in the US) or +1-978-646-2777.

NATURE PUBLISHING GROUP LICENSE TERMS AND CONDITIONS

Mar 28, 2016

This is an Agreement between Alena Grebe ("You") and Nature Publishing Group ("Nature Publishing Group"). It consists of your order details, the terms and conditions provided by Nature Publishing Group, and the payment terms and conditions.

All payments must be made in full to CCC. For payment instructions, please see information listed at the bottom of this form.

License Number	3837600360302
License date	Mar 28, 2016
Licensed Content Publisher	Nature Publishing Group
Licensed Content Publication	Nature Reviews Drug Discovery
Licensed Content Title	Cyclodextrin-based pharmaceutics: past, present and future
Licensed Content Author	Mark E. DavisandMarcus E. Brewster
Licensed Content Date	Dec 1, 2004
Volume number	3
Issue number	12
Type of Use	reuse in a dissertation / thesis
Requestor type	academic/educational
Format	print and electronic
Portion	figures/tables/illustrations
Number of figures/tables/illustrations	3
High-res required	no
Figures	Figure 1, Figure 2, Figure 3
Author of this NPG article	no
Your reference number	None
Title of your thesis / dissertation	Targeting cholesterol crystals in atherosclerosis with cholesterol solubilizing 2-hydroxypropyl-β-cyclodextrin
Expected completion date	Apr 2016
Estimated size (number of pages)	150
Total	**0.00 EUR**
Terms and Conditions	

Terms and Conditions for Permissions

Nature Publishing Group hereby grants you a non-exclusive license to reproduce this material for this purpose, and for no other use,subject to the conditions below:

1. NPG warrants that it has, to the best of its knowledge, the rights to license reuse of this material. However, you should ensure that the material you are requesting is original to Nature Publishing Group and does not carry the copyright of another entity (as credited in the published version). If the credit line on any part of the material you have requested indicates that it was reprinted or adapted by NPG with permission from another source, then you should also seek permission from that source to reuse the material.

2. Permission granted free of charge for material in print is also usually granted for any electronic version of that work, provided that the material is incidental to the work as a whole and that the electronic version is essentially equivalent to, or substitutes for, the print version.Where print permission has been granted for a fee, separate permission must be obtained for any additional, electronic re-use (unless, as in the case of a full paper, this has already been accounted for during your initial request in the calculation of a print run).NB: In all cases, web-based use of full-text articles must be authorized separately through the 'Use on a Web Site' option when requesting permission.

3. Permission granted for a first edition does not apply to second and subsequent editions and for editions in other languages (except for signatories to the STM Permissions Guidelines, or where the first edition permission was granted for free).

4. Nature Publishing Group's permission must be acknowledged next to the figure, table or abstract in print. In electronic form, this acknowledgement must be visible at the same time as the figure/table/abstract, and must be hyperlinked to the journal's homepage.

5. The credit line should read:
   Reprinted by permission from Macmillan Publishers Ltd: [JOURNAL NAME] (reference citation), copyright (year of publication)
   For AOP papers, the credit line should read:
   Reprinted by permission from Macmillan Publishers Ltd: [JOURNAL NAME], advance online publication, day month year (doi: 10.1038/sj.[JOURNAL ACRONYM].XXXXX)

   Note: For republication from the *British Journal of Cancer,* the following credit lines apply.
   Reprinted by permission from Macmillan Publishers Ltd on behalf of Cancer Research UK: [JOURNAL NAME] (reference citation), copyright (year of publication)For AOP papers, the credit line should read:
   Reprinted by permission from Macmillan Publishers Ltd on behalf of Cancer Research UK: [JOURNAL NAME], advance online publication, day month year (doi: 10.1038/sj.[JOURNAL ACRONYM].XXXXX)

6. Adaptations of single figures do not require NPG approval. However, the adaptation should be credited as follows:

   Adapted by permission from Macmillan Publishers Ltd: [JOURNAL NAME] (reference citation), copyright (year of publication)

   Note: For adaptation from the *British Journal of Cancer,* the following credit line applies.
   Adapted by permission from Macmillan Publishers Ltd on behalf of Cancer Research UK: [JOURNAL NAME] (reference citation), copyright (year of publication)

7. Translations of 401 words up to a whole article require NPG approval. Please visit http://www.macmillanmedicalcommunications.com for more information.Translations of up to a 400 words do not require NPG approval. The translation should be credited as follows:

   Translated by permission from Macmillan Publishers Ltd: [JOURNAL NAME] (reference citation), copyright (year of publication).

   Note: For translation from the *British Journal of Cancer,* the following credit line applies.
   Translated by permission from Macmillan Publishers Ltd on behalf of Cancer Research UK: [JOURNAL NAME] (reference citation), copyright (year of publication)

We are certain that all parties will benefit from this agreement and wish you the best in the use of this material. Thank you.
Special Terms:
v1.1

Questions? customercare@copyright.com or +1-855-239-3415 (toll free in the US) or +1-978-646-2777.

JOHN WILEY AND SONS LICENSE TERMS AND CONDITIONS

Mar 28, 2016

This Agreement between Alena Grebe ("You") and John Wiley and Sons ("John Wiley and Sons") consists of your license details and the terms and conditions provided by John Wiley and Sons and Copyright Clearance Center.

License Number	3837600554929
License date	Mar 28, 2016
Licensed Content Publisher	John Wiley and Sons
Licensed Content Publication	Journal of Pharmacy and Pharamacology
Licensed Content Title	Pharmaceutical applications of cyclodextrins: basic science and product development
Licensed Content Author	Thorsteinn Loftsson,Marcus E. Brewster
Licensed Content Date	Jul 20, 2010
Pages	15
Type of Use	Dissertation/Thesis
Requestor type	University/Academic
Format	Print and electronic
Portion	Figure/table
Number of figures/tables	1
Original Wiley figure/table number(s)	Figure 1
Will you be translating?	No
Title of your thesis / dissertation	Targeting cholesterol crystals in atherosclerosis with cholesterol solubilizing 2-hydroxypropyl-β-cyclodextrin
Expected completion date	Apr 2016
Expected size (number of pages)	150
Requestor Location	Alena Grebe WInzerstr. 6-8 None None Bonn, Germany 53129 Attn: Alena Grebe
Billing Type	Invoice
Billing Address	Alena Grebe WInzerstr. 6-8 None None Bonn, Germany 53129 Attn: Alena Grebe
Total	**0.00 EUR**
Terms and Conditions	

TERMS AND CONDITIONS

This copyrighted material is owned by or exclusively licensed to John Wiley & Sons, Inc. or one of its group companies (each a"Wiley Company") or handled on behalf of a society with which a Wiley Company has exclusive publishing rights in relation to a particular work (collectively "WILEY"). By clicking "accept" in connection with completing this licensing transaction, you agree that the following terms and conditions apply to this transaction (along with the billing and payment terms and conditions established by the Copyright Clearance Center Inc., ("CCC's Billing and Payment terms and conditions"), at the time that you opened your RightsLink account (these are available at any time at http://myaccount.copyright.com).

Terms and Conditions

- The materials you have requested permission to reproduce or reuse (the "Wiley Materials") are protected by copyright.
- You are hereby granted a personal, non-exclusive, non-sub licensable (on a stand-alone basis), non-transferable, worldwide, limited license to reproduce the Wiley Materials for the purpose specified in the licensing process. This license, **and any CONTENT (PDF or image file) purchased as part of your order,** is for a one-time use only and limited to any maximum distribution number specified in the license. The first instance of republication or reuse granted by this license must be completed within two years of the date of the grant of this license (although copies prepared before the end date may be distributed thereafter). The Wiley Materials shall not be used in any other manner or for any other purpose, beyond what is granted in the license. Permission is granted subject to an appropriate acknowledgement given to the author, title of the material/book/journal and the publisher. You shall also duplicate the copyright notice that appears in the Wiley publication in your use of the Wiley Material. Permission is also granted on the understanding that nowhere in the text is a previously published source acknowledged for all or part of this Wiley Material. Any third party content is expressly excluded from this permission.
- With respect to the Wiley Materials, all rights are reserved. Except as expressly granted by the terms of the license, no part of the Wiley Materials may be copied, modified, adapted (except for minor reformatting required by the new Publication), translated, reproduced, transferred or distributed, in any form or by any means, and no derivative works may be made based on the Wiley Materials without the prior permission of the respective copyright owner.**For STM Signatory Publishers clearing permission under the terms of the STM Permissions Guidelines only, the terms of the license are extended to include subsequent editions and for editions in other languages, provided such editions are for the work as a whole in situ and does not involve the separate exploitation of the permitted figures or extracts,** You may not alter, remove or suppress in any manner any copyright, trademark or other notices displayed by the Wiley Materials. You may not license, rent, sell, loan, lease, pledge, offer as security, transfer or assign the Wiley Materials on a stand-alone basis, or any of the rights granted to you hereunder to any other person.
- The Wiley Materials and all of the intellectual property rights therein shall at all times remain the exclusive property of John Wiley & Sons Inc, the Wiley Companies, or their respective licensors, and your interest therein is only that of having possession of and the right to reproduce the Wiley Materials pursuant to Section 2 herein during the continuance of this Agreement. You agree that you own no right, title or interest in or to the Wiley Materials or any of the intellectual property rights therein. You shall have no rights hereunder other than the license as provided for above in Section 2. No right, license or interest to any trademark, trade name, service mark or other branding ("Marks") of WILEY or its licensors is granted hereunder, and you agree that you shall not assert any such right, license or interest with respect thereto

- NEITHER WILEY NOR ITS LICENSORS MAKES ANY WARRANTY OR REPRESENTATION OF ANY KIND TO YOU OR ANY THIRD PARTY, EXPRESS, IMPLIED OR STATUTORY, WITH RESPECT TO THE MATERIALS OR THE ACCURACY OF ANY INFORMATION CONTAINED IN THE MATERIALS, INCLUDING, WITHOUT LIMITATION, ANY IMPLIED WARRANTY OF MERCHANTABILITY, ACCURACY, SATISFACTORY QUALITY, FITNESS FOR A PARTICULAR PURPOSE, USABILITY, INTEGRATION OR NON-INFRINGEMENT AND ALL SUCH WARRANTIES ARE HEREBY EXCLUDED BY WILEY AND ITS LICENSORS AND WAIVED BY YOU.

- WILEY shall have the right to terminate this Agreement immediately upon breach of this Agreement by you.

- You shall indemnify, defend and hold harmless WILEY, its Licensors and their respective directors, officers, agents and employees, from and against any actual or threatened claims, demands, causes of action or proceedings arising from any breach of this Agreement by you.

- IN NO EVENT SHALL WILEY OR ITS LICENSORS BE LIABLE TO YOU OR ANY OTHER PARTY OR ANY OTHER PERSON OR ENTITY FOR ANY SPECIAL, CONSEQUENTIAL, INCIDENTAL, INDIRECT, EXEMPLARY OR PUNITIVE DAMAGES, HOWEVER CAUSED, ARISING OUT OF OR IN CONNECTION WITH THE DOWNLOADING, PROVISIONING, VIEWING OR USE OF THE MATERIALS REGARDLESS OF THE FORM OF ACTION, WHETHER FOR BREACH OF CONTRACT, BREACH OF WARRANTY, TORT, NEGLIGENCE, INFRINGEMENT OR OTHERWISE (INCLUDING, WITHOUT LIMITATION, DAMAGES BASED ON LOSS OF PROFITS, DATA, FILES, USE, BUSINESS OPPORTUNITY OR CLAIMS OF THIRD PARTIES), AND WHETHER OR NOT THE PARTY HAS BEEN ADVISED OF THE POSSIBILITY OF SUCH DAMAGES. THIS LIMITATION SHALL APPLY NOTWITHSTANDING ANY FAILURE OF ESSENTIAL PURPOSE OF ANY LIMITED REMEDY PROVIDED HEREIN.

- Should any provision of this Agreement be held by a court of competent jurisdiction to be illegal, invalid, or unenforceable, that provision shall be deemed amended to achieve as nearly as possible the same economic effect as the original provision, and the legality, validity and enforceability of the remaining provisions of this Agreement shall not be affected or impaired thereby.

- The failure of either party to enforce any term or condition of this Agreement shall not constitute a waiver of either party's right to enforce each and every term and condition of this Agreement. No breach under this agreement shall be deemed waived or excused by either party unless such waiver or consent is in writing signed by the party granting such waiver or consent. The waiver by or consent of a party to a breach of any provision of this Agreement shall not operate or be construed as a waiver of or consent to any other or subsequent breach by such other party.

- This Agreement may not be assigned (including by operation of law or otherwise) by you without WILEY's prior written consent.

- Any fee required for this permission shall be non-refundable after thirty (30) days from receipt by the CCC.

- These terms and conditions together with CCC's Billing and Payment terms and conditions (which are incorporated herein) form the entire agreement between you and WILEY concerning this licensing transaction and (in the absence of fraud) supersedes all prior agreements and representations of the parties, oral or written. This Agreement may not be amended except in writing signed by both parties. This Agreement shall be binding upon and inure to the benefit of the parties' successors, legal representatives, and authorized assigns.

- In the event of any conflict between your obligations established by these terms and conditions and those established by CCC's Billing and Payment terms and conditions, these terms and conditions shall prevail.

- WILEY expressly reserves all rights not specifically granted in the combination of (i) the license details provided by you and accepted in the course of this licensing transaction, (ii) these terms and conditions and (iii) CCC's Billing and Payment terms and conditions.

- This Agreement will be void if the Type of Use, Format, Circulation, or Requestor Type was misrepresented during the licensing process.

- This Agreement shall be governed by and construed in accordance with the laws of the State of New York, USA, without regards to such state's conflict of law rules. Any legal action, suit or proceeding arising out of or relating to these Terms and Conditions or the breach thereof shall be instituted in a court of competent jurisdiction in New York County in the State of New York in the United States of America and each party hereby consents and submits to the personal jurisdiction of such court, waives any objection to venue in such court and consents to service of process by registered or certified mail, return receipt requested, at the last known address of such party.

WILEY OPEN ACCESS TERMS AND CONDITIONS

Wiley Publishes Open Access Articles in fully Open Access Journals and in Subscription journals offering Online Open. Although most of the fully Open Access journals publish open access articles under the terms of the Creative Commons Attribution (CC BY) License only, the subscription journals and a few of the Open Access Journals offer a choice of Creative Commons Licenses. The license type is clearly identified on the article.

The Creative Commons Attribution License

The Creative Commons Attribution License (CC-BY) allows users to copy, distribute and transmit an article, adapt the article and make commercial use of the article. The CC-BY license permits commercial and non-

Creative Commons Attribution Non-Commercial License

The Creative Commons Attribution Non-Commercial (CC-BY-NC)License permits use, distribution and reproduction in any medium, provided the original work is properly cited and is not used for commercial purposes.(see below)

Creative Commons Attribution-Non-Commercial-NoDerivs License

The Creative Commons Attribution Non-Commercial-NoDerivs License (CC-BY-NC-ND) permits use, distribution and reproduction in any medium, provided the original work is properly cited, is not used for commercial purposes and no modifications or adaptations are made. (see below)

Use by commercial "for-profit" organizations

Use of Wiley Open Access articles for commercial, promotional, or marketing purposes requires further explicit permission from Wiley and will be subject to a fee.
Further details can be found on Wiley Online Library http://olabout.wiley.com/WileyCDA/Section/id-410895.html

Other Terms and Conditions:

v1.10 Last updated September 2015

Questions? customercare@copyright.com or +1-855-239-3415 (toll free in the US) or +1-978-646-2777.

JOHN WILEY AND SONS LICENSE TERMS AND CONDITIONS

Mar 28, 2016

This Agreement between Alena Grebe ("You") and John Wiley and Sons ("John Wiley and Sons") consists of your license details and the terms and conditions provided by John Wiley and Sons and Copyright Clearance Center.

License Number	3837600554929
License date	Mar 28, 2016
Licensed Content Publisher	John Wiley and Sons
Licensed Content Publication	Journal of Pharmacy and Pharamacology
Licensed Content Title	Pharmaceutical applications of cyclodextrins: basic science and product development
Licensed Content Author	Thorsteinn Loftsson,Marcus E. Brewster
Licensed Content Date	Jul 20, 2010
Pages	15
Type of Use	Dissertation/Thesis
Requestor type	University/Academic
Format	Print and electronic
Portion	Figure/table
Number of figures/tables	1
Original Wiley figure/table number(s)	Figure 1
Will you be translating?	No
Title of your thesis / dissertation	Targeting cholesterol crystals in atherosclerosis with cholesterol solubilizing 2-hydroxypropyl-β-cyclodextrin
Expected completion date	Apr 2016
Expected size (number of pages)	150
Requestor Location	Alena Grebe WInzerstr. 6-8 None None Bonn, Germany 53129 Attn: Alena Grebe
Billing Type	Invoice
Billing Address	Alena Grebe WInzerstr. 6-8 None None Bonn, Germany 53129 Attn: Alena Grebe
Total	**0.00 EUR**
Terms and Conditions	

TERMS AND CONDITIONS

This copyrighted material is owned by or exclusively licensed to John Wiley & Sons, Inc. or one of its group companies (each a"Wiley Company") or handled on behalf of a society with which a Wiley Company has exclusive publishing rights in relation to a particular work (collectively "WILEY"). By clicking "accept" in connection with completing this licensing transaction, you agree that the following terms and conditions apply to this transaction (along with the billing and payment terms and conditions established by the Copyright Clearance Center Inc., ("CCC's Billing and Payment terms and conditions"), at the time that you opened your RightsLink account (these are available at any time at http://myaccount.copyright.com).

Terms and Conditions

- The materials you have requested permission to reproduce or reuse (the "Wiley Materials") are protected by copyright.
- You are hereby granted a personal, non-exclusive, non-sub licensable (on a stand-alone basis), non-transferable, worldwide, limited license to reproduce the Wiley Materials for the purpose specified in the licensing process. This license, **and any CONTENT (PDF or image file) purchased as part of your order,** is for a one-time use only and limited to any maximum distribution number specified in the license. The first instance of republication or reuse granted by this license must be completed within two years of the date of the grant of this license (although copies prepared before the end date may be distributed thereafter). The Wiley Materials shall not be used in any other manner or for any other purpose, beyond what is granted in the license. Permission is granted subject to an appropriate acknowledgement given to the author, title of the material/book/journal and the publisher. You shall also duplicate the copyright notice that appears in the Wiley publication in your use of the Wiley Material. Permission is also granted on the understanding that nowhere in the text is a previously published source acknowledged for all or part of this Wiley Material. Any third party content is expressly excluded from this permission.
- With respect to the Wiley Materials, all rights are reserved. Except as expressly granted by the terms of the license, no part of the Wiley Materials may be copied, modified, adapted (except for minor reformatting required by the new Publication), translated, reproduced, transferred or distributed, in any form or by any means, and no derivative works may be made based on the Wiley Materials without the prior permission of the respective copyright owner.**For STM Signatory Publishers clearing permission under the terms of the STM Permissions Guidelines only, the terms of the license are extended to include subsequent editions and for editions in other languages, provided such editions are for the work as a whole in situ and does not involve the separate exploitation of the permitted figures or extracts,** You may not alter, remove or suppress in any manner any copyright, trademark or other notices displayed by the Wiley Materials. You may not license, rent, sell, loan, lease, pledge, offer as security, transfer or assign the Wiley Materials on a stand-alone basis, or any of the rights granted to you hereunder to any other person.
- The Wiley Materials and all of the intellectual property rights therein shall at all times remain the exclusive property of John Wiley & Sons Inc, the Wiley Companies, or their respective licensors, and your interest therein is only that of having possession of and the right to reproduce the Wiley Materials pursuant to Section 2 herein during the continuance of this Agreement. You agree that you own no right, title or interest in or to the Wiley Materials or any of the intellectual property rights therein. You shall have no rights hereunder other than the license as provided for above in Section 2. No right, license or interest to any trademark, trade name, service mark or other branding ("Marks") of WILEY or its licensors is granted hereunder, and you agree that you shall not assert any such right, license or interest with respect thereto

- NEITHER WILEY NOR ITS LICENSORS MAKES ANY WARRANTY OR REPRESENTATION OF ANY KIND TO YOU OR ANY THIRD PARTY, EXPRESS, IMPLIED OR STATUTORY, WITH RESPECT TO THE MATERIALS OR THE ACCURACY OF ANY INFORMATION CONTAINED IN THE MATERIALS, INCLUDING, WITHOUT LIMITATION, ANY IMPLIED WARRANTY OF MERCHANTABILITY, ACCURACY, SATISFACTORY QUALITY, FITNESS FOR A PARTICULAR PURPOSE, USABILITY, INTEGRATION OR NON-INFRINGEMENT AND ALL SUCH WARRANTIES ARE HEREBY EXCLUDED BY WILEY AND ITS LICENSORS AND WAIVED BY YOU.

- WILEY shall have the right to terminate this Agreement immediately upon breach of this Agreement by you.

- You shall indemnify, defend and hold harmless WILEY, its Licensors and their respective directors, officers, agents and employees, from and against any actual or threatened claims, demands, causes of action or proceedings arising from any breach of this Agreement by you.

- IN NO EVENT SHALL WILEY OR ITS LICENSORS BE LIABLE TO YOU OR ANY OTHER PARTY OR ANY OTHER PERSON OR ENTITY FOR ANY SPECIAL, CONSEQUENTIAL, INCIDENTAL, INDIRECT, EXEMPLARY OR PUNITIVE DAMAGES, HOWEVER CAUSED, ARISING OUT OF OR IN CONNECTION WITH THE DOWNLOADING, PROVISIONING, VIEWING OR USE OF THE MATERIALS REGARDLESS OF THE FORM OF ACTION, WHETHER FOR BREACH OF CONTRACT, BREACH OF WARRANTY, TORT, NEGLIGENCE, INFRINGEMENT OR OTHERWISE (INCLUDING, WITHOUT LIMITATION, DAMAGES BASED ON LOSS OF PROFITS, DATA, FILES, USE, BUSINESS OPPORTUNITY OR CLAIMS OF THIRD PARTIES), AND WHETHER OR NOT THE PARTY HAS BEEN ADVISED OF THE POSSIBILITY OF SUCH DAMAGES. THIS LIMITATION SHALL APPLY NOTWITHSTANDING ANY FAILURE OF ESSENTIAL PURPOSE OF ANY LIMITED REMEDY PROVIDED HEREIN.

- Should any provision of this Agreement be held by a court of competent jurisdiction to be illegal, invalid, or unenforceable, that provision shall be deemed amended to achieve as nearly as possible the same economic effect as the original provision, and the legality, validity and enforceability of the remaining provisions of this Agreement shall not be affected or impaired thereby.

- The failure of either party to enforce any term or condition of this Agreement shall not constitute a waiver of either party's right to enforce each and every term and condition of this Agreement. No breach under this agreement shall be deemed waived or excused by either party unless such waiver or consent is in writing signed by the party granting such waiver or consent. The waiver by or consent of a party to a breach of any provision of this Agreement shall not operate or be construed as a waiver of or consent to any other or subsequent breach by such other party.

- This Agreement may not be assigned (including by operation of law or otherwise) by you without WILEY's prior written consent.

- Any fee required for this permission shall be non-refundable after thirty (30) days from receipt by the CCC.

- These terms and conditions together with CCC's Billing and Payment terms and conditions (which are incorporated herein) form the entire agreement between you and WILEY concerning this licensing transaction and (in the absence of fraud) supersedes all prior agreements and representations of the parties, oral or written. This Agreement may not be amended except in writing signed by both parties. This Agreement shall be binding upon and inure to the benefit of the parties' successors, legal representatives, and authorized assigns.

- In the event of any conflict between your obligations established by these terms and conditions and those established by CCC's Billing and Payment terms and conditions, these terms and conditions shall prevail.

- WILEY expressly reserves all rights not specifically granted in the combination of (i) the license details provided by you and accepted in the course of this licensing transaction, (ii) these terms and conditions and (iii) CCC's Billing and Payment terms and conditions.

- This Agreement will be void if the Type of Use, Format, Circulation, or Requestor Type was misrepresented during the licensing process.

- This Agreement shall be governed by and construed in accordance with the laws of the State of New York, USA, without regards to such state's conflict of law rules. Any legal action, suit or proceeding arising out of or relating to these Terms and Conditions or the breach thereof shall be instituted in a court of competent jurisdiction in New York County in the State of New York in the United States of America and each party hereby consents and submits to the personal jurisdiction of such court, waives any objection to venue in such court and consents to service of process by registered or certified mail, return receipt requested, at the last known address of such party.

WILEY OPEN ACCESS TERMS AND CONDITIONS

Wiley Publishes Open Access Articles in fully Open Access Journals and in Subscription journals offering Online Open. Although most of the fully Open Access journals publish open access articles under the terms of the Creative Commons Attribution (CC BY) License only, the subscription journals and a few of the Open Access Journals offer a choice of Creative Commons Licenses. The license type is clearly identified on the article.

The Creative Commons Attribution License

The Creative Commons Attribution License (CC-BY) allows users to copy, distribute and transmit an article, adapt the article and make commercial use of the article. The CC-BY license permits commercial and non-

Creative Commons Attribution Non-Commercial License

The Creative Commons Attribution Non-Commercial (CC-BY-NC)License permits use, distribution and reproduction in any medium, provided the original work is properly cited and is not used for commercial purposes.(see below)

Creative Commons Attribution-Non-Commercial-NoDerivs License

The Creative Commons Attribution Non-Commercial-NoDerivs License (CC-BY-NC-ND) permits use, distribution and reproduction in any medium, provided the original work is properly cited, is not used for commercial purposes and no modifications or adaptations are made. (see below)

Use by commercial "for-profit" organizations

Use of Wiley Open Access articles for commercial, promotional, or marketing purposes requires further explicit permission from Wiley and will be subject to a fee.
Further details can be found on Wiley Online Library http://olabout.wiley.com/WileyCDA/Section/id-410895.html

Other Terms and Conditions:

v1.10 Last updated September 2015

Questions? customercare@copyright.com or +1-855-239-3415 (toll free in the US) or +1-978-646-2777.

Media centre

Cardiovascular diseases (CVDs)

Fact sheet N°317
Updated January 2015

KEY FACTS

- CVDs are the number 1 cause of death globally: more people die annually from CVDs than from any other cause.
- An estimated 17.5 million people died from CVDs in 2012, representing 31% of all global deaths. Of these deaths, an estimated 7.4 million were due to coronary heart disease and 6.7 million were due to stroke .
- Over three quarters of CVD deaths take place in low- and middle-income countries.
- Out of the 16 million deaths under the age of 70 due to noncommunicable diseases, 82% are in low and middle income countries and 37% are caused by CVDs.
- Most cardiovascular diseases can be prevented by addressing behavioural risk factors such as tobacco use, unhealthy diet and obesity, physical inactivity and harmful use of alcohol using population-wide strategies.
- People with cardiovascular disease or who are at high cardiovascular risk (due to the presence of one or more risk factors such as hypertension, diabetes, hyperlipidaemia or already established disease) need early detection and management using counselling and medicines, as appropriate.

What are cardiovascular diseases?

Cardiovascular diseases (CVDs) are a group of disorders of the heart and blood vessels and they include:

- coronary heart disease – disease of the blood vessels supplying the heart muscle;
- cerebrovascular disease – disease of the blood vessels supplying the brain;
- peripheral arterial disease – disease of blood vessels supplying the arms and legs;
- rheumatic heart disease – damage to the heart muscle and heart valves from rheumatic fever, caused by streptococcal bacteria;
- congenital heart disease – malformations of heart structure existing at birth;
- deep vein thrombosis and pulmonary embolism – blood clots in the leg veins, which can dislodge and move to the heart and lungs.

Heart attacks and strokes are usually acute events and are mainly caused by a blockage that prevents blood from flowing to the heart or brain. The most common reason for this is a build-up of fatty deposits on the inner walls of the blood vessels that supply the heart or brain.

Strokes can also be caused by bleeding from a blood vessel in the brain or from blood clots. The cause of heart attacks and strokes are usually the presence of a combination of risk factors, such as tobacco use, unhealthy diet and obesity, physical inactivity and harmful use of alcohol, hypertension, diabetes and hyperlipidaemia.

What are the risk factors for cardiovascular disease?

The most important behavioural risk factors of heart disease and stroke are unhealthy diet, physical inactivity, tobacco use and harmful use of alcohol. The effects of behavioural risk factors may show up in individuals as raised blood pressure, raised blood glucose, raised blood lipids, and overweight and obesity. These “intermediate risks factors” can be measured in primary care facilities and indicate an increased risk of developing a heart attack, stroke, heart failure and other complications.

Cessation of tobacco use, reduction of salt in the diet, consuming fruits and vegetables, regular physical activity and avoiding harmful use of alcohol have been shown to reduce the risk of cardiovascular disease. In addition, drug treatment of diabetes, hypertension and high blood lipids may be necessary to reduce cardiovascular risk and prevent heart attacks and strokes. Health policies that create conducive environments for making healthy choices affordable and available are essential for motivating people to adopt and sustain healthy behaviour.

There are also a number of underlying determinants of CVDs or "the causes of the causes". These are a reflection of the major forces driving social, economic and cultural change – globalization, urbanization and population ageing. Other determinants of CVDs include poverty, stress and hereditary factors.

What are common symptoms of cardiovascular diseases?

Symptoms of heart attacks and strokes

Often, there are no symptoms of the underlying disease of the blood vessels. A heart attack or stroke may be the first warning of underlying disease. Symptoms of a heart attack include:

- pain or discomfort in the centre of the chest;
- pain or discomfort in the arms, the left shoulder, elbows, jaw, or back.

In addition the person may experience difficulty in breathing or shortness of breath; feeling sick or vomiting; feeling light-headed or faint; breaking into a cold sweat; and becoming pale. Women are more likely to have shortness of breath, nausea, vomiting, and back or jaw pain.

The most common symptom of a stroke is sudden weakness of the face, arm, or leg, most often on one side of the body. Other symptoms include sudden onset of:

- numbness of the face, arm, or leg, especially on one side of the body;
- confusion, difficulty speaking or understanding speech;
- difficulty seeing with one or both eyes;
- difficulty walking, dizziness, loss of balance or coordination;
- severe headache with no known cause; and

- fainting or unconsciousness.

People experiencing these symptoms should seek medical care immediately.

What is rheumatic heart disease?

Rheumatic heart disease is caused by damage to the heart valves and heart muscle from the inflammation and scarring caused by rheumatic fever. Rheumatic fever is caused by an abnormal response of the body to infection with streptococcal bacteria, which usually begins as a sore throat or tonsillitis in children.

Rheumatic fever mostly affects children in developing countries, especially where poverty is widespread. Globally, about 2% of deaths from cardiovascular diseases is related to rheumatic heart disease.

Symptoms of rheumatic heart disease

- Symptoms of rheumatic heart disease include: shortness of breath, fatigue, irregular heart beats, chest pain and fainting.
- Symptoms of rheumatic fever include: fever, pain and swelling of the joints, nausea, stomach cramps and vomiting.

Why are cardiovascular diseases a development issue in low- and middle-income countries?

- At least three quarters of the world's deaths from CVDs occur in low- and middle-income countries.
- People in low- and middle-income countries often do not have the benefit of integrated primary health care programmes for early detection and treatment of people with risk factors compared to people in high-income countries.
- People in low- and middle-income countries who suffer from CVDs and other noncommunicable diseases have less access to effective and equitable health care services which respond to their needs. As a result, many people in low- and middle-income countries are detected late in the course of the disease and die younger from CVDs and other noncommunicable diseases, often in their most productive years.
- The poorest people in low- and middle-income countries are affected most. At the household level, sufficient evidence is emerging to prove that CVDs and other noncommunicable diseases contribute to poverty due to catastrophic health spending and high out-of-pocket expenditure.
- At macro-economic level, CVDs place a heavy burden on the economies of low- and middle-income countries.

How can the burden of cardiovascular diseases be reduced?

“Best buys” or very cost effective interventions that are feasible to be implemented even in low-resource settings have been identified by WHO for prevention and control of cardiovascular diseases. They include two types of interventions: population-wide and individual, which are recommended to be used in combination to reduce the greatest cardiovascular disease burden.

Examples of population-wide interventions that can be implemented to reduce CVDs include:

- comprehensive tobacco control policies
- taxation to reduce the intake of foods that are high in fat, sugar and salt
- building walking and cycle paths to increase physical activity
- strategies to reduce harmful use of alcohol
- providing healthy school meals to children.

At the individual level, for prevention of first heart attacks and strokes, individual health-care interventions need to be targeted to those at high total cardiovascular risk or those with single risk factor levels above traditional thresholds, such as hypertension and hypercholesterolemia. The former approach is more cost-effective than the latter and has the potential to substantially reduce cardiovascular events. This approach is feasible in primary care in low-resource settings, including by non-physician health workers.

For secondary prevention of cardiovascular disease in those with established disease, including diabetes, treatment with the following medications are necessary:

- aspirin
- beta-blockers
- angiotensin-converting enzyme inhibitors
- statins.

The benefits of these interventions are largely independent, but when used together with smoking cessation, nearly 75% of recurrent vascular events may be prevented. Currently there are major gaps in the implementation of these interventions particularly at the primary health care level.

In addition costly surgical operations are sometimes required to treat CVDs. They include:

- coronary artery bypass
- balloon angioplasty (where a small balloon-like device is threaded through an artery to open the blockage)
- valve repair and replacement
- heart transplantation
- artificial heart operations

Medical devices are required to treat some CVDs. Such devices include pacemakers, prosthetic valves, and patches for closing holes in the heart.

WHO response

Under the leadership of the WHO, all Member States (194 countries) agreed in 2013 on global mechanisms to reduce the avoidable NCD burden including a "Global action plan for the prevention and control of NCDs 2013-2020". This plan aims to reduce the number of premature deaths from NCDs by 25% by 2025 through nine voluntary global targets. Two of the global targets directly focus on preventing and controlling CVDs.

Global action plan for the prevention and control of NCDs 2013-2020

The sixth target in the Global NCD action plan calls for 25% reduction in the global prevalence of raised blood pressure. Raised blood pressure is one of the leading risk factors of cardiovascular disease. The global prevalence of raised blood pressure (defined as systolic and/or diastolic blood pressure ≥140/90 mmHg) in adults aged 18 years and over was around 22% in 2014.

Reducing the incidence of hypertension by implementing population-wide policies to reduce behavioural risk factors, including harmful use of alcohol, physical inactivity, overweight, obesity and high salt intake, is essential to attaining this target. A total-risk approach needs to be adopted for early detection and cost-effective management of hypertension in order to prevent heart attacks, strokes and other complications.

The eighth target in the Global NCD action plan states at least 50% of eligible people should receive drug therapy and counselling (including glycaemic control) to prevent heart attacks and strokes. Prevention of heart attacks and strokes through a total cardiovascular risk approach is more cost-effective than treatment decisions based on individual risk factor thresholds only and should be part of the basic benefits package for pursuing universal health coverage. Achieving this target will require strengthening key health system components, including health-care financing to ensure access to basic health technologies and essential NCD medicines.

In 2015, countries will begin to set national targets and measure progress on the 2010 baselines reported in the "Global status report on noncommunicable diseases 2014". The UN General Assembly will convene a third high-level meeting on NCDs in 2018 to take stock of national progress in attaining the voluntary global targets by 2025.

Global status report on noncommunicable diseases 2014

Related links

WHO action plan for the strategy for prevention and control of noncommunicable

Global atlas on cardiovascular disease prevention and control

Deaths from cardiovascular diseases and diabetes

Health topic: cardiovascular diseases

Related

Stroke, Cerebrovascular accident

Explore WHO

Congenital anomalies

Potential impact of single-risk-factor versus total risk management for the prevention of cardiovascular events in Seychelles

Indicator 18: Drug therapy to prevent heart attacks and strokes

The availability and affordability of selected essential medicines for chronic diseases in six low- and middle-income countries

mhGAP Evidence Resource Centre

About HIV/AIDS

Health financing policy and financial protection